

TR diss
2684

**Synthesis and Coordination Behaviour of
N-alkylamino Sugars and Derivatives**

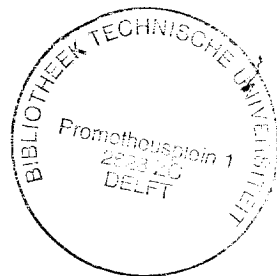
Synthesis and Coordination Behaviour of N-alkylamino Sugars and Derivatives

PROEFSCHRIFT

ter verkrijging van de graad van doctor
aan de Technische Universiteit Delft,
op gezag van de Rector Magnificus Prof. ir. K.F. Wakker,
in het openbaar te verdedigen ten overstaan van een commissie,
door het College van Dekanen aangewezen,
op maandag 11 december 1995 te 10.30 uur
door

Hendrik LAMMERS

scheikundig doctorandus
geboren te Aalten



Dit proefschrift is goedgekeurd door de promotor:

Prof. dr. ir. H. van Bekkum

en de toegevoegd promotor: Dr. ir. J.A. Peters

Samenstelling promotiecommissie:

| | |
|-------------------------------------|--|
| Rector Magnificus | Technische Universiteit Delft |
| Prof. dr. ir. H. van Bekkum | Technische Universiteit Delft |
| Dr. ir. J.A. Peters | Technische Universiteit Delft |
| Prof. dr. A.E. Merbach | Universiteit van Lausanne, Zwitserland |
| Prof. dr. R.N. Muller | Universiteit van Mons-Hainaut, België |
| Prof. dr. R.A. Sheldon | Technische Universiteit Delft |
| Dr. C.L. Habraken | Rijksuniversiteit Leiden |
| Dr. E. Boelema | Akzo Nobel Central Research |
| Prof. dr. J. Schoonman (reservelid) | Technische Universiteit Delft |

Published and distributed by:

Delft University Press

Stevinweg 1

2628 CN Delft

The Netherlands

Telephone +31 15 2783254

Fax +31 15 2781661

CIP-DATA KONINKLIJKE BIBLIOTHEEK, DEN HAAG

Lammers, Hendrik

Synthesis and coordination behaviour of N-alkylamino sugars and derivatives / Hendrik Lammers. - Delft : Delft University Press. - Ill.

Thesis Delft University of Technology. - With ref. - With summary in Dutch.

ISBN 90-407-1186-0

NUGI 841

Subject heading: amino sugars.

Copyright © 1995 by H. Lammers

All rights reserved.

No part of the material protected by this copyright notice may be reproduced or utilized in any form or by any means, electronic or mechanical, including photocopying, recording or by any information storage and retrieval system, without permission from the publisher: Delft University Press, Stevinweg 1, 2628 CN Delft, The Netherlands.

Printed in The Netherlands

*'But science, unadulterated, is not satisfying:
men need also passion and art and religion.
Science may set limits to knowledge, but should not
set limits to imagination.'*

Bertrand Russell in *History of Western Philosophy*,
Routledge; London **1991**, p36.

CONTENTS

| | page |
|--|------|
| Chapter 1: General Introduction | 1 |
| Chapter 2: Magnetic Resonance Imaging: General Information | 17 |
| Chapter 3: Reductive Amination of Aldohexoses with Mono- and Bifunctional Alkyl Amines: Conversion of Carbohydrates into EDTA Type Complexing Agents | 35 |
| Chapter 4: Reaction Kinetics of the Aqueous Phase Reductive Amination of D-Galactose with Propylamine (in Aqueous Medium) over Platinum on (Activated) Carbon | 55 |
| Chapter 5: Formation of Borate Esters from, and Sequestration of Metal Ions by Bis(polyhydroxyalkyl)amines and their N-Carboxymethyl Derivatives Studied by ^{11}B- and ^{13}C NMR Spectroscopy | 71 |
| Chapter 6: Coordination of Cd(II) by N-alkylamino Sugars in Aqueous Solution as Studied by Potentiometry and ^{113}Cd NMR Spectroscopy | 89 |
| Chapter 7: Determination of Stability Constants of Metal Complexes from NMR Chemical Shifts and Relaxation Rates using a Spreadsheet Computer Program | 105 |
| Chapter 8: Structure and Dynamics of Ln(III) Complexes of Sugar-Based DTPA-bis(amides) in Aqueous Solution: A Multinuclear NMR Study | 125 |
| Chapter 9: Protonation and Metal Ion Coordination Studies of a Sugar-Based DTPA-bis(amide) Derivative as Studied by Potentiometry and Multinuclear NMR Spectroscopy | 167 |
| Summary | 189 |
| Samenvatting | 193 |

Dankwoord

197

Curriculum vitae

199

Chapter 1

GENERAL INTRODUCTION

INTRODUCTION

Naturally occurring N-containing carbohydrates

Carbohydrates form the major class of renewables. Examples include the polysaccharides cellulose and starch with glucose as the monomeric unit. Together with sucrose, a disaccharide consisting of glucose and fructose, they form the three most abundant carbohydrates. Various natural carbohydrates contain functional groups, e.g. carboxylate groups are found in the alginates and pectins, pyruvate acetals are present in xanthan gum and sulfate groups occur in agar.

Also nitrogen-containing carbohydrates are found in nature. Most of these aminosugars make up building blocks of oligo- and polysaccharides possessing an N-containing group as the substituent. An exception is nojirimycin (1) in which the amino group is incorporated into the sugar ring (Figure 1). Aminosugars possessing this type of piperidine ring structure have generated a great deal of interest because they are able to function as glycosidase inhibitors.^{1,2} As such these compounds have therapeutic potential as antiviral, anti-HIV, antidiabetic and anticancer agents.^{3,4}

2-Amino-2-deoxy- β -D-glucose (2), or D-glucosamine, exemplifies an aminosugar in which the amine function is present in the form of an appended substituent. It occurs as its

acetylated analogue in chitin (3) (Figure 2), which is a (1-4)-linked aminopolysaccharide found in the exoskeletons of crustacea.

The biosynthesis of D-glucosamine is accomplished via condensation of D-fructose (a 2-ketohexose) with ammonia followed by rearrangement of the imine to form D-glucosamine.⁵ This reaction is a specific example of the very complex cascade of reactions taking place between reducing sugars and the free amino group of amines, amino acids and proteins during food processing and ageing. The reaction was first investigated by Maillard and is commonly known as the Maillard or "browning" reaction.⁵

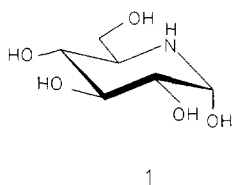


Figure 1. The structure of nojirimycin (1).

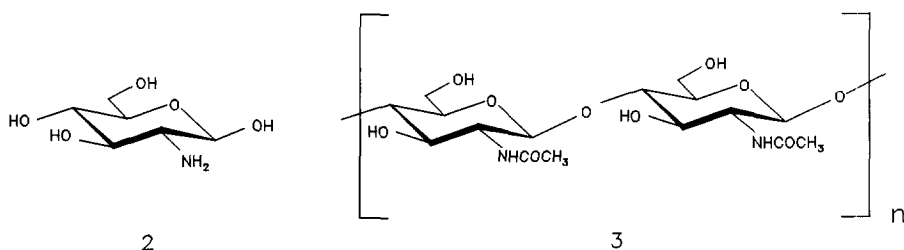


Figure 2. The structures of β -D-glucosamine (2) and chitin (3).

Synthetic N-containing carbohydrates

A variety of alternative synthetic reaction routes to form nitrogen-containing carbohydrates are known.⁶ In this thesis, the attention will be focused on the synthesis of acyclic aminosugars starting from readily available carbohydrates. The amino function is introduced by making use of the carbonyl group present in reducing carbohydrates. In this introductory chapter, the most effective approaches to synthesize acyclic aminosugars are

discussed as well as the (potential) applications of the products obtained. The so-called glycosylamines (see Figure 3) are the reaction intermediates in the synthetic methods described. The formation and applications of glycosylamines are also described.

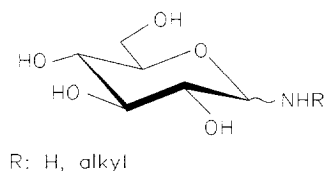


Figure 3. The structural formula of α,β -D-glycosylamines.

On a laboratory scale a commonly used procedure for the synthesis of aminosugars is the reaction of sugars with hydroxylamine followed by the reduction of the oximes formed with metal hydrides⁷ or by catalytic hydrogenation.⁸ A useful example of the latter method, depicted in Figure 4, is the synthesis of 5-amino-5-deoxy-D-glucono- δ -lactam (6), which has been used for establishing the configuration of nojirimycin (1) starting from 5-keto-D-gluconic acid potassium salt (4).⁹

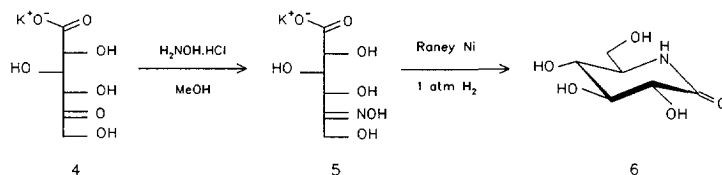


Figure 4. The synthesis of 5-amino-5-deoxy-D-glucono- δ -lactam (6).

The superior route towards nitrogen-containing carbohydrates is the reductive amination by the action of a (noble) metal catalyst.¹⁰⁻¹⁷ The initial step in the reductive amination corresponds to the first step in the Maillard reaction. As an example the speciation of a D-glucose/ ammonia mixture in water is given in Figure 5.¹⁸ The imine (9) is formed by the nucleophilic attack of ammonia on the acyclic form (8) of (α,β) -D-glucose (7). The (α,β) -D-glycosylamine (10), formed by cyclization of the imine (9), contains a primary amino group. Consequently, a nucleophilic attack on a second D-glucose molecule may occur

resulting via imine (11) in an (α,β)-D-diglycosylamine (12).^{19,20} The latter process is called dimerization²¹ or transglycosylation.²²

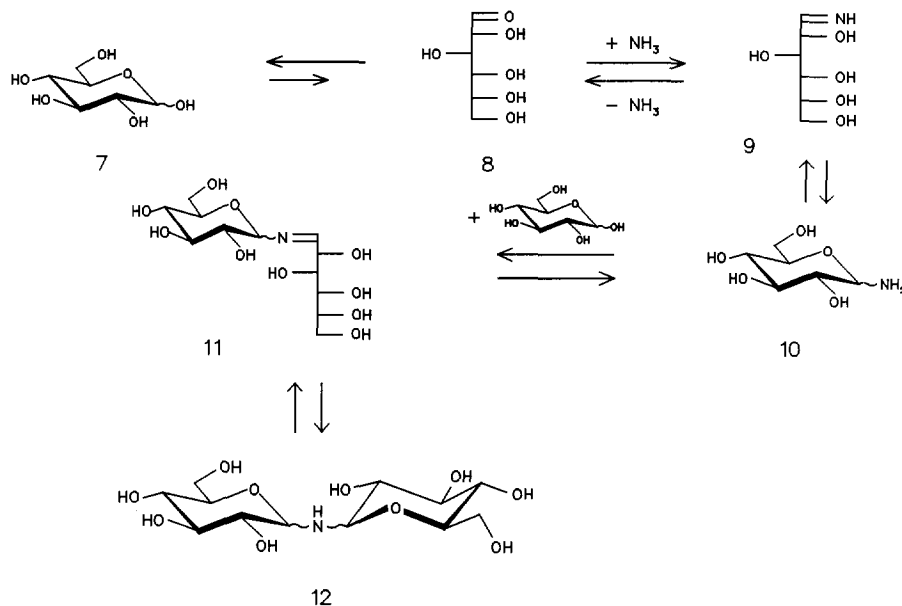


Figure 5. Equilibria occurring in an aqueous solution of D-glucose (7) and ammonia.

Glycosylamines are well-known carbohydrate derivatives.^{23,24} The first synthetic compounds were prepared by Schiff by heating aniline or *p*-toluidine with D-glucose.^{25,26} Since then, many reports concerning the isolation and characterization of glycosylamines have been published.^{23,24} In addition to this, the mutarotation, hydrolysis and rearrangement reactions of glycosylamines in water as well as in organic solvents have been extensively studied.^{20,27} Several glycosylamines are of interest in nucleoside and glycopeptide chemistry as valuable synthetic intermediates. Their high solubility has been exploited in their use as biological carriers while their pharmaceutical activity is generally the same as that of the corresponding bases.²⁸ It should be noted, however, that glycosylamines are also able to react with nitrosating species (e.g. nitrogen oxides) forming N-nitrosoglycosylamines, some of which exhibit mutagenic behaviour.²⁹ Recently, Lubineau et al. reported an efficient method for the synthesis of N-acyl-

glucosylamines, which are unlike glycosylamines stable compounds (Figure 6).³⁰ The N-acylglucosylamines exhibited promising micellar properties. The peracetylated N-acyl-D-glucosylamine turned out to be an excellent bleaching booster for detergents.³⁰

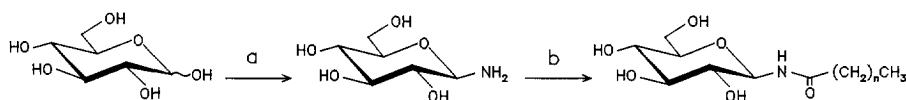
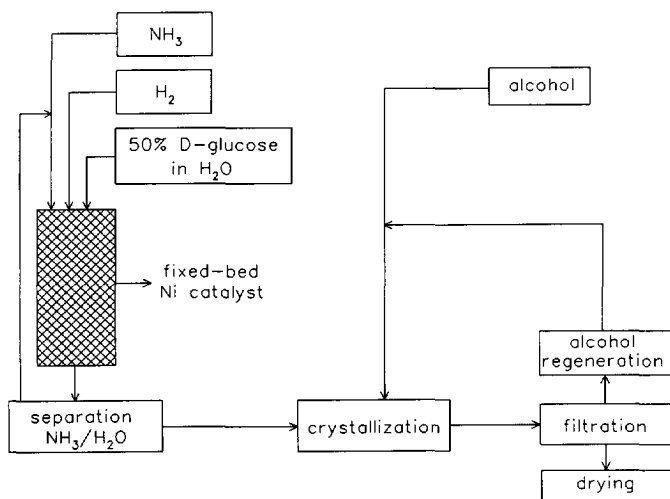


Figure 6. The synthesis of N-acylglucosylamines ($6 < n < 12$); a: 0.2 M D-glucose/0.2 M NH_4HCO_3 /16 M NH_3 /42 °C/36 h; b: EtOH/ H_2O /1 eq Na_2CO_3 /4 eq acyl chloride/0 °C.

A similar type of amphiphilic molecules showing excellent surface active properties are the long chain N-alkyllactosylamines. Their synthesis and characterization has been described by Latgé and co-workers.³¹⁻³³

The next step in the synthesis of amino sugars via reductive amination is the hydrogenation of the sugar/amine mixtures. It is believed that the formation of the amino sugar proceeds via hydrogenolysis of the corresponding glycosylamine. The hydrogenation step is carried out either directly on the sugar/amine mixture or after isolation of the glycosylamine. The former procedure is more attractive from a commercial point of view. The first patents appearing in the 1930s, described the (direct) reductive amination of readily available carbohydrates with primary alkylamines using Raney Ni or Ni supported on silica as the catalyst.¹¹ The starting sugars predominantly used were the aldohexoses D-glucose and D-galactose; the products obtained have been named systematically as 1-alkylamino-1-deoxy-D-alditols with the trivial name 'glycamines'.

A commercial process has been developed by Hüls AG, and involves the reductive amination of D-glucose with ammonia, producing D-glucamine or 1-amino-1-deoxy-D-glucitol (13).¹⁸ This process is carried out by continuous reductive amination of an aqueous solution of D-glucose and ammonia using hydrogen in a fixed-bed process over a Ni catalyst (Scheme 1).



Scheme 1. Flow diagram of the continuous reductive amination of D-glucose with ammonia (Hüls AG, Germany).¹⁸

It can be concluded from Figure 5 that the hydrogenation of this solution will result in a mixture containing the aminosugars D-glucamine (13), di-D-glucitylamine (14) and D-glucitol (15) (for the structures of the hydrogenated products see Figure 7). The aminosugars 13 and 14 are being formed as a result of the presence of the species 10 and 12, respectively, D-glucitol (15) is formed by the hydrogenation of D-glucose (7). The best results are obtained when the sugar solution and ammonia are pumped into the reactor tube in separate streams (Scheme 1). Water and ammonia are partially recycled in the reactor. The degree of amination is controlled by the temperature, the space velocity and the ratio of reactants. The reaction temperature is approximately 150 °C and the hydrogen pressure is 200 bar. The final product crystallizes upon addition of either methanol or ethanol to the reaction mixture. Under the applied reaction conditions, the selectivity to D-glucamine (13) is approximately 90%. The purity of the crystallized D-glucamine is more than 99%. The product contains less than 0.1% of D-glucitol (15) and di-D-glucitylamine (14) is not present in detectable amounts.

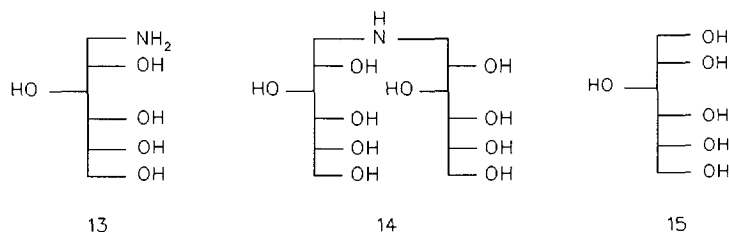


Figure 7. The products formed during the reductive amination of *D*-glucose (7) with ammonia.

The reductive amination can also be applied to disaccharides (Südzucker AG, Germany).³⁴ Sucrose (16) is the most attractive disaccharide to utilize since the world market price continues to be low but it is lacking a carbonyl group. Consequently, either by isomerization or by oxidation reactions, a carbonyl function has to be introduced into sucrose prior to the reductive amination. For example, the reducing sugar isomaltulose (17) is obtained by enzymatic isomerization of sucrose with *Protaminobacter rubrum* CBS 574.77.^{35,36} In the first step of the reductive amination of isomaltulose (17) with ammonia³⁷ (Figure 8), the formation of the ketosylamine (19) via the open form (18) is very slow. Therefore, a pre-equilibration time is necessary prior to hydrogenation of approximately 17 h at 20 °C. After hydrogenation at 150 bar and 50 °C using Raney Ni as the catalyst, 80% of an equimolar mixture of 2-amino-2-deoxy-6-O-(α -*D*-glucopyranosyl)-*D*-mannitol (20) and 2-amino-2-deoxy-6-O-(α -*D*-glucopyranosyl)-*D*-glucitol (21) has been obtained. In order to minimize side reactions, e.g. the Amadori-rearrangement and the Maillard-reaction, the reaction mixture must be well stirred and kept at room temperature.

The 3-keto-sucrose (22), formed during the oxidation of sucrose (16) with *Agrobacterium tumefaciens*³⁸, has been converted into an amino-disaccharide (23) by reductive amination with ammonia³⁹ (Figure 9). 1-Amino-1-deoxy-4-O-*D*-alditols derived from the disaccharides *D*-cellobiose, *D*-lactose and *D*-maltose have been synthesized in 80-90% yield. This was accomplished via reductive amination with benzylamine using sodium borohydride and subsequent catalytic removal of the benzyl group at atmospheric hydrogen pressure using Pd on activated carbon as the catalyst.⁴⁰

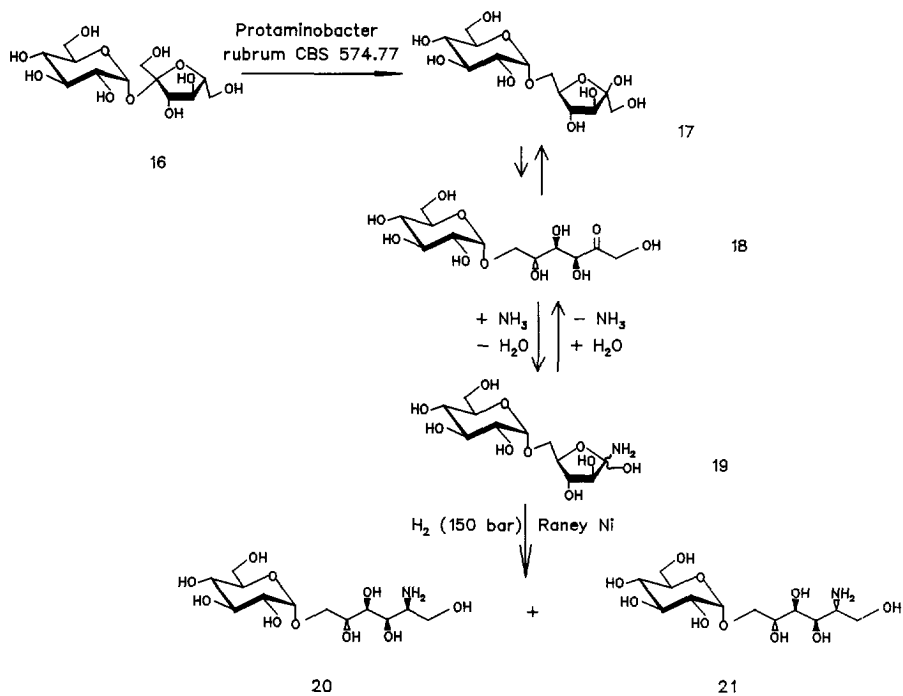


Figure 8. The reductive amination of isomaltulose (17) with ammonia.

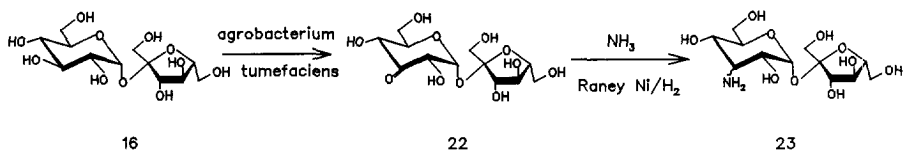


Figure 9. The formation and the reductive amination with ammonia of 3-keto sucrose (22).

POSSIBLE INDUSTRIAL APPLICATIONS OF GLYCAMINES

Recent developments in the detergent industry have been driven by a strong consumer demand for naturally-derived products. Detergent manufacturers have responded to this demand by supplying the requisite products and advertising slogans such as "fully biodegradable", "natural" or even "double natural" in order to gain the edge over their competitors. The most important challenge in recent years to the detergent industry has been to find a solution for the eutrophication of surface waters partially caused by polyphosphates (pentasodiumtripolyphosphate) present in detergent powders.⁴¹ A relatively quick response to this by the manufacturers was the introduction of phosphate-free products. These were followed by the development of a new generation of detergents, firstly the liquid detergents and subsequently the high density compact-powder detergents. The new generation detergents typically contains about 30% surfactant. Surfactants are amphiphilic, surface active substances, which dissolve (in a molecular and micellar form) and remove stains.

The heterofunctional nature of glycamines provides easy access to a novel type of surfactants called glycamides (Figure 10). Glycamides (mainly derived from D-glucose) have been under the scrutiny of detergents manufactures since three years ago. The sugar-based surfactants are readily biodegradable and do not cause any skin irritant effects. These compounds were first described in the 1930s but were ignored until reawakened interest started in the 1980s.⁴² Procter & Gamble in the 1990s has submitted approximately 20 patent applications for the manufacture and use of glucamides in their detergent formulations.⁴²

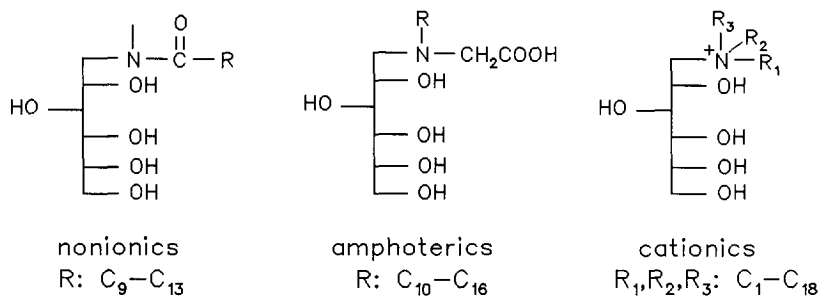
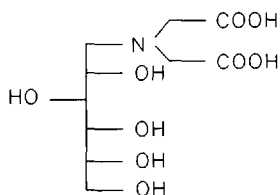


Figure 10. Several types of surfactants based on glucamine.

Surfactants based on the amino-sucrose derivatives (Figure 9) show low skin-degreasing effects and are non skin-irritating. They also exhibit superior skin moisturizing behaviour and therefore are of potential interest in cosmetic applications.³⁹

Builders and co-builders, making up the largest proportion of detergents, have the function of complexing calcium and magnesium ions in water. These metal ions cause the permanent hardness in water and result in precipitation of insoluble carbonates and soap salts on the fabric (incrustation) as well as scaling in the washing machine. Polyphosphates performed the metal ion complexing function for many years, however due to the notorious side effect (eutrophication) the use of phosphates was partially abandoned initially in the 1980's, and nowadays they almost completely vanished in W-Europe from use. Today, mainly silicate types, such as Zeolite NaA, are used as builder in combination with synthetic polycarboxylate copolymers, e.g. the acrylic acid/maleic acid copolymer, as co-builder. The zeolite functions as an insoluble suspended inorganic cation exchanger. Recently, Unilever introduced another zeolite, MAP, with improved properties compared to zeolite NaA. Substances such as EDTA (ethylenediaminetetraacetic acid) and NTA (nitrilotriacetic acid) have been investigated as potential phosphate replacers. The biodegradability of the former compound and of the synthetic polycarboxylates however is insufficient to meet today's standards. Polymers derived from natural polysaccharides, such as dicarboxystarch and dicarboxyinulin, are being investigated as potential substitutes.^{43,44} In addition to this, the di-carboxymethylated product of D-glucamine 24 has been investigated as a potential builder and shows promising calcium sequestering capacities.¹⁸



24

Figure 11. The structure of D-glucamine-N,N-diacetic acid (24).

Several other potential applications of glycamines are mentioned in the literature. Klein et

al. proposed new types of semi-synthetic polymers based on well-defined monosaccharides containing a polymerizable double bond.⁴⁵ The aminopolyols obtained after reductive amination are converted to reactive vinyl compounds using a suitable vinyl compound, e.g. 2-isocynoethyl methyl acrylate, and subsequently polymerized. The resulting linear polymers of the urea type have been characterized and their properties were investigated by using viscometry, light scattering and surface tension measurements. An important microscopic effect of these water-soluble polymers, is the viscosity enhancement in aqueous solution. By varying of the monomer ratio of amphiphilic monomers and other hydrophilic co-monomers, the authors were able to prepare polymers of high molecular weight with interesting surfactant properties.⁴⁵ Liquid crystalline compounds represent another possible future application of glycamines as well as of glycosylamines. Studies on the liquid crystalline behaviour of several types of glycamines and glycosylamines are still at an exploratory stage.⁴⁶ Finally, glycamines have also been suggested as sweeteners.⁴⁷ The concerning research was based on the notion that increased hydrophobicity potentially results in increased sweetness. The authors prepared therefore a number of amides of 1-amino-1-deoxy-D-glucitol and 1-deoxy-1-methylamino-D-glucitol by reaction with carboxylic acid anhydrides, chlorides and methyl esters. It was found that sweetness could not be induced by increasing the hydrophobicity of the parent molecule, even though the compounds investigated, seemed to match the existing models describing sweetness-structure relationships.

METAL ION - AMINOSUGAR INTERACTIONS IN SOLUTION

The complexes of metal ions with carbohydrates were initially thought to be of little interest. However since the 1970's, interest has increased profoundly, and complex formation between metal ions and carbohydrates is currently being studied in areas such as bioinorganic chemistry, environmental chemistry and industrial applications.^{48,49} Sugar acids and related polyhydroxy carboxylic acids have been studied as potential sequestering agents for over forty years.⁴⁹ Of these compounds the sodium salt of D-gluconate has found widespread use as a chelating agent under conditions of extreme alkalinity, e.g. for bottle washing and metal cleaning.^{50,51} The metal ion sequestering capacities of aqueous

solutions of polyhydroxy carboxylic acids are known to increase substantially upon addition of boric acid at $\text{pH} > 9$.⁵² The Ca(II) ion complexation of mixtures of borate and polyhydroxy carboxylates has been studied extensively in our laboratory.⁵²⁻⁵⁴ In these systems, a synergistic Ca(II) sequestration originates from the linkage of two organic ligands by the borate anion, creating strong metal ion coordinating sites.

By virtue of the presence of the amino group in aminosugars, these ligands form generally much stronger complexes than nitrogen-free sugars do with most metal ions.⁴⁸ The already mentioned aminopolysaccharide chitin (3) and its N-deacetylated analogue chitosan (polyglucosamine), are well-known examples of naturally-occurring chelators. The chelating abilities of these aminopolysaccharides have been investigated by Muzzarelli and coworkers.⁵⁵⁻⁵⁷ Chitosan derivatives have been used to remove Cu(II) from waste water, and these polymers have also been proposed as chelating supports for pre-concentrating trace elements and recovering uranium from dilute solutions of natural waters.^{57,58}

The selective removal and sequestration of Cd(II) is of interest from an environmental and pharmaceutical point of view. Moreover, the interaction of Cd(II) with organic ligands is interesting because Cd(II) is used to mimic NMR "silent" metal ions such as Ca(II), Zn(II) and Mg(II) in a variety of metallo-enzymes.⁵⁸⁻⁶⁰ ¹¹³Cd NMR studies of metallo-enzymes in which the native metal ions are replaced by Cd(II), have provided useful information on the metal binding sites in these proteins.⁶⁰⁻⁶²

SCOPE OF THIS THESIS

The reductive amination of aldohexoses e.g. D-glucose, D-galactose and D-mannose with mono- and bifunctional amines and the metal ion coordination of the thus-obtained aminosugars and various derivatives thereof are the two main themes in this thesis. The aminosugars derived from bifunctional amines are converted into poly(aminocarboxylates), derived from DTPA (diethylenetriaminepentaacetic acid), possessing potential value in magnetic resonance imaging (MRI), a rapidly evolving non-invasive diagnostic method based upon nuclear magnetic resonance.⁶³ In Chapter 2, the main chemical and physical principles of MRI will be discussed. The speciation of a D-galactose/n-propylamine

mixture is investigated extensively using ^1H and ^{13}C NMR spectroscopy and is described in Chapter 3.⁶⁴ The reductive amination of aldohexoses with n-propylamine, ethylenediamine and 1,3-diaminopropane using a Pt on carbon catalyst as well as the subsequent conversion of the ethylenediamine sugar derivatives into EDTA-type complexes are also described in Chapter 3.⁶⁴ So far, kinetic studies on the reductive amination of carbohydrates have not been published in the literature and therefore a (preliminary) kinetic study on the continuous reductive amination of D-galactose with n-propylamine using platinum on activated carbon as the catalyst is described in Chapter 4. The synthesis of bis(polyhydroxyalkyl)amines using the 'hydroxylamine method', and the preparation of their N-carboxymethyl derivatives is reported in Chapter 5.⁶⁵ The borate ester formation of these compounds is studied using ^{11}B and ^{13}C NMR spectroscopy. Preliminary results on the Ca(II) and Cd(II) sequestration of these compounds and their mixtures with borate are provided. The coordination of Cd(II) by N-alkylamino sugars in aqueous solution as studied by potentiometry and ^{113}Cd NMR spectroscopy is reported in Chapter 6.⁶⁶ The Cd(II) stability constants were also determined from NMR chemical shifts using a spreadsheet computer program which is discussed in Chapter 7.⁶⁷ Moreover, two other examples demonstrating the versatility of NMR for determining stability constants are described in Chapter 7. The compounds derived from the reductive amination of aldohexoses with bifunctional amines, described in Chapter 3, are used for the synthesis of sugar-based DTPA-bis(amides), which is reported in Chapter 8.⁶⁸ The structures and dynamics of the corresponding lanthanide(III) complexes in aqueous solution using multinuclear NMR spectroscopy (^1H , ^{13}C , ^{17}O) are reported also in Chapter 8. The water exchange rate on and the rotational correlation time of the corresponding Gd(III) complexes, which are important parameters for the efficacy of a MRI contrast agent, are determined using variable temperature ^{17}O NMR. The mechanism of water exchange is determined using variable pressure ^{17}O NMR. This latter research has been carried out in collaboration with the University of Lausanne. The so-called ^1H NMRD profiles of the Gd(III) complexes concerned were recorded at the University of Mons and will be interpreted also in Chapter 8. The hydroxyl groups present in these molecules may be potential binding sites for metal ions such as Cd(II) and Zn(II). The formation of ternary complexes of the sugar-based DTPA-bis(amides) with Ln(III) and borate, respectively (as a model for Cd(II) and Zn(II)) has been investigated using ^{11}B as well as

^{13}C NMR spectroscopy and is discussed in Chapter 9.⁶⁹ In addition, a study on the transmetallation of the Ln(III) DTPA-bis(amides) with Zn(II) using ^{13}C and ^{139}La NMR spectroscopy is described in Chapter 9.

REFERENCES

1. Truscheit, E.; Frommer, W.; Junge, B.; Muller, L.; Schmidt, D.D.; Wingerder, W. *Angew. Chem. Int. Ed. Engl.* **1981**, *20*, 744.
2. Fleet, G.W.J. *Chem. Brit.* **1989**, 287.
3. Spearman, M.A.; Jamieson, J.C.; Wright, J.A. *Expt. Cell Res.* **1987**, *168*, 116.
4. Tsukamoto, K.; Uno, A.; Shimada, S.; Imokaw, G. *Clin. Res.* **1989**, *37A*, 722.
5. Ledl, F.; Schleicher, E. *Angew. Chem. Int. Ed. Engl.* **1990**, *29*, 565.
6. Long, J.W.; Bollenback, G.N. In *Methods in Carbohydrate Chemistry*, Vol. II; Whistler, R.L.; Wolfrom, M.L., Eds; Academic Press: London, **1963**, 79.
7. Pelyvás, S.; Hasegawa, A.; Whistler, R.L. *Carbohydr. Res.* **1986**, *146*, 193.
8. Brimacombe, J.S.; Hanna, R.; Saeed, M.S.; Tucker, L.C.N. *Carbohydr. Res.* **1982**, *100*, C10.
9. Inouye, S.; Tsuruoka, T.; Ito, T.; Niida, T. *Tetrahedron* **1968**, *24*, 2125.
10. Ling, A.R.; Nanji, D.R. *J. Chem. Soc.* **1922**, *121*, 1682.
11. Flint, R.B.; Salzberg, P.L. *US* 2,016,962, **1934**; *Chem. Abstr.* **1935**, *29*, 8007.
12. Wayne, W.; Adkins, H.J. *J. Am. Chem. Soc.* **1940**, *62*, 3314.
13. Holly, F.W.; Peel, E.W.; Mazingo, R.; Folkers, K. *J. Am. Chem. Soc.* **1950**, *72*, 5416.
14. Kagan, F.; Rebenstorf, M.A.; Heinzelman, R.V. *J. Am. Chem. Soc.* **1957**, *79*, 3541.
15. Lemieux, R.U. *US* 2,830,983, **1958**; *Chem. Abstr.* **1958**, *52*, 14668.
16. Tronchet, J.M.J.; Baehler, B.; Zumwald, J.-B. *Helv. Chim. Acta* **1977**, *60*, 1932.
17. Larkin, J.M.; Yeakey, E.L. Watts, Jr. L.W. *US* 4,540,821, **1985**; *Chem. Abstr.* **1985**, *104*, 110120.
18. Kelkenberg, H. *Tenside Surf. Det.* **1988**, *25*, 1.
19. Mitts, E.; Hixon, R.M. *J. Am. Chem. Soc.* **1944**, *66*, 483.
20. Isbell, H.S.; Frush, H.L. *J. Org. Chem.* **1958**, *23*, 1309.
21. Linek, K.; Alföldi, J.; Defaye, J. *J. Carbohydr. Res.*, **1987**, *164*, 195.
22. Paul, B.; Korytnyk, W. *Carbohydr. Res.* **1978**, *67*, 457.
23. Ellis, G.P.; Honeyman, J. In *Adv. Carbohydr. Chem.*, Vol. 10; Wolfrom, M.L., Ed.;

- Academic Press: London, **1955**, 95.
24. Paulsen, H.; Pflughaupt, W. In *The Carbohydrates*, Vol. 1B; Pigman, W.; Horton, D., Eds.; Academic Press: London, **1980**, 881.
 25. Schiff, H. *Ann. Chem. Pharm.* **1866**, 140, 123.
 26. Schiff, H. *Ann. Chem. Pharm.* **1870**, 154, 30.
 27. Capon, B. *Chem. Rev.* **1969**, 69, 407.
 28. Wiegandt, H.; Ziegler, W. *Physiol. Chem.* **1974**, 355, 11.
 29. Pignatelli, B.; Malaveille, C.; Friesen, M.; Hautefeuille, A.; Bartsch, H.; Piskorska, D.; Descotes, G. *Food Chem. Toxic.* **1987**, 25, 669.
 30. Lubineau, A.; Augé, J.; Drouillat, B. *Carbohydr. Res.* **1995**, 266, 211.
 31. Latgé, P.; Rico, I.; Lattes, A.; Godefroy, L. *FR* 2,661,413, **1991**; *Chem. Abstr.* **1992**, 116, 194795v.
 32. Latgé, P.; Rico, I.; Garelli, R.; Lattes, A. *J. Disp. Sci. Technol.* **1991**, 12, 227.
 33. Garelli-Calvet, R.; Latgé, P.; Rico, I.; Lattes, A.; Puget, A. *Biochim. Biophys. Acta* **1992**, 1109, 55.
 34. van Bekkum, H.; Lammers, H. In *Sugar Technology*; van der Poel, P.W.; Rich, J.E.A.; Schiweck, H., Eds.; in press
 35. Nakajima, Y.; *Proc. Res. Soc. Japan Refineries Technol.* **1984**, 33, 55.
 36. Kaga, T.; Mitzutani, T.; *Proc. Res. Soc. Japan Refineries Technol.* **1985**, 34, 45.
 37. Klein, J.; Behrens, W.; Kunz, M. *EP* 255,033, **1987**; *Chem. Abstr.* **1989**, 110,95711j.
 38. Buchholz, K.; Stoppok, E.; Matalla, K.; Reh, K.-D.; Jördening, H.-J. In *Carbohydrates as Organic Raw Materials*; Lichtenthaler, F.W., Ed.; VCH Verlag: Weinheim, **1991**, 155.
 39. Kunz, M. *Zuckerind.* **1988**, 113, 273.
 40. Christiansen-Brams, I.; Meldal, M.; Bock, K. *J. Carbohydr. Chem.* **1992**, 11, 813.
 41. Berth, P.; Krings, P.; Verbeek, H. *Tenside Surf. Det.* **1985**, 22, 169.
 42. Koch, H.; Beck, R.; Röper, H. *Starch* **1993**, 1, 2.
 43. Floor, M.; PhD Thesis, Delft, **1989**.
 44. Besemer, A.C.; PhD Thesis, Delft, **1993**.
 45. Klein, J.; Kunz, M.; Kowalczyk, J. *Makromol. Chem.* **1990**, 191, 517.
 46. van Doren, H.; van der Geest, R.; de Ruijter, C.F.; Kellogg, R.M.; Wynberg, H. *Liq. Crystals* **1990**, 8, 109.
 47. Ellis, J.W.; Malehorn, S.H.; Browning, L.M.; Heischmidt, T.A. *J. Carbohydr. Chem.* **1992**, 11, 761.
 48. Angyal, S.J. *Adv. Carbohydr. Chem. Biochem.* **1989**, 47, 1.

49. Geraldes, C.F.C.G.; Castro, M.M.C.A. *Metal Speciation in the Environment*, Vol. G 23; NATO ASI Series; Springer-Verlag: Berlin 1990, 105.
50. Mehlretter, C.L.; Alexander, B.H.; Rist, C.E. *Ind. Eng. Chem.* **1953**, 45, 2782.
51. Prescott, F.J.; Shaw, J.K.; Bilello, J.P.; Cragwall, G.O. *Ind. Eng. Chem.* **1953**, 45, 338.
52. van Duin, M.; Peters, J.A.; Kieboom, A.P.G.; van Bekkum, H. *J. Chem. Soc., Perkin Trans 2* **1987**, 473.
53. van Duin, M.; Peters, J.A.; Kieboom, A.P.G.; van Bekkum, H. *Carbohydr. Res.* **1987**, 162, 65.
54. van Duin, M.; Peters, J.A.; Kieboom, A.P.G.; van Bekkum, H. *J. Chem. Soc., Dalton Trans.* 1987, 2051.
55. Muzzarelli, R.A.A.; Jeuniaux, C.; Gooday, G.W. *Proc. Int. Conf. Chitin-Chitosan 1986*; *Chem. Abstr.* **1986**, 107, 40236r.
56. Muzzarelli, R.A.A.; Tanfani, F.; Emanuelli, M.; Mariotti, S. *Carbohydr. Res.* **1982**, 27, 532.
57. Muzzarelli, R.A.A.; Raithand, G.; Tubertini, O. *J. Chrom.* **1970**, 47, 414.
58. Hirano, S.; Kondo, Y.; Nakazawa, Y. *Carbohydr. Res.* **1982**, 100, 431.
59. Marchetti, P.S.; Bank, S.; Bell, T.W.; Kennedy, M.A.; Ellis P.D. *J. Am. Chem. Soc.* **1989**, 111, 2063.
60. Good, M.; Hollenstein, R.; Sadler, P.J.; Vašák, M. *Biochemistry* **1988**, 27, 7163.
61. Summers, M.F.; van Rijn, J.; Reedijk, J.; Marzilli, L.G. *J. Am. Chem. Soc.* **1986**, 108, 4254.
62. Rivera, E.; Kennedy, M.A.; Adams, R.D.; Ellis, P.D. *J. Am. Chem. Soc.* **1990**, 112, 1400.
63. Lauffer, R.B. *Chem. Rev.* **1987**, 87, 901.
64. Lammers, H.; Peters, J.A.; van Bekkum, H. *Tetrahedron* **1994**, 50, 8103.
65. van Haveren, J.; Lammers, H.; Peters, J.A.; Batelaan, J.G.; van Bekkum, H. *Carbohydr. Res.* **1993**, 243, 259.
66. Lammers, H.; van Bekkum, H.; Peters, J.A.; *submitted to Carbohydr. Res.*
67. Huskens, J.; Lammers, H.; van Bekkum, H.; Peters, J.A. *Magn. Reson. Chem.* **1994**, 32, 691.
68. Lammers, H.; Maton, F.; Pubanz, D.; van Laren, M.W.; van Bekkum, H.; Merbach, A.E.; Muller, R.N.; Peters, J.A. *to be submitted to Inorg. Chem.*
69. Lammers, H.; van der Heijden, A.M.; Peters, J.A.; van Bekkum, H. *to be submitted to Inorg. Chem.*

Chapter 2

MAGNETIC RESONANCE IMAGING: GENERAL INFORMATION

INTRODUCTION

In 1973, Lauterbur added an entirely new aspect to the already vast array of emerging NMR methodologies, namely that of image formation based on NMR principles. It was possible to produce a "nuclei density" image of an object by spatially encoding the signal.¹ This achievement has led to the highly successful development of NMR imaging (or MRI) to a useful technique in clinical medicine.²⁻⁴ In comparison with X-ray and radioisotope methods, MRI makes use of energy at the other end of the electromagnetic spectrum; no permanent harmful side effects of MRI have as yet been reported. The energy involved in MRI is nine orders of magnitude lower than that of X-rays and radioisotope techniques. After Lauterbur's discovery, it took only eight years for the first whole-body MRI machines to be used for clinical applications. These machines were, however, crude prototypes in comparison with the equipment of today.⁵ In 1982, there were around a dozen research groups working with whole-body imagers. Today, approximately 6,000 machines are operational worldwide, most of them in the United States and Japan. By the end of the century, it is predicted that there will be at least one machine per 100,000 inhabitants in the United States, Japan and the EC.⁵

At present, MRI influences decisions in most areas of medicine; neurology; orthopedics;

pediatrics and radiation therapy. Owing to high soft-tissue contrast, lack of adverse side effects, 3-D capabilities and high patient acceptance, MRI is more versatile than radiology.

The development of a new class of pharmacological products called contrast agents started approximately 10 years ago in order to evolve MRI as a non-invasive diagnostic tool. Administration to patients is designed to either enhance the contrast between normal and diseased tissue (brain, gastrointestinal tract) or to indicate the status of organ function or blood flow. The early development of these contrast agents is reviewed extensively by Lauffer⁶ and Goldstein.⁷ The contrast enhancement agents used in MRI and X-ray computed tomography (CT; tomography is slice photography) operate by entirely different mechanisms. X-ray CT agents function directly by their ability to scatter or absorb X-ray photons. The observed X-ray attenuation is the weighted average of native tissue attenuation plus attenuation caused by the contrast agent. MRI contrast agents on the other hand function indirectly by altering the local magnetic environment of tissue. The physics distinguishing the various diagnostic modalities (nuclear medicine, X-ray, MRI) dictates that fundamentally different materials as contrast media need to be used. The properties of these classes of agents are summarized in Table 1.⁸

Table 1. Comparison of basic chemical and biologic properties of pharmaceuticals for diagnostic imaging.⁸

| Property | MRI | X-ray/CT | Radiopharmaceuticals |
|---------------------------------|------------------------|--------------------------|-------------------------------------|
| active component | paramagnetic metal ion | iodine/BaSO ₄ | gamma ray-emitting isotope |
| molecular weight ^{a,b} | < 1000 | < 2000 | < 1000 |
| water solubility | high | high | variable |
| in vivo stability | high | high | high |
| in vivo metabolism | no | no | yes/no |
| dosage ^c | 0.05-10 | 50-150 | 10 ⁻⁹ -10 ⁻¹¹ |
| biodistribution | extracellular | extracellular | extra/intracellular |

^a in Daltons; ^b blood-pool contrast agent not included; ^c in g/kg active component

PRINCIPLES OF CONTRAST ENHANCEMENT

The search for contrast agents has been focused on paramagnetic substances which reduce the relaxation times of protons. Bloch first described the use of a paramagnetic salt, ferric nitrate, to enhance the relaxation rates of water protons.⁹ The standard theory describing solvent nuclear relaxation rates in the presence of dissolved paramagnetic substances was developed by Bloembergen and Solomon.¹⁰⁻¹⁴ Lauterbur and his co-workers demonstrated the feasibility of paramagnetic agents for the purpose of tissue discrimination by making use of differential water proton relaxation times.¹⁵ In their experiments, a salt of manganese(II), a cation known to localize in normal myocardial tissue in preference to infarcted regions, was injected into dogs with occluded coronary arteries. The proton relaxation rates of tissue samples was correlated with Mn(II) concentration and thus normal myocardium could be distinguished from the infarcted zone by relaxation behaviour alone. The first human MRI study involving a paramagnetic agent was performed by Young et al., the orally-administered ferric chloride was used to enhance the gastrointestinal tract.¹⁶

MRI relies on detecting the spatially localized NMR signals of water protons. Water is the most abundant substance in the human body (approximately 75 percent) and, therefore, the most sensitive resonance to detect *in vivo*. The spatial information is obtained by inducing the water frequency to become position-dependent. This is achieved by imposing a gradient magnetic field in contrast to the static field that is used in high-resolution NMR spectrometers. Water protons in the tissue sample resonate at slightly different frequencies according to their position in the gradient field, resulting in a spatially encoded signal that can be decoded computationally to provide a digitised image. The image intensity in proton NMR depends on longitudinal and transverse relaxation times, T_1 and T_2 respectively, and on the type of pulse sequences applied. The largest effect arises from the reduction of T_1 , which enhances the MRI signal by allowing the magnetic field vector to return to equilibrium between the rapid frequency pulses used in MRI and this reduces imaging times significantly.

The high electron spin ($S = 7/2$) and slow electronic relaxation of gadolinium(III), makes this element an especially attractive candidate as a MRI contrast agent. The general strategy that has been adopted, is to encapsulate the highly toxic Gd(III) ion with an

organic ligand so as to form complexes of relatively low toxicity.

GENERAL REQUIREMENTS FOR CONTRAST AGENTS

NMR imaging contrast agents must be biocompatible pharmaceuticals. Apart from standard pharmaceutical features such as water solubility and shelf-life stability, the requirements relevant to metal complex-based agents can be classified into three main general categories.

Relaxivity

The efficiency with which the complex enhances the proton relaxation rates of water, is referred to as the relaxivity. It must be sufficiently large as to significantly increase the relaxation rates of target tissue. The appropriate dosage of the Gd(III)-complex which results in changes in tissue relaxation rates must be non-toxic. The solvent relaxation rates are influenced linearly by the concentration of the paramagnetic species and relaxivity may be defined in terms of this dependence in units of $M^{-1}s^{-1}$ or, more commonly $mM^{-1}s^{-1}$.

Specificity

Contrast agents should ideally have the ability to concentrate in specific tissues. This can be accomplished in two ways: firstly, the agents accumulate in the neighbourhood of the target tissues (concentration differences) or secondly the relaxivity of the agents is higher when present in target tissue. The first approach is rather difficult to implement and can hardly be influenced by different administration of the drug. Locations where the drug accumulates depend mainly on the hydrophobic/hydrophilic character of the drug. Hydrophilic compounds will be filtered out relatively fast by the kidneys. Compounds more hydrophobic in nature, will be removed via the so-called hepatobiliary excretion pathway (via the liver). Compounds which are very lipophilic may however be accumulated in fat tissues or membranes and this may lead to chronic toxicity. In addition, residual contrast agent in the blood may accumulate in the liver or spleen cells. The specificity caused by local concentration differences can successfully be used in e.g.

brain scans. The brain capillaries are impermeable to contrast agents (the so-called "blood-brain barrier"), while the capillaries of tumors tolerate the passage of contrast agents which leads to selective enhancement.

The second option accomplishing preferential enhancement, by means of higher relaxivities of contrast agents when present in the target tissues, is to chemically link the contrast agent with the target tissue and thus alter the relaxivity with respect to the non-target tissue.

A third approach to improve tissue targeting is the use of paramagnetically labelled monoclonal antibodies.¹⁷

In-vivo stability, excretability and non-toxicity

The acute and chronic toxicity of an intravenously administered metal complex is related to its in vivo stability and tissue clearance behaviour (the removal of the drug from target tissue). The Gd(III) cation (and several other paramagnetic transition-metal ions), as already stated above, are toxic at the doses required for NMR relaxation rate changes. Thus the dissociation of the complex should not occur to any significant degree. An additional requirement is that the diagnostic agent must be excreted within hours of administration.

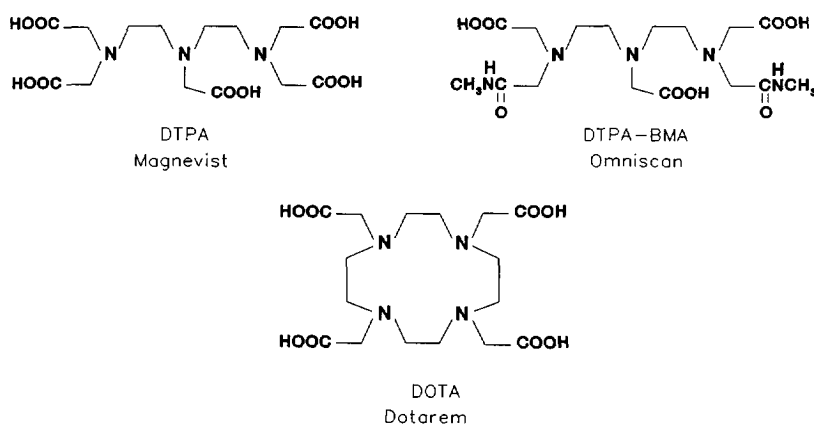


Figure 1. The ligand structures and commercial names of contrast agents currently in use.

Three contrast agents, with Gd(III) as the paramagnetic centre, are commercially available.¹⁸ These involve the organic ligands diethylenetriaminepentaacetic acid (DTPA, Magnevist), 1,4,7,10-tetraazacyclododecanetetraacetic acid (DOTA, Dotarem) and diethylenetriaminepentaacetic acid-bis(methylamide) (DTPA-BMA, Omniscan), as depicted in Figure 1. In Figure 2 an (MR) image of a brain before and after administration of contrast agent is presented.⁵

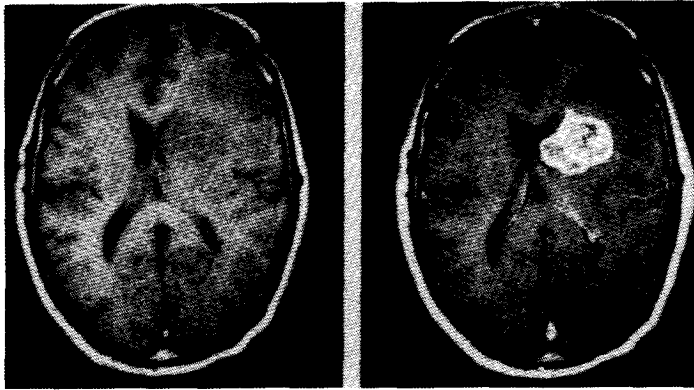


Figure 2. The MR image of a brain before (left) and after (right) administration of $Gd(DTPA)^{2-}$; after administration the malignant tumor becomes evidently visible.

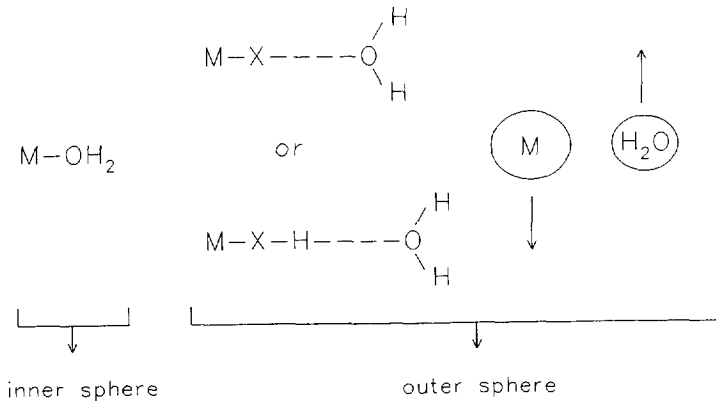


Figure 3. The schematic representation of the inner and outer sphere relaxation processes induced by the metal centre (M) or the ligands (X and $X-H$).

PRINCIPLES OF RELAXIVITY

When situated round a paramagnetic ion, the bulk water proton relaxation rates are enhanced both due to long-range interactions ("outer sphere" relaxation) and short-range interactions ("inner sphere" relaxation). In Figure 3, the difference between the two types of interactions is illustrated. The inner sphere contribution to the relaxivity is described in the Solomon-Bloembergen-Morgan theory.^{10-14,19} The mathematical equations designating this theory are given in Appendix I.

The magnetic field dependence of proton relaxivity, the so-called nuclear magnetic relaxation dispersion (NMRD) profile, is being widely used to develop an understanding of the function of Gd(III) complexes as MRI contrast agents.²⁰ In order to interpret these profiles correctly, it is desirable to investigate the physicochemical properties determining the relaxation process by independent measurements. In the next section several parameters influencing these physicochemical properties will be discussed briefly.

The water exchange rate, τ_m

The strongest relaxivity effect of water molecules is in the inner coordination sphere of the complex. This effect is transmitted to bulk water molecules by rapid water exchange as illustrated in Figure 4. The inner sphere contribution to the relaxivity ($1/T_{is}$) experienced by the bulk water is given by:

$$\frac{1}{T_{is}} = \frac{[Gd(III)]q}{55.6} \left(\frac{1}{T_{1m} + \tau_m} \right)$$

where q is the number of inner sphere water molecules and T_{1m} the longitudinal proton relaxation of the bound water molecule. The commercialized contrast agents (Gd(DTPA)²⁻, Gd(DOTA)⁻ and Gd(DTPA-BMA), Figure 1) contain one inner sphere water molecule in the first coordination sphere of the Gd(III) ion. In the early days of MRI contrast agent design, a fundamental trade-off existed between relaxivity on the one hand and stability and toxicity on the other hand. Chelation of a metal ion with a multidentate ligand, though resulting in a stable and non-toxic complex, causes an enormous drop in

relaxivity. This decrease may be ascribed to the loss of coordinated water molecules in the Gd(III) complexes. The higher doses of such a chelate which are necessary in order to alter tissue relaxation rates, partially offset the decrease in toxicity. At present, the paramount importance of safety in diagnostic examinations makes this "trade-off" redundant: paramagnetic contrast agents must be safe at their effective dosage. Also, in order to prevent chronic effects, they must not dissociate *in vivo* to any appreciable degree. Targeting and *in vivo* stability requirements conclusively overrule those of relaxivity.

The efficiency of transfer of the relaxivity is reduced when the exchange rate, k_{ex} , is slower than the proton relaxation rate in the inner sphere, $1/T_{1m}$ ($\tau_m > T_{1m}$).

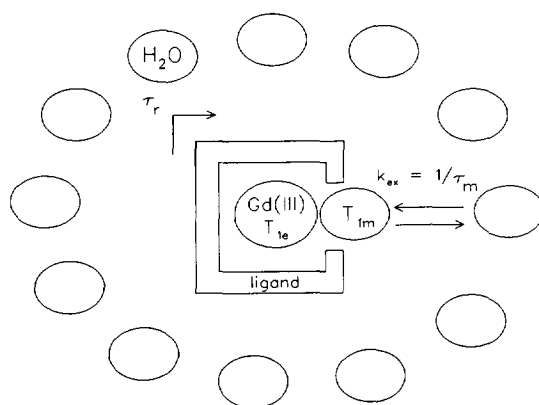


Figure 4. Detailed view of the inner sphere contribution to the relaxivity.

Water exchange is also an important factor because the dipole-dipole interaction diminishes when a water molecule leaves the inner sphere. The dipole-dipole relaxation rate, which largely dominates the longitudinal proton relaxation (T_{1m}), depends on the overall correlation time, τ_c , which is composed of (Appendix I):

$$\frac{1}{\tau_c} = \frac{1}{T_{1e}} + \frac{1}{\tau_m} + \frac{1}{\tau_r}$$

where τ_r is the rotational correlation time of the entire complex and T_{1e} the longitudinal

electron spin relaxation time of the paramagnetic species. In general, longer τ_c values lead to larger inner sphere relaxivity. Therefore an ideal water exchange rate would lie in the following range:

$$\frac{1}{T_{1m}} < k_{ex} < \frac{1}{\tau_r}, \frac{1}{T_{1e}}$$

The water exchange should be sufficiently fast to allow for efficient transfer of the inner sphere relaxivity to the bulk water, but not so fast as to shorten the correlation times for the dipole-dipole interactions. The optimal value normally falls in the range $10^6 - 10^9 \text{ s}^{-1}$. The close proximity of the oxygen atoms of the inner sphere water molecules with the Gd(III) ion results in stronger scalar (contact) as well as dipole-dipole (through space) interactions between the electron spins of Gd(III) and the nuclear spins of the oxygen atoms. The current understanding of water exchange in metal chelates has stemmed largely from the ^{17}O NMR technique for estimating τ_m developed by Swift and Connick.²¹ The water exchange rate is the upper limit for the proton exchange rate. The mechanism of the water exchange of the inner sphere water molecule can be determined using variable pressure ^{17}O NMR spectroscopy at high magnetic fields as described by Merbach et al.²²⁻²⁴ It has been demonstrated that the water exchange in current commercial contrast agents is 200 to 2000 times slower than in the Gd(III) aquo ion (Table 2). It has also been shown that the water exchange in the Gd(III) aquo ion takes place via an associative pathway (positive sign of the activation volume, ΔV^\ddagger), and via a dissociative pathway in the Gd(III) monoaqua poly(amino carboxylate) complexes (cf Chapter 8 of this thesis). Without the assistance of the incoming water molecule in breaking bonds, the exchange requires a higher enthalpy of activation and therefore deceleration takes place. This change in mechanism may be understood in terms of a change of coordination number from eight for the Gd(III) aquo ion to nine for the poly(amino carboxylate) complexes (the multidentate ligand occupies eight sites and the inner sphere water molecule the ninth). The limiting effect of the slow water exchange on their proton relaxivity, and hence their efficacy, for the commercially produced contrast agents (Figure 1) is marginal.

Table 2. Water exchange rates and activation volumes for different Gd(III) complexes.²²⁻²⁴

| Complex | k_{ex}^{298} (s ⁻¹) | ΔV_0^\ddagger (cm ³ mol ⁻¹) |
|--|--|--|
| [Gd(H ₂ O) ₉] ³⁺ | $(8.30 \pm 0.9) \times 10^8$ | -3.3 ± 0.2 |
| [Gd(DTPA)(H ₂ O)] ²⁻ | $(4.10 \pm 0.3) \times 10^6$ | +12.5 ± 0.2 |
| [Gd(DOTA)(H ₂ O)] ⁻ | $(4.8 \pm 0.4) \times 10^6$ | +10.5 ± 0.2 |
| [Gd(DTPA-BMA)(H ₂ O)] | $(4.3 \pm 0.2) \times 10^5$ | +7.3 ± 0.2 |

The rotational correlation time, τ_r

In general, the higher the τ_r of a chelate (the slower its molecular tumbling), the higher its relaxivity potential. A stage is reached at a certain value of τ_r where upon further increase of this parameter does not result in additional benefits to the relaxivity. Three basic strategies exist to reduce the rotational mobility of metal complexes in vivo: (1) Distribution of the agent into a tissue or tissue compartment with high microviscosity; (2) Covalent attachment of the complex to a larger molecule such as a protein; (3) Noncovalent binding of the complex in tissue or macromolecules.

The electronic spin relaxation time, T_{1e}

The choice of Gd(III) as an optimal relaxation agent is because of its long T_{1e} and large magnetic moment. Gd(III) has a stable, half-filled *f*-shell and the pathway for electronic relaxation is rather inefficient compared to other electronic configurations.²⁵ In general, increasing T_{1e} results in higher relaxivities, however, limited by the τ_m or τ_r value. No comprehensive theory for electron spin relaxation of metals ions in solution has been developed. The Solomon-Bloembergen equations adequately describe the magnetic field dependence of the longitudinal and transverse relaxivities in simple aquo ion solutions such as those of Mn(II). Bloembergen and Morgan developed a theory for the field dependence of T_{1e} . For $S > 1/2$ ions, collisions between the complex and solvent molecules (or "wagging" motions of the primary coordination sphere water molecules²⁶) are thought to induce distortions in the octahedral symmetry that in turn, lead to transient zero-field splitting (ZFS) of the electronic spin levels. Electronic relaxation occurs as a result of this ZFS modulation in which τ_v is the correlation time characterizing these fluctuations (for the relevant equation, see Appendix I). The exact nature of τ_v , i.e., what

it is physically defined by, is unknown for the case of metal chelates. The need for long T_{1e} values therefore translates into a desire to minimize ZFS in metal complexes. It may be possible to tune this parameter by changing ligand field strength and complex symmetry.

FUTURE TRENDS

Magnetic resonance angiography (MRA) has recently become a very powerful technique competing successfully with conventional X-ray angiography. MRA produces images of the bulk or macroscopic flow of blood in vessels. Considering that cardiovascular diseases are worldwide the main cause of death (50%), the development of diagnostic technologies for vascular and cardiovascular diseases which are reliable, safe, rapid and inexpensive is of the utmost importance. In contrast to X-ray angiography, MRA does not require the use of contrast agents, rather the blood itself is used as an intrinsic contrast agent. However there are general problems with all the MRA techniques which are difficult to overcome. Such problems include flow voids or regions of low signal intensity where turbulent flow prevails and there are difficulties in depicting smaller vessels. These pitfalls could be overcome if suitable angiographic contrast agents could be designed. The only agents available for intravascular use, are the low molecular weight (small molecular volume) commercialized contrast agents as depicted in Figure 1. Their distribution through the vascular system is hampered by extravasation (dispersion) into most tissues with the exception of those areas possessing specialised vascular barriers, such as the brain. These agents therefore enhance not only the blood vessels but also the perivascular space which limits the required angiographic contrast.

As a consequence, attention has been focused on the design of specific blood pool agents possessing improved contrast-to-noise ratio and enhance vascular structures without being influenced by turbulent flow. If MRA is to overcome such problems it needs powerful contrast agents, which should be able to attain proton relaxivities greater than $100 \text{ s}^{-1} \text{ mmol}^{-1}$ in comparison with values of 3 to $4 \text{ s}^{-1} \text{ mmol}^{-1}$ currently found in commercial Gd(III) contrast agents. The attention will be focussed on compounds with high molecular weights (large molecular volume) in order to develop contrast media which will remain in

the blood pool. Due to the increase of the molecular weight the rotational correlation time, τ_r , will increase (slower molecular tumbling) resulting in an enlargement of the inner sphere relaxivity. Higher water exchange rates than those observed for the present commercial agents are necessary if this increase in inner sphere proton relaxivity is to be translated into relaxivity of the surrounding water. It is therefore important to understand the factors influencing the water exchange rates in lanthanide(III) poly(amino carboxylate) complexes as an initial step towards synthesizing effective blood pool agents in the future. Several oligo- and polymeric Gd(III) complexes have been proposed as contrast agents for MRA. The chelating units for the Gd(III) ion should meet the general requirements that hold for low-molecular weight contrast agents, such as a high thermodynamic and kinetic stability. Most of the compounds under scrutiny for potential use as blood pool agents contain DTPA as the chelating unit.

For example, the polysaccharide dextran can be functionalized with DTPA units according to several well documented synthetic routes.²⁷ In this way the size is increased to above an average molecular weight of 9400 g/mol. This type of sugar-based contrast agent exhibited an increase of the vascular retention, however, lower proton relaxivities than expected were found. The presence of sugar moieties near to the Gd(III) ion may influence the various parameters governing the relaxivity. Therefore the water exchange kinetics of the Gd(III) complexes of several sugar-based DTPA-bis(amides) (Figure 5), useful as model compounds for the polysaccharides, have been investigated (see Chapter 8 in this thesis).²⁸ It is shown that the water exchange rates, k_{ex} , and the corresponding activation parameters of these compounds are similar to those found for Gd(DTPA-BMA). Further examples of potential contrast agents for MRA are the dendrimer Gd(III) polychelates.²⁹ Various StarburstTM products, a type of cascade polymer, are already commercially available. The dendrimers have near-spherical shapes and the synthetic routes used provide for unique control of critical molecular design parameters such as size, shape and interior flexibility. These compounds possess a large number of surface amino groups, which are good anchoring groups for the DTPA moiety. The corresponding Gd(III) complexes have enhancement factors, i.e., the ratio of the relaxivity per Gd(III) ion to that of Gd(DTPA)²⁻, of as much as ten. It has been suggested that this new and powerful class of contrast agents is very likely to play an important role as MRA contrast agents in the future.

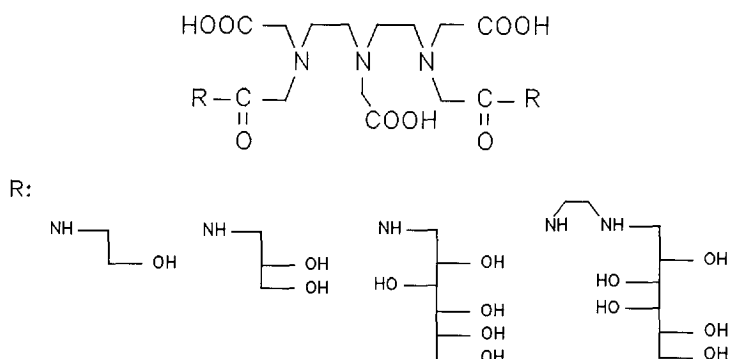


Figure 5. The structures of several sugar-based DTPA-bis(amides).

MARKET PROSPECTS

The largest market for diagnostic imaging contrast agents is in the United States and is undergoing major changes since recent acquisitions have given European companies (Nycomed/Salutar, Bracco/Squibb Diagnostics, Schering and Mallinckrodt/Guerbet) market control. Currently, 25-30% of MRI procedures worldwide are contrast-enhanced and this is expected to increase to more than 50% by the year 2000. According to US industry analysts, MRI procedures are running at near full capacity, as has been the case since 1991. Therefore future growth in the number of procedures will be to a large extent linked to reduced scanning times and extended applications, both of which are possible with new imaging agents presently under development. The forecast predicts that the MRI contrast agent market will grow worldwide from 0.5 billion US dollars in 1993 to 1.5 billion US dollars in the year 2000.¹⁸

REFERENCES

1. Lauterbur, P.C. *Nature* **1973**, *242*, 190.

2. Hinshaw, W.S.; Bottomley, P.A.; Holland, G.N. *Nature (London)* **1977**, *270*, 722.
3. Andrew, E.R.; Bottomley, P.A.; Hinshaw, W.S.; *Phys. Med. Biol.* **1977**, *22*, 971.
4. Damadian, R.; Goldsmith, M.; Minkoff, L. *Physiol. Chem. Phys.* **1977**, *9*, 97.
5. Rinck, P.A., Ed. *Magnetic Resonance in Medicine*, 3rd ed.; Blackwell Scientific Publications: Oxford, 1993.
6. Lauffer, R.B. *Chem. Rev.* **1987**, *87*, 901.
7. Goldstein, H.; Lumma, W.; Rudzik, *Ann. Rep. Med. Chem.* **1989**, *24*, 265.
8. Rocklage, S.M.; Watson, A.D.; Carvlin, M.J. In *Magnetic Resonance Imaging*, 2nd ed.; Stark, D.D.; Bradley, W.G., Eds.; Mosby: St. Louis, 1992, Chapter 14.
9. Bloch, F.; Hansen, W.W.; Packard, M. *Phys. Rev.* **1948**, *70*, 474.
10. Bloembergen, N.; Purcell, E.M.; Pound, R.V. *Phys. Rev.* **1948**, *73*, 678.
11. Bloembergen, N. *J. Chem. Phys.* **1957**, *27*, 572.
12. Kubo, R.; Tomita, K. *J. Phys. Soc. Jpn.* **1954**, *9*, 888.
13. Solomon, I. *Phys. Rev.* **1955**, *99*, 559.
14. Eisinger, J.; Shulman, R.G.; Blumberg, W.E. *Nature* **1961**, *192*, 963.
15. Lauterbur, P.C.; Mendoca-Dias, M.H.; Rudin, A.M. In *Frontier of Biological Energetics*; Dutton, P.L.; Leigh, L.S.; Scarpa, A., Eds.; Academic: New York, 1978; p 752.
16. Young, I.R.; Clarke, G.J.; Gales, D.R. *Comput. Tomogr.* **1981**, *5*, 534.
17. Gansow, O.A.; Brechbiel, M.W.; Mirzadeh, S.; Colcher, D.; Roselli, M. *Cancer Treatment Research* **1990**, *51*, 153.
18. Halter, P. Technology Report in Medical Imaging International 1995.
19. Bloembergen, N.; Morgan, L.O. *J. Chem. Phys.* **1961**, *34*, 842.
20. Koenig, S.H.; Brown, R.D., III. *Prog. Nucl. Magn. Reson. Spectrosc.* **1990**, *22*, 487 and references therein.
21. Swift, T.J.; Connick, R.E. *J. Chem. Phys.* **1962**, *37*, 307.
22. Micskei, K.; Helm, L.; Brücher, E.; Merbach, A.E. *Inorg. Chem.* **1993**, *32*, 3844.
23. Micskei, K.; Powell, D.H.; Helm, L.; Brücher, E.; Merbach, A.E. *Magn. Reson. Chem.* **1993**, *31*, 1011.
24. González, G.; Powell, D.H.; Tissières, V.; Merbach, A.E. *J. Phys. Chem.* **1994**, *98*, 53.
25. La Mar, G.N.; Horrocks, W.D.; Holm, R.G., Eds. *NMR of Paramagnetic Molecules*; Academic: New York, 1973.
26. Friedman, H.L. In *Protons and Ions Involved in Fast Dynamics Phenomena*; Laszlo, P., Ed.; Elsevier: Amsterdam, 1978; pp 27-42.

27. Armitage, F.E.; Richardson, D.E.; Li, K.C.P. *Bioconjugate Chem.* **1990**, *1*, 365.
28. Lammers, H.; Maton, F.; Pubanz, D.; van Laren, M.W.; Merbach, A.E.; Muller, R.N.; Peters, J.A.; van Bekkum, H. *submitted to Inorg. Chem.*
29. Wiener, E.C.; Brechbiel, M.W.; Brothers, H.; Magin, R.L.; Gansow, O.A.; Tomalia, D.A.; Lauterbur, P.C. *Magn. Reson. Med.* **1994**, *31*, 1.

APPENDIX I

Inner sphere relaxation: Solomon-Bloembergen-Morgan equations

As already mentioned in the text the longitudinal relaxation contribution from the inner sphere results from a chemical exchange of the water molecule between the primary coordination sphere of the paramagnetic metal ion (Gd(III)) and the bulk solvent as given in eq 1. The value of the relaxation time of the bound water, T_{1m} , is the sum of dipolar ("through-space") and scalar, or contact ("through-bonds") contributions and is given by:

$$\frac{1}{T_{1m}} = \left(\frac{\mu_0}{4\pi}\right)^2 \frac{2}{15} \frac{\gamma_I^2 g^2 S(S+1)\beta^2}{r^6} \left[\frac{7\tau_c}{1 + \omega_S^2 \tau_c^2} + \frac{3\tau_c}{1 + \omega_I^2 \tau_c^2} \right] + \frac{2}{3} S(S+1) \left(\frac{A}{\hbar}\right)^2 \left[\frac{\tau_e}{1 + \omega_S^2 \tau_e^2} \right]$$

"dipolar-term"

"scalar-term"

where γ_I is the proton gyromagnetic ratio, g is the electron Landé factor, S is the total electron spin of the metal ion, β is the Bohr magneton, r is the proton-metal ion distance, ω_S and ω_I are the electronic and proton Larmor precession frequencies, respectively, and A/\hbar (rad s⁻¹) is the electron-nuclear hyperfine coupling constant. The dipolar and scalar relaxation mechanisms are modulated by the correlation τ_c and τ_e :

$$\frac{1}{\tau_c} = \frac{1}{T_{1e}} + \frac{1}{\tau_m} + \frac{1}{\tau_r}$$

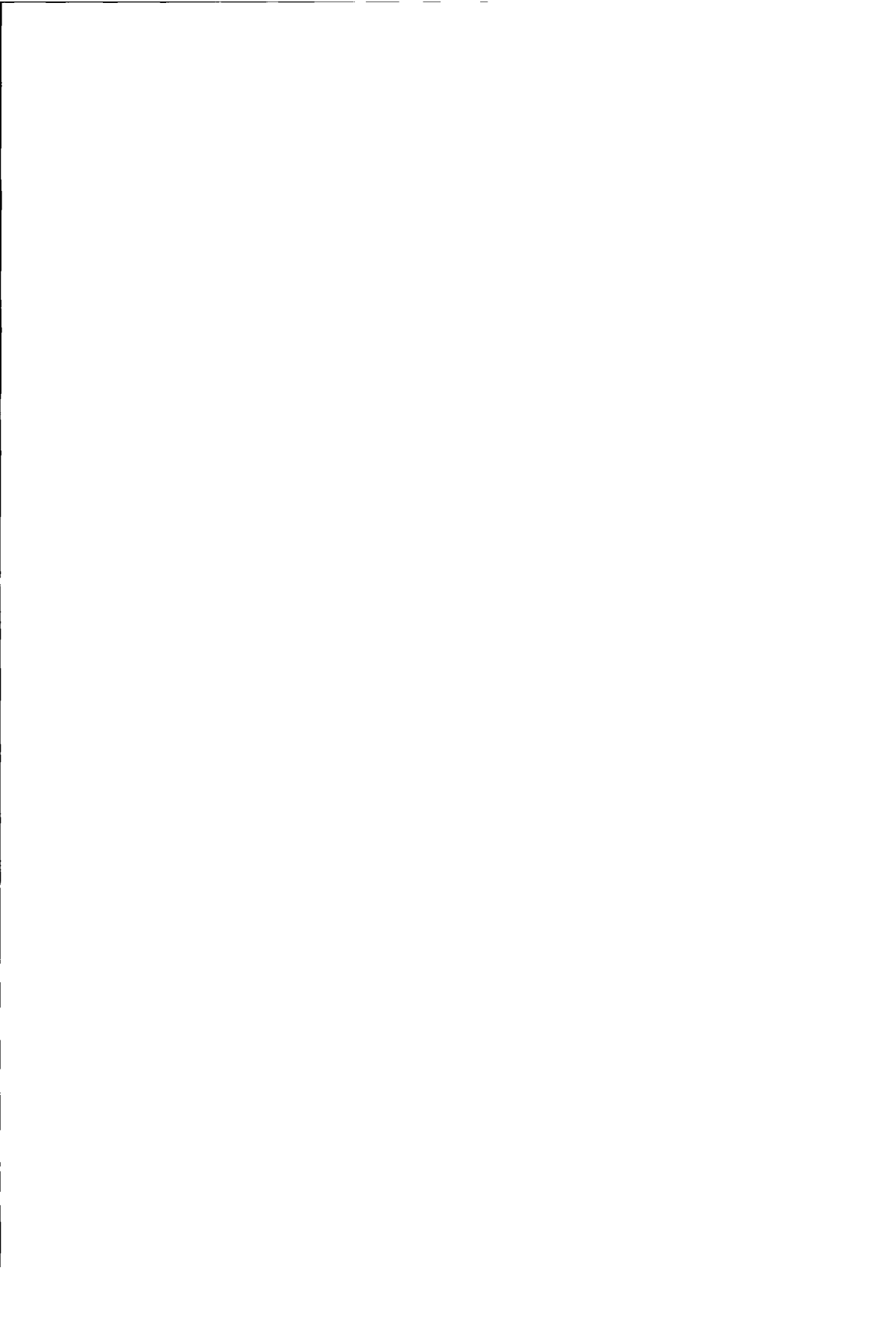
$$\frac{1}{\tau_e} = \frac{1}{T_{1e}} + \frac{1}{\tau_m}$$

T_{1e} is the longitudinal electron spin relaxation time, τ_m the bound water residence time, and τ_r is the rotational tumbling time of the entire metal-water unit.

The electronic relaxation occurs as a result of the already mentioned ZFS modulation and can be expressed as:

$$\frac{1}{T_{1e}} = B \left[\frac{\tau_v}{1 + \omega_s^2 \tau_v^2} + \frac{4\tau_v}{1 + 4\omega_s^2 \tau_v^2} \right]$$

where the constant B is related to the magnitude of the transient ZFS and τ_v is the correlation characterizing these fluctuations.



Chapter 3

REDUCTIVE AMINATION OF ALDOHEXOSES WITH MONO- AND BIFUNCTIONAL ALKYL AMINES: CONVERSION OF CARBOHYDRATES INTO EDTA TYPE COMPLEXING AGENTS*

ABSTRACT

It is shown by ^1H and ^{13}C NMR spectroscopy (1D and 2D) that β -N-propylgalactosylamine (5a) is the major species present in an equimolar aqueous solution of D-galactose (1a) and propylamine (PA). In equimolar solutions of aldohexoses (1a-c) and ethylenediamine (EN) or 1,3-diaminopropane (DAP) in addition to mono- (9) and diglycosylamines (12) tetrahydro-imidazole (8, n=1) and hexahydropyrimidine derivatives (8, n=2), respectively, are formed. Hydrogenation of equimolar solutions of aldohexoses (1a-c) and primary amines (PA, EN, and DAP) at 100 atm. and 50 °C, using 5% Pt on carbon as the catalyst, gave amino sugars 13-16 in good yields. Carboxymethylation of 14a-b resulted in sugar based EDTA type complexing agents (17a-b) with promising chelating abilities towards Cd(II) and Ca(II) at high pH.

* Lammers, H.; Peters, J.A.; van Bekkum, H. *Tetrahedron* **1994**, *50*, 8103.

INTRODUCTION

There are a variety of synthetic pathways leading towards 1-(alkyl)-amino-1-deoxyalditols,¹ of which catalytic reductive amination of reducing carbohydrates through the action of a (noble) metal catalyst is the most used one.²⁻⁹ A direct, commercially applied, route to 1-amino-1-deoxy-D-glucitol, is the reductive amination of D-glucose with ammonia using a fixed-bed Ni catalyst.¹⁰ The synthesis of 1-alkylamino-1-deoxy-D-glucitol has been described as a two-step process in which the first step is the formation of the N-alkylglycosylamine which is then hydrogenated in the second step in the presence of a Ni catalyst.¹¹ Catalytic reductive aminations of several disaccharides have also been reported. Isomaltamine, the equimolar mixture of D-glucopyranosyl- α (1,6)-2-amino-2-deoxy-D-mannitol and its D-glucitol (sorbitol) analogue, is obtained by reductive amination with ammonia or hydrazine of isomaltulose, an isomerization product of sucrose, using Raney Ni as the catalyst¹². 1-Amino-1-deoxyalditols derived from cellobiose, lactose and maltose were synthesized *via* reductive amination with benzylamine and subsequent catalytic removal of the benzyl group at atmospheric pressure.¹³ N-alkyllactamines are obtained by a similar two-step process as mentioned above using either Raney Ni or Pd (10%) on carbon as the catalyst. Higher yields, however, were obtained by reduction with NaBH₄.¹⁴

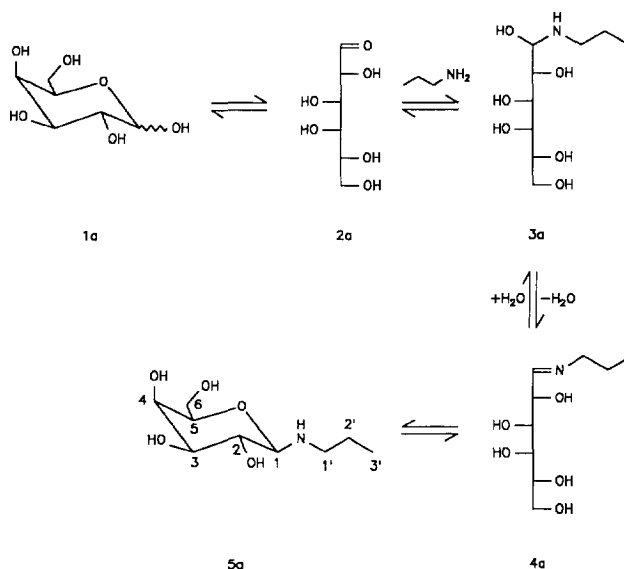
N-alkyl substituted amino sugar derivatives are readily biodegradable and do not cause any skin irritant effects and are therefore being studied as new components for detergents and cosmetics¹⁰. Further potential applications are as surfactants,¹⁵ polymers,¹⁶ sweeteners¹⁷ and as liquid crystalline compounds.¹⁸

In this paper we report the reductive amination of the aldohexoses D-galactose (1a), D-mannose (1b), and D-glucose (1c) with propylamine (PA), ethylenediamine (EN) and 1,3-diaminopropane (DAP) through the action of a Pt catalyst. The equilibria and species involved in these reactions are investigated with the aid of ¹H and ¹³C NMR. The amino sugars obtained by reductive amination with EN are converted into EDTA (ethylenediaminetetraacetic acid) type complexing agents by carboxymethylation. The Cd(II) and Ca(II) sequestering capacities of the newly synthesized ligands are given.

RESULTS AND DISCUSSION

Study of Aqueous Solutions Containing Aldohexoses and Primary Amines

Upon addition of an equimolar amount of PA to an aqueous solution of an aldohexose, a new set of signals appeared in the ^{13}C NMR spectrum next to the signals of the starting compounds. These signals have to be ascribed to an adduct of the amine and the aldohexose. Characteristically this new species has a signal at about 90 ppm and no signal for an imine function ($\delta = 150 - 170$ ppm). In order to elucidate its structure, the system D-galactose (1a)/ PA was studied in more detail. The possible equilibria involved are outlined in Scheme 1.



Scheme 1

The first step is a nucleophilic addition of the primary amine onto the acyclic form (2a) yielding the acyclic carbinolamine (3a). This latter species can be in equilibrium with the imine (4a) and/ or with the N-propylgalactosylamine (5a). As no imine is observed, the new species present in solution is either 3a or 5a. In a 0.5 M solution of D-galactose containing an excess of PA (5 eq., pH= 11.6) a nearly complete conversion of D-

reductive amination of aldohexoses with mono- and bifunctional alkyl amines

galactose into the new species took place. The ^{13}C and ^1H NMR parameters of this compound are summarized in Table 1.

Table 1. NMR Data of β -N-propylgalactosylamine (5a) in D_2O at pH 11.6 and 25 °C.^a

| Chemical shifts (ppm) | | | | | | | | | | | |
|-----------------------------|----------------|------|----------------------|------|------|------|------|--------------------|------|------------------|------|
| | 1 | 2 | 3 | 4 | 5 | 6a | 6b | 1'a | 1'b | 2' | 3' |
| $^{13}\text{C}^b$ | 91.6 | 72.1 | 75.3 | 70.6 | 77.4 | 62.7 | 62.7 | 48.5 | 48.5 | 23.8 | 12.6 |
| $^1\text{H}^c$ | 3.89 | 3.38 | 3.55 | 3.87 | 3.58 | 3.69 | 3.73 | 2.79 | 2.57 | 1.43 | 0.85 |
| H-H coupling constants (Hz) | | | | | | | | | | | |
| | $J(1,2) = 9.2$ | | $J(5,6a) = 7.6$ | | | | | $J(1'a,2'a) = 8.7$ | | $J(2',3') = 7.5$ | |
| | $J(2,3) = 9.8$ | | $J(5,6b) = 4.3$ | | | | | $J(1'a,2'b) = 6.6$ | | | |
| | $J(3,4) = 3.7$ | | $J(6a,6b) = -12.0$ | | | | | $J(1'b,2'a) = 6.1$ | | | |
| | $J(4,5) = 1.2$ | | $J(1'a,1'b) = -11.6$ | | | | | $J(1'b,2'b) = 8.5$ | | | |

^a obtained from a sample prepared from 0.5 M D-galactose (1a) and 2.5 M PA;^b 100.6 MHz;

^c 400 MHz

It is known that free alditols in water prefer a planar carbon chain except when this results in a 1,3 parallel arrangement of two C-O bonds.^{19,20} Therefore when carbinolamine 3a would be present in solution the coupling constants $^3J_{3,4}$ and $^3J_{4,5}$ would be about 2 and 10 Hz²¹, respectively, which is not in agreement with the observed values. Since the $^3J_{\text{H-H}}$ coupling constants of the carbohydrate moiety closely resemble those of D-galactose,²² it can be concluded that the compound formed is N-propyl-galactosylamine (5a). The large diaxial $\text{H}_1\text{-H}_2$ coupling constant ($^3J_{1,2} = 9.2$ Hz) shows that we are dealing with the β -anomer which strongly prefers the $^4\text{C}_1$ conformation.²³

Pure 5a could be obtained by reacting D-galactose (1a) with 1.1 eq. PA in a minimum amount of water²⁴. After 2h the N-propylgalactosylamine crystallized from the reaction mixture. Dissolution of pure 5a (0.55 M) resulted, after 1h, in a mixture with the same

composition as that obtained when D-galactose (1a) and PA (0.55 M) were mixed in equimolar amounts, demonstrating that the thermodynamic equilibrium was reached. When the pH of equimolar mixtures of aldohexoses and primary amines was lowered the molar concentration of the starting aldohexose and primary amine increased. At low pH (<6) a complete hydrolysis to the starting aldohexose and primary amine occurred.^{25,26} Since in the solutions studied only 1a, 5a and PA were observed, we suppose that the ring opening of these compounds is rate determining in the establishment of the equilibrium. The equilibrium is reached relatively slow starting from 5a. Therefore, the ring opening of 5a is probably slower than that of 1a, which is consistent with the molar ratio 5a/ 1a in the equilibrium (Table 2).

In equimolar solutions of aldohexoses and the bifunctional amines EN or DAP similar species were observed by ¹³C NMR, but in addition to that two other new compounds could be detected. One of them resembled that of the glycosylamines (Table 1). The relative intensities of the signals for this compound as a function of the molar ratio aldohexose/ amine suggested that it was the diglycosylamine. In the case of EN this was supported by characteristic signals at 46 and 90 ppm, for the ethylenediamine function and C1, respectively. Because of the S₂-symmetry of the diglycosylamine, the methylene groups of the ethylenediamine unit give one signal at 46 ppm. The ¹³C resonances in the carbohydrate region (60 - 80 ppm) of the diglycosylamine coincide with those of the monoglycosylamine. The diglycosylamines derived from aldohexoses and DAP similarly show characteristic resonances at 30 (β-CH₂), 44 (α-CH₂), and 90 ppm (C1). The ¹³C resonances in the carbohydrate region of the DAP derived diglycosylamines also coincide with those of the corresponding monoglycosylamines. Diglycosylamines derived from D-glucose and ammonia already have been described, but no spectral data have been reported up to now.²⁷ In an equimolar solution of D-galactose (1a) and DAP the other new species is the major component (Figure 1). The signals at 39.8 and 35.6 ppm are corresponding to DAP. The resonances with the highest intensities at 73.1, 72.9, 71.8, 71.0, 70.9, 64.8, 45.8, 45.7, and 27.0 ppm indicate the presence of a hexahydropyrimidine derivative (8a, n=2; Scheme 2). Due to the presence of the chiral carbohydrate moiety the α-methylene carbons are not equivalent resulting in two resonances (45.8 and 45.7 ppm), the signal for the β-methylene group of the heterocyclic ring is located at 27.0 ppm. The chemical shift of C6 (64.8 ppm) is characteristic for alditol derivatives.²² In solutions of

reductive amination of aldohexoses with mono- and bifunctional alkyl amines

aldohexoses and EN a similar species is observed, but in a much lower concentration. Consequently the signals were difficult to observe in this case, especially in the carbohydrate region signals do overlap. The C6 resonance at 64 ppm and the (coinciding) NCH₂CH₂N signals at 46 ppm, however, were easily observed.

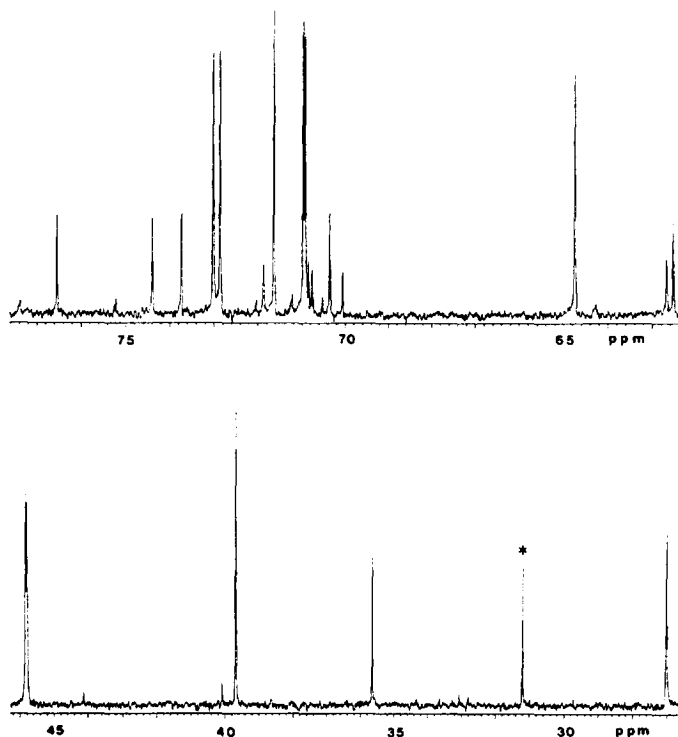


Figure 1. 100.6 MHz ¹³C NMR spectrum of 0.5 M D-galactose (1a) and 0.5 M DAP in D₂O at pH 11.7 and 25 °C. * internal standard (*t*-BuOH).

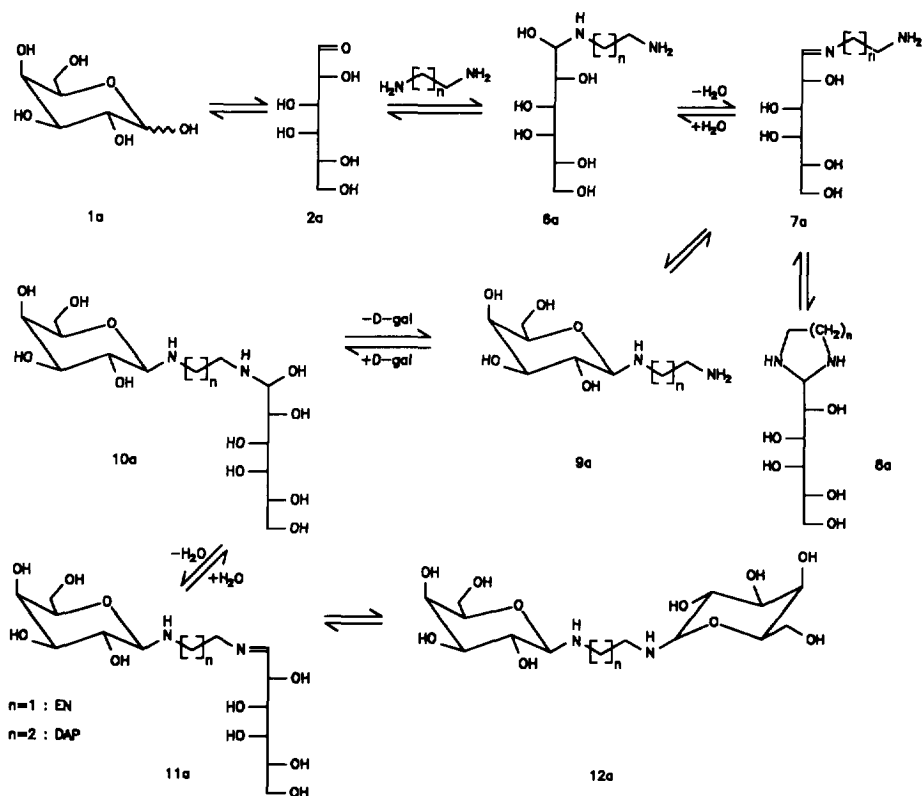
On the basis of the species identified, it can be concluded that, for example, the equilibria given in Scheme 2 occur in solutions of D-galactose (1a) and EN (n=1) or DAP (n=2). The imine 7a is formed after elimination of water from the carbinolamine 6a. Nucleophilic attack of the primary amino group on the imine C-atom results in the formation of 8a. The nucleophilic attack of the C5 hydroxyl group results in the

galactosylamine 9a, which is in equilibrium with the digalactosylamine 12a via intermediates 10a and 11a.

The equilibria of D-galactose (1a) or D-mannose (1b) with the primary amines PA, EN, and DAP are established relatively fast (0.5h) compared to those of D-glucose (1c) (7h) with these primary amines. At 50 °C the equilibria for D-glucose (1c) were reached in 1.5 h. A decrease of the N-glycosylamine concentration occurred after 2h due to non-enzymatic browning.²⁸ Also in solutions containing D-galactose (1a) or D-mannose (1b) and primary amines non-enzymatic browning occurred after 2h at 50 °C. The speciations in aqueous solutions of aldohexoses and mono- and bifunctional amines as determined at pH 11.6 by quantitative ¹³C NMR are summarized in Table 2. The results show that the hexahydropyrimidines (8a-c, n=2) are thermodynamically more stable than the tetrahydroimidazole derivatives (8a-c, n=1).

Table 2. Distribution of Aldohexoses and Derivatives in Equimolar Solutions of Aldohexoses and Amines (mol %) at pH 11.6 and at room temperature.

| aldohexose | amine | 1 | 5 | 8 | 9 | 12 |
|------------|-------|----|----|----|----|----|
| 1a | PA | 30 | 70 | | | |
| 1a | EN | 5 | | 10 | 60 | 25 |
| 1a | DAP | 10 | | 60 | 25 | 5 |
| 1b | PA | 25 | 75 | | | |
| 1b | EN | 10 | | 10 | 60 | 20 |
| 1b | DAP | 10 | | 55 | 25 | 10 |
| 1c | PA | 25 | 75 | | | |
| 1c | EN | 15 | | 5 | 60 | 20 |
| 1c | DAP | 10 | | 30 | 45 | 15 |



Scheme 2

Reductive Amination of Aldohexoses with Mono- and Bifunctional Amines

All reductive aminations were carried out at 50 °C in aqueous medium (0.55 M based on aldohexose) using 5% platinum supported on carbon as the catalyst using a hydrogen pressure of 100 atm. Similar reaction conditions were applied for the synthesis of dialditylamines via hydrogenation of the corresponding aldoximes.²⁹ Heating of the reaction mixture prior to hydrogenation must be carried out in the absence of catalyst in order to avoid dehydrogenation of the aldohexose towards the corresponding aldonic acid.³⁰ At temperatures above 50 °C non-enzymatic browning occurred during hydrogenation. From ¹³C NMR data of the hydrogenated products it can be concluded that during the reductive amination there is retention of configuration of the polyhydroxy

chain. The reductive amination of a 0.55 M D-galactose (1a) solution with 1 mol equivalent PA was monitored by quantitative ^{13}C NMR using dioxane as the internal standard (Figure 2). The hydrogenation, was started immediately after mixing D-galactose and PA, and was completed within 2 h. Under the reaction conditions applied a considerable amount of D-galactitol is obtained (15 mol %) as a result of the direct hydrogenation of D-galactose. The molar ratio of 13a/ alditol in the final product is higher than that of 5a/ 1a at $t = 0$, and the hydrogenation rate of 5a is higher than that of 1a. Apparently conversion of 1a into 5a (Scheme 1) is relatively fast with respect to the hydrogenation rates.

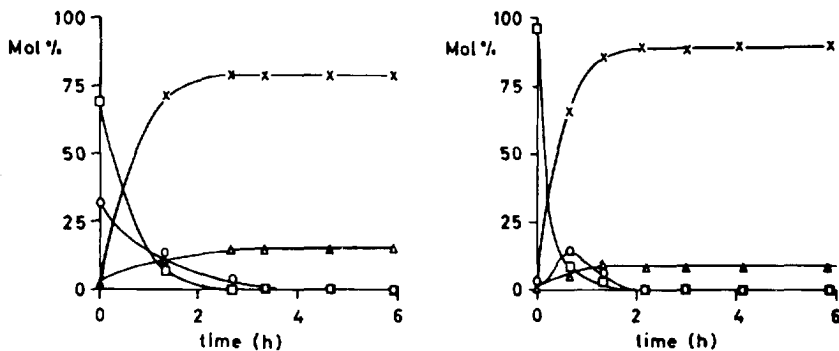


Figure 2. Product distribution of the hydrogenation of an equimolar mixture (0.55 M) D-galactose (1a) and propylamine (left) and of a 0.55 M solution N-propylgalactosylamine (5) (right); (\square) N-propylgalactosylamine (5); (\circ) D-galactose (1a); (\times) 1-Deoxy-1-(propylamino)-D-galactitol (13a); (\triangle) D-galactitol).

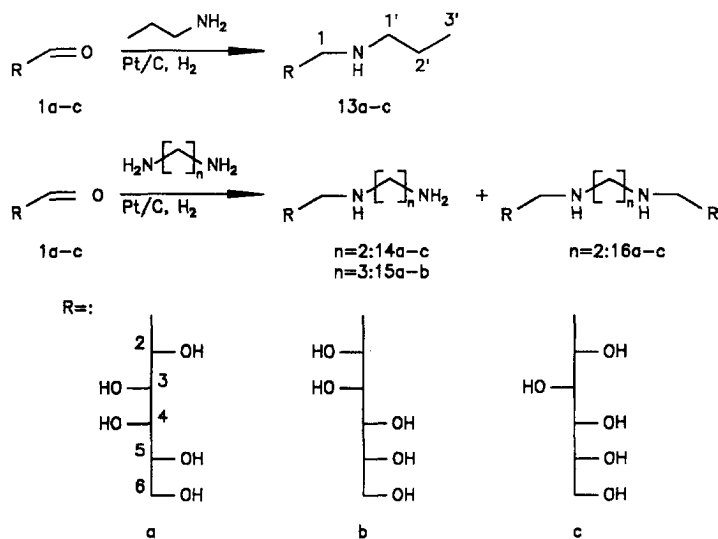
The non-enzymatic browning, as mentioned earlier, is observable after 2 h at 50 °C. At higher reaction temperatures considerable browning was observed, which was expected since it is known that the rate of non-enzymatic browning has an exponential dependence on the temperature.²⁸

The hydrogenation of a 0.55 M solution of 5a in water was also followed by quantitative ^{13}C NMR (Figure 2). During hydrogenation the concentration of 1a initially increases due

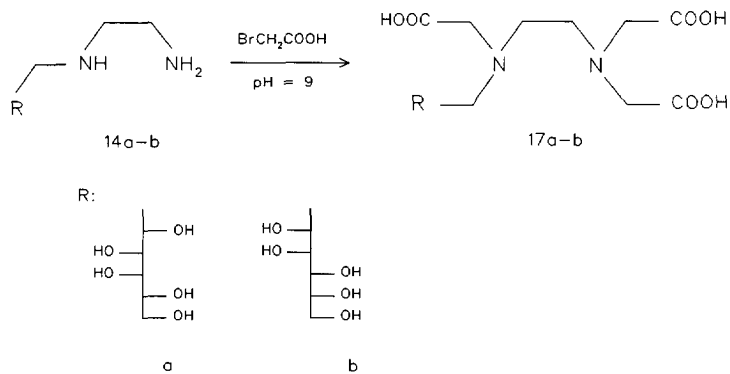
reductive amination of aldohexoses with mono- and bifunctional alkyl amines

to the hydrolysis of 5a and a relatively low hydrogenation rate of 1a. The hydrolysis of 5a, however, is rather slow resulting in a higher molar ratio 5a/1a at the initial stage of the hydrogenation in comparison with the above described reaction starting from an equimolar sugar/amine solution, and consequently the molar ratio of 13a/ galactitol in the final product is higher in this case. This behaviour is in agreement with the conclusion of the speciation studies on solutions of 1a and PA, that ring opening of 5a is relatively slow with respect to that of 1a.

The reductive amination of 1a-c with 1 mol equivalent PA gave the corresponding amino sugars 13a-c in good yields (70%), when a 5-fold excess of amine was used higher yields (85%) were obtained (Scheme 3). Using 1 mol equivalent EN in the reductive amination resulted in mixtures of mono- and diadducts (and alditol). The monoadducts 14a-c and diadducts 16a-c were obtained in yields of 55%, and 15%, respectively. All compounds were isolated as white solids except 14c which was obtained as a syrup from which sorbitol could not be removed. The ratio mono-/diglycosylamine in the starting solutions of aldohexoses and EN closely resembles the ratio mono-/diadduct in the hydrogenated products. Since the equilibration of D-glucose with EN is rather slow (7h at 25 °C), hydrogenation must start after the equilibration is completed. Hydrogenation before equilibrium is reached results in different product compositions and lower yields of the amino sugars. The product composition can be altered in favour of the monoadduct by application of 5 mol equivalents of EN. This resulted in higher yields (75%) of 14a-c, compound 14c was still obtained as a syrup containing sorbitol. The amino sugars 15a and 15b were obtained in 50% yield by reductive amination of D-galactose (1a), and D-mannose (1b), respectively with 5 mol equivalents DAP.



Scheme 3



Scheme 4

Cadmium(II) and Calcium(II) Sequestering Capacities of the Compounds 14a-b and their Carboxymethylated Adducts 17a-b

The monoadducts 14a-b were carboxymethylated using bromoacetate with a yield of 45% (Scheme 4). The thus obtained compounds 17a-b are EDTA type complexing agents in which one of the acetate groups is substituted by a sugar moiety. In Table 3 the Cd(II) and Ca(II) sequestering capacities (CdSC and CaSC, respectively) of the ligands 14a-b, 15a-b, and 17a-b and EDTA at pH 11.6 are presented. The monoadducts 14a-b are poor Ca(II) sequestrants, attachment of the acetate groups increases their Ca(II) sequestering abilities significantly. The ligands 14a-b possess good CdSC abilities, the attachment of acetate groups did not improve the Cd(II) complexing abilities as much as with the sequestering capacities of the hard Ca(II)³¹ cation. The CaSC of 15a-b are comparable with those of ligands 14a-b. The CdSC of 15a-b are significantly lower than those of 14a-b. The decrease in complex stability of the Cd(II) complexes caused by increase of the chelate ring size from five- to six-membered can be ascribed to an enthalpy effect.³² The strong CdSC and CaSC of the sugar-based EDTA type ligands 17a-b can be ascribed to additional coordination of one of the hydroxyl groups of the polyhydroxy chain besides the coordination of the nitrogen-atoms and carboxylate groups. Further studies on the structures of this type of complexes are described in Chapter 6.³³

Table 3. Cadmium(II) and Calcium(II) Sequestering Capacities in mg/gram (mol/mol) Ligand at pH 11.6 and at room temperature.

| ligand | CdSC | | CaSC | |
|--------|------|-------|------|--------|
| 14a | 224 | (0.4) | 20 | (0.1) |
| 14b | 279 | (0.7) | 8 | (0.04) |
| 15a | 82 | (0.2) | 10 | (0.05) |
| 15b | 68 | (0.1) | 15 | (0.08) |
| 17a | 225 | (0.9) | 90 | (1.0) |
| 17b | 226 | (0.9) | 86 | (1.0) |
| EDTA | 342 | (1.0) | 142 | (1.3) |

CONCLUSIONS

The major species present in equimolar aqueous solutions (0.55 M) of aldohexoses and PA or EN are the N-alkylglycosylamines, with DAP as the amine hexahydropyrimidines are predominant. Hydrogenation of the aqueous solutions with the primary amines (PA, EN, and DAP) at 50 °C and 100 atm. H₂, using a 5% Pt on carbon catalyst, gave the desired amino sugars in good yields. The amino sugars 14a-b obtained by reductive amination of 1a-b with EN can be carboxymethylated to give the sugar based EDTA type complexing agents 17a-b, which show promising Cd(II) and Ca(II) sequestering properties at high pH.

EXPERIMENTAL

The ¹³C NMR spectra were recorded at 50.3 MHz with a Nicolet NT-200 WB NMR spectrometer or at 100.6 MHz with a Varian VXR-400 S NMR spectrometer with D₂O/H₂O (4:1 v/v) as the solvent and t-butanol as the internal reference (δ (ppm): 31.2 (methyl)). The quantitative ¹³C NMR spectra were recorded with 45° flip angle, an acquisition delay of 30 s, 32 K datapoints with ¹H decoupling during the acquisition only. Product ratios were determined by deconvolution of the ¹³C signals using Lorentzian line shapes. ¹H NMR spectra were recorded using the Varian VXR-400 S NMR spectrometer with D₂O/H₂O (4:1 v/v) as the solvent and t-butanol as internal reference (δ (ppm); 1.20). The complete ¹H and ¹³C NMR analysis of 5a was carried out by means of ¹H homonuclear correlation spectroscopy, ¹H-¹³C chemical shift correlation spectroscopy (HETCOR) and selective proton decoupling experiments. With J-resolved 2D NMR the ³J_{H-H} coupling constants (first order systems) could be determined. FAB mass spectra were obtained with a VG 70-250 SE mass spectrometer.

The starting materials were all purchased from Janssen Chimica. The hydrogenations were carried out in a 300 ml Hastelloy C276 autoclave model 4562, manufactured by Parr. The autoclave was equipped with a motor-driven impeller stirrer, a sampling device and a temperature programming system (M 4841 Parr). The aldohexose/ amine solutions were thermostatted at 50 °C by a water bath before transferring to the autoclave. The catalyst

(5% Pt/C) was added and the mixtures were hydrogenated for 12 h at 100 atm. H_2 and 50 °C. After hydrogenation the catalyst was filtered off, the solvent and amine were removed by evaporation. Purification of the reaction product was carried out by recrystallization. When using DAP, the amine could not be removed by evaporation. The products derived from DAP crystallized upon addition of MeOH to the crude reaction mixture after removal of the solvent. The quantitative ^{13}C NMR analyses were carried out with 3 ml samples taken at certain intervals. From the samples the catalyst was removed by centrifugation, 0.8 ml D_2O was added and then the ^{13}C NMR spectrum was measured. Dioxane was used as internal standard (δ (ppm): 66.6). The pH values given are direct meter readings.

Metal-ion sequestering capacities were determined according to a procedure used by Akzo Chemicals Research Center Deventer³⁴ or according to Mehlretter et al.³⁵ Cadmium(II) and calcium(II) sequestering capacities, at ambient temperature, were determined by adding a solution of Cd(II) or Ca(II) chloride to a solution containing approximately 100 mg ligand. The CdSC and CaSC were determined at pH 11.6 using NaOH/ Na_2CO_3 as indicator. As endpoint of a titration the first turbidity that not disappeared within 30 seconds was taken. The estimated errors in the metal-ion sequestering capacities are 20%.

1-Deoxy-1-(propylamino)-D-galactitol (13a). To a mixture of 15 g (83 mmol) D-galactose (1a) and 24.6 g (417 mmol) PA dissolved in 150 ml H_2O 2 g catalyst were added. Recrystallization of the hydrogenated mixture from MeOH/ H_2O (9/1) and drying in vacuo yielded 15.8 g (85%) pure 13a. 1H NMR (pH = 10.7): δ (ppm) 3.98 (ddd, 1H, H2, J_{21a} = 8.7 Hz, J_{21b} = 4.2 Hz, J_{23} = 1.6 Hz); 3.92 (m, 1H, H5, J_{54} = 1.4 Hz, J_{56} = 6.7 Hz); 3.65 (d, 2H, H6); 3.62 (dd, 1H, H4, J_{43} = 9.3 Hz); 3.54 (dd, 1H, H3); 2.75 (dd, 1H, H1a, J_{1a1b} = -12.7 Hz); 2.67 (dd, 1H, H1b); 2.55 (m, 2H, H1', $J_{1'a1'b}$ = -11.7 Hz); 1.45 (m, 2H, H2', $J_{2'3'}$ = 7.3 Hz); 0.88 (t, 3H, H3'). ^{13}C NMR (pH = 11.6): δ (ppm) 72.4, 71.7, 71.0 (C3, C4, C5); 69.9 (C6); 52.9, 51.9 (C1, C1'); 23.3 (C2'); 12.6 (C3'). FAB-MS (glycerol matrix): m/z 224 ($M + H^+$).

1-Deoxy-1-(propylamino)-D-mannitol (13b). The procedure described for 13a was followed. From 15 g (83 mmol) D-mannose (1b) 15.3 g (82 %) pure 13b was obtained. 1H NMR (pH = 10.5): δ (ppm) 3.81 (dd, 1H, H6a, J_{6a5} = 2.4 Hz, $J_{6a,6b}$ = -11.6 Hz); 3.78-3.66 (m, 4H, H2, H3, H4, H5); 3.61 (dd, 1H, H6b, J_{6b5} = 5.9 Hz); 2.87 (dd, 1H, H1a, J_{1a2}

=4.0 Hz, $J_{1a1b} = -12.7$ Hz); 2.62 (dd, 1H, H1b, $J_{1b2} = 8.3$ Hz); 2.54-2.50 (m, 2H, H1'); 1.46 (m, 2H, H2', $J_{2,3} = 7.3$ Hz); 0.88 (t, 3H, H3'). ^{13}C NMR (pH = 10.4): δ (ppm) 72.9, 72.4, 70.9 (C3, C4, C5); 70.4 (C2); 64.8 (C6); 52.5, 51.8 (C1, C1'); 22.7 (C2'); 12.4 (C3'). FAB-MS (glycerol matrix): 224 ($\text{M} + \text{H}^+$).

1-Deoxy-1-(propylamino)-D-glucitol (13c). The procedure described for 13a was followed. From 15 g (83 mmol) D-glucose (1c) 14.8 g (80%) pure 13c was obtained. ^1H NMR (pH = 10.6): δ (ppm) 3.85 (ddd, 1H, H2, $J_{21a} = 3.7$ Hz, $J_{21b} = 8.1$ Hz, $J_{23} = 6.0$ Hz); 3.78 (dd, 1H, H6a, $J_{6a6b} = -11.7$ Hz, $J_{6a5} = 2.9$ Hz); 3.72 (m, 1H, H5, $J_{56b} = 6.3$ Hz, $J_{54} = 8.1$ Hz); 3.70 (dd, 1H, H3, $J_{34} = 2.1$ Hz); 3.60 (dd, 1H, H6b); 3.59 (dd, 1H, H4); 2.70 (dd, 1H, H1a, $J_{1a1b} = -12.7$ Hz); 2.61 (dd, 1H, H1b); 2.54 (dt, 1H, H1'a, $J_{1'a1'b} = -11.7$ Hz, $J_{1'a2'} = 7.3$ Hz); 2.49 (dt, 1H, H1'b, $J_{1'b2'} = 7.3$ Hz); 1.45 (m, 2H, H2', $J_{2,3} = 7.3$ Hz); 0.88 (t, 3H, H3'). ^{13}C NMR (pH = 11.6): δ (ppm) 72.6 (broad, C3, C4, C5); 72.4 (C2); 64.4 (C6); 51.9, 51.8 (C1, C1'); 23.2 (C2'); 12.5 (C3'). FAB-MS (glycerol matrix): 224 ($\text{M} + \text{H}^+$).

1-(2-Aminoethylamino)-1-deoxy-D-galactitol (14a). To a mixture of 10 g (55 mmol) D-galactose (1a) and 16.7 g (278 mmol) EN dissolved in 100 ml H_2O 1.5 g catalyst was added. Recrystallization of the hydrogenated mixture from $\text{MeOH}/\text{H}_2\text{O}$ (1/1) and drying in vacuo yielded 9.3 g (75 %) pure 14a. ^1H NMR (pH = 10.5): δ (ppm) 3.97 (ddd, 1H, H2, $J_{21a} = 4.2$ Hz, $J_{21b} = 8.8$ Hz, $J_{23} = 1.5$ Hz); 3.92 (dt, 1H, H5, $J_{56} = 6.0$ Hz, $J_{54} = 1.5$ Hz); 3.63 (d, 2H, H6); 3.61 (dd, 1H, H4, $J_{34} = 9.3$ Hz); 3.54 (dd, 1H, H3); 2.77 (dd, 1H, H1a, $J_{1a1b} = -12.6$ Hz); 2.66 (dd, 1H, H1b); 2.74-2.60 (m, 4H, H1', H2'). ^{13}C NMR (pH = 11.7): δ (ppm) 72.5, 71.8, 71.1 (C3, C4, C5); 70.0 (C2); 64.8 (C6); 53.0 (C1); 52.0 (C1'); 41.4 (C2'). FAB-MS (glycerol matrix): 225 ($\text{M} + \text{H}^+$).

1-(2-Aminoethylamino)-1-deoxy-D-mannitol (14b). The procedure for 14a was followed. From 10 g (55 mmol) D-mannose (1b) 9.0 g (72 %) pure 14b was obtained. ^1H NMR (pH = 10.5): δ (ppm) 3.81 (dd, 1H, H6a, $J_{6a5} = 2.5$ Hz, $J_{6a6b} = -11.6$ Hz); 3.75 (m, 1H, H2, $J_{21a} = 3.7$ Hz, $J_{21b} = 8.3$ Hz); 3.70 (m, 3H, H3, H4, H5); 3.61 (dd, 1H, H6b, $J_{6b5} = 5.6$ Hz); 2.90 (dd, 1H, H1a, $J_{1a1b} = -12.7$ Hz); 2.64 (dd, 1H, H1b); 2.78-2.66 (m, 4H, H1', H2'). ^{13}C NMR (pH = 11.4): δ (ppm) 72.9, 72.4, 70.9 (C3, C4, C5); 70.8 (C2); 52.8 (C1); 51.4 (C1'); 41.1 (C2'). FAB-MS (glycerol matrix): 225 ($\text{M} + \text{H}^+$).

1-(2-Aminoethylamino)-1-deoxy-D-glucitol (14c). The procedure for 14a was followed. From 10 g (55 mmol) D-glucose (1c) 9.0 g of a mixture containing 14c and sorbitol was

obtained as a syrup. Estimated yield of 70% based on quantitative ^{13}C NMR. ^{13}C NMR (pH = 11.4): δ (ppm) 72.7 (broad, C3, C4, C5); 72.5 (C2); 64.4 (C6); 52.0, 51.9 (C1, C1'); 41.4 (C2').

1-(3-Aminopropylamino)-1-deoxy-D-galactitol (15a). To a mixture of 10 g (55 mmol) D-galactose (1a) and 20.6 g (278 mmol) DAP 1.5 g catalyst was added. Removal of the solvent and subsequent addition of MeOH to the remaining solution resulted in the precipitation of 15a. After filtration and drying in vacuo 6.0 g (45%) pure 8a was obtained. ^1H NMR (pH = 10.4): δ (ppm) 3.97 (dd, 1H, H2, J_{21a} = 8.7 Hz, J_{21b} = 4.0 Hz, J_{23} = 1.4 Hz); 3.92 (m, 1H, H5, J_{56} = 6.6 Hz, J_{54} = 1.2 Hz); 3.65 (d, 2H, H6); 3.61 (dd, 1H, H4, J_{43} = 9.3 Hz); 3.55 (dd, 1H, H3); 2.76 (dd, 1H, H1a, J_{1a1b} = -12.5 Hz); 2.67 (dd, 1H, H1b); 2.62 (m, 4H, H1', H3'); 1.61 (m, 2H, H2'). ^{13}C NMR (pH = 11.4): δ (ppm) 72.5, 71.8, 71.1 (C5, C4, C3); 70.0 (C2); 64.8 (C6); 53.0, 47.7, 40.1 (C1, C1', C3'); 32.7 (C2'). FAB-MS (glycerol matrix): 239 (M + H⁺).

1-(3-Aminopropylamino)-1-deoxy-D-mannitol (15b). The procedure described for 15a was followed. From 10 g (55mmol) D-mannose (1b) 6.4 g (48%) pure 15b was obtained. ^1H NMR (pH = 10.6): δ (ppm) 3.80 (dd, 1H, H6a, J_{6a5} = 2.6 Hz, J_{6a6b} = -11.9); 3.82-3.66 (m, 4H, H2, H3, H4, H5); 3.61 (dd, 1H, H6b, J_{6b5} = 5.8 Hz); 2.87 (dd, 1H, H1a, J_{1a2} = 3.8 Hz, J_{1a1b} = -12.5 Hz); 2.63 (dd, 1H, H1b, J_{1b2} = 8.1 Hz); 2.67-2.57 (m, 4H, H1', H3'); 1.66-1.54 (m, 2H, H2'). ^{13}C NMR (pH = 11.4): δ (ppm) 73.0, 72.4, 71.0 (C3, C4, C5); 70.9 (C2); 64.8 (C6); 52.8, 47.7, 40.2 (C1, C1', C3'); 32.9 (C2'). FAB-MS (glycerol matrix): 239 (M + H⁺).

N,N'-ethylenedi-(1-imino-1-deoxy-D-galactitol) (16a). To a mixture of 10 g (55 mmol) D-galactose (1a) and 3.33 g (55 mmol) EN 1.5 g catalyst was added. Recrystallization of the hydrogenated mixture from MeOH and drying in vacuo yielded 1.62 g (15%) pure 16a. ^1H NMR (pH = 10.3): δ (ppm) 3.99 (ddd, 2H, H2, J_{21a} = 8.8 Hz, J_{21b} = 4.1 Hz, J_{23} = 1.6 Hz); 3.92 (dt, 2H, H5, J_{56} = 6.0 Hz, J_{54} = 1.6 Hz); 3.64 (d, 4H, H6); 3.62 (dd, 2H, H4, J_{43} = 9.4 Hz); 3.55 (dd, 2H, H3); 2.80 (dd, 2H, H1a, J_{1a1b} = -12.6 Hz); 2.68 (dd, 2H, H1b); 2.80-2.70 (m, 4H, H1'). ^{13}C NMR (pH = 11.2): δ (ppm) 72.5, 71.8, 71.1 (C3, C4, C5); 70.0 (C2); 64.8 (C6); 53.0, 49.1 (C1, C1'). FAB-MS (glycerol matrix): 389 (M + H⁺).

N,N'-ethylenedi-(1-imino-1-deoxy-D-mannitol) (16b). The procedure for 16a was followed. From 10 g D-mannose (1b) 1.2 g (11%) pure 16b was obtained. ^1H NMR (pH =

10.2): δ (ppm) 3.81 (dd, 2H, H6a, $J_{6a5} = 2.7$ Hz, $J_{6a6b} = -11.8$ Hz); 3.78-3.68 (m, 8H, H2, H3, H4, H5); 3.62 (dd, 2H, H6b, $J_{6b5} = 5.6$ Hz); 2.94 (dd, 2H, H1a, $J_{1a2} = 3.5$ Hz, $J_{1a1b} = -12.6$ Hz); 2.85-2.75 (m, 4H, H1'); 2.68 (dd, 2H, H1b, $J_{1b2} = 8.3$ Hz). ^{13}C NMR (pH = 11.3): δ (ppm) 72.9, 72.3, 70.9 (C3, C4, C5); 70.6 (C2); 64.8 (C6); 52.9, 48.9 (C1, C1'). FAB-MS (glycerol matrix): 389 ($\text{M} + \text{H}^+$).

N,N'-ethylenedi-(1-imino-1-deoxy-D-glucitol) (16c). The procedure for 16a was followed. From 10 g (55 mmol) D-glucose (1c) 1.1 g (10%) pure 16c was obtained. ^1H NMR (pH = 10.3): δ (ppm) 3.87 (ddd, 2H, H2, $J_{21a} = 3.7$ Hz, $J_{21b} = 8.5$ Hz, $J_{23} = 2.1$ Hz); 3.78 (dd, 2H, H6a, $J_{6a6b} = -11.7$ Hz, $J_{6a5} = 3.0$ Hz); 3.73 (dd, 2H, H5, $J_{56b} = 6.2$ Hz, $J_{54} = 8.1$ Hz); 3.71 (dd, 2H, H3, $J_{34} = 2.1$ Hz); 3.60 (dd, 2H, H6b); 3.59 (dd, 2H, H4); 2.76 (dd, 2H, H1a, $J_{1a1b} = -12.6$ Hz); 2.70-2.75 (m, 4H, H1'); 2.68 (dd, 2H, H1b). ^{13}C NMR (pH = 11.4): δ (ppm) 72.6, 72.5 (C3, C4, C5); 72.3 (C2); 52.0, 49.1 (C1, C1'). FAB-MS (glycerol matrix): 389 ($\text{M} + \text{H}^+$).

1-Deoxy-1-(2-aminoethylamino)-D-galactitol-N-triacetate (17a). In 40 ml H_2O 2 g (9 mmol) 14a and 7.45 g (54 mmol) bromoacetic acid were dissolved. The pH was raised to 11 with LiOH. The reaction mixture was heated for 5 h at 90 °C. The reaction mixture was concentrated in vacuo and fractionated on a Dowex 50W (H^+) cation exchange column. A gradient was applied from 0 to 0.7 M NH_4OH . The fractions were concentrated, 1.74 g (43 %) pure 17a was obtained. ^{13}C NMR (pH = 1.5): δ (ppm) 172.3, 172.2 ($-\text{CH}_2\text{COOH}$); 71.9, 71.6, 70.9 (C3, C4, C5); 67.3 (C2); 64.8 (C6); 59.6 ($-\text{CH}_2\text{COOH}$); 58.9 (2 x CH_2COOH); 58.1, 53.1, 52.8, (C1, C1', C2'). FAB-MS (glycerol matrix): 399 ($\text{M} + \text{H}^+$).

1-Deoxy-1-(2-aminoethylamino)-D-mannitol-N-triacetate (17b). The procedure described for 10a was followed. From 2 g (14b) (9 mmol) 1.76 g (44%) pure 17b was obtained. ^{13}C NMR (pH = 1.6): δ (ppm) 176.3, 176.0 ($-\text{CH}_2\text{COOH}$); 72.7, 72.4, 70.6, (C3, C4, C5); 68.1 (C2); 64.8 (C6); 59.8 ($-\text{CH}_2\text{COOH}$); 59.0 ($-\text{CH}_2\text{COOH}$); 58.2, 53.2, 52.6, (C1, C1', C2'). FAB-MS (glycerol matrix): 399 ($\text{M} + \text{H}^+$).

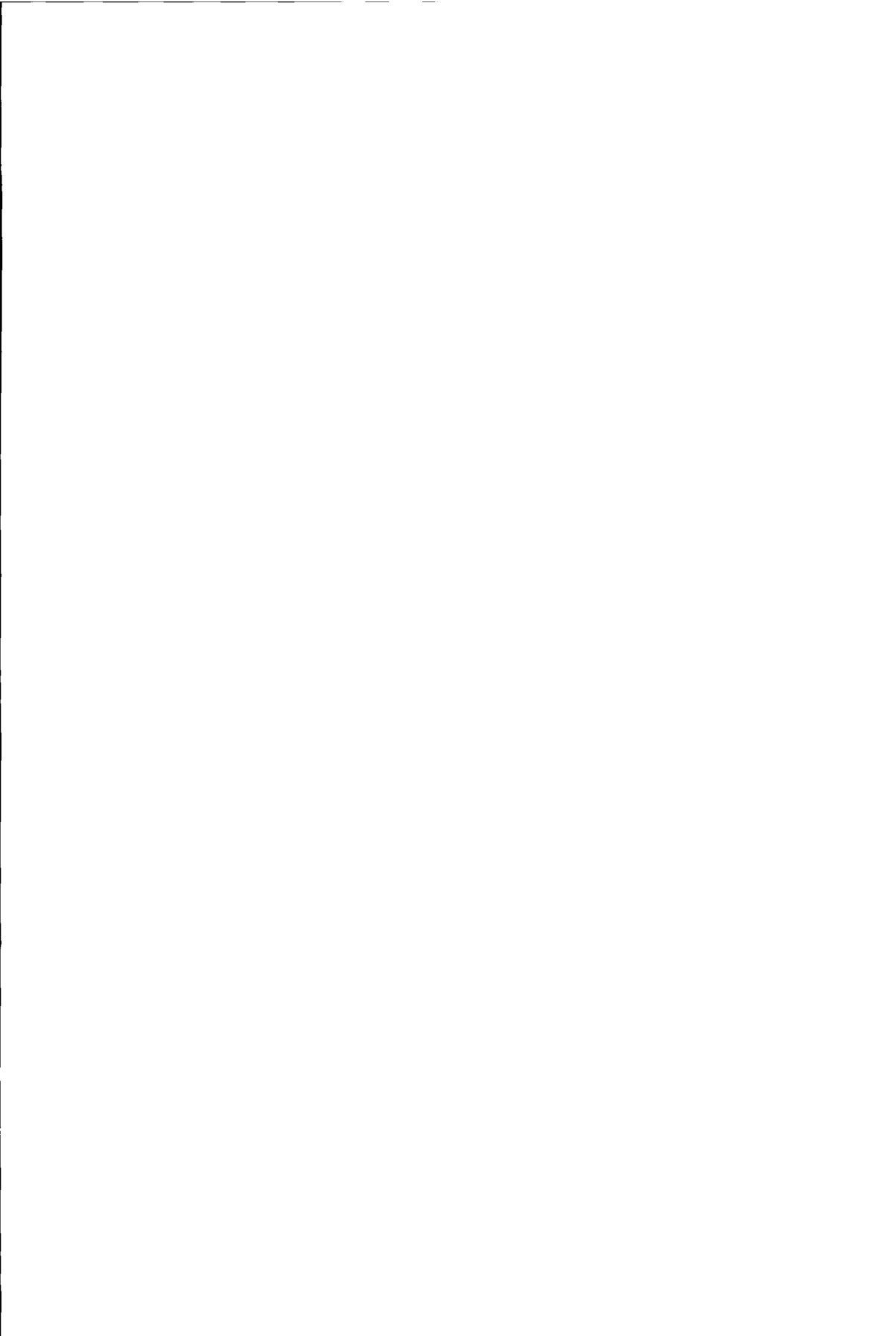
ACKNOWLEDGEMENTS

This investigation was carried out with support of the Dutch National Innovation Program Carbohydrates. We are grateful to Akzo Nobel Central Research (ACR) for their financial support. Thanks are due to Dr. J.G. Batelaan, Dr. E. Boelema, Dr. C.M. Navarro, and Dr. J.C. Speelman, all from Akzo Nobel Central Research (ACR), for their fruitful discussions. Mr. A. Sinnema is thanked for recording part of the NMR spectra, Mrs. A. H. Knol-Kalkman for measuring the FAB mass spectra, and Mr. E. Wurtz for carrying out the hydrogenation experiments. Dr. L. Maat is thanked for his assistance in naming several compounds.

REFERENCES

1. Long, J.W.; Bollenback, G.N. *Methods in Carbohydrate Chemistry*, Vol. II; Whistler, R.L.; Wolfrom, M.L., Eds.; Academic Press, **1963**, pp. 79-83.
2. Ling, A.R.; Nanji, D.R. *J. Chem. Soc.* **1922**, 121, 1682.
3. Flint, R.B.; Salzberg, P.L. *US* 2,016,962, **1974**; *Chem. Abstr.* **1935**, 29, 8007.
4. Wayne, W.; Adkins, H. *J. Am. Chem. Soc.* **1940**, 62, 3314.
5. Holly, F.W.; Peel, E.W.; Mozingo, R.; Folkers, K. *J. Am. Chem. Soc.* **1950**, 72, 5416.
6. Kagan, F.; Rebenstorf, M.A.; Heinzelman, R.v. *J. Am. Chem. Soc.* **1957**, 79, 3541.
7. Lemieux, R.U. *US* 2,830,983, **1958**; *Chem. Abstr.* **1958**, 52, 14668.
8. Tronchet, J.M.J.; Baehler, B.; Zumwald, J.-B. *Helv. Chim. Acta* **1977**, 60, 1932.
9. Larkin, J.M.; Yeakey, E.L.; Watts, Jr. L.W. *US* 4,540,821, **1985**; *Chem. Abstr.* **1985**, 104, 110120
10. Kelkenberg, H. *Tens. Surf. Det.* **1988**, 25, 8.
11. Shumate, R.E.; Burdsall, D.C.; Scheibel, J.J.; Connor, D.S. *WO* 08687, **1992**; *Chem. Abstr.* **1992**, 117, 215006b.
12. Klein, J.; Behrens, W.; Kunz, M. *EP* 225,033, **1987**; *Chem. Abstr.* **1989**, 110, 95711j.
13. Christiansen-Brams, I.; Meldal, M.; Bock, K. *J. Carbohydr. Chem.* **1992**, 11, 813.
14. Latgé, P.; Rico, I.; Lattes, A.; Godefroy, L. *FR* 2,661,413, **1991**; *Chem. Abstr.* **1992**, 116, 194795v.
15. Koch, H.; Beck, R.; Röper, H. *Starch* **1993**, 45, 2.
16. Klein, J.; Kunz, M.; Kowalczyk, J. *Makromol. Chem.* **1990**, 191, 517.

17. Ellis, J.W.; Malehorn, S.H.; Browning, L.M.; Heischmidt, T.A. *J. Carbohydr. Chem.* **1992**, *11*, 761.
18. Jeffrey, G.A.; Wingert, L.M. *Liq. Crystals* **1992**, *12*, 179.
19. Schnarr, G.W.; Vyas, D.M.; Szarek, W.A. *J. Chem. Soc., Perkin Trans. I* **1979**, 496.
20. Angyal, S.J.; Le Fur, R. *Carbohydr. Res.* **1980**, *84*, 201.
21. Hawkes, G.E.; Lewis, D. *J. Chem. Soc. Perkin Trans. II* **1984**, 2073.
22. Bock, K.; Thogersen, H. *Annu. Rep. NMR Spectrosc.* **1982**, *13*, 2.
23. Paulsen, H.; Gyorgydeak, Z.; Friedman, M. *Chem. Ber.* **1974**, *107*, 1590.
24. Votoček, E.; Valentin, F. *Collect Czech. Chem. Commun.* **1934**, *6*, 77.
25. Ellis, G.P.; Honeyman, J. *Adv. Carbohydr. Chem.*, Vol. 10; Wolfrom, M.L., Ed.; Academic Press, **1955**, Chapter 2, pp. 95-168.
26. Capon, B. *Chem. Rev.* **1969**, *69*, 407.
27. Mitts, E.; Hixon, R.M. *J. Am. Chem. Soc.* **1944**, *66*, 483.
28. Leal, F.; Schleicher, E. *Angew. Chem. Int. Ed. Eng.* **1990**, *29*, 565.
29. van Haveren, J.; Lammers, H.; Peters, J.A.; Batelaan, J.G.; van Bekkum, H. *Carbohydr. Res.* **1993**, *243*, 259.
30. de Wit, G.; de Vlieger, J.J.; Kock-van Dalen, A.C.; Heus, R.; Laroy, R.; van Hengstum, A.J.; Kieboom, A.P.G.; van Bekkum, H. *Carbohydr. Res.* **1981**, *91*, 125.
31. Hancock, R.D.; Martell, A.E. *Chem. Rev.* **1989**, *89*, 1875.
32. Hancock, R.D. *J. Chem. Educ.* **1992**, *8*, 615.
33. Lammers, H.; van Bekkum, H.; Peters J.A., submitted to *Carbohydr. Res.*
34. Bekendam, G. (Akzo Chemicals Research Center Deventer), Technical Leaflet 104.
35. Mehlretter, C.L.; Alexander, B.H.; Rist, C.E. *Ind. Eng. Chem.* **1953**, *45*, 2782.



Chapter 4

REACTION KINETICS OF THE AQUEOUS PHASE REDUCTIVE AMINATION OF D-GALACTOSE WITH PROPYLAMINE (IN AQUEOUS MEDIUM) OVER PLATINUM ON (ACTIVATED) CARBON

ABSTRACT

The reductive amination of D-galactose (1) with propylamine (PA) over a platinum-on-graphite catalyst in water was investigated in a three-phase continuous stirred tank reactor. The hydrogen pressure was varied from 5 to 20 bar, the D-galactose (1) concentration from 125 to 750 mol m⁻³, the amine concentration from 125 to 500 mol m⁻³ and the reaction temperature was fixed at 323 K. The reaction kinetics of the hydrogenation can be described satisfactorily over the range of the reaction conditions applied, using a relatively simple rate equation.

INTRODUCTION

The catalytic reductive amination of carbohydrates using a (noble) metal catalyst is the most commonly used method for the introduction of an amino function in a sugar molecule.¹⁻⁸ The starting reactants are readily available mono- and disaccharides and either ammonia or short chain (C<5) primary alkyl amines. In the case of monosaccharides reducing aldohexoses such as D-glucose, D-galactose and D-mannose are

used. Sucrose, a non-reducing disaccharide linked through its two anomeric centers, can also be used in the reductive amination with ammonia⁹ but requires, prior to the reductive amination, conversion into a disaccharide, e.g. by isomerization, containing a reducing unit.

Due to the presence of the amino function, the amino sugars can be converted into surfactant molecules.¹⁰ Recently, several patent applications for the manufacture and use of this new type of sugar-based surfactants, mainly based on D-glucose, in detergents have been published.^{11,12} Further potential applications are as polymers¹³, sweeteners¹⁴ and as liquid crystalline compounds.¹⁵

The only known continuous process carried out on an industrial scale is the reductive amination of D-glucose with ammonia, resulting in 1-amino-1-deoxy-D- glucitol. A high hydrogen pressure (200 atm. H₂) is applied in a fixed-bed process over a Ni catalyst.¹⁶ In this way the formation of side products is suppressed and high yields and selectivities are obtained. To the best of our knowledge, no literature data on the reaction kinetics of the catalytic reductive amination of carbohydrates with ammonia or alkyl amines are available. In the present study the reaction kinetics of the reductive amination of D-galactose (1) with PA, in a continuous process, using a platinum-on-graphite catalyst has been investigated. Previously, we reported on the speciation in aqueous solution of D-galactose and PA to gain insight into the equilibria involved in the reductive amination.¹⁷ In Figure 1 the equilibria and species present in an aqueous solution of D-galactose (1) and one mol equivalent PA at pH = 11.5 are given. It has been shown using ¹H and ¹³C NMR that the major species present is the β-N-propylgalactosylamine (5).¹⁷ The carbinolamine (3) as well as the imine (4) could not be detected. At low pH (< 6) complete hydrolysis to 1 and PA occurred. After hydrogenation of this mixture (batch process) the reaction mixture obtained comprised the desired amino sugar (6) and D-galactitol (7). The latter compound is invariably obtained as the by-product in the reductive amination due to direct hydrogenation of 1.

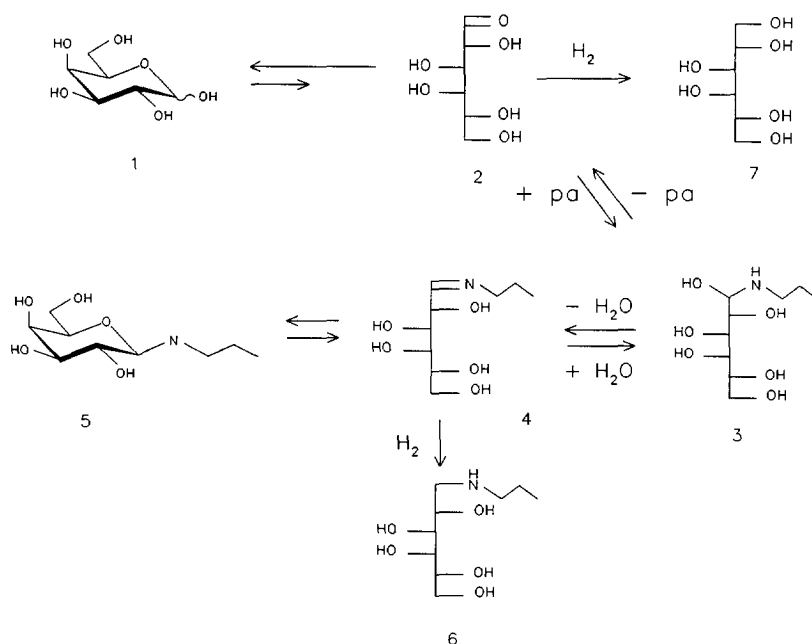


Figure 1. The equilibria occurring in an aqueous equimolar solution of D-galactose (1) and PA together with the irreversible hydrogenations to 1-deoxy-1-(propylamino)-D-galactitol (6) and D-galactitol (7), respectively.

EXPERIMENTAL

Chemicals

A 5 wt% platinum-on-graphite catalyst from Johnson Matthey (Type 287) was used. D-Galactose, D-galactitol and propylamine were obtained from Janssen Chimica and used without any further purification.

Experimental set-up

A continuous stirred three phase slurry reactor, CSTR, in which the catalyst was retained by a filter, was used for the experiments (Figure 2). This type of reactor offers good contraction of the three phases and thus assures good isothermality, and when using

sufficiently fine catalyst powder, absence of mass transfer limitations.

At the start of an experiment the reactor is filled with catalyst and 350 ml of an aqueous solution containing 1 and PA in the desired molar ratio. After closure, the reactor is purged with nitrogen for about 10 minutes to remove the oxygen, while maintaining the stirrer speed at 18.3 rps. This process of purging with nitrogen is time-limited and must be carried out at room temperature to avoid the dehydrogenation of D-galactose to D-galactonic acid.¹⁸ After adjustment of the reaction temperature to 323 K and admission of hydrogen, the reaction pressure is increased to the desired hydrogen pressure.

The reaction conditions are summarized in Table 1. It was established that under these reaction conditions the obtained production rates were free of any mass transfer limitations. The mass balance was based on carbon and determined for the sugar containing species and nitrogen containing species and amounted typically to 90-95%:

$$C\text{-balance}\% = \frac{\sum C_i n_{C,i}}{\sum C_{i,0} n_{C,i}} 100\% \quad (1)$$

in which $n_{C,i}$ is the number of carbon atoms in a molecule i . Equation 1 can be used as the mass balance only if the flow of liquid (F_L) in and out of the reactor are equal and if the carbon containing components are not present in significant amounts in the gas phase. These conditions were fulfilled during the experiments reported here.

The reaction was monitored using a HPLC set-up (Spectra Physics) which consisted of a HPLC pump (SP 8800), a column heater (SP 8790) and a Waters Assoc. differential refractometer (RI-401). The data obtained after integration (SP 4600) were combined with TSP PC Winner on windows. We were not able to separate all species on one particular column, therefore two analyses were developed. The separation of 1 and 7 was achieved on a 280 x 4.6 ID mm Lichroma SS column slurry packed with a Benson type of cation-exchange resin (BA-X8, 7 - 10 μ) which was brought into the Ca(II)-form by pumping overnight with a 0.01 M CaCl_2 solution in water. With a 0.03 M HCl solution as the eluent and a liquid flow of 1 ml/min the retention times for 1 and 7 were typically 7.5 and 9.2 min, respectively. The analysis of PA and amino sugar 6 was carried out on a similar column as described above which was brought into the Na^+ -form by pumping

overnight with a 0.1 M NaCl solution. An acidified (2.5 ml conc. HCl in 1 L water) 0.3 N trisodium citrate solution was applied as the eluent which gave retention times for 6 and PA of 6.3 and 11.6 min, respectively. An acidic eluent was used in both separation methods in order to establish a complete hydrolysis of 5 to 1 and PA.¹⁹ During an experiment, one of the above mentioned analyses was performed on-line while at the same time intervals samples were taken which were analyzed off-line in the second type of analysis. The samples taken for the off-line analysis were stored at 5 °C to avoid non-enzymatic browning (Maillard reaction)²⁰ when they were not analyzed immediately after sampling.

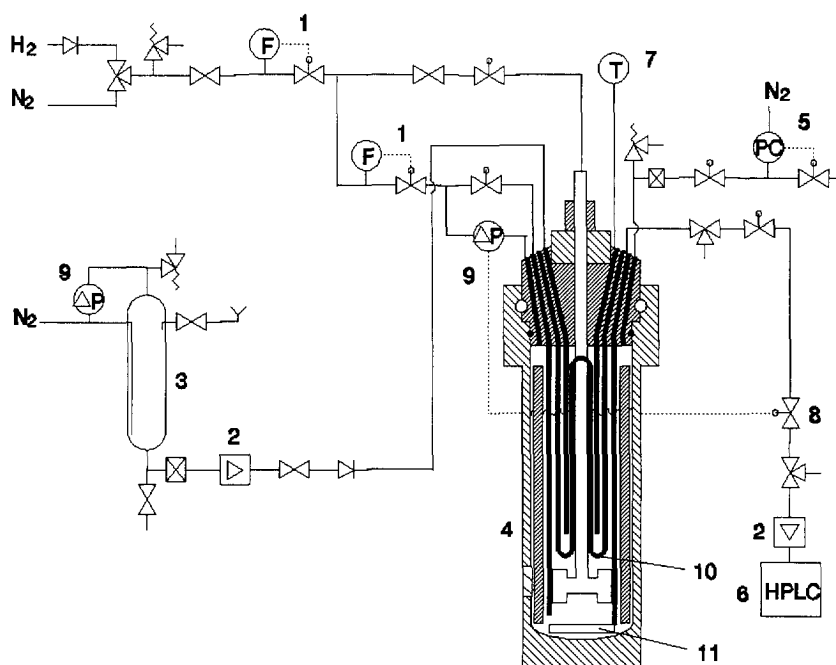


Figure 2. Schematic representation of reactor set-up; 1. mass flow controller; 2. HPLC pump; 3. vessel; 4. reactor; 5. backward pressure regulator; 6. HPLC analysis section; 7. temperature sensor; 8. proportional valve; 9. differential pressure sensor; 10. cooling coil; 11. liquid outlet filter.

Table 1. Reaction conditions.

| | | |
|----------------------|---|---|
| $p(\text{H}_2)$ | = | 5 - 20 bar (= P_{total}) |
| T | = | 323 K |
| W_{cat} | = | 1 g |
| C_1^0 | = | 125 - 750 mol m ⁻³ |
| C_{PA}^0 | = | 125 - 500 mol m ⁻³ |
| F_L | = | 6 ml min ⁻¹ |
| F_G | = | 120 ml min ⁻¹ H ₂ |
| N_{stirrer} | = | 18.3 rps |

RESULTS AND DISCUSSION

The overall equilibrium present in an aqueous solution of 1 and PA can be written as:

$$C_5 = K_a * C_1 * C_{\text{PA}} \quad (2)$$

The value of K_a (14.2 mol⁻¹ L) was determined by quantitative ¹³C NMR spectroscopy of samples prepared by mixing of known amounts of 1 and PA. The mass balances (neglecting C_2 , C_3 and C_4) of the nitrogen-containing (eq 3) and of the sugar-containing components (eq 4) are defined as:

$$C_{\text{PA}}^0 = C_{\text{PA}} + C_5 + C_6 \quad (3)$$

$$C_1^0 = C_1 + C_5 + C_6 + C_7 \quad (4)$$

in these equations C_1 , C_5 and C_{PA} are to be determined; C_{PA}^0 and C_1^0 are the weighed amounts of PA and 1, respectively; C_6 and C_7 are obtained from HPLC analysis. Assuming that the same species and equilibria, as given in Figure 1, are present in mixtures of 1 and PA under the reaction conditions applied, the concentration of 1, 5 and PA can be calculated using eqs 2-4. From these results the net specific formation rates of 6 and 7 and the net specific disappearance rate of H₂ are calculated:

$$R_{w,6} = F_{V,L} \cdot \frac{C_6}{W} \quad (5)$$

$$R_{w,7} = F_{V,L} \cdot \frac{C_7}{W} \quad (6)$$

$$-R_{w,H_2} = F_{V,L} \cdot \frac{C_6 + C_7}{W} \quad (7)$$

in which R_w is the specific production/disappearance rate ($\text{mol kg}_{\text{cat}}^{-1} \text{s}^{-1}$), $F_{V,L}$ is the volumetric flow rate ($\text{m}^3 \text{s}^{-1}$), C the concentration of products (mol m^{-3}) and W is the catalyst mass (kg).

The selectivity to 6 (S_6) can be calculated from:

$$S_6 = \frac{C_6}{C_6 + C_7} \quad (8)$$

The data, summarized in Table 2, are used as such in the regression analysis (11 points). In Table 2, the initial compositions of the reaction mixtures are also given. The regression analysis was performed as outlined by Froment and Hosten²¹ implementing the two reaction models which will be described later. The regression was performed by minimization of the sum of squared residuals of the observed and calculated reaction rates to obtain maximum probability estimates b for the proposed kinetic parameters:

$$S(b) = \sum_{i=1}^{n_{\text{obs}}} (R_{w,i} - R_w(x_i, b))^2 \rightarrow \text{MIN} \quad (9)$$

in which n_{obs} is the number of observations, $R_{w,i}$ is the observed specific production/disappearance rate of the observation i and $R_w(x_i, b)$ is the calculated specific production/disappearance rate under the reaction conditions x_i of the observation i and parameter estimates b .

This minimization was performed using the Marquardt algorithm.²² The significance of the results of the global regression was expressed by the F-ratio, the ratio of the mean regression sum of squares to the mean residual sum of squares:

$$F\text{-ratio} = \frac{(n_{obs} - n_{par}) \sum_{i=1}^{n_{obs}} R_{w,i}^2}{n_{par} \sum_{i=1}^{n_{obs}} [R_{w,i} - R_w(x_i, b)]^2} \quad (10)$$

in which n_{par} is the number of parameters. A high value of this F-ratio, which is distributed according to the in statistics known F distribution²³, indicates a high significance of the global regression. The significance of the individual parameter estimates is expressed as the calculated t-value which is given by the ratio of the parameter estimate b_i , and the estimated standard error of the parameter, $s(b_i)$:

$$t_i = \frac{b_i}{\sqrt{\text{variance}(b_i)}} = \frac{b_i}{s(b_i)} \quad (11)$$

As a rule of thumb these calculated t-values should be larger than 2 to indicate a parameter estimate significantly different from 0. The two sided $1 - \alpha$ confidence intervals for the parameters were calculated from tabulated critical t-values as:

$$b_i - t(n_{obs} - p_{par}, 1 - 1/2\alpha) s(b_i) \leq \beta_i \leq b_i + t(n_{obs} - p_{par}, 1 - 1/2\alpha) s(b_i) \quad (12)$$

in which β is the proposed kinetic parameter.

Table 2. The kinetic data used in the regression analysis of the hydrogen disappearance rate.^{a,b,c}

| exp | $p_{H_2}^d$ | C_1^{0e} | C_{PA}^{0e} | C_1^f | C_{PA}^f | C_5^f | C_6^g | C_7^g | $R_{w,6}^h$ | $R_{w,7}^h$ | $-R_{w,H_2}^h$ | S_6^i |
|------------------|-------------|------------|---------------|-------------------|------------|---------|---------|---------|-------------|-------------|----------------|---------|
| Formulation Feed | | | | Reaction Mixtures | | | | | | | | |
| 1 | 10 | 0.50 | 0.50 | 0.13 | 0.14 | 0.25 | 0.11 | 0.008 | 10.7 | 0.8 | 11.5 | 93 |
| 2 | 10 | 0.50 | 0.50 | 0.13 | 0.14 | 0.25 | 0.11 | 0.009 | 11.4 | 0.9 | 12.3 | 93 |
| 3 | 15 | 0.50 | 0.50 | 0.12 | 0.14 | 0.24 | 0.13 | 0.011 | 12.8 | 1.1 | 13.9 | 92 |
| 4 | 5 | 0.50 | 0.50 | 0.14 | 0.15 | 0.30 | 0.07 | 0.007 | 6.5 | 0.7 | 7.2 | 90 |
| 5 | 10 | 0.25 | 0.50 | 0.03 | 0.30 | 0.13 | 0.08 | 0.007 | 7.5 | 0.7 | 8.2 | 92 |
| 6 | 10 | 0.125 | 0.50 | 0.01 | 0.40 | 0.06 | 0.05 | 0.005 | 5.2 | 0.5 | 5.7 | 91 |
| 7 | 7.5 | 0.50 | 0.50 | 0.13 | 0.14 | 0.26 | 0.09 | 0.006 | 8.8 | 0.6 | 9.4 | 94 |
| 8 | 20 | 0.50 | 0.50 | 0.14 | 0.13 | 0.25 | 0.10 | 0.011 | 13.4 | 1.5 | 14.9 | 90 |
| 9 | 10 | 0.75 | 0.50 | 0.32 | 0.07 | 0.33 | 0.09 | 0.013 | 9.5 | 1.3 | 10.8 | 88 |
| 10 | 10 | 0.50 | 0.25 | 0.27 | 0.03 | 0.12 | 0.08 | 0.010 | 8.3 | 1.0 | 9.3 | 89 |
| 11 | 10 | 0.50 | 0.125 | 0.38 | 0.014 | 0.075 | 0.04 | 0.007 | 3.6 | 0.7 | 4.3 | 84 |

^a see Table 1 for the reaction conditions; ^b concentrations in mol m⁻³; ^c flow rate = 6 ml min⁻¹; ^d in bar; ^e initial amounts in mol m⁻³; ^f calculated using eq 2-4; ^g determined using HPLC; ^h in mmol kg_{cat}⁻¹ s⁻¹; ⁱ in % (see eq 8)

In Figure 3 it is shown that the net disappearance rate of H₂, $-R_{w,H_2}$, increases as the hydrogen partial pressure increases. Upon further increase of the hydrogen partial pressure, the increase of $-R_{w,H_2}$ levels off. Increasing the concentration of β -N-propylgalactosylamine 5 resulted in an increase of $-R_{w,H_2}$; this effect, less pronounced than for H₂, levels off at higher concentrations of 5 as visualized in Figure 4.

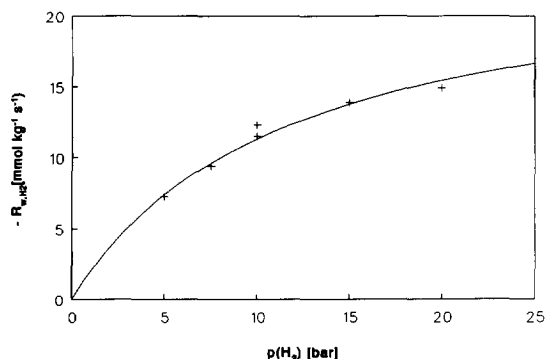


Figure 3. Plot of the net disappearance rate of H_2 ($-R_{w,H_2}$) versus H_2 partial pressure.

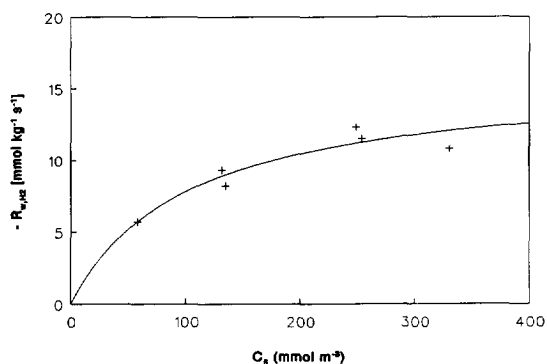
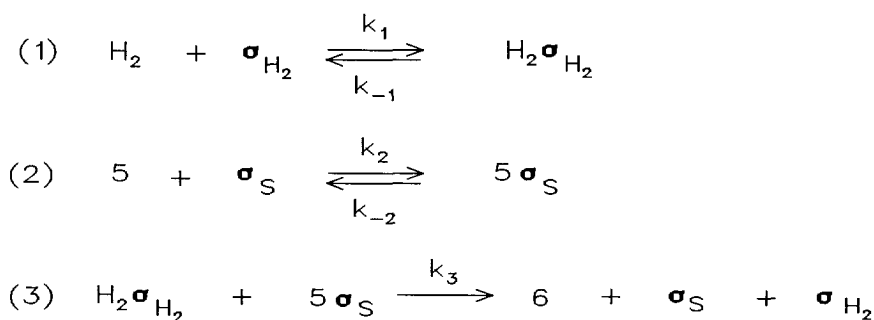


Figure 4. Plot of the net disappearance rate of H_2 ($-R_{w,H_2}$) versus concentration of β -N-propylgalactosylamine (C_3) at $p_{H_2} = 10$ bar.

All compounds (reactants as well as products) of Figure 1 will adsorb on the catalyst surface. From the data obtained it can be assumed that the adsorption of 1 (or 2) and 5 (or 4) leads to conversion (to 7 and 6, respectively). It is not known whether the formation of 6 proceeds via hydrogenation of 4 or 5, respectively. In our reaction models (see below) we assume that the formation of the amino sugar 6 occurs via hydrogenation of the β -N-propylgalactosylamine (5). Competitive adsorption between 1 and 5 is likely due to similarity in molecular size and shape. On the other hand no competitive

adsorption between hydrogen and 1 or 5 is to be expected. Therefore the adsorption of hydrogen will occur at a different adsorption site ($\sigma_t^{H_2}$) than the adsorption of 1 and 5 (σ_t^S). It was observed that at higher ratios C_5/C_1^0 (> 0.2) the selectivity to 6 remained constant (91%) (Table 2). Surprisingly, the experiments using an excess of PA (exp 2, 5 and 6) gave slightly lower selectivities. This might be ascribed to poisoning of the catalyst surface by PA.

In order to describe reaction sequences and rate equations two situations will be discussed. Firstly, the situation in which only the hydrogenation of 5 is considered. In the second model, the hydrogenation of 5 as well as 1 are taken into account. In order to describe the hydrogenation of 5 (in the absence of 1) only data with a low concentration of 1 in comparison to 5 are used in the data treatment (exp 1-8). A simplified reaction sequence in which both the adsorption of hydrogen and 5 are equilibrated is depicted in Scheme 1. Here, σ_s and σ_{H_2} denote surface adsorption sites for organics and hydrogen, respectively.



Scheme 1

reaction kinetics of the reductive amination of D-galactose with propylamine

Table 3. Parameter estimates with 95 % confidence limits and their corresponding t-values for the model in which only the hydrogenation of 5 is taken into account (rate equation 13).

| parameter | estimate | t-value |
|---|-----------------|---------|
| 1 ($k_3 K_1 K_2 / H_{H_2}$) $\sigma_{H_2} \sigma_S$ | 0.0290 ± 0.0112 | 5.22 |
| 2 (K_1 / H_{H_2}) | 0.0877 ± 0.0376 | 4.67 |
| 3 (K_2) | 0.0098 ± 0.0005 | 4.21 |

F-ratio = 928

Applying the steady-state approximation the following rate equation is obtained:

$$-R_{w,H_2} = \frac{k_3 K_1 \frac{p_{H_2}}{H_{H_2}} K_2 C_5}{(1 + K_1 \frac{p_{H_2}}{H_{H_2}}) (1 + K_2 C_5)} \sigma_{H_2} \sigma_S \quad (13)$$

in which K_1 and K_2 are the overall adsorption constants for H_2 and 5, respectively; k_3 is the reaction rate constant for step 3 in the simplified reaction sequence of Scheme 1. The regression results for this model are presented in Table 3. Assuming that $-R_{w,H_2} = R_{w,6}$, it can be seen clearly from the F-ratio (and the fitted curves in Figures 3 and 4) that this model can adequately describe the experimental data.

The reaction sequence in which the adsorption of 5, 1 and hydrogen are equilibrated is presented in Scheme 2. In this reaction sequence two responses are used, i.e. $-R_{w,H_2}$ (eq 14) and $+R_{w,6}$ (eq 15). All kinetic data, presented in Table 2, are used in the regression analysis.

$$-R_{W,H_2} = \frac{K_1 \frac{P_{H_2}}{H_{H_2}} (k_3 K_2 C_5 + k_5 K_4 C_1)}{(1 + K_1 \frac{P_{H_2}}{H_{H_2}}) (1 + K_2 C_5 + K_4 C_1)} \sigma_{H_2} \sigma_S \quad (14)$$

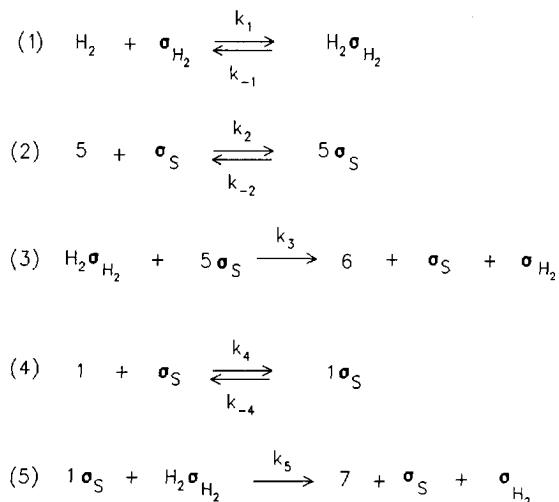
$$+R_{W,6} = \frac{k_5 K_1 \frac{P_{H_2}}{H_{H_2}} K_2 C_5}{(1 + K_1 \frac{P_{H_2}}{H_{H_2}}) (1 + K_2 C_5 + K_4 C_1)} \sigma_{H_2} \sigma_S \quad (15)$$

The regression results for this model are given in Table 4. It can be seen that the adsorption of 1 cannot be estimated significantly from zero. This might be due to the fact that only a few datapoints (exps 9-11) are used in the minimization routine in which an excess of 1 in the reaction mixture is present, resulting in a significant formation of 7. Another reason might be that the adsorption of 1 on the catalyst surface is negligible.

Table 4. Parameter estimates with 95 % confidence limits and their corresponding t-values for the model in which the hydrogenation of 5 as well as 1 is described (rate equations 14 and 15).

| parameter | estimate | t-value |
|---------------------|---------------|---------|
| 1 (K_1/H_{H_2}) | 0.0792±0.0572 | 2.77 |
| 2 ($k_5 K_4$) | 0.0241±0.0114 | 3.52 |
| 3 (K_2) | 0.0063±0.0044 | 2.80 |
| 4 ($k_3 K_2$) | 0.0008±0.0008 | 2.04 |
| 5 (K_4) | 0.0012±0.0020 | 1.16 |

F-ratio = 400



Scheme 2

CONCLUSIONS

The reaction kinetics of the platinum catalyzed hydrogenation of an aqueous mixture of D-galactose (1) and propylamine can be described adequately over a range of reaction conditions by a relatively simple rate equation. Including the adsorption of D-galactose (1) on the catalyst surface into the model does not give an improvement of the fit of the experimental data. This might be due to the fact that the adsorption of 1 is negligible.

ACKNOWLEDGEMENTS

This investigation, mainly carried out at the Schuit Institute of Catalysis of the University of Technology in Eindhoven, was financially supported by the Dutch National Innovation Program Carbohydrates. Thanks are due to Prof. G.B. Marin and Dr. B.F.M. Kuster for their supervision of this part of the project. Special thanks are due to Mr. G. Ingenbleek

for performing the larger part of the reactions as well as to Mrs. M. Kuppens and Mr. W. Groenland for carrying out the HPLC-analyses.

REFERENCES

1. Ling, A.R.; Nanji, D.R. *J. Chem. Soc.* **1922**, 121, 1682.
2. Flint, R.B.; Salzberg, P.L. *US 2,016,962*, **1974**; *Chem. Abstr.* **1935**, 29, 8007.
3. Wayne, W.; Adkins, H. *J. Am. Chem. Soc.* **1940**, 62, 3314.
4. Holly, F.W.; Peel, E.W.; Mozingo, R.; Folkers, K. *J. Am. Chem. Soc.* **1950**, 72, 5416.
5. Kagan, F.; Rebenstorf, M.A.; Heinzelman, R.V. *J. Am. Chem. Soc.* **1957**, 79, 3541.
6. Lemieux, R.U. *US 2,830,983*, **1958**; *Chem. Abstr.* **1958**, 52, 14668.
7. Tronchet, J.M.J.; Baehler, B.; Zumwald, J.-B. *Helv. Chim. Acta* **1977**, 60, 1932.
8. Larkin, J.M.; Yeakey, E.L.; Watts, Jr. L.W. *US Pat.* 4,540,821, **1985**; *Chem. Abstr.* **1985**, 104, 110120.
9. Klein, J.; Behrens, W.; Kunz, M. *EP 225,033*, **1987**; *Chem. Abstr.* **1989**, 110, 95711j.
10. Koch, H.; Beck, R.; Röper, H. *Starch* **1993**, 45, 2.
11. Connor, D.S.; Scheibel, J.J.; Kao, J.N. *WO 9,206,072*, **1990**; *Chem. Abstr.* **1992**, 117, 72094r.
12. Connor, D.S.; Scheibel, J.J.; Severson, R.G. *WO 9,206,073*, **1990**; *Chem. Abstr.* **1992**, 117, 114043f.
13. Klein, J.; Kunz, M.; Kowalczyk, J. *Makromol. Chem.* **1990**, 191, 517.
14. Ellis, J.W.; Malehorn, S.H.; Browning, L.M.; Heischmidt, T.A. *J. Carbohydr. Chem.* **1992**, 11, 761.
15. Jeffrey, G.A.; Wingert, L.M. *Liq. Crystals* **1992**, 12, 517.
16. Kelkenberg, H. *Tens. Surf. Det.* **1988**, 25, 8.
17. Lammers, H.; Peters, J.A.; van Bekkum, H. *Tetrahedron* **1994**, 50, 27, 8103.
18. de Wit, G.; de Vlieger, J.J.; Kock-van Dalen, A.C.; Heus, R.; Laroy, R.; van Hengstum, A.J.; Kieboom, A.P.G.; van Bekkum, H. *Carbohydr. Res.* **1981**, 91, 125.
19. Capon, B. *Chem. Rev.* **1969**, 69, 407.
20. Leal, F.; Schleicher, E. *Angew. Chem. Int. Ed. Eng.* **1990**, 29, 565.
21. Froment, G.F.; Hosten, L.H. *Catalysis Science and Technology*; Anderson, J.R.; Boudart, M., Eds.; Springer Verlag (Berlin), **1981**, Chapter 3.

reaction kinetics of the reductive amination of D-galactose with propylamine

22. Marquardt, D.W. *J. Soc. Indust. Appl. Math.* **1963**, *11*, 431.
23. Draper, N.R.; Smith, H. *Applied Regression Analysis*, Wiley, New York, 1966.

Chapter 5

FORMATION OF BORATE ESTERS FROM, AND SEQUESTRATION OF METAL IONS BY BIS(POLY-HYDROXYALKYL)AMINES AND THEIR N-CARBOXY-METHYL DERIVATIVES STUDIED BY ^{11}B - AND ^{13}C NMR*

ABSTRACT

Catalytic hydrogenation of aldose oximes affords bis(polyhydroxyalkyl)amines. These compounds and their N-carboxymethyl derivatives react with borate ions to give macrocyclic diborate diesters. The presence of an N-carboxymethyl group raises the capacities for the sequestration of Ca^{2+} , Cu^{2+} , and Cd^{2+} . The N-carboxymethyl derivatives possess strong affinity for Ca^{2+} ($\text{pH}>11$) and Cd^{2+} both in the absence and presence of borate.

INTRODUCTION

Aldonic acids and oxidized polysaccharides have promising metal ion chelating properties.¹⁻³ Such systems are possible substitutes for sodium triphosphate in detergent formulations since they have strong metal ion sequestering capacities with good

* van Haveren, J.; Lammers, H.; Peters, J.A.; Batelaan, J.G.; van Bekkum, H. *Carbohydr. Res.* **1993**, *243*, 259.

biodegradabilities. Substituted polyhydroxyamines also possess strong metal ion chelating properties and are used in detergents and cosmetics⁴ and bis(polyhydroxyalkyl)amines have potential as metal ion chelating agents for use in plant therapeutics.⁵

For aldonic acids, the metal ion sequestering capacities at pH>9 increase upon addition of borate.⁶⁻⁸ In these systems, the borate anion links two aldonic acid molecules and strong metal ion coordinating sites are formed. Borate esters formed from polyhydroxy compounds that contain functional groups other than carboxylate and hydroxyl, also exhibit good metal ion sequestering capacities. Thus, mixtures of borate and amino aldonic acids or (amino) aldose oximes coordinate transition metal ions more selectively than aldonic acids.^{9,10}

Hodge et al.⁵ reported that the capacity of bis(D-gluco-2,3,4,5,6-pentahydroxyhexyl)amine (2d) to sequester Cu²⁺, Ca²⁺, Sr²⁺, and Fe³⁺ is substantially higher than that of the equally basic N-methyl-D-gluco-2,3,4,5,6-pentahydroxyhexylamines. The authors concluded that two freely-rotating polyhydroxy alkyl chains in one molecule result in better metal ion sequestering than a single such chain and predicted that attachment of a third such chain would further increase the metal ion chelating properties. However, attempts to react bis(D-gluco-2,3,4,5,6-pentahydroxyhexyl)amine with D-glucose or tetra-O-acetyl- α -D-glucopyranosyl bromide failed. We now report that the metal ion complexing abilities of these compounds can be enhanced by the formation of (a) N-carboxymethyl (NCH₂COOH) derivatives and (b) borate esters.

Bis(polyhydroxyalkyl)amines have been prepared by hydrogenation of dialdosylamines¹¹ and by hydrogenolysis of N-benzyl(polyhydroxyalkyl)amines.¹² We have synthesized bis(polyhydroxyalkyl)amines by catalytic hydrogenation of aldose oximes. Although alkyl or aryl oximes can be transformed easily into primary and secondary amines by catalytic hydrogenation¹³, there has been no report of the application of this reaction to prepare bis(polyhydroxyalkyl)amines.

RESULTS AND DISCUSSION

Synthesis of bis(polyhydroxyalkyl)amines and their N-carboxymethyl derivatives

Hydrogenation (Pt/C) of D-arabinose oxime (1a), D-mannose oxime (1b), and D-galactose

oxime (1c) gave the corresponding bis(polyhydroxyalkyl)amines 2a-c in yields of 26-80% (Figure 1). These compounds were characterized by ^{13}C NMR spectroscopy and FAB MS.

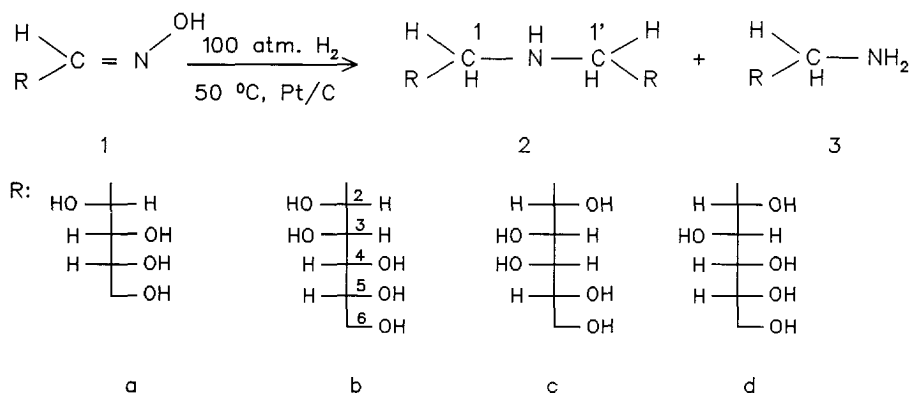


Figure 1. The synthesis of the bis(polyhydroxyalkyl)amines.

Heard et al.¹⁴ reported the formation of 2a as a byproduct [D-arabino-2,3,4,5-tetrahydroxypentylamine (3a) was the main product] during the hydrogenation of D-arabinose oxime over Pt at ambient temperature and 1 atm. ^{13}C NMR of the crude reaction mixtures showed however clearly that, at 50° and 100 atm, 2a was the major product.

D-Glucose oxime (1d) was reduced much more slowly than the oximes 1a-c. After 24 h at 50° and 100 atm, reduction was incomplete and bis(D-gluco-2,3,4,5,6-pentahydroxyhexyl)amine (2d) could not be crystallized from the reaction mixture. Also, on electrochemical reduction, the conversion of D-glucose oxime into D-gluco-2,3,4,5,6-pentahydroxyhexylamine (3d) was much slower¹⁵ than that of the oximes 1a-c. This may be ascribed to the considerable proportion of cyclic forms present in the solution of glucose oxime, in contrast to the other oximes.¹⁶ Catalytic hydrogenation of a mixture of D-glucose and D-gluco-2,3,4,5,6-pentahydroxyhexylamine (3d), however, afforded almost exclusively 2d, which could be purified by crystallization.

The N-carboxymethyl derivatives 4b-d, were synthesized by reacting the bis(polyhydroxyalkyl)amines with lithium bromoacetate as depicted in Figure 2.

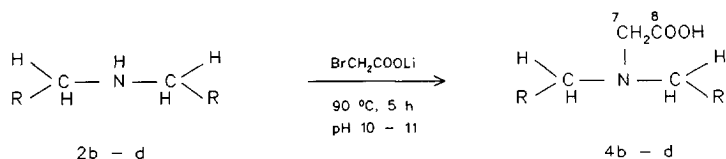
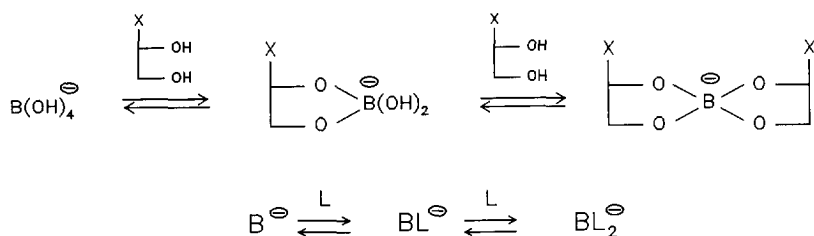


Figure 2. The synthesis of the N-carboxymethyl derivatives $R=(\text{CHOH})_5\text{CH}_2\text{OH}$.

Formation of borate esters

The formation of borate esters from D-gluco-2,3,4,5,6-pentahydroxyhexylamine (3d), the bis(polyhydroxyalkyl)amines 2a-d, and the N-carboxymethyl derivatives 4b-d was investigated using ^{11}B - and ^{13}C NMR. Studies with ^{11}B NMR^{17,18} and other techniques¹⁹ have shown that alditols, aldonic acids, aldaric acids, and aldose oximes, react with boric acid/borate to give monoesters (B^-L) and diesters (B^-L_2) that are formed from 1,2- and 1,3-diols (Scheme 1).



Scheme 1. The equilibria between borate (B^-) and a diol function of a polyhydroxy compound ($\text{X} = \text{CHOH}, \text{CH}_2\text{OH}, \text{COO}^-, \text{C}=\text{NOH}$).

The exchange between B^- , B^-L and B^-L_2 is slow on the ^{11}B NMR time scale so that the chemical shifts, line widths, and association constants of the various boron-containing species can be determined. Thus, in studying the reaction of 2a-d and 4b-d with borate as a function of pH and at a ligand-to-borate ratio of 0.5 or 1.0, the ^{11}B signals could be assigned easily to B^-L or B^-L_2 on the basis of literature values (Table 1).^{17,18} For most of the ligands, however, there was an unusually high proportion of borate diester species.

Table 1. ^{11}B NMR data (chemical shifts and line widths) for the borate esters (D_2O , 25°).

| Ligand | Ester type | δ (ppm) | | $\Delta\nu_{1/2}$ (Hz) | |
|--------|-----------------------|----------------|-------------------------------|------------------------|-------------------------------|
| | | B'L | B'L ₂ ^a | B'L | B'L ₂ ^a |
| 2a | threo-2,3 | -13.7 | -9.1 | 71 | 137 |
| | syn/anti ^b | -18.1 | | 19 | |
| 2b | threo-3,4 | -13.6 | -9.1 | 49 | 167 |
| | erythro | -14.3 | | 23 | |
| | syn/anti | -18.3 | | 11 | |
| 2c | threo | -13.7 | -9.7 | 94 | 153 |
| 2d | threo | -13.5 | -9.2 | 65 | 208 |
| | erythro | -14.2 | | 44 | |
| | syn/anti | -18.1 | | | |
| 3d | threo | -13.5 | -9.4 | 52 | 109 |
| | erythro | -14.4 | | 58 | |
| | syn/anti | -18.3 | | 31 | |
| 4b | threo-3,4 | -13.3 | -9.0 | 89 | 209 |
| | erythro | -14.4 | | 27 | |
| | syn/anti | -18.1 | | | |
| 4c | threo | -13.5 | -9.0 | 91 | 166 |
| | erythro | -14.4 | | 25 | |
| | syn/anti | -18.2 | | 16 | |
| 4d | threo | -13.5 | -9.3 | 76 | 187 |
| | erythro | -14.4 | | 45 | |
| | syn/anti | -18.2 | | 17 | |

^a Structures I, III, VI, or VII; ^b syn and anti refer to 1,3-diol type esters

^{11}B NMR measurements for D-gluco-2,3,4,5,6-polyhydroxyhexylamine (3d), as a function of the ligand-to-borate ratio (ρ), revealed mainly threo borate monoesters at $\rho=1$ and mainly borate diesters at $\rho=2$, (Figure 3). This pattern of borate ester formation resembles those of D-glucitol, D-mannitol and D-arabinitol.^{20,21} Figure 3 also demonstrates that, at pH 12 for the secondary amines 2a-d and a ligand-to-borate ratio of 1, practically all of the borate anion is incorporated in a borate diester species ($\delta \sim -9$) with an apparent relatively high stability.

However, a borate anion complexed to such an extent via two diol functions of different

ligands (i.e. $B^{\cdot}L_2$ in Scheme 1), is impossible at a ligand:borate ratio (ρ) of ~ 1 . Therefore, borate diester species other than those mentioned in literature may be present. The presence of 8-10 hydroxyl groups in the various bis(polyhydroxyalkyl)amines creates several possibilities (I - VII) for the formation of borate diesters at $\rho=1-2$ as exemplified in Figure 4.

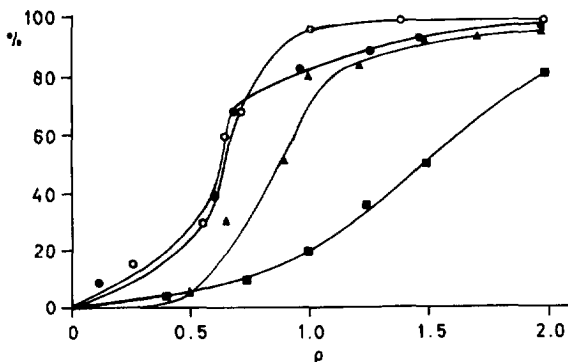


Figure 3. Percentage of the total boron involved in a borate diester species (structure I, III, VI, or VII), as a function of the ligand-to-borate ratio (ρ) with 0.05-0.20 M borate and 0-0.31 M ligand, pH 12.2-12.7, D_2O , 25 °C; \circ 2a, \bullet 2c, \blacktriangle 2d, \blacksquare 3d.

For the bis(polyhydroxyalkyl)amines 2a-d the chemical shifts of the ^{11}B resonances of the main 1,2-diol-type borate monoesters are characteristic of threo structures in agreement with the finding^{20,22} that such monoesters are more stable than the erythro isomers. Therefore, it is likely that, in the borate diester species also, the borate is bound at threo positions. This inference was confirmed for 2a, 2b, and 2d by ^{13}C NMR substituent effects, at $\rho=1$ and 2, on the formation of borate esters (Table 2). The down-field shifts of only 0.2 -0.3 ppm for the signals of C-6,6' (C-5,5' of 2a) on the formation of borate esters indicate that C-5,5' (C-4,4' of 2a) and C-6,6' are not involved in the borate ester ring.²³ Furthermore, since the substituent effect (-1.2 ppm) for C-1,1' of 2b indicates a threo-3,4-borate ester²³, it can be concluded that for 2a, 2b, and 2d the borate moiety in the borate diester species is bound at the threo positions. Therefore borate esters of structures II, IV, and V are not present. For 2c ^{13}C NMR results indicate that the borate can be bound at both threo positions (2,3 or 4,5). Borate esters of structures II, IV, and V are unlikely to be formed with 2c since the separation of the oxygens of the two borate units is only 1 Å.

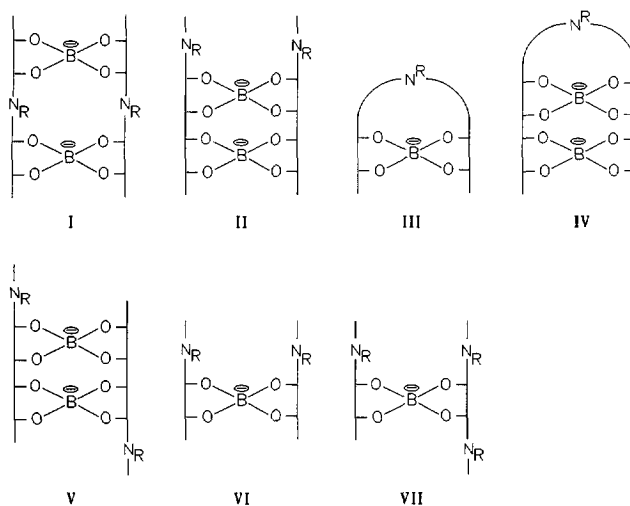


Figure 4. Schematic representation of possible structures of borate diester species of bis(polyhydroxyalkyl)amines 2a-d ($R=H$) and 4b-d ($R=CH_2COOH$).

For the bis(polyhydroxyalkyl)amines 2a-d the ^{13}C NMR spectra at $\rho=1$ ($pH > 12$) showed nearly all of the ligand to be complexed, indicating the existence of borate diesters of structures I or III. At $\rho=1$, for 2a and 2b, the ^{13}C spectra contained only five and six signals, respectively, suggesting that only one type of borate diester was present with structure I or III. For 2c and 2d at $\rho=1$, more than six signals were present, which reflects the presence of two different threo-diol functions. At $\rho=2$, 2a-d appeared to be present as 50-70% of free ligand which shows that the borate diesters of structure I or III have a relatively high stability. In addition, relatively weak ^{13}C signals, attributed to borate esters other than those at $\rho=1$, were discerned (Figure 5) possibly of structure VI or VII.

metal ion sequestration by bis(polyhydroxyalkyl)amines

Table 2. ^{13}C NMR data^a (δ in ppm) for 2a-2d, 3d and 4d and their borate diester species in D_2O , pH 12.2-12.7, 25 °C.

| Assignment | Species | 2a | 2b | 2c | 2d | 3d | 4d |
|------------|------------------------|-------------------|------|-------------------------|------|-------------------|-------------------|
| C-1,1' | L | 52.7 | 52.7 | 52.9 | 51.8 | 44.3 | 60.6, 59.9 |
| | B^-L_2 | 54.6 ^b | 51.5 | 55.2, 53.1 ^b | | 54.3 ^b | 45.0 ^b |
| | | 55.2 ^c | | 54.6, 53.3 ^c | | 52.6 ^c | 44.9 ^c |
| C-5,5' | L | 64.5 | | | | | |
| | B^-L_2 | 64.7 | | | | | |
| C-6,6' | L | | 64.7 | 64.8 | 64.4 | 64.4 | 64.4 |
| | B^-L_2 | | 64.9 | 65.3 | 64.7 | 64.7 | 64.7 |
| | | | | 66.0 | | | |

^a The CHOH signals of the ligand and the borate diester species could not be assigned unambiguously; ^b Predominant signal at $\rho=1$; ^c Predominant signal at $\rho=2$

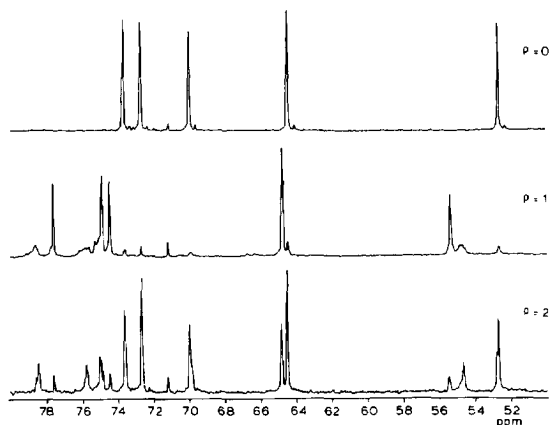


Figure 5. ^{13}C NMR spectra of bis(D-arabino-2,3,4,5-tetrahydroxypentyl)amine (2a) and borate at $\rho=0, 1, \text{ and } 2$, D_2O , pH 12.2-12.7, 25 °C.

For the N-carboxymethyl derivatives 4b-d, the formation of borate esters at pH 12.2-12.7 was also studied as a function of ρ (Figure 6 for 2d and 4d). As is clear from Figure 6, at $\rho=1$, less of the boron is included in a borate diester species than for the bis(polyhydroxyalkyl)amines. On the other hand, for the N-carboxymethyl derivative 4d,

much more ligand is present in a borate diester species, at $\rho=1$, than for D-gluco-2,3,4,5,6-pentahydroxyhexylamine (3d). The fact that, at $\rho=1$ for the N-carboxymethyl derivatives, 55-65% of the total borate is present as a borate diester and 30-40% as a borate monoester (not shown in Figure 3), points to the occurrence of boron-containing species having structures I or III, which are apparently less stable than the corresponding borate esters of the unsubstituted bis(polyhydroxyalkyl)amines. This difference may reflect steric hindrance by the carboxymethyl groups or repulsive interactions of the negatively charged borate and carboxylate groups.

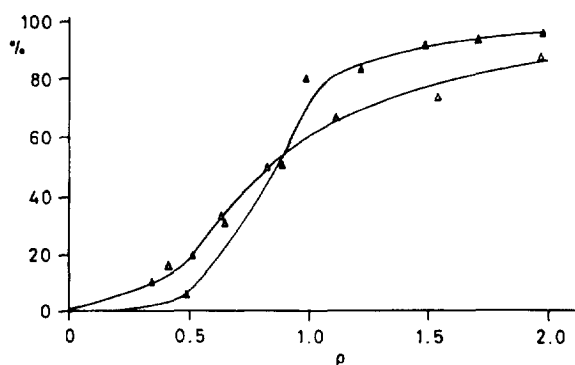


Figure 6. Percentage of the total borate involved in a borate diester species (structures I, III, VI, or VII) as a function of the borate-to-ligand ratio at pH 12.2-12.7, 0.05 M borate and 0-0.31 M ligand, D_2O , 25 °C; ▲ 2d, △ 4d.

Although the borate diester species of 2a-d and 4b-d showed only one ^{11}B resonance, this does not exclude diborate diesters of structure I since, in these species, the borate moieties have similar environments. A further indication of the presence of borate esters of structure I or III can be obtained from the line-widths of the ^{11}B signals which are dominated by quadrupolar relaxation²⁴ as approximated by the equation²⁵

$$\frac{1}{T_2} = \left(\frac{3\pi^2 (2I + 3)}{10 I^2(2I - 1)} \chi^2 (1 + \eta^2/3) \right) \left(\frac{4\pi r^3 \eta_s}{3k_B T} \right) \quad (1)$$

where χ is the quadrupolar coupling constant in Hz, η is the electric-field gradient asymmetry, η_s is the viscosity of the solution, and r is the radius of the molecule which is considered as a rigid sphere. Line-widths of $B'L_2$ signals increase going from small diols such as ethylene glycol or 1,2-propanediol to C_5 or C_6 alditols or aldonic acids. For D-

metal ion sequestration by bis(polyhydroxyalkyl)amines

gluco-2,3,4,5,6-pentahydroxyhexylamine, a line-width for the borate diester signal of 109 Hz was found, close to that found for borate diesters of other ligands containing 5 or 6 carbon atoms.^{22,26} For the bis(polyhydroxyalkyl)amines 2a-d and the N-carboxymethyl derivatives 4b-d, line-widths of the borate diester species (~9 ppm) were substantially larger (Table 1). The electric-field asymmetry (η) will be nearly the same for all borate diester species and therefore, assuming equal viscosities of the solutions, the larger line widths indicate that the molecular radii for the borate diester species of the bis(polyhydroxyalkyl)amines are larger than those for alditols and aldonic acids. The line widths at $\rho \approx 1$ were in agreement with those estimated for structure I, using eq 1 and molecular radii from molecular models.

It is concluded that, in solutions of borate and bis(polyhydroxyalkyl)amines, diborate diesters of structure I are formed. The existence of such diborate diesters is of interest with regard to cation sequestration for in these structures crown ether like coordinating cavities are formed.

Table 3. Ca^{2+} and Cd^{2+} sequestering capacities^a (mg/g of ligand) of the N-carboxymethyl derivatives in the absence and presence of 1 mol equiv. of borate.

| Ligand | pH | CdSC | | CaSC | |
|----------------|------|----------------|-------------|----------------|-------------|
| | | without borate | with borate | without borate | with borate |
| 4b (D-manno) | 7.0 | 220 | 220 | <1 | <1 |
| | 11.5 | 340 | 360 | 140 | 200 |
| 4c (D-galacto) | 6.7 | 160 | 160 | <1 | <1 |
| | 12.3 | 240 | 330 | 120 | 150 |
| 4d (D-gluco) | 7.0 | 170 | 200 | <1 | <1 |
| | 11.5 | 150 | 280 | 130 | 150 |

^a Determined by adding solution of Ca^{2+} or Cd^{2+} chloride to a solution containing ~ 100 mg of ligand and indicator (oxalate at pH 6.7 and $\text{NaOH}/\text{Na}_2\text{CO}_3$ at pH 11.5-12.3). The estimated errors are $\pm 20\%$.

Sequestration of Cd^{2+} and Ca^{2+} by borate N-carboxymethylbis(polyhydroxyalkyl)-amine systems

The sequestration of Cd^{2+} and Ca^{2+} by 4b-d was studied in the presence and absence of borate since their complexation can be enhanced by addition of borate.⁶⁻¹⁰ The sequestration of Cu^{2+} by 2a-2d and 4d was studied also. The capacities (CdSC and CaSC, respectively) for the sequestration of Cd^{2+} and Ca^{2+} by 4b-d, were determined at pH 6.7-7.0 and 11.5-12.3, in the absence and presence of 1 mol equiv. borate using a titration procedure.¹ The results in Table 3 show that the N-carboxymethyl derivatives are poor Ca^{2+} sequestrants at pH 7, probably as a result of the inability of Ca^{2+} to deprotonate the ammonium functions at that pH, but strong Ca^{2+} chelators at pH > 11, at which pH about 1 mmol of Ca^{2+} is sequestered per mmol of ligand.

Compounds 4b-d possess good CdSC at both pH 7 and 11.5-12.3, amounting to 0.7 and ~1 mmol of Cd^{2+} sequestered per mmol of ligand, respectively. For compounds 2a-c only 20-30 mg of Cd^{2+} per g of ligand was sequestered at pH 11.5 which shows that the N-carboxymethyl group increases their Cd^{2+} -sequestering abilities significantly. The Cu^{2+} -sequestering abilities of 2a-2d as well as of their N-carboxymethyl derivatives were high at both pH 7 and 11-12. For 2a-2d at neutral pH, ~1 mmol of Cu^{2+} is sequestered per mmol of ligand, which rises to 1.5-2 mmol at pH 11-12. The N-carboxymethyl derivatives sequester 2-3 mmol of Cu^{2+} per mmol of ligand at neutral pH and as much as 4 mmol at high pH. Addition of borate to solutions of 2a-2d or 4d did not increase the sequestering abilities. The higher abilities of 2a-2d to sequester Cu^{2+} than Ca^{2+} and Cd^{2+} can be explained by the higher effective charge of the Cu^{2+} ion, thereby causing a stronger interaction of the bis(polyhydroxyalkyl)amine and the metal ion. The strong CdSC and CaSC of the N-carboxymethyl derivatives may be rationalized by assuming coordination of the metal ions via the nitrogen atom and the carboxylate group, while the alditol chains assist in the complexation by encapsulating the metal ions.

¹¹B NMR on mixtures of the N-carboxymethyl derivatives 4b-d and borate, at $\rho=0.9$ (Table 4), showed that the addition of Ca^{2+} did not alter the ratios of B^- , B^-L , and B^-L_2 . Also addition of Ba^{2+} to mixtures of borate and 4b had no influence on these ratios. Thus Ca^{2+} and Ba^{2+} are not coordinated preferentially by one of the borate esters. Addition of Cd^{2+} resulted in an increase in the proportion of B^-L_2 species for 4b and 4d and the CdSC increased upon adding borate (Table 3).

metal ion sequestration by bis(polyhydroxyalkyl)amines

Table 4. Effect of the addition^a of CaCl₂ (0.16M) or CdCl₂ (0.05M) on the percentage borate diester species present in solutions of borate and the N-carboxymethyl derivatives, at pH 12, as determined by ¹¹B NMR.

| Ligand | pH | B ⁻ L ₂ ^{b,c} | | B ⁻ L ₂ ^{b,c} | |
|----------------|------|--|----------------------|--|----------------------|
| | | C _{Ca,0.0} | C _{Ca,0.16} | C _{Cd,0.0} | C _{Cd,0.05} |
| 4b (D-manno) | 6.3 | 56 | 75 | 55 | 71 |
| | 12.3 | 74 | 73 | 53 | 72 |
| 4c (D-galacto) | 7.2 | 66 | 80 | 69 | 63 |
| | 12.7 | 78 | 75 | 68 | 65 |
| 4d (D-gluco) | 6.8 | 67 | 69 | 72 | 78 |
| | 12.7 | 53 | 48 | 55 | 82 |

^a For Ca²⁺ C_B = 0.1 M and C_{4b-4d} = 0.1 M, for Cd²⁺ C_B = 0.05 M and C_{4b-4d} = 0.05 M;^b The percentage borate included in a borate diester species is given in the absence (C_{Ca,0} or C_{Cd,0}) and presence (C_{Ca,0.16} and C_{Cd,0.05}) of Ca²⁺ and Cd²⁺, respectively. The sum of the borate diesters, including their metal ion complexes is given;^c B⁻L₂ represents a borate ester of structure I or III

Although the results in Tables 3 and 4 indicate that addition of borate to solutions of the N-carboxymethyl derivatives has only a small synergistic effect on the sequestration of Cd²⁺ and Ca²⁺, the borate diester species form complexes with Cd²⁺ and Ca²⁺ of strength equal or higher than those in the absence of borate. In the diborate diesters, with the borate bound at the threo-2,3-position (4c and 4d), 16-membered rings are formed, wherein 2 carboxylate groups, 2 nitrogen and, 4 oxygen atoms can assist in metal ion coordination. In diborate diesters of structure I, with the borate bound at the threo-3,4-position (4b and 4d), complexing cavities are formed that are somewhat larger than that of the 18-crown-6-ether ligand (Figure 7). Strong metal ion coordination by diborate diesters of the N-carboxymethyl derivatives might be hampered by their high flexibility or the dynamics of the borate ester formation. For synergistic metal ion sequestration the latter effect may be an advantage, for the metal ions can be removed easily from their diborate diester complexes by lowering the pH, thus inducing dissociation of the diborate diesters.

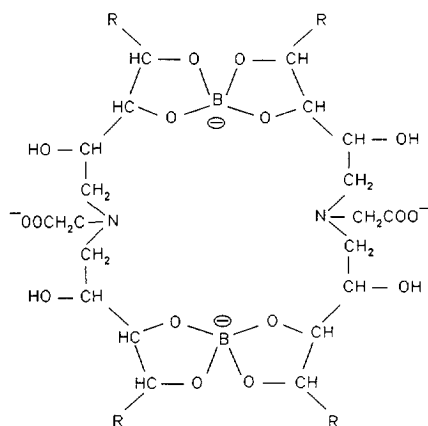


Figure 7. The proposed diborate ester structure for 4b and 4d with the borate bound at the threo-3,4 positions $R=CHOHCH_2OH$.

CONCLUSIONS

We have been able to synthesize bis(polyhydroxyalkyl)amines via catalytic hydrogenation of polyhydroxy oximes. The corresponding N-carboxymethyl derivatives have shown to possess strong Ca(II) and Cd(II) sequestering properties, both in the absence and presence of borate. ^{11}B and ^{13}C NMR measurements have revealed that in mixtures of borate and bis(polyhydroxyalkyl)amines and their N-carboxymethyl derivatives a new type of borate esters, probably cyclic diborate diesters, is formed.

EXPERIMENTAL

NMR measurements

^{11}B NMR spectra (external 0.1 M boric acid in D_2O) were recorded at 25 °C with Varian VXR-400 S (128.3 MHz) or Nicolet NT-200 WB (64.2 MHz) spectrometers. Baseline

correction was applied to remove the broad signal of the boron incorporated in the glass sample tube and in the insert. Usually a deconvolution program was used to obtain all the signal characteristics. ^{13}C NMR spectra (internal t-butanol, δ 31.2) were recorded at the same spectrometers at 100.6 and 50.3 MHz, respectively. Samples were prepared by dissolution of the appropriate amounts of boric acid and ligand in D_2O . The total boron concentration was 0.05-0.20 M whereas the concentrations of the bis(polyhydroxyalkyl)amines and their N-carboxymethyl derivatives were 0.00-0.31 M. The pH was adjusted with NaOH or HCl and was measured with a calibrated MI 412 micro-combination probe (Microelectrodes, Inc.) or with a calibrated Z11,344-1 combination pH electrode (Aldrich). The pH values are direct meter readings.

Ca^{2+} , Cu^{2+} , Cd^{2+} , and Ba^{2+} ions were added to the borate ligand systems as their chloride salts. Metal ion sequestering capacities were determined according to Mehlretter et al.¹ Cd^{2+} and Ca^{2+} sequestering capacities (CdSC and CaSC, respectively), were determined at ambient temperature by adding a solution of Cd^{2+} or Ca^{2+} chloride to a solution containing 50-100 mg of ligand. CdSC and CaSC, were determined at pH 6.9, by using oxalate as the indicator. Solutions of ligand and Cd^{2+} slowly turned turbid. As the end point of a titration, the first turbidity that appeared within 2 min after the last addition of Cd^{2+} was taken. At pH 11.5, CdSC and CaSC were determined with the use of NaOH/ Na_2CO_3 as the indicator. As end point of a titration the first turbidity that had not disappeared within 30 s was taken.

FAB mass spectra

A VG 70-250 SE mass spectrometer was used with glycerol as the matrix.

Synthesis

Bis(D-arabino-2,3,4,5-tetrahydroxypentyl)amine (2a). - To a solution of D-arabinose oxime (17.94 g, 109 mmol) in water (150 mL), 5% Pt/C (1.4 g) was added, and the mixture was hydrogenated during 24 h at 50° and 100 atm H_2 . The mixture was filtered, concentrated, and the residue was crystallized from 3:2 methanol-water to give 2a (4.06 g, 26.1 %), m.p. 175-176 °C (dec.); $[\alpha]_{\text{D}}^{25} + 14.1^\circ$ (c, 0.9, water); ^{13}C NMR data (pD 10.6, D_2O): δ 52.7 (C-1,1'), 69.9, 72.6, 73.5 (C-2,2',3,3',4,4'), 64.5 (C6,6'); FAB mass spectrum: m/z 286 [100% (M + H)⁺]. Anal. Calc. for $\text{C}_{10}\text{H}_{23}\text{NO}_8$: C, 42.08; H, 8.13; N,

4.91. Found: C, 42.01; H, 8.19; N, 4.92.

Bis(D-manno-2,3,4,5,6-pentahydroxyhexyl)amine (2b). - Prepared from D-mannose oxime (15.03 g) according to the procedure described above 2b, (6.54 g, 49.2%), m.p. 185-186 °C (dec.); $[\alpha]_{D}^{25} + 2.44^{\circ}$ (c 0.9, water); ^{13}C NMR data (pD 11.0, D_2O): δ 52.8 (C-1,1'), 70.6, 70.9, 72.4, 72.9 (C-2,2',3,3',4,4',5,5') 64.8 (C-6,6'); FAB mass spectrum: m/z 346 [100%, (M + H)⁺]. Anal. Calc. for $\text{C}_{12}\text{H}_{27}\text{NO}_{10}$: C, 41.72; H, 7.88; N, 4.06. Found: C, 41.50; H, 7.54; N, 3.97.

Bis(D-galacto-2,3,4,5,6-pentahydroxyhexyl)amine (2c). - Prepared from D-galactose oxime (5.0 g) according to the procedure described above. 2c (3.51 g, 79.5%), m.p. 195-196 °C (dec.); $[\alpha]_{D}^{25} - 11.7^{\circ}$ (c 0.9, water); ^{13}C NMR data (pD 10.8, D_2O): δ 52.9 (C-1,1'), 69.9, 71.1, 71.8, 72.6 (C-2,2',3,3',4,4',5,5'), 64.8 (C-6,6'); FAB mass spectrum: m/z 346 [100%, (M + H)⁺]. Anal. Calc. for $\text{C}_{12}\text{H}_{27}\text{NO}_{10}$: C, 41.72; H, 7.88; N, 4.06. Found: C, 41.52; H, 7.89; N, 4.02.

Bis(D-gluco-2,3,4,5,6-pentahydroxyhexyl)amine (2d). - To a solution of D-glucose (20.6 g, 111 mmol) and D-gluco-2,3,4,5,6-pentahydroxyhexylamine (23.6 g, 130 mmol) in H_2O (100 mL, pH 11.4), 5% Pt/C (1.5 g) was added, and the mixture was hydrogenated during 24 hr at 50° and 100 atm H_2 . The mixture was filtered, concentrated and the residue was crystallized from 1:1 methanol-water to give 2d (12.1 g, 31.6%), m.p. 180-181 °C (dec.); $[\alpha]_{D}^{25} - 19.2^{\circ}$ (c 0.9, water); ^{13}C NMR data (pD 9.8, D_2O): δ 51.8 (C-1,1'), 72.2, 72.3, 72.6 (C-2,2',3,3',4,4',5,5'), 64.4 (C-6,6'); FAB mass spectrum m/z 346 [78%, (M + H)⁺]. Anal. Calc. for $\text{C}_{12}\text{H}_{27}\text{NO}_{10}$: C, 41.72; H, 7.88; N, 4.06. Found: C, 41.45; H, 7.62; N, 4.07.

N-methylenecarboxybis(D-manno-2,3,4,5,6-pentahydroxyhexyl)amine (4b). -The pH of a solution of 2b (4 g, 11.6 mmol) and bromoacetic acid (3.2 g, 23.2 mmol) in water (40 mL) was raised to 10-11 with LiOH. The mixture was heated for 5 h at 90° when no 2b remained. The mixture was concentrated in vacuo and the residue was eluted from a column (50 x 3 cm) of Dowex 50 W (H^+) resin with a gradient of 0 → 0.7 M NH_4OH . The fractions obtained were concentrated and analyzed by ^{13}C NMR spectroscopy. Pure 4b (1.5 g, 32.1%) was isolated; ^{13}C NMR data (pD 1.3, D_2O): δ 57.6 (C-1,1'), 66.3 (C-2,2'), 70.4, 72.2, 72.8 (C-3,3',4,4',5,5') 64.6 (C-6,6'), 59.9 (b, C-7), 170.6 (C-8); FAB mass spectrum: m/z 404 [42%, (M + H)⁺], 346 [14%, ($\text{M}^+ - \text{CH}_2\text{COO}$)].

N-methylenecarboxybis(D-galacto-2,3,4,5,6-pentahydroxyhexyl)amine (4c). -Treatment

of 2c (2 g, 5.8 mmol) bromoacetic acid (1.6 g, 11.6 mmol) as described for 2b gave 4c (0.9 g, 39%); ^{13}C NMR data (pD 0.6, D_2O): δ 56.8 (C-1,1'), 65.8 (C-2,2'), 70.8, 71.4, 71.8 (C-3,3',4,4',5,5'), 64.6 (C-6,6'), 60.1 (b, C-7), 170.1 (C-8); FAB mass spectrum: m/z 404 [33%, (M + H) $^+$].

N-Methylenecarboxybis(D-gluco-2,3,4,5,6-pentahydroxyhexyl)amine (4d). -Treatment of 2d (7.0 g, 20.3 mmol) with bromoacetic acid (5.5 g, 39.6 mmol), as described for 2b, gave 4d (2.4 g 29.3%); ^{13}C NMR data (pD 6.7, D_2O): δ 58.6 (C-1,1'), 68.2 (C-2,2'), 72.2, 72.3, 72.5 (C-3,3',4,4',5,5'), 64.3 (C-6,6'), 58.3 (b, C-7) 172.08 (C-8); FAB mass spectrum: m/z 404 [10%, (M + H) $^+$].

ACKNOWLEDGEMENTS

This investigation was supported by the Dutch National Innovation Oriented Program Carbohydrates (IOP-k) and Akzo Nobel Central Research. We thank Mr. A. Sinnema for recording some of the NMR spectra and Mrs. A. Knol-Kalkman for measuring the FAB mass spectra, and Hüls Aktiengesellschaft for kindly supplying D-gluco-2,3,4,5,6-pentahydroxyhexylamine (D-glucamine).

REFERENCES

1. Mehlretter, C.L.; Alexander, B.H.; Rist, C.E. *Ind. Eng. Chem.* **1953**, *45*, 2782.
2. Floor, M.; Hofsteede, L.P.M.; Groenland, W.P.T.; Verhaar, L.A.Th.; Kieboom, A.P.G.; van Bekkum, H. *Recl. Trav. Chim. Pays-Bas* **1989**, *108*, 384.
3. Floor, M.; Koek, J.H.; Smeets, F.L.M.; Niemantsverdriet, R.E.; Peters, J.A.; van Bekkum, H.; Kieboom, A.P.G. *Carbohydr. Res.* **1990**, *203*, 19.
4. Kelkenberg, H. *Tens. Surf. Det.* **1988**, *25*, 8.
5. Hodge, J.E.; Nelson, E.C.; Moy, B.F. *Agric. Food Chem.* **1963**, *11*, 126.
6. van Duin, M.; Peters, J.A.; Kieboom, A.P.G.; van Bekkum, H. *J. Chem. Soc., Perkin Trans. 2* **1987**, 473.
7. van Duin, M.; Peters, J.A.; Kieboom, A.P.G.; van Bekkum, H. *Carbohydr. Res.* **1987**, *162*, 65.

8. van Duin, M.; Peters, J.A.; Kieboom, A.P.G.; van Bekkum, H. *J. Chem. Soc., Dalton Trans.* **1987**, 2051.
9. van Haveren, J.; Peters, J.A.; Batelaan, J.G.; Kieboom, A.P.G.; van Bekkum, H. *J. Chem. Soc., Dalton Trans.* **1991**, 2649.
10. van Haveren, J.; Peters, J.A.; Batelaan, J.G.; Kieboom, A.P.G.; van Bekkum, H. *Inorg. Chim. Acta* **1993**, 205, 1.
11. Hodge, J.E.; Moy, B.F. *J. Org. Chem.* **1963**, 28, 2784.
12. Kagan, F.; Rebenstorf, M.A.; Heinzelmann, R.V. *J. Am. Chem. Soc.* **1957**, 79, 3541.
13. Paul, R. *Bull. Soc. Chim. Fr.* **1937**, 4, 1121.
14. Heard, D.D.; Hudson, B.G.; Barker, R. *J. Org. Chem.* **1970**, 35, 464.
15. Ryan, G.; Utley, J.H.P. *Tetrahedron Lett.* **1988**, 29, 3699.
16. Finch, P.; Merchant, Z. *J. Chem. Soc. Perkin Trans. 1* **1975**, 1682.
17. Henderson, W.G.; How, M.J.; Kennedy, G.R.; Mooney, E.F. *Carbohydr. Res.* **1973**, 28, 1.
18. van Duin, M.; Peters, J.A.; Kieboom, A.P.G.; van Bekkum, H. *Tetrahedron* **1984**, 40, 2901.
19. Böeseken, J. *Adv. Carbohydr. Chem.* **1949**, 4, 189.
20. Bell, C.F.; Beauchamp, R.D.; Short, E.L. *Carbohydr. Res.* **1989**, 185, 39.
21. Makkee, M.; Kieboom, A.P.G.; van Bekkum, H. *Carbohydr. Res.* **1985**, 138, 225.
22. van Duin, M.; Peters, J.A.; Kieboom, A.P.G.; van Bekkum, H. *Tetrahedron* **1985**, 4, 3411.
23. van Duin, M.; Peters, J.A.; Kieboom, A.P.G.; van Bekkum, H. *Recl. Trav. Chim. Pays-Bas* **1986**, 105, 488.
24. Nöth, H.; Wrackmeyer, B. *NMR Basic Princ. Prog.* **1978**, 14, 6.
25. Abragam, A. In *The principles of Nuclear Magnetism* **1961** Clarendon Press; Oxford.
26. Chapelle, S.; Verchere, J.F. *Tetrahedron* **1988**, 44, 4469.



Chapter 6

COORDINATION OF Cd(II) BY N-ALKYLAMINO SUGARS IN AQUEOUS SOLUTION AS STUDIED BY POTENTIOMETRY AND ^{113}Cd NMR SPECTROSCOPY

ABSTRACT

The Cd(II) coordination of 1-deoxy-1-(2-aminoethylamino)-D-alditols (1a-b) and of 1-deoxy-1-(2-aminopropylamino)-D-alditols (2a-b) was investigated by means of ^{113}Cd NMR spectroscopy and potentiometry. The protonation constants of 1a-b and 2a-b, determined from plots of ^{13}C chemical shifts versus pH, were in good agreement with those obtained by potentiometry. The Cd(II) stability constants for ligands 1a-b and 2a-b and the Ni(II) stability constants for 1a were determined by potentiometry. The geometry of the Cd(II) complexes of 1a-b and 2a-b was studied by ^{113}Cd NMR spectroscopy. For 1a-b three separate ^{113}Cd resonances for free Cd(II), CdL, and CdL₂ are observed, indicating these species to be in slow exchange. From the ^{113}Cd chemical shifts for CdL and CdL₂, it could be concluded that at neutral pH both primary and secondary N-atoms are involved in coordination. At high pH additional coordination of one of the hydroxyl groups of the carbohydrate chain occurs.

INTRODUCTION

The study of interactions between sugars and metal ions has become important in

bioinorganic chemistry, environmental chemistry and chemical technology.^{1,2} Amino sugars are in general able to form more stable metal ion complexes than neutral nitrogen-free sugars. Current research on the interactions of metal ions with amino sugars is focused mainly on 2-amino-2-deoxy sugar derivatives³⁻⁸ and on N-glycosides derived from readily available aldohexoses and bifunctional amines such as ethylenediamine (EN) and 1,3-diaminopropane (DAP).^{9,10} Metal ion complexes derived from amino sugars might be useful as (chiral) catalyst. Tanase et al. described the first example of a catalytic reaction mediated by metal complexes containing N-glycosides.¹¹ They used Cu(II) N-glycosides complexes derived from readily available aldohexoses (D-glucose and D-mannose) and EN as the catalyst in the epoxidation of several prochiral olefins.

Recently we described the synthesis of 1-alkylamino-alditols (1a-b and 2a-b).¹² The amino sugars were obtained by reductive amination of D-galactose and D-mannose with EN and DAP using platinum (5%) on activated carbon as the catalyst.

In the present paper, a study on the coordinating versatility of this type of amino sugars to Cd(II) and Ni(II) in aqueous media is reported. The protonation constants were determined by ¹³C NMR spectroscopy and are compared with those obtained by potentiometry. The stability constants of Cd(II) and Ni(II) complexes with 1a-b and 2a-b are presented.

¹¹³Cd NMR spectroscopy is a powerful technique for determining the number and type of coordinating groups around a Cd(II) metal centre and has, therefore, become an important tool in bio-organic chemistry.^{13,14} It has been principally used in the study of metalloproteins in which Zn(II), Cu(II), Mg(II), or Ca(II) ions are replaced by Cd(II). The deshielding of ¹¹³Cd by the ligand donor site increases in the order O < N < S, and the chemical shift range exceeds 900 ppm.¹⁵ The structures of the Cd(II) complexes of 1a-b and 2a-b were investigated by ¹¹³Cd NMR spectroscopy.

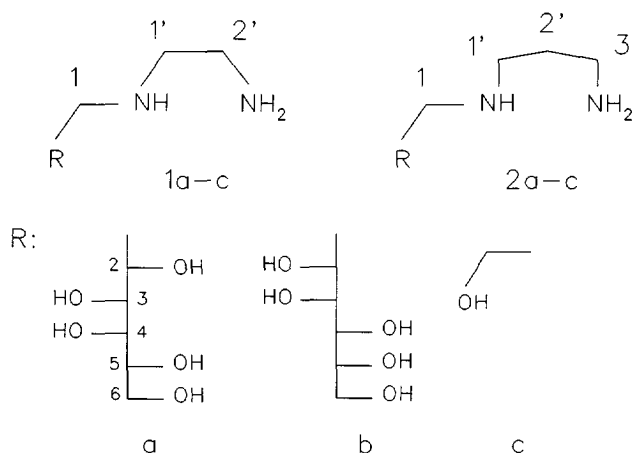


Figure 1. The structures of the N-alkylamino sugars (1a-c and 2a-c) discussed in this work.

RESULTS AND DISCUSSION

Protonation

Plots of ^{13}C chemical shifts as a function of pH may be useful for the assignment of ^{13}C NMR resonances of molecules possessing basic functionalities. They also afford the protonation schemes of compounds, which are of interest in relation to the coordination with metal ions. The plots obtained are typical titration curves and (microscopic) pK_a values of the various amino groups in a ligand can be obtained by applying the Henderson-Hasselbach equation¹⁶ to the δ values near the point of inflection. The effect of protonation on the ^{13}C chemical shift of amines has been studied extensively.^{17,18} Christiansen-Brans et al. have described the ^{13}C chemical shift pH titration curves of 1-amino alditols derived from cellobiose, lactose, and maltose and determined pK_a values (9.4) for this type of amino sugars.¹⁹ Here we extend this to 1-alkylamino-D-alditols possessing a primary as well as a secondary amino function.

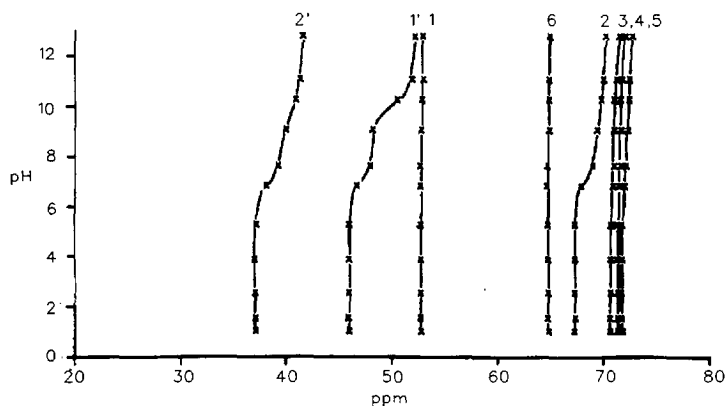


Figure 2. ^{13}C NMR pH titration curve of a 0.02 M solution of 1a measured at 50.3 MHz and 293 K; numbering of carbons as in Figure 1.

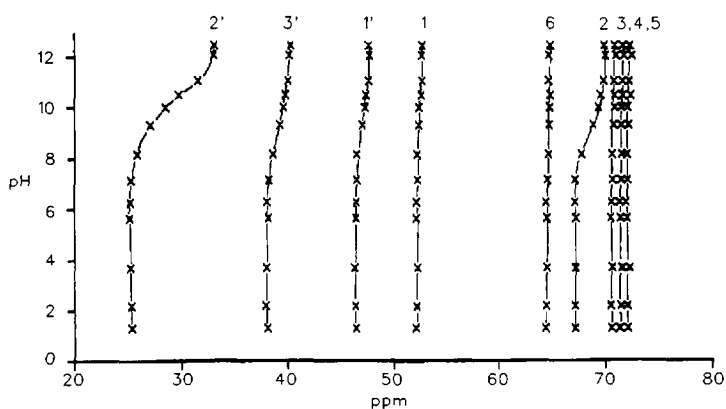


Figure 3. ^{13}C NMR pH titration curve of a 0.02 M solution of 2a measured at 50.3 MHz and 293 K; numbering of carbons as in Figure 1.

In Figures 2 and 3 the ^{13}C NMR chemical shift pH titration curves of 1a and 2a are presented. Ligands 1b and 2b exhibit similar plots except for the characteristic sugar window ($\delta = 65 - 75$ ppm). The protonation shifts ($\Delta_c = \delta$ protonated form - δ free base) appear to be upfield.^{17,18} The protonation of the N-atoms has a relatively large influence on the ^{13}C chemical shift of β -positioned carbon atoms owing to electrical field effects.

Upon decreasing the pH, protonation of 1a occurs initially at the primary amine function as demonstrated by a $\Delta_{C-1'}$ of -5.9 ppm and relatively small protonation shifts of the ^{13}C nuclei of the sugar chain. Subsequent protonation of the secondary amine function causes substantial shifts of both C-2 ($\Delta_{C-2} = -2.7$ ppm) and C-2' ($\Delta_{C-2'} = -4.2$ ppm). The ^{13}C chemical shift titration curve of 2a (Figure 3) shows a relatively large protonation shift of C-2' ($\Delta_{C-2'} = -7.1$ ppm) as a consequence of a double β -effect. Protonation of the secondary amine function results in a protonation shift of C-2 of -2.6 ppm. The pK_a values obtained from these NMR titration curves are given in Table 1.

Table 1. Protonation constants as determined by NMR (measured at 50.3 MHz, $I = 0.25$ M and 295 K) and potentiometry (measured at 295 K and $I = 0.1$ M).

| Compound | Method | pK_{a1}^a | pK_{a2}^a | ΣpK_a |
|---------------|----------------------------|--------------------|--------------------|---------------------|
| 1a | NMR ^b | 9.9 | 7.2 | 16.7 |
| | potentiometry ^c | 9.48 | 6.39 | 15.87 |
| 1b | NMR | 9.7 | 7.3 | 16.6 |
| | potentiometry | 9.27 | 6.59 | 15.86 |
| 2a | NMR | 10.6 | 8.9 | 19.1 |
| | potentiometry | 10.63 | 8.46 | 19.09 |
| 2b | NMR | 10.5 | 8.6 | 19.0 |
| | potentiometry | 10.75 | 8.52 | 19.27 |
| 1c (hen-(OH)) | NMR | 9.8 | 6.6 | 16.0 |
| | potentiometry ^d | 9.59 | 6.64 | 16.23 |
| 2c (hep-(OH)) | NMR | 10.3 | 8.0 | 17.9 |
| | potentiometry ^d | 10.19 | 7.95 | 18.14 |
| EN | potentiometry ^d | 10.0 | 7.1 | 17.1 |
| DAP | potentiometry ^d | 10.5 | 8.7 | 19.2 |

^a pK_{a1} is assigned to the deprotonation of the protonated primary amino function, and pK_{a2} to that of the secondary one (see text); ^b error ± 0.1 ; ^c error ± 0.05 ; ^d ref. 20

We determined pK_a values for 1a,b, 2a,b, 1-amino-2-((2-hydroxyethyl)amino)ethane (hen-(OH), 1c), and 1-amino-3-((2-hydroxyethyl)amino)propane (hep-(OH), 2c) by potentiometry. These data are included in Table 1. It can be seen that the pK_a values obtained by NMR agree well with those obtained by potentiometry.

Comparison of the pK_a values of ethylamine and ethanolamine (10.81 and 9.50,²⁰

respectively) shows that the presence of a β -hydroxyl group generally results in a decrease of the pK_a . For all ligands under study the pK_a of the secondary amine function appears to be lower than that of the primary amine function due to inductive effects caused by the C-2 hydroxyl group. This effect is also observed for hen-(OH) (1c) and hep-(OH) (2c) when plotting the ^{13}C chemical shift versus pH. The pK_{a1} values of 1a-c and 2a-c are similar to those of EN and DAP, respectively. This indicates that the substituent effect on the primary amine function for all these compounds is of the same order. The results show that the configuration of the carbohydrate chain, either D-galacto or D-manno, does not affect the protonation.

Metal Ion Sequestering Capacities

A practical way to obtain information on the complexation behaviour and crystal growth inhibition is to carry out metal ion sequestering experiments. The Cd(II) sequestering capacities (CdSC) at ambient temperature and pH 11.6 are presented in Table 2. Ligands 1a-b possess good CdSC abilities in comparison to 2a-b. This can be ascribed to a decrease in complex stability of the Cd(II) complexes caused by an increase of the chelate ring size from five- to six membered as the result of an enthalpy effect.²¹ The corresponding model compounds, hen-(OH) (1c) and hep-(OH) (2c) show comparable CdSC properties.

Table 2. Cadmium(II) sequestering capacities (CdSC) measured at pH 11.6 and 295 K.

| Ligand | CdSC |
|--------|-------------------------------------|
| 1a | 224 ^a (0.4) ^b |
| 1b | 279 (0.6) |
| 1c | 650 (0.6) |
| 2a | 82 (0.2) |
| 2b | 68 (0.1) |
| 2c | 175 (0.2) |

^a mg Cd/ g ligand; ^b mol Cd/ mol ligand

The ligand stability constants for Cd(II) of the ligands under study and their

corresponding structural analogues as determined by potentiometry are summarized in Table 3. The Cd(II) stability constants of 1a obtained in this way are in excellent agreement with those determined by ^{113}Cd NMR speciation.²²

Table 3. Cd(II) and Ni(II) stability constants of 1a-b, 2a-b, 1c, EN and DAP as determined by potentiometry at 295 K and $I = 0.1$ M.

| Ligand | $\log \beta$ (Cd(II)) ^a | $\log \beta$ (Ni(II)) ^a |
|------------------|------------------------------------|------------------------------------|
| 1a | 4.54, 8.41 | 6.01, 10.70 |
| 1b | 5.24, 9.97 | |
| 1c ^b | 4.9, 9.2 | 6.8, 12.4 |
| 2a | 4.31, 7.68 | |
| 2b | 4.50, 7.63 | |
| EN ^b | 5.45, 9.98, 11.74 | 7.3, 13.5, 17.7 |
| DAP ^b | 4.50, 7.20, 8.0 | |

^a values for $[\text{ML}]/[\text{M}][\text{L}]$, $[\text{ML}_2]/[\text{M}][\text{L}]^2$, and $[\text{ML}_3]/[\text{M}][\text{L}]^3$, ^b ref. 20

The complexation constants β_{CdL} and β_{CdLL} of the equilibrium shown in Eqn. (1), are defined in Eqn. (2).



$$\beta_{\text{CdL}} = [\text{CdL}] / [\text{Cd}][\text{L}] \quad (2a)$$

$$\beta_{\text{CdLL}} = [\text{CdL}_2] / [\text{Cd}][\text{L}]^2 \quad (2b)$$

There is generally a linear correlation for a series of complexes of a particular M^{n+} ion between ΣpK_a of (multiprotic) ligands (L) and the logarithm of the stability constant β . When the Cd(II) stability constants of 1a-b and 2a-b are compared to those of EN and DAP, respectively, it is obvious that 1a has an exceptional complexation behaviour. Its Cd(II) stability constants are substantially lower than those of 1b and EN although the ΣpK_a values for all these ligands are similar. The Cd(II) stability constants of hen-(OH) (1c) are in between those of 1a and 1b. In the case of 2a, 2b and DAP, also having similar ΣpK_a values, there is no significant difference in the determined Cd(II) stability constants. Apparently, the above described conformational preference involved in the

coordination of Cd(II) by N-alkylamino sugars

complexation of Cd(II) does not occur in this type of ligands.

The ligands 1a-b and 2a-b form complexes with 1:1 and 1:2 metal:ligand stoichiometry. The 1:3 complexes are not observed. Probably the stability of these latter complexes is low due to the steric interactions between the polyhydroxy chains. In the parent systems (EN and DAP), however, the 1:3 complexes do occur.

The magnitudes of the stability constants of the Cd(II) complexes of the sugar derivatives are the same as those of EN and DAP, which suggests that the coordination of Cd(II) is similar for these ligands; probably all ligands coordinate to Cd(II) in a bidentate fashion via the two N-atoms.

The ligand stability constants for Ni(II) complexes of 1a, 1c and EN as determined by potentiometry are about two orders of magnitude larger than those of the corresponding Cd(II) complexes (Table 3). The trends observed in these stability constants, however, are the same as in the Cd(II) complexes.²³

Table 4. ¹¹³Cd chemical shifts of Cd(II) complexes of 1a-c and 2a,b^{a,b}, measured at 88.7 MHz and 295 K.

| Ligand | δ_{obs} | |
|-----------------|-----------------------|------------------|
| | CdL | CdL ₂ |
| 1a | 110 | 240 |
| 1b | 108 | 242 |
| 1c | 108 | 239 |
| 2a ^c | - | 209 |
| 2b ^c | - | 212 |

^a for 1a-c Cd(II)/ L = 1; for 2a,b Cd(II)/ L = 0.25; 0.1M Cd(ClO₄)₂ is used as reference; ^b δ_{calcd} for all ligands: 126 ppm (CdL) and 252 (CdL₂), assuming that the N atoms are the donor sites; ^c CdL species could not be observed for 2a,b

¹¹³Cd NMR Spectroscopy

The observed and calculated ¹¹³Cd chemical shifts for ligands 1a,b, 2a,b and hen-(OH) (1c) in aqueous solution at pH 7 are presented in Table 4. Summers and Marzilli^{24,25} reported that ¹¹³Cd chemical shifts can be calculated within 5% by implementing the following relationship:

$$^{113}\text{Cd} \text{ chemical shift} = 75A + 51B + 31C$$

where A, B, and C are the numbers of primary, secondary and tertiary amine donors, respectively. Since chelate ring size and chelate basicity have also a large effect on the ^{113}Cd chemical shift, the above mentioned relationship must be used cautiously.²⁶

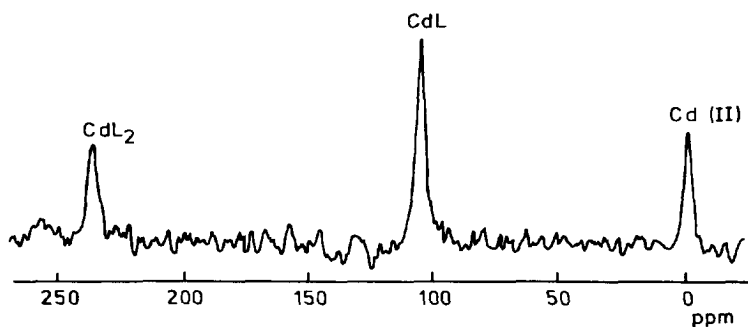


Figure 4. ^{113}Cd spectrum of a 0.1 M solution of 1a with (Cd(II)/L) molar ratio (ρ) = 1 and pH = 7.50 measured at 88.7 MHz and 295 K.

In Figure 4 the ^{113}Cd NMR spectrum of 1a at (Cd(II)/L) molar ratio (ρ) 1 and at pH 7.50 is illustrated. Three signals are observed at 0, 110 and 240 ppm. Upon altering ρ , the chemical shifts of these signals do not change, indicating that the corresponding species are in slow exchange on the ^{113}Cd NMR time scale. On the basis of the intensities of the signals as a function of ρ , these signals are assigned to free (hydrated) Cd, CdL and CdL₂, respectively. With the use of the Summers-Marzilli additivity relationship it can be concluded that for CdL and CdL₂ both the primary and secondary N-atom are involved in coordination, which is in agreement with the results of potentiometry described above.

Owing to precipitation occurring at higher ρ values ($0.6 < \rho < 2$) only ^{113}Cd spectra (pH ± 7) at lower ρ values ($\rho < 0.5$) could be obtained for 2a and 2b. Only a single signal is observed at 240 ppm. Upon altering ρ , the chemical shift of this signal does not change and no other signals were observed, indicating CdL₂ to be the only cadmium complex present. As mentioned before the ligand basicity and the chelate ring size profoundly affect the ^{113}Cd chemical shift. The ^{113}Cd nucleus deshielding (higher chemical shifts) increases with increasing ligand basicity due to metal-ligand σ -bond formation.²⁶ The

deshielding order with regard to the chelate ring size is five- > six- > seven-membered chelate ring. It is obvious from the data summarized in Table 4 that the chelate ring strain compensates the effect of change in basicity because the ΣpK_a values of 1a,b are approximately 2.5 pK_a units lower than those of 2a,b (Table 1). The ^{113}Cd NMR spectrum of hen-(OH) (1c) closely resembles that of 1a and 1b implying that the hydroxyl groups HO-3, HO-4, HO-5 and HO-6 in 1a and 1b are not involved in the Cd(II) coordination. The ^{13}C NMR spectrum of 1a and 1b at $\rho = 1$ and at pH = 7.5 shows one set of 8 signals indicating the present cadmium species and free ligand to be in fast exchange on the ^{13}C NMR time scale.

Increasing the pH of a solution of 1a at $\rho = 1$ starting at pH = 7.50 initially causes precipitation, but upon increasing the pH to 12.2 a clear solution is obtained. Several signals between 225 and 240 ppm are observed by ^{113}Cd NMR. The corresponding ^{13}C NMR spectrum shows several sets of resonances which are relatively broad. Increasing the pH presumably gives a oligomeric mixture containing several CdL species. At $\rho = 0.75$ and pH = 12.2 in the ^{113}Cd NMR two signals at 231 and 277 ppm are observed; the ^{13}C NMR spectrum shows two sets of 8 signals. Upon further lowering of ρ , the intensity of the signal in the ^{113}Cd NMR spectrum at 277 increases at the expense of that at 231 ppm. The chemical shifts of these signals do not change, suggesting these species to be in slow exchange on the ^{113}Cd NMR time scale. Based on the intensities of the signals as a function of ρ the signals at 231 and 277 ppm are assigned to CdL and CdL₂, respectively. Application of the Summers-Marzilli relationship and correcting for a pH effect it can be concluded that for the CdL₂ species only the primary and secondary N-atoms are involved in the coordination. The observed ^{113}Cd chemical shift at high pH for the CdL (231 ppm) species and that obtained by calculation (125 ppm) differ significantly which cannot be ascribed to a pH effect only. The ^{113}Cd chemical shift increment of ionized hydroxyl groups of Cd(II) complexes in solution is unknown. From the ^{113}Cd chemical shift of solid Cd(OH)₂ (158 ppm),²⁷ this increment can be estimated to be roughly 80 ppm. It, therefore, can be concluded that in the CdL species additional coordination of OH⁻ or one of the ionized hydroxyl groups of the sugar chain occurs.

At lower ρ values two sets of eight resonances are observed in the ^{13}C NMR spectra. From the intensities of these signals obtained at various ρ values one set of signals is assigned to CdL. The other set of signals is assigned to an equilibrium of a CdL₂ species

and free ligand, which are in fast exchange on the ^{13}C NMR time scale. One of the carbon resonances in the sugar window (76.7 ppm) assigned to CdL is downfield compared to the corresponding carbon signals (69.9 - 72.3 ppm) of free ligand at pH = 12.2. This suggests that one of the hydroxyl groups from the polyhydroxy chain is involved in the additional coordination mentioned above. This is supported by the presence of a weak cross peak in the sugar region of a solution at $\rho = 0.66$ and pH = 12.2 using $^1\text{H} - ^{113}\text{Cd}$ heteronuclear multiple quantum correlation (HMQC) spectroscopy. Two-bond $^{13}\text{C} - ^{113}\text{Cd}$ scalar couplings are usually small and could not be observed in the ^{13}C NMR spectrum.

From the NMR data obtained it can be concluded that one of the hydroxyl groups in the polyhydroxy chain is involved in the coordination. It is not clear which hydroxyl group, either HO-2 or HO-3, is actually involved due to severe overlap in the ^1H NMR spectrum.

CONCLUSIONS

The pK_a values obtained for 1a-b and 2a-b by ^{13}C NMR spectroscopy are in good agreement with those obtained by potentiometry. The ΣpK_a values of 2a-b are approximately 2.5 pK_a units higher than those of 1a-b. Due to the large effect of chelate ring strain compared to the change in basicity higher Cd(II) stability constants are found for 1a-b. The configuration of the carbohydrate chain does not influence protonation of the free ligand. From the determined Cd(II) and Ni(II) stability constants it may be concluded that the attachment of a substituent containing a neutral oxygen donor does not result in a significant drop in stability of Cd(II) and Ni(II) complexes. From the ^{113}Cd NMR study it is obvious that at neutral pH both the primary and secondary amine function of 1a and 1b are involved in Cd(II)-coordination. At high pH one of the hydroxyl groups of the polyhydroxy chain is also coordinated.

EXPERIMENTAL

Materials

The reagents used were purchased from Janssen Chimica (Analytical Grade). $\text{Cd}(\text{ClO}_4)_2 \cdot x\text{H}_2\text{O}$ was obtained from Alfa Products. The Cd content of $\text{Cd}(\text{ClO}_4)_2 \cdot x\text{H}_2\text{O}$ was determined using complexometric methods.²⁸ The synthesis of 1a-b and 2a-b has been published elsewhere.¹² The compounds were purified by recrystallization from MeOH/ H_2O (1/9 v/v).

Potentiometry

The potentiometric titrations were conducted at 298 K in a double-walled vessel. Millivolt readings obtained with a glass electrode were converted to pH values using a calibration curve which was determined from standard buffer solutions. The ionic strength was maintained at 0.1 M using NaClO_4 . The protonation constants were determined by titration of a 0.01 M ligand solution with 0.02 M HCl. The Cd(II) and Ni(II) stability constants were determined by titration of 0.01 M $\text{Cd}(\text{ClO}_4)_2$ or 0.01 M NiCl_2 with a 0.01 M ligand solution. All calculations for the potentiometric titrations were performed using a spreadsheet program.^{29,30} The speciation and the stability constants were determined for each point in the titration. The stability constant obtained was used in a speciation simulation generating pH values. In all cases good agreement between the calculated and the experimental pH curve was observed.

Cadmium(II) sequestering capacities

The Cd(II) sequestering capacities were determined according to a procedure of Mehlretter³¹ modified by Akzo Chemicals Research Center in Deventer.³² The CdSC values were obtained by adding aqueous 0.1 M $\text{Cd}(\text{ClO}_4)_2$ to a solution containing 100 mg ligand at room temperature and pH 11.6 using $\text{NaOH}/\text{Na}_2\text{CO}_3$ as the indicator. The turbidity which remained for more than 30 s was taken to be the endpoint of the titration.

NMR spectroscopy

The ^{13}C NMR spectra were recorded at 295 K on a Nicolet NT-200 WB NMR spectrometer (50.3 MHz) and on a Varian VXR-400 S NMR spectrometer (100.6 MHz)

using 30% D₂O (for locking) in water as the solvent with *t*-butanol ($\delta = 31.2$ ppm) as the internal reference. The ¹³C spectra (50.3 MHz) were recorded using 16K datapoints, a spectral width of 12 KHz, broadband ¹H decoupling and an acquisition delay of 10 s. For ¹³C NMR 0.02 M solutions of amino sugar, hen-(OH) or hep-(OH) were used. The pH was adjusted to 1 using 1 M HCl. Subsequently, the pH was raised from 1 to 12 in intervals of approximately 1 using 1 M NaOH. The pH was measured with a calibrated Z11,344-1 Aldrich combination pH electrode. The values given are direct meter readings. The ¹¹³Cd NMR spectra were recorded on a Varian VXR-400 S NMR spectrometer at 88.7 MHz using 48K datapoints, a spectral width of 50 KHz, and 0.1M Cd(ClO₄)₂ as an external reference. A 60° pulse was applied and the acquisition delay was 2.5 s. Solutions were prepared by dissolving the appropriate amounts of Cd(ClO₄)₂·xH₂O and ligand in D₂O. The total Cd(II) concentration was 0.1 M. The pH was adjusted to 7 using diluted solutions of 60% aqueous HClO₄. The ionic strength was approximately 0.25 M. The ¹H-¹¹³Cd correlated spectra were obtained with the HMQC method.³³

ACKNOWLEDGEMENTS

This investigation was carried out with support of the Dutch National Innovation Program Carbohydrates. We are grateful to Akzo Nobel Central Research (ACR) for their financial support and to Dr. J. Huskens and Miss A.D. Kennedy for performing some of the potentiometric titration experiments.

REFERENCES

1. Angyal, S.J. *Adv. Carbohydr. Chem. Biochem.* **1989**, 47, 1.
2. Geraldes, G.F.G.C.; Castro, M.M.C.A. In *Metal Speciation in the Environment*, Springer-Verlag: Berlin, 1990, NATO ASI Series, vol. G 23, p 105.
3. Hirano, S.; Kondo, Y.; Nakazawa, Y. *Carbohydr. Res.* **1982**, 100, 431.
4. Muzzarelli, R.A.A.; Tanfani, F.; Emanuelli, M.; Mariotti, S. *Carbohydr. Res.* **1982**, 107, 199.
5. Muzzarelli, R.A.A.; Raithand, G.; Tubertini, O. *J. Chrom.* **1970**, 47, 414.

6. Dobbetti, L.; Delben, F. *Carbohydr. Polymers* **1992**, *18*, 273.
7. Kozłowski, H.; Decock, P.; Olivier, I.; Micera, G.; Pusino, A.; Pettit, L.D. *Carbohydr. Res.* **1990**, *197*, 109.
8. Bunel, S.; Ibarra, C.; Moraga, E.; Calvo, V.; Blaskó, A.; Bunton, C.A. *Carbohydr. Res.* **1993**, *239*, 185.
9. Tanase, T.; Takei, T.; Hidai, M.; Yano, S. *J. Chem. Res. (S)* **1992**, 252.
10. Yamauchi, T.; Fukushima, K.; Yanagihara, R.; Osanai, S.; Yoshikawa, S. *Carbohydr. Res.* **1990**, *204*, 233.
11. Tanase, T.; Mano, K.; Yamamoto, Y. *Inorg. Chem.* **1993**, *32*, 3995.
12. Lammers, H.; Peters, J.A.; van Bekkum, H. *Tetrahedron* **1994**, *50*, 8103.
13. Summers, M.F. *Coord. Chem. Rev.* **1988**, *86*, 43.
14. Coleman, J.E. in *Methods in Enzymology (Metallobiochemistry Pt. D. Physical and spectroscopic methods for probing metal ion environments in metalloproteins)* Riordan, J.F.; Vallee, B.L., eds.; Academic Press: San Diego, 1993, vol. 227, pp. 16-43.
15. Ellis, P.D. *Science* **1983**, *221*, 1141 and references therein.
16. Breitmaier, E.; Völler, W. *Carbon-13 NMR Spectroscopy*, 3rd ed.; VCH: New York, 1987, pp. 122-123.
17. Sarneski, J.E.; Suprenant, H.L.; Molen, F.K.; Reilley, C.N. *Anal. Chem.* **1975**, *47*, 2116.
18. Batchelor, J.G.; Feeney, J.; Roberts, G.C.K. *J. Magn. Res.* **1975**, *20*, 19.
19. Christiansen-Brams, I.; Meldal, M.; Bock, K. *J. Carbohydr. Chem.* **1992**, *11*, 813.
20. Smith, R.M.; Martell, A.E. *Critical Stability Constants* Plenum Press: New York, 1975, vol. 2.
21. Hancock, R.D. *J. Chem. Educ.* **1992**, *8*, 615.
22. Huskens, J.; Lammers, H.; van Bekkum, H.; Peters, J.A. *Magn. Res. Chem.* **1994**, *32*, 691.
23. Hancock, R.D.; Martell, A.E. *Chem. Rev.* **1989**, *89*, 1875.
24. Summers, M.F.; Marzilli, L.G. *Inorg. Chem.* **1984**, *23*, 523.
25. Summers, M.F.; van Rijn, J.; Reedijk, J.; Marzilli, L.G. *J. Am. Chem. Soc.* **1986**, *108*, 4254.
26. Munkata, M.; Kitagawa, S.; Yagi, F. *Inorg. Chem.* **1986**, *25*, 964.
27. Goodfellow, R.J. In *Multinuclear NMR*, Mason, J., ed.; Plenum Press: New York, 1987, p. 576.
28. Schwarzenbach, G.; Flaschka, H. *Complexometric Titrations*, 2nd ed.; Methuen & Co Ltd: London, 1969, pp. 268-271.

29. van Westrenen, J.; Khizhnyak, P.L.; Choppin, G.R. *Comput. Chem.* **1991**, *15*, 121.
30. Huskens, J.; Peters, J.A.; van Bekkum, H. *Comput. Chem.*, in print.
31. Mehlretter, C.L.; Alexander, B.H.; Rist, C.E.; *Ind. Eng. Chem.* **1953**, *45*, 2782.
32. Bekendam, G. (Akzo Chemicals Research Center Deventer), Technical Leaflet 104.
33. Frey, M.H.; Wagner, G.; Vařák, M.; Sørensen, O.W.; Neuhaus, D.; Wörgötter, E.; Kägi, J.H.R.; Ernst, R.R.; Wüthrich, K. *J. Am. Chem. Soc.* **1985**, *107*, 6847.



Chapter 7

DETERMINATION OF STABILITY CONSTANTS OF METAL COMPLEXES FROM NMR CHEMICAL SHIFTS AND RELAXATION RATES USING A SPREADSHEET COMPUTER PROGRAM.*

ABSTRACT

The versatility of multinuclear magnetic resonance techniques in the determination of stability constants of metal complexes is demonstrated for three cases in which potentiometry is impossible or less suitable. The complexation of trimetaphosphate to lanthanide aminopolycarboxylate complexes is investigated in a dilution experiment using ^{31}P NMR shifts. The stabilities of CdL and CdL_2 ($\text{L} = 1\text{-}(2\text{-aminoethylamino})\text{-1-deoxy-D-galactitol}$) are determined by ^{113}Cd NMR speciation, in which the occurring species were in slow exchange. Competition experiments using both ^{31}P NMR shifts and ^{13}C and ^{31}P relaxation rate enhancements are performed to determine the stabilities of $\text{Nd}(\text{NTA})(\text{PPP})$ and $\text{Nd}(\text{PPP})_2$ (PPP : tripolyphosphate). Where possible, the results are compared with potentiometry data and found to be in good agreement.

* Huskens, J.; Lammers, H.; van Bekkum, H.; Peters, J.A. *Magn. Reson. Chem.* 1994, 32, 691.

INTRODUCTION

Potentiometry is a powerful tool for the determination of metal-ligand stability constants,^{1,2} but is subject to some constraints. The amount of ligand participating in the protonation equilibrium can be obtained, which allows indirect determination of the amount of ligand complexed to the metal ion. In order to be able to observe a pH effect, the titration experiment has to be performed at a pH lower than the (highest) pK_a of the ligand. The accuracy of the metal-ligand complexation constant is highly dependent on the accuracy of both the pH measurement in the titration and the pK_a of the ligand. This propagation of errors is especially observed in the determination of stabilities of mixed ligand ternary complexes, where the accuracy is further diminished by errors in the binary metal-ligand complexation constants. Another disadvantage of potentiometry is that from pH titration experiments no information on the molecular structures of the species involved in the equilibria can be obtained.

By contrast, multinuclear magnetic resonance data, such as metal and ligand induced shifts and paramagnetic metal induced relaxation rate enhancements, can provide valuable information on both speciations and structures.³ In general, the metal-ligand complexation equilibrium is studied directly, so there are no limitations on the pH at which these measurements can be performed. In fact, measurements at a pH higher than the (highest) pK_a of the ligand can facilitate the calculation of the stability constant, and eliminate any substantial contribution of an error in pH to the total error. Particularly, NMR can be very helpful in the determination of the stabilities of ternary complexes, because of the direct observation of the metal-ligand equilibria involved.

In this study, we determined stabilities of metal-ligand complexes by NMR in three different situations, where potentiometry is impossible or less favourable. First, the complexation of a "pH-silent" ligand, trimetaphosphate (P_{3m}), with lanthanide(III) (Ln) aminopolycarboxylate complexes was studied by Ln(III)-induced ^{31}P shifts. Knowledge of the stabilities of these ternary complexes was required for the interpretation of kinetic data on the hydrolysis of trimetaphosphate catalyzed by Ln(III) complexes.⁴ Measurement at a pH higher than the highest pK_a of P_{3m} ⁵ (value: 2.0) is required, because substantial decomplexation of the aminopolycarboxylate ligand occurs at $pH < 4$. The equilibria involved resemble in this case the complexation of organic substrates with Ln(III) shift

reagents.⁶ A combination of an elegant experimental dilution technique,^{7,8} and a simple though rigorous calculation method is provided.

Second, an example is given of Cd(II) complexes with an ethylenediamine carbohydrate conjugate, in which separate Cd(II) species were observed by ¹¹³Cd NMR. Potentiometry is possible for this system but yields no information on the stoichiometries of the complexes involved. As will be shown even for nuclei with a low sensitivity such as Cd(II), stabilities can be determined from the integrals in the NMR spectra with an accuracy comparable to potentiometry.

Third, the stability of a ternary complex is determined in a competition experiment using both Nd(III)-induced shifts and relaxation rate enhancements. Potentiometry gives in this case values with a rather low accuracy because of the already mentioned propagation of errors. Competition experiments are mainly used in the field of the determination of the stability of very strong binary complexes, such as observed for metal-ligand complexes used in magnetic resonance imaging.⁹ We extended the use of these competition experiments to the determination of the stability of ternary complexes.

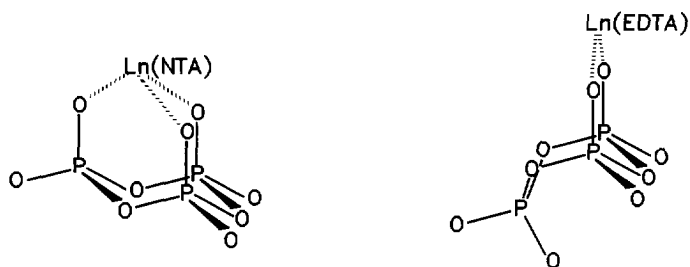
All calculations were performed using a spreadsheet program previously developed in our laboratory.^{10,11} Advantages of this program are (i) the convenient handling of experimental data, (ii) the complete overview of the speciation during and after the calculations, (iii) the versatility in handling different mathematical models, and (iv) the easy graphical presentation.

RESULTS AND DISCUSSION

Determination of the Stability of the Complexes Ln(L₁)(P_{3m}) by ³¹P NMR Shift Measurements

Trimetaphosphate (P_{3m}) forms weak (ternary) complexes with Ln(III) aminopolycarboxylate complexes, LnL₁ (L₁ = NTA³⁻ (nitrilotriacetate), EDTA⁴⁻ (ethylenediaminetetraacetate)), at neutral pH. With Ln(NTA), P_{3m} binds in a tridentate fashion to the Ln(III) ion, whereas with Ln(EDTA), a bidentate coordination mode was observed,⁴ as shown in Scheme 1. The highest pK_a of P_{3m} is too low (about 2)⁵ to allow potentiometric determination. The ³¹P NMR spectrum is simple: a single very sharp

resonance was observed, which was independent of the pH (between 4 and 10). Stepwise addition of LnL_1 to an aqueous solution of $\text{P}_{3\text{m}}$ caused a shift of the ^{31}P resonance of $\text{P}_{3\text{m}}$. Apparently, exchange of $\text{P}_{3\text{m}}$ between the free ligand and the complexed form (with LnL_1) is rapid on the NMR time scale.



Scheme 1

The stability constant of the binary complex LnL_1 is much higher than the formation constant of the ternary complex with $\text{P}_{3\text{m}}$. Therefore, dissociation of LnL_1 is negligible and LnL_1 is denoted as M. A dilution experiment was performed, starting at a total concentration of $\text{P}_{3\text{m}}$, $[\text{L}]_{\text{tot}}$, of 0.1 mmol ml^{-1} . The ratio $\rho = [\text{M}]_{\text{tot}}/[\text{L}]_{\text{tot}}$ was kept constant in this experiment at about 1. Under this condition, both L and ML occur in solution and the formation of complexes ML_n and M_nL ($n > 1$) can be excluded. The complexation constant K of the formation equilibrium of ML shown in Eqn (1), is defined in Eqn (2).



$$K = [\text{ML}] / [\text{M}][\text{L}] \quad (2)$$

The ratio $y = \Delta\delta/\Delta\delta_b$ yields the ratio between complexed and total L, according to Eqn (3), in which $\Delta\delta$ is the difference between the ^{31}P chemical shift of the concerning mixture of M and L and the chemical shift of the free ligand, and $\Delta\delta_b$ is the difference between the shift of the complex ML and the free ligand L.

$$y = \Delta\delta / \Delta\delta_b = [\text{ML}] / [\text{L}]_{\text{tot}} \quad (3)$$

Similar models have been derived for Ln(III) shift reagents in the analysis of Ln(III)-induced shifts in order to obtain structural information about the formed complexes. Several methods have been developed and reviewed⁶ to obtain reliable bound shifts and stabilities simultaneously. For low stabilities as found in our system, only one method⁸ seems to provide reliable values, using elegant dilution experiments. However, this method is subject to the restriction that ρ has to be 1 to allow graphical analysis of the results. We used a similar method, also using dilution experiments,⁷ in which simple though rigorous spreadsheet calculations provide values with the same accuracy, but which is not restricted to the condition $\rho = 1$. Because the complexes ML are weak and the concentration $[\text{M}]_{\text{tot}}$ is limited to about 0.1 mmol ml⁻¹ for solubility reasons, $\Delta\delta_b$ could not be determined independently, but was obtained simultaneously with the stability constant K of the complex ML in this minimization routine.³ The mass balances for M and L are given in Eqs (4) and (5), from which Eqn (6) can be derived.

$$[\text{M}]_{\text{tot}} = [\text{M}] + [\text{ML}] \quad (4)$$

$$[\text{L}]_{\text{tot}} = [\text{L}] + [\text{ML}] \quad (5)$$

$$[\text{M}]_{\text{tot}} - [\text{L}]_{\text{tot}} = [\text{M}] - [\text{L}] \quad (6)$$

The stability constant K was calculated with the following iteration process. From initial estimates for $\log K$, $\Delta\delta_b$, and the free ligand concentration $[\text{L}]$, $[\text{M}]$ was calculated with the use of Eqn (6). The complex concentration $[\text{ML}]$ was then derived from Eqn (2). $[\text{L}]$ was varied until the mass balance for L (Eqn (5)) was valid. Then, values for $\Delta\delta$ were calculated with Eqn (3). K and $\Delta\delta_b$ were varied until the differences between experimental and calculated values for $\Delta\delta$ were minimized.

The results are listed in Table 1. Figure 1 demonstrates the good agreement between calculated and experimental values of y as a function of $[\text{L}]_{\text{tot}}$ for $\text{M} = \text{La}(\text{NTA})$ and $\text{Nd}(\text{NTA})$.

The accuracy of the NMR method is high, thanks to the narrow signals ($\Delta\nu_{1/2} = 4$ Hz) in the case of the diamagnetic La(III) complexes, and, therefore, the error in the experimental chemical shifts (0.01 ppm) is small. For the Nd(III) complexes, the error in

stability constants by NMR

the shift is 0.1 ppm, due a larger linewidth ($\Delta\nu_{1/2} = 25$ Hz). This does, however, not lead to a reduced accuracy for the calculated stability constant, since the relative errors are still small as a result of the higher bound shifts.

In contrast to the known dilution procedure with graphical determination of K ,^{6,8} our method is in general not restricted to low K values. However, for higher K values, lower concentrations have to be used, and therefore, the applicability is determined by the sensitivity of the nucleus under investigation.

Table 1. Stabilities and bound ^{31}P shifts of P_{3m} in $\text{Ln}(\text{L}_1)(\text{P}_{3m})$ ($\text{Ln} = \text{La}, \text{Nd}$; $\text{L}_1 = \text{NTA}, \text{EDTA}$) and the estimated errors, as measured at 81.0 MHz and 295 K.

| Ln | L_1 | $\log K^a$ | $\Delta\delta_b$ (ppm) |
|-------------|--------------|-----------------|------------------------|
| La | NTA | 1.84 ± 0.03 | 0.94 ± 0.03 |
| Nd | NTA | 1.97 ± 0.03 | 15.1 ± 0.4 |
| La | EDTA | 1.15 ± 0.03 | 1.14 ± 0.04 |
| Nd | EDTA | 1.00 ± 0.06 | 9.5 ± 0.8 |

^a K (see Eqn (2)) in M^{-1}

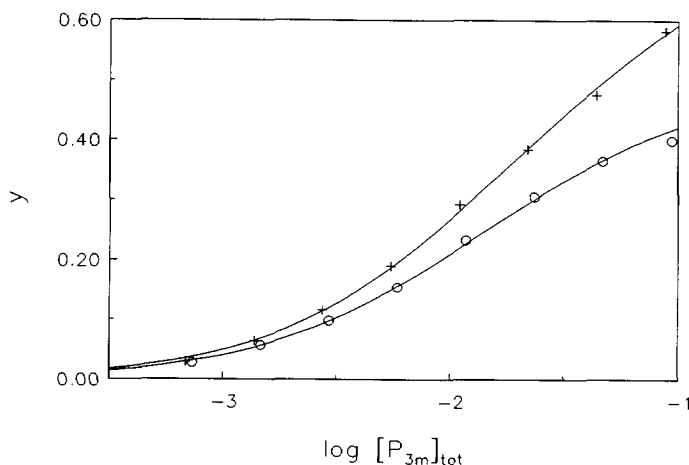


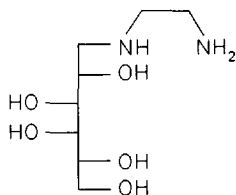
Figure 1. The bound fraction y of P_{3m} versus $\log [P_{3m}]_{tot}$ for $La(NTA)$ (+; $\rho = 0.8$) and $Nd(NTA)$ (O; $\rho = 0.5$), as measured at 81.0 MHz and 295 K; the solid lines were calculated with stabilities and bound shifts as given in Table 1.

Determination of the Stability of the Cd(II) Complexes with 1-(2-Aminoethylamino)-1-deoxy-D-galactitol by ^{113}Cd Speciation

^{113}Cd NMR spectroscopy is a powerful technique for the determination of the number and type of coordinating groups around a Cd(II) metal centre and, therefore, has become a valuable tool in cadmium chemistry and bioinorganic chemistry.¹² The deshielding of ^{113}Cd increases in the order $\text{O} < \text{N} < \text{S}$, and the scale of observed resonances exceeds 900 ppm.

In our study on carbohydrate-based metal sequestering agents, the ligand 1-(2-aminoethylamino)-1-deoxy-D-galactitol (L; see Scheme 2) was synthesized from D-galactose and ethylenediamine by reductive amination.¹³ Here, we observed separate ^{113}Cd resonances for free Cd(II) (0 ppm), CdL (108 ppm), and CdL₂ (239 ppm) in aqueous solution at room temperature, as illustrated in Figure 2, indicating these species and the free ligand L to be in slow exchange. From the ^{113}Cd chemical shifts obtained for CdL and CdL₂, it was concluded that both the primary and secondary N-atom are involved in coordination. The additional coordination of one of the hydroxyl groups in the

carbohydrate chain, at the pH values measured, can be excluded.¹⁴



Scheme 2

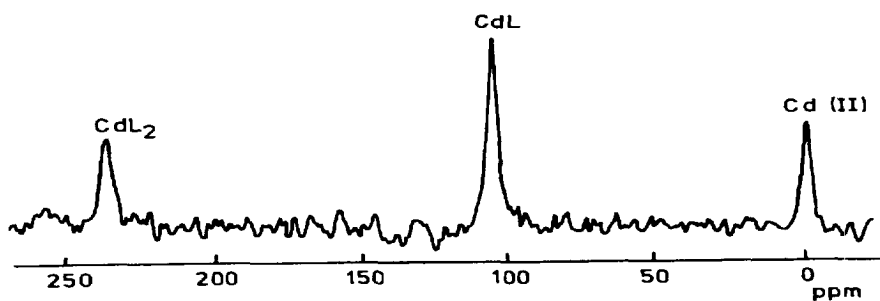
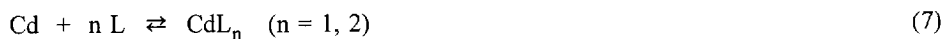


Figure 2. Characteristic ^{113}Cd spectrum at $[L]_{\text{tot}}/[Cd]_{\text{tot}} = 1$, $\text{pH} = 7.35$, measured at 88.7 MHz and 295 K.

The complexation constants β_{101} and β_{102} of the equilibrium shown in Eqn (7), are defined in Eqn (8).



$$\beta_{101} = [\text{CdL}] / [\text{Cd}][\text{L}] \quad (8a)$$

$$\beta_{102} = [\text{CdL}_2] / [\text{Cd}][\text{L}]^2 \quad (8b)$$

From the integrals, I , obtained by ^{113}Cd NMR, the concentrations of CdL_n ($n = 0, 1, 2$) were calculated with Eqn (9), in which $[\text{Cd}]_{\text{tot}}$ is given by Eqn (10).

$$[\text{CdL}_n] = (I_n / \sum I_n) * [\text{Cd}]_{\text{tot}} \quad (9)$$

$$[\text{Cd}]_{\text{tot}} = [\text{Cd}] + [\text{CdL}] + [\text{CdL}_2] \quad (10)$$

The total free ligand concentration $[\text{L}]_f$, which is the sum of the concentrations of the free ligand and its protonated forms according to Eqn (11), was obtained from the ligand mass balance, Eqn (12).

$$[\text{L}]_f = [\text{L}] (1 + \beta_{\text{HL}}[\text{H}] + \beta_{\text{H}_2\text{L}}[\text{H}]^2) \quad (11)$$

$$[\text{L}]_{\text{tot}} = [\text{L}]_f + [\text{CdL}] + 2 [\text{CdL}_2] \quad (12)$$

The protonation constants β_{011} and β_{021} are defined according to Eqn (13) and were determined by potentiometry (log values: 9.48 and 15.87, respectively).¹⁴

$$\beta_{011} = [\text{HL}] / [\text{H}][\text{L}] \quad (13a)$$

$$\beta_{021} = [\text{H}_2\text{L}] / [\text{H}]^2[\text{L}] \quad (13b)$$

The concentration $[\text{L}]$ was then calculated from Eqn (11) and used in Eqn (8) to yield the complexation constants.

The stabilities of CdL and CdL₂ were determined by measuring the ¹¹³Cd speciation at different ligand-to-metal ratios, $[\text{L}]_{\text{tot}}/[\text{Cd}]_{\text{tot}}$, at a pH of about 7. The results are given in Table 2, together with the standard deviations in log β . For comparison, results obtained by potentiometry are included. Although potentiometry gave some indication for the formation of CdL₃, this was excluded by the NMR measurements, because, even at high $[\text{L}]_{\text{tot}}$ (4 times $[\text{Cd}]_{\text{tot}}$) and high pH (about 9.5), no signal was observed for this species. The chemical shift of the CdL₃ complex can be estimated to be about 350 ppm on the basis of the analogous complex with ethylenediamine.¹⁵

The errors are mainly determined by the errors of the integrals, which are large (about 10 %) due to the low signal-to-noise ratio, particularly when the free Cd or the CdL₂ species are present in only small amounts. The errors resulting from inaccuracies in the pH and the pK_as are of only little importance and, therefore, the errors in the stability constants compare well with those obtained by potentiometry. It is clear that the ¹¹³Cd speciation technique is especially useful for obtaining both the stabilities and the structure of the concerning complexes with a single experiment.

Table 2. Stabilities and standard deviations of CdL and CdL₂ (L = 1-(2-aminoethylamino)-1-deoxy-D-galactitol), measured at 88.7 MHz and 295 K.

| complex | method | log β_{10n} ^a |
|------------------|---------------|--------------------------------|
| CdL | NMR | 4.6 ± 0.3 |
| | potentiometry | 4.5 ± 0.1 |
| CdL ₂ | NMR | 8.7 ± 0.4 |
| | potentiometry | 8.4 ± 0.2 |

^a β (see Eqn (8)) in mlⁿ mmol⁻ⁿ

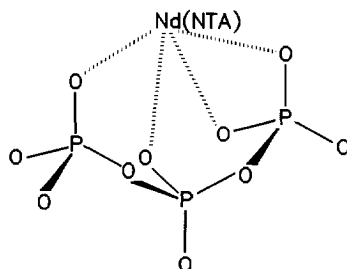
Determination of the Stability of the Complexes Nd(NTA)(PPP) and Nd(PPP)₂ by Nd(III) Induced ³¹P NMR Shifts and ³¹P and ¹³C Relaxation Rate Enhancements

Tripoly-phosphate (PPP) forms 1:1 complexes with Ln(III) ions which have rather low solubilities. Therefore, the stabilities of Ln(PPP) are not accurately known. We performed a competition experiment, according to Eqn (14a) and (14b), to determine the stabilities of Nd(NTA)(PPP) (β_{111}) and Nd(PPP)₂ (β_{102}).



The equilibrium between Nd(NTA)(PPP) and Nd(NTA)₂ in Eqn (14a) was investigated by ³¹P NMR shifts and longitudinal relaxation rate enhancements (RE), yielding the ratio between free and complexed PPP. The shift of P₁ (the terminal phosphate group) of PPP could not be used, because the exchange between free and bound PPP was slow on the NMR time scale for this nucleus, while for the shift of P₂ (the middle phosphate group) and for the REs of both P₁ and P₂, the exchange was fast on the NMR time scale, as has been reported previously.¹⁶ The equilibrium between Nd(NTA)(PPP) and Nd(PPP)₂ in Eqn (14b) was studied by ¹³C NMR REs, yielding the ratio between free and complexed NTA. It has been shown, also by ³¹P and ¹³C REs, that PPP binds in a tetradentate (see Scheme 3) and NTA in a tridentate fashion to Nd(III) in the mixed complex Nd(NTA)(PPP),⁴ excluding the formation of Nd(III) complexes with three ligands. Analogously to Ln(PPP)₂,¹⁶ the overall tetradentate coordination of PPP in

Nd(NTA)(PPP) contains mono- and bidentate contributions of all three phosphate groups.⁴



Scheme 3

The total concentrations of Nd(III) ($[M]_{\text{tot}}$), NTA ($[L_1]_{\text{tot}}$), and PPP ($[L_2]_{\text{tot}}$) were chosen such that the concentrations of the free metal M and of the 1:1 complexes ML_1 and ML_2 could be ignored ($[M]_{\text{tot}} = 0.01$ M, $[L_1]_{\text{tot}} + [L_2]_{\text{tot}} > 0.02$ M). This complete occupation of sites on M was necessary for the competition experiment and facilitated the calculations. The stability of ML_2^1 (β_{120}) and the protonation constants of L_1 and L_2 were obtained from the literature.¹⁷ The metal-ligand complexation constants β_{1mn} are defined according to Eqn (15).

$$\beta_{1mn} = [M(L_1)_m(L_2)_n] / [M][L_1]^m[L_2]^n \quad (m, n = 0, 1, 2; m+n = 1, 2) \quad (15)$$

Because the ^{31}P shift of free L_2 is pH dependent, the pH was kept constant at 7.0. The equilibrium of Eqn (14a), of which the stability β_{111} is given by Eqn (15) ($m=n=1$), was studied by addition of L_1 to a solution of ML_1L_2 , yielding the ratio y between free and complexed L_2 , according to Eqn (16).^{18,19}

$$y = [ML_1L_2] / [L_2]_{\text{tot}} = \Delta\delta_i / \Delta\delta_{b,i} \quad (16a)$$

$$= RE_i / RE_{b,i} \quad (16b)$$

In Eqn (16b), RE_i is given by Eqn (17), where $(1/T_1)_i$ and $(1/T_1)_{f,i}$ are the longitudinal relaxation rates of the nucleus P_i of L_2 in the competition experiment or the free ligand

form, respectively.

$$RE_i = (1/T_1)_i - (1/T_1)_{f,i} \quad (17)$$

The various concentrations are related by the mass balances given in Eqs (18), (19), and (20).

$$[M]_{\text{tot}} = [M] + [ML_1] + [ML_2] + [ML_2^1] + [ML_2^2] + [ML_2L_2] \quad (18)$$

$$[L_1]_{\text{tot}} = [L_1]_f + [ML_1] + 2 [ML_1L_1] + [ML_1L_2] \quad (19)$$

$$[L_2]_{\text{tot}} = [L_2]_f + [ML_2] + [ML_1L_2] + 2 [ML_2L_2] \quad (20)$$

All terms concerning the species M, ML_1 , ML_2 , and ML_2L_2 can be neglected. Then, Eqs (21) and (22) can be derived from (18) to (20) to facilitate the computations.

$$[L_1]_{\text{tot}} + [L_2]_{\text{tot}} - 2 [M]_{\text{tot}} = [L_1]_f + [L_2]_f \quad (21)$$

$$[L_1]_{\text{tot}} - [M]_{\text{tot}} = [L_1]_f + [ML_1L_1] \quad (22)$$

Analogous to Eqn (11), $[L_1]_f$ and $[L_2]_f$ are given by Eqn (23), in which the protonation constants are defined analogous to Eqn (13).

$$[L_i]_f = [L_i] (1 + \beta_{HL,i}[H] + \beta_{H_2L,i}[H]^2 + \beta_{H_3L,i}[H]^3 + \beta_{H_4L,i}[H]^4) \quad (23)$$

The calculation of β_{111} was performed as follows. Starting values were used for β_{111} , $\Delta\delta_{b,2}$ and $RE_{b,i}$ (the values for the complex ML_1L_2), and the total free NTA concentration, $[L_1]_f$. Then $[L_2]_f$ and $[ML_1L_1]$ were calculated from $[L_1]_f$ using Eqs (21) and (22), respectively. Subsequently, the free ligand concentrations $[L_1]$ and $[L_2]$ were calculated with Eqn (23). From $[ML_1L_1]$, the free metal concentration $[M]$ was calculated using Eqn (15) and the literature value for β_{120} . With β_{111} , $[ML_1L_2]$ was calculated. $[L_1]_f$ was varied until the mass balance for L_1 (Eqn (19)) was valid. Subsequently, $\Delta\delta_2$ and RE_i were calculated with Eqn (16). The complexation constant β_{111} , $\Delta\delta_{b,2}$ and $RE_{b,i}$ were varied in an iterative process until an optimal fit between experimental and calculated values for $\Delta\delta_2$ and RE_i was obtained.

Because the complex formation was strong under these conditions, $\Delta\delta_{b,2}$ and $(1/T_1)_{b,i}$ could be determined directly by measuring $\Delta\delta_2$ and $(1/T_1)_i$ for ML_1L_2 . However, because the error in the Nd(III)-induced shift (± 0.1 ppm) and RE (± 0.5 s $^{-1}$) measurements is rather high, both $\Delta\delta_{b,2}$ and $(1/T_1)_{b,i}$ were optimized in the above described minimization routine. The optimized values agreed with the actual values within the experimental error. Measurement of a sample of the free ligand L_2 gave $(1/T_1)_{f,i}$.

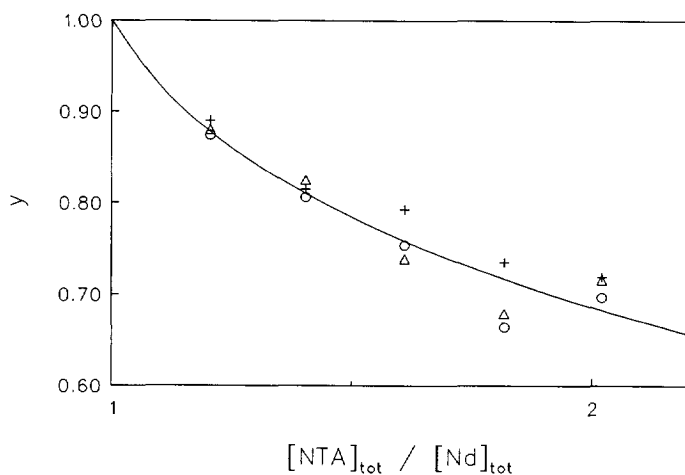


Figure 3. The bound fraction y of PPP versus $[NTA]_{tot}/[Nd]_{tot}$ as obtained using the shift of P_2 (+), the RE of P_1 (o), and the RE of P_2 (Δ), as measured at 81.0 or 50.3 MHz and 295 K; the solid line was calculated with the stability as given in Table 3.

Analogously, the equilibrium between ML_1L_2 and ML_2L_2 (Eqn (14b)) was investigated by ^{13}C REs of the nuclei C_1 (the CH_2 carbon) and C_2 (the carboxylate carbon), yielding fractions $y' = [ML_1L_2] / [L_1]_{tot}$ according to Eqn (16b), in which RE_i is now the longitudinal relaxation rate enhancement of the ^{13}C nucleus C_i of L_1 . In this case, all terms concerning the species M, ML_1 , ML_2 , and ML_1L_1 can be neglected.

The results for the equilibrium of Eqn (14a) are shown in Figure 3, in which y versus $[NTA]_{tot} / [Nd]_{tot}$ is plotted. The estimated errors, the values for the bound shifts and REs, and the results for the equilibrium of Eqn (14b) are compiled in Table 3.

The stabilities obtained by NMR are in excellent agreement with the values determined by

potentiometry. It should be mentioned that these potentiometric titrations were also performed as competition experiments.⁴ The strength of the NMR determination lies in the fact that information about the denticity of the ligands is obtained concurrently, which is necessary to check the feasibility of a competition experiment. The error in the determined stabilities contains contributions from the experimental errors in the NMR parameters and the literature values for the pK_a s as well as the stability of $Nd(NTA)_2$. The pH affects the shift of the free ligand PPP, but it has only a very limited influence on the calculated speciations.

Table 3. Stabilities and their standard deviations, and the bound shifts and REs of $Nd(NTA)(PPP)$ and $Nd(PPP)_2$, measured at 81.0 (^{31}P) or 50.3 (^{13}C) MHz and 295 K.

| complex | method | $\log \beta_{1mn}^a$ | bound value ^b |
|-------------------------------|--------------------|----------------------|--------------------------|
| $Nd(NTA)(PPP)$ ($m=n=1$) | $\Delta\delta P_2$ | 18.70 ± 0.15 | 3.2 |
| | RE P_1 | 18.57 ± 0.11 | 13.7 |
| | RE P_2 | 18.52 ± 0.15 | 12.3 |
| | overall | 18.57 ± 0.14 | |
| | potentiometry | 18.4 ± 0.4 | |
| $Nd(PPP)_2$ ($m=0, n=2$) | RE C_1 | 17.6 ± 0.3 | 7.4 |
| | RE C_2 | 17.6 ± 0.3 | 5.5 |
| | overall | 17.6 ± 0.3 | |
| | potentiometry | 17.5 ± 0.5 | |

^a β_{111} and β_{102} (see Eqn(15)) in $ml^2 mmol^{-2}$; ^b Bound shift (in ppm; ± 0.1 ppm) or bound RE (in s^{-1} ; $\pm 0.5 s^{-1}$)

CONCLUSIONS

Multinuclear magnetic resonance techniques are very powerful in the determination of stability constants. The stabilities of several ternary complexes were determined, using ^{31}P shift and relaxation rate data. The speciation of $Cd(II)$ complexes with an ethylenediamine carbohydrate derivative was investigated by ^{113}Cd NMR and used to determine the stabilities of the occurring complexes. Some of the results are compared with

potentiometric data, and found to correlate very well. The magnitude of the errors is dependent on the particular NMR technique used, and the pK_a s of the ligands. In contrast to potentiometry, the pH and the proton balance do not contribute much to the error.

EXPERIMENTAL

Materials

All compounds were purchased from Janssen Chimica. $LaCl_3$ was obtained as a mixed hydrate; the La(III) content was determined by complexometric titration.²⁰ $NdCl_3$ and $Cd(ClO_4)_2$ were obtained as the hexahydrate, NTA as the free acid, and EDTA as the trisodium salt; all were used as such. Trimetaphosphate (P_{3m}) was obtained as the trisodium salt and tripolyphosphate (PPP) as the pentasodium salt, both in technical grade; both were recrystallized from water-ethanol mixtures.²¹ The ligand 1-(2-aminoethylamino)-1-deoxy-D-galactitol was synthesized from galactose and ethylenediamine, and purified by anion exchange column chromatography.¹³

Nuclear Magnetic Resonance Spectroscopy

The ^{13}C and ^{31}P spectra were recorded on a Nicolet NT-200 WB NMR spectrometer at 295 K with 30 % D_2O (for locking) in water as the solvent. The ^{31}P shift and RE measurements were recorded at 81.0 MHz using 16 K data-points, a spectral width of 6 kHz, and 1 % phosphoric acid as an external standard. A 90° pulse was applied and the acquisition delay was 10 s. The relaxation times were determined using an inversion recovery pulse sequence with a composite 180° pulse and calculated with the aid of a non-linear least squares three parameters curve fitting routine.²² The ^{13}C spectra were recorded at 50.3 MHz using 16 K data-points, a spectral width of 12 KHz, and *t*-butanol in D_2O as the external standard. The ^{113}Cd spectra were recorded on a Varian VXR-400 S NMR spectrometer at 88.7 MHz using 48 K data-points, a spectral width of 50 KHz, and 0.1 M $HClO_4$ as an external reference. A 60° pulse was applied and the acquisition delay was 2.5 s.

Computations

All calculations were performed with a spreadsheet program described previously.¹⁰ Some adaptations were made to enable the calculation of stabilities from NMR and potentiometric data.¹¹

Determination of the Stability of $\text{Ln}(\text{L}_1)(\text{P}_{3m})$ by ^{31}P NMR Shift Measurements

Starting solutions were prepared by dissolving the appropriate amounts of metal salt and ligands in 6 ml 30 % D_2O in water. The initial concentration of P_{3m} was 0.1 mmol ml^{-1} and the concentration of LnL_1 was about $0.08 \text{ mmol ml}^{-1}$. After the shift measurement, 3 ml of this sample was transferred to another tube and diluted with 3 ml 30 % D_2O in water. This procedure was repeated 6 or 7 times. No corrections for the decrease of ionic strength were made. The experimental results are shown in Table 4.

Table 4. Experimental ^{31}P shifts ($\Delta\delta^a$) of P_{3m} at 81.0 MHz and 295 K in the dilution experiments of $\text{LnL}_1\text{-P}_{3m}$.

| n^b | La(NTA) | Nd(NTA) | La(EDTA) | Nd(EDTA) |
|----------------------|---------|---------|----------|----------|
| 0 | 0.550 | 6.01 | 0.453 | 3.49 |
| 1 | 0.449 | 5.50 | 0.320 | 2.52 |
| 2 | 0.363 | 4.59 | 0.201 | 1.55 |
| 3 | 0.276 | 3.50 | 0.132 | 0.84 |
| 4 | 0.180 | 2.32 | 0.076 | 0.45 |
| 5 | 0.110 | 1.48 | 0.041 | 0.25 |
| 6 | 0.061 | 0.84 | 0.020 | 0.16 |
| 7 | 0.028 | 0.41 | | |
| $L_{\text{tot},i}^c$ | 0.0879 | 0.0939 | 0.0965 | 0.0949 |
| ρ | 0.810 | 0.502 | 0.853 | 0.822 |

^a Values in ppm; absolute shift of P_{3m} (free ligand): -21.60 ppm ;^b Dilution exponential, cf. note c;

^c Initial L_{tot} at $n=0$ (in mmol ml^{-1}); at other dilution steps: $L_{\text{tot}} = L_{\text{tot},i}/2^n$.

Determination of the Stability of the Cd(II) Complexes with 1-(2-Aminoethylamino)-1-deoxy-D-galactitol by ^{113}Cd Speciation

Starting solutions were prepared by dissolving the appropriate amounts of metal salt and ligand in 20 % D_2O in water. The total Cd(II) concentration was 0.1 mmol ml^{-1} . The pH was adjusted to about 7 using 60 % aqueous perchloric acid. The ligand-to-metal ratio ($[\text{L}]_{\text{tot}}/[\text{Cd}]_{\text{tot}}$) was raised from 0.2 to 2 with intervals of 0.2. The ionic strength was about $0.25 \text{ mmol ml}^{-1}$. Experimental data are summarized in Table 5.

Table 5. Integrals (I) of Cd, CdL, and CdL₂ obtained by ^{113}Cd NMR at 88.7 MHz and 295 K.

| $[\text{Cd}]_{\text{tot}}^{\text{a}}$ | $[\text{L}]_{\text{tot}}^{\text{a}}$ | pH | I_{Cd}^{b} | $I_{\text{CdL}}^{\text{b}}$ | $I_{\text{CdL}_2}^{\text{b}}$ |
|---------------------------------------|--------------------------------------|------|----------------------------|-----------------------------|-------------------------------|
| 0.102 | 0.021 | 6.66 | 82.2 | 17.8 | |
| 0.096 | 0.037 | 6.72 | 70.1 | 29.9 | |
| 0.099 | 0.059 | 6.70 | 58.3 | 41.7 | |
| 0.098 | 0.077 | 6.80 | 42.5 | 57.5 | |
| 0.097 | 0.096 | 7.00 | 31.8 | 49.1 | 19.1 |
| 0.098 | 0.118 | 6.66 | 35.9 | 44.4 | 19.7 |
| 0.104 | 0.145 | 6.55 | 35.0 | 47.4 | 17.6 |
| 0.099 | 0.156 | 6.45 | 28.8 | 44.1 | 27.1 |
| 0.098 | 0.200 | 6.55 | 26.0 | 46.6 | 27.4 |

^a In mmol ml^{-1} ; ^b Values in percentage of total integral

Determination of the Stability of the Complexes Nd(NTA)(PPP) and Nd(PPP)₂ by Nd(III) Induced ^{31}P NMR Shifts and ^{31}P and ^{13}C REs

Starting solutions were prepared by dissolving the appropriate amounts of NdCl_3 , NTA, and PPP in 30 % D_2O in water, providing a concentration of $0.15 \text{ mmol ml}^{-1}$ of Nd(NTA)(PPP). After measurement of the ^{31}P shift and REs, NTA was added in five portions, finally reaching a total NTA concentration, $[\text{NTA}]_{\text{tot}}$, of $0.25 \text{ mmol ml}^{-1}$, in order to study the equilibrium of Eqn (14a). The experimental results are shown in Table 6. The equilibrium of Eqn (14b) was studied by addition of 3 portions of PPP, starting from the same initial solution and measuring the ^{13}C REs of NTA, finally reaching a total NTA concentration, $[\text{NTA}]_{\text{tot}}$, of $0.33 \text{ mmol ml}^{-1}$. The experimental results are shown in

stability constants by NMR

Table 7. In each case, the pH was adjusted to about 7 using either 4 mmol ml⁻¹ aqueous NaOH or 2 mmol ml⁻¹ aqueous HCl. The ionic strength was between 1 and 2 mmol ml⁻¹.

Table 6. Experimental ³¹P shifts, $\Delta\delta_2$, and RE_i of PPP in the competition experiment of Nd(NTA)(PPP) with NTA (Eqn (14a)).

| [NTA] _{tot} ^a | [Nd(PPP)] _{tot} ^a | pH | $\Delta\delta_2$ (ppm) ^b | RE ₁ (s ⁻¹) ^c | RE ₂ (s ⁻¹) ^d |
|-----------------------------------|---------------------------------------|------|-------------------------------------|---|---|
| 0.141 | 0.141 | 7.02 | 3.16 | 13.8 | 12.3 |
| 0.170 | 0.141 | 6.92 | 2.82 | 12.1 | 10.8 |
| 0.189 | 0.135 | 7.21 | 2.58 | 11.4 | 9.9 |
| 0.211 | 0.131 | 6.98 | 2.51 | 10.2 | 9.3 |
| 0.232 | 0.127 | 7.19 | 2.32 | 9.3 | 8.2 |
| 0.253 | 0.125 | 6.94 | 2.28 | 9.8 | 8.6 |

^a In mmol ml⁻¹; ^b Absolute shift of P₂ in PPP (free ligand): -20.84 ppm; ^c (1/T₁)_{1,f} = 0.04 s⁻¹;

^d (1/T₁)_{2,f} = 0.07 s⁻¹

Table 7. Experimental ¹³C REs, RE_i, of NTA in the competition experiment of Nd(NTA)(PPP) with PPP (Eqn (14b)).

| [PPP] _{tot} ^a | pH | RE ₁ (s ⁻¹) ^b | RE ₂ (s ⁻¹) ^c |
|-----------------------------------|------|---|---|
| 0.165 | 7.02 | 7.4 | 5.5 |
| 0.221 | 7.08 | 5.2 | 3.8 |
| 0.278 | 7.00 | 3.0 | 2.4 |
| 0.332 | 7.14 | 2.5 | 1.7 |

^a In mmol ml⁻¹; [Nd(NTA)]_{tot} = 0.165 mmol ml⁻¹; ^b (1/T₁)_{1,f} = 1.7 s⁻¹; ^c (1/T₁)_{2,f} = 0.3 s⁻¹

ACKNOWLEDGEMENTS

This research was supported by the Netherlands Organization for Scientific Research (NWO), under the auspices of the Netherlands Foundation for Chemical Research (SON) (J.H.), and by the Dutch National Innovation Oriented Program Carbohydrates (IOP-k; H.L.). We gratefully acknowledge Ms. Anna D. Kennedy for performing the potentiometric titration experiments.

REFERENCES

1. Martell, A.E.; Motekaitis, R.J. In *Determination and Use of Stability Constants*, VCH Publishers, Inc., New York (1988).
2. Leggett, D.J. *Am. Lab.* **1982**, 29.
3. Erb, H.-P.; Bluhm, T. *J. Phys. Chem.* **1984**, 88, 4158.
4. Huskens, J.; Kennedy, A.D.; van Bekkum, H.; Peters, J.A. *J. Am. Chem. Soc.* **1995**, 117, 375.
5. Hirokawa, T.; Kobayashi, S.; Kiso, Y. *J. Chromatogr.* **1985**, 318, 195.
6. Raber, D.J.; Hardee, L.E. *Org. Magn. Reson.* **1982**, 20, 125.
7. Inagaki, F.; Takahashi, S.; Tasumi, M.; Miyazawa, T. *Bull. Chem. Soc. Jpn.* **1975**, 48, 853.
8. Bouquant, J.; Chuche, J. *Tetrahedron Lett.* **1972**, 23, 2337.
9. Sherry, A.D.; Cacheris, W.P.; Kuan, K.-T. *Magn Reson. Med.* **1988**, 8, 180.
10. van Westrenen, J.; Khizhnyak, P.L.; Choppin, G.R. *Comput. Chem.* **1991**, 15, 121.
11. Huskens, J.; van Bekkum, H.; Peters, J.A. *Comput. Chem* in press.
12. Summers, M.F. *Coord. Chem. Rev.* **1988**, 86, 43.
13. Lammers, H.; Peters, J.A.; van Bekkum, H. *Tetrahedron* **1994**, 50, 8103.
14. Lammers, H.; Peters, J.A.; van Bekkum, H. submitted to *Carbohydr. Res.*
15. Summers, M.F.; Marzilli, L.G. *Inorg. Chem.* **1984**, 23, 523.
16. Nieuwenhuizen, M.S.; Peters, J.A.; Sinnema, A.; Kieboom, A.P.G.; van Bekkum, H. *J. Am. Chem. Soc.* **1985**, 107, 12.
17. Martell, A.E.; Smith, R.M. In *Critical Stability Constants*, Plenum Press, New York, **1977**, Vol. 3; **1982**, Vol. 5; **1989**, Vol. 6.
18. Leigh, Jr. J.S. *J. Magn. Reson.* **1971**, 4, 308.
19. McLaughlin, A.C.; Leigh, Jr. J.S. *J. Magn. Reson.* **1973**, 9, 296.
20. Woyski, M.M.; Harris, R.E. In *Treatise on Analytical Chemistry*, Kolthoff, I.M.;

stability constants by NMR

- Elving, P.J. (eds.), Interscience-Wiley, New York; **1963**, Vol. 8, part II, 54.
21. Quimby, O.T. *J. Phys. Chem.* **1954**, *58*, 603.
 22. Canet, D.; Levy, G.C.; Peat, I.R. *J. Magn. Reson.* **1975**, *18*, 199.

Chapter 8

STRUCTURES AND DYNAMICS OF Ln(III) COMPLEXES OF SUGAR-BASED DTPA-BIS(AMIDES) IN AQUEOUS SOLUTION: A MULTINUCLEAR NMR STUDY

ABSTRACT

The structure and dynamics of the lanthanide(III) complexes of DTPA-BGLUCA³⁻ (DTPA-bis(glucamide)) and DTPA-BENGALAA³⁻ (DTPA-bis(ethylenegallactamine-amide)) and of the model compounds DTPA-BEA³⁻ (DTPA-bis(ethanolamide)) and DTPA-BPDA³⁻ (DTPA-bis(propanediolamide)) in aqueous solution have been investigated using ¹³C and ¹⁷O NMR. Longitudinal ¹³C relaxation times of the Nd(III) complexes show that the organic ligand is bound to the lanthanide(III) ion in an octadentate fashion via the three nitrogens of the diethylenetriamine backbone, the three carboxylate groups, and the two amide oxygens. The sugar side chains are not involved in the coordination. ¹⁷O NMR measurements indicate that the coordination sphere is completed by one water ligand. Inversion of the lanthanide-bound nitrogens is precluded and therefore four diastereomeric pairs of isomers are possible for these complexes. The number of diastereoisomers is doubled due to the chirality of the sugar chain.

In addition, we performed a variable temperature and pressure ¹⁷O NMR study at 9.4 T on the Gd(III) complexes of DTPA-BGLUCA³⁻, DTPA-BENGALAA³⁻ and DTPA-BPDA³⁻ to evaluate their water exchange kinetics. These complexes may be of relevance as potential MRI contrast agents, and the water exchange rate is one of the crucial

parameters determining the efficacy of a contrast agent. The water exchange rates, k_{ex} , on [Gd(DTPA-BPDA)(H₂O)], [Gd(DTPA-BGLUCA)(H₂O)] and [Gd(DTPA-BENGALAA)(H₂O)] are 3.6 ± 0.3 , 3.9 ± 0.2 , and $2.1 \pm 0.1 \times 10^5 \text{ s}^{-1}$, and the activation volumes are +6.5, +6.4, and +5.2 cm³mol⁻¹ ($\pm 0.2 \text{ cm}^3\text{mol}^{-1}$) respectively, indicating that the exchange reaction is strongly dissociatively activated. The activation enthalpies and entropies are reported, as well as the rotational correlation times of these complexes. A comparison is made with [Gd(DTPA-BMA)(H₂O)] (DTPA-bis(methylamide), and the conclusion is drawn that structural changes in the second coordination sphere do not influence the activation parameters for water exchange on these complexes.

The nuclear magnetic relaxation dispersion (NMRD) profiles of [Gd(DTPA-BPDA)(H₂O)], [Gd(DTPA-BGLUCA)(H₂O)] and [Gd(DTPA-BENGALAA)(H₂O)] at several temperatures are presented. The data confirm the relatively slow water exchange process of the single inner-sphere water molecule.

INTRODUCTION

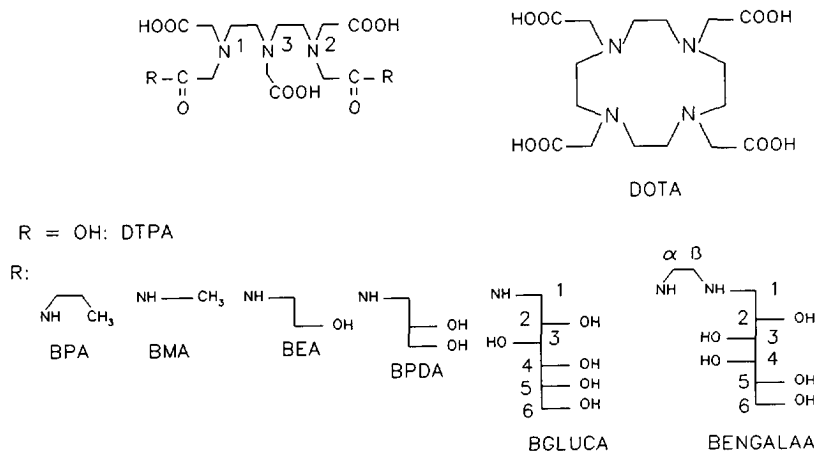
The rapid development of biomedical Magnetic Resonance Imaging (MRI) as a clinical modality provoked a prodigious growth in interest in lanthanide(III) complexes for application as contrast agents.¹⁻³ These agents enhance proton relaxation rates ($1/T_1$ and $1/T_2$) of water, and since these parameters determine the intensity of the NMR signal, the contrast of images may improve. All current commercially available MRI contrast reagents for clinical use are polyaminopolycarboxylate complexes of Gd(III). The Gd(III) ion is especially suitable because of its high electron spin ($S=7/2$) and relatively slow electronic relaxation. Therefore high relaxivity is produced by the fluctuating dipole-dipole interaction between the electron spin of the paramagnetic center and the proton nuclear spin.

Around a paramagnetic ion, the bulk water proton relaxation rates are enhanced due to long-range interactions ("outer sphere" relaxation) and to short-range interactions ("inner sphere" relaxation). The latter process is mediated by the chemical exchange of inner sphere water molecules with the bulk. The water exchange rate is a lower limit for the proton exchange rate. At physiological pH, however, proton exchange occurs via the

exchange of entire water molecules. Inner sphere relaxation is governed by four correlation times: the time for rotation of the complex, τ_r ; the residence time of a water proton in the inner coordination sphere, τ_m ; and the electronic longitudinal and transverse relaxation rates ($1/T_{1e}$ and $1/T_{2e}$) of the metal center.⁴ The outer sphere relaxivity is determined by the relative diffusional motion of outer sphere water molecules and the complex, and by $1/T_{1e}$ and $1/T_{2e}$.⁴ The current commercial MRI contrast agents contain one water molecule in their inner coordination sphere. The presence of one inner sphere molecule ensures a high proton relaxivity effect via rapid exchange of inner sphere water with the bulk water. The "inner sphere" and "outer sphere" contributions to the proton relaxivity in these complexes are similar in magnitude.

The evolution of the MRI technique has given rise to an increasing demand for contrast agents which are more effective and specific than the ones currently commercially available, such as the Gd(III) complexes of diethylenetriamine-N,N',N'',N'''-pentaacetate (Gd(DTPA)²⁻) and 1,4,7,10-tetraazacyclododecane-N,N',N'',N'''-tetraacetate (Gd(DOTA)⁻). Theory predicts that it should be possible to make contrast agents with a relaxivity that is 100 times higher than that of the contrast agents presently in use. The rational design of improved contrast agents requires insight into the relation between structure and proton relaxation enhancement.⁵

An option to achieve higher relaxivities, is to couple the Gd-chelates covalently to high molecular weight compounds, such as polysaccharides. This type of high molecular weight contrast agents are being investigated on their potential use as blood pool agents. The introduction of sugar compounds in the proximity of the Gd(III) ion may influence the various parameters governing the relaxivity. Here we report on a multinuclear NMR study of the structure and dynamics of the Ln(III) complexes of DTPA-BGLUCA³⁻ and DTPA-BENGALAA³⁻ and of the model compounds DTPA-BEA³⁻ and DTPA-BPDA³⁻ in aqueous solution (see Scheme 1 for the structures) which may serve as model compounds for DTPA-linked polysaccharides. The various Ln(III) complexes of a particular ligand are usually nearly isostructural. Therefore one can profit from the different NMR properties of the various Ln(III) ions in structural analysis of these complexes.^{6,7} A comprehensive study of the parameters governing the relaxivity has been undertaken using variable temperature and pressure ¹⁷O measurements, and NMRD profiles recorded at several temperatures.



Scheme 1. The structural formulas of the different ligands discussed in this work.

RESULTS AND DISCUSSION

Ln(III)-Induced Water ^{17}O shifts

Upon addition of Dy(III) to a 0.08 M solution of one of the ligands under study in D_2O , the water ^{17}O shift decreased linearly as the molar ratio Dy(III)/ L (ρ_L) increased. At $\rho_L = 1.0$, a large increase occurred in the magnitude of the (negative) induced shift. The exchange of water between the Dy(III) complex and the bulk is fast on the ^{17}O NMR time scale under the conditions applied (4.7 T, 75°C). Apparently all ligands form 1:1 complexes at $\rho_L \leq 1$. For DTPA-BGLUCA (Figure 1) the slope of the line $\rho_L > 1$ was 8.1 times larger than that of the line $\rho_L < 1$ and identical to the slope of the line obtained when the titration with Dy(III) was performed in the absence of DTPA-BGLUCA. Similar plots were obtained with DTPA-BEA and DTPA-BPDA, but the plot for DTPA-BENGALAA had a different shape (Figure 1). There the slope at $\rho_L > 1$ was only 2.7 times larger than that of the line at $\rho_L < 1$, and at $\rho_L > 1.4$ a precipitate formed.

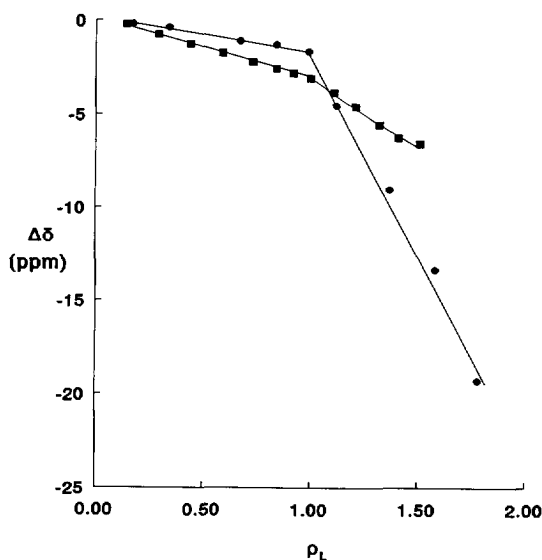


Figure 1. Plots of the Dy(III)-induced water ^{17}O shift versus the molar ratio Dy(III)/organic ligand (ρ_L) for 0.08 M solutions of DTPA-BGLUCA³⁻ (●) and DTPA-BENGALAA³⁻ (■) in D_2O at 75 °C.

Previously, the Dy(III)-induced ^{17}O water shifts were shown to be independent of the other ligands chelated to the Dy(III) ion and to be predominant of contact origin ($\geq 85\%$).⁸ Consequently the slope of a plot of the Dy(III)-induced shift versus the molar ratio Dy(III)/water (ρ_w) is proportional to the hydration number of the Dy(III) complex. If it is assumed that the Dy(III) aquo-ion contains 8 water ligands,⁹ then it can be concluded that all complexes under study contain one water molecule in the first coordination sphere of the Dy(III) ion at $\rho_L \leq 1$. Commonly, the Ln(III) ion in complexes of this type has a coordination number nine. This suggests that the organic ligand is coordinated in an octadentate fashion. Most likely the donor sites are the same as for the previously investigated DTPA-BPA³⁻ ligand: the three nitrogens of the diethylenetriamine group; three carboxylate oxygens; and the two amide oxygens.¹⁰ The deviation of the Dy-DTPA-BENGALAA³⁻ system at $\rho_L > 1$ can be explained by the formation of a di- or oligonuclear species at these concentrations. Further studies on the structure of this

structures and dynamics of Ln(III) complexes of sugar-based DTPA-bis(amides)

complex are in progress.

Table 1. Lanthanide-Induced Water ^{17}O Shifts (ppm) for 0.1 M Ln(DTPA-BEA), Ln(DTPA-BPDA) and Ln(DTPA-BGLUCA) Complexes in D_2O at pH 7 and 75 °C.

| Ln(III) | δ (ppm) ^a | | |
|------------|-----------------------------|-------------------------|---------------------------|
| | DTPA-BEA ³⁻ | DTPA-BPDA ³⁻ | DTPA-BGLUCA ³⁻ |
| La | 964 | 790 | 431 |
| Pr | 935 | 1171 | 938 |
| Nd | 1174 | 1074 | 681 |
| Eu | -80 | -175 | -362 |
| Tb | -1985 | -2305 | -2110 |
| Dy | -1672 | -2085 | -1938 |
| Ho | -1107 | -998 | -1410 |
| Er | -88 | 24 | -44 |
| Tm | 600 | 580 | 639 |
| Yb | 772 | 670 | 716 |
| Lu | 729 | 921 | 363 |
| <i>n</i> F | -68 | -78 | -74 |
| <i>n</i> G | 11.0 | 7.2 | 8.7 |

^a The shifts were obtained using plots analogous to that given in Figure 1.

The values are extrapolated to a molar ratio of Ln(III)/water (ρ_w) = 1. The relative errors are 5%. In order to obtain the number of inner-sphere water molecules in the other Ln(III) complexes, a more extended treatment of the Ln(III)-induced water ^{17}O shifts is required. The induced shifts (Δ) comprise diamagnetic (Δ_d), contact (Δ_c) and pseudocontact shifts (Δ_p). The value of Δ_d can be estimated from an interpolation of the induced shifts for La(III) and Lu(III). The contact contribution results from a through-bond transmission of unpaired spin density, whereas the pseudocontact shift arises from a through-space dipolar interaction between the magnetic moments of the unpaired electrons of the Ln(III) ion and the ^{17}O nucleus. Both Δ_c and Δ_p can be written as the product of a term that is characteristic of the Ln(III) ion but independent of the complex structure ($\langle S_z \rangle$ and C^D respectively) and a second term that is characteristic of the complex but that is independent of the Ln(III) ion (F and G , respectively).^{11,12}

$$\Delta' = \Delta - \Delta_d = \Delta_c + \Delta_p = \langle S_z \rangle F + C^D G \quad (1)$$

Values for $\langle S_z \rangle$ and C^D are tabulated in the literature.¹¹⁻¹⁵ When the various Ln(III) complexes are isostructural, eq 1 can be rearranged in a linear form:¹⁶

$$\Delta' / C^D = \langle S_z \rangle F / C^D + G \quad (2)$$

Thus, when a series of Ln(III) complexes yields a linear plot of Δ'/C^D versus $\langle S_z \rangle/C^D$, this indicates that they are isostructural.^{16,17}

The water ^{17}O shifts for the various Ln-complexes of DTPA-BEA³⁻, DTPA-BPDA³⁻, and DTPA-BGLUCA³⁻ at 75 °C were extrapolated to $\rho_w = 1$ (Table 1). The values obtained correspond to $n\Delta$, where n is the number of the bound waters in the concerning complex. The plots of the shifts according to eq 2 gave straight lines for the three ligands.

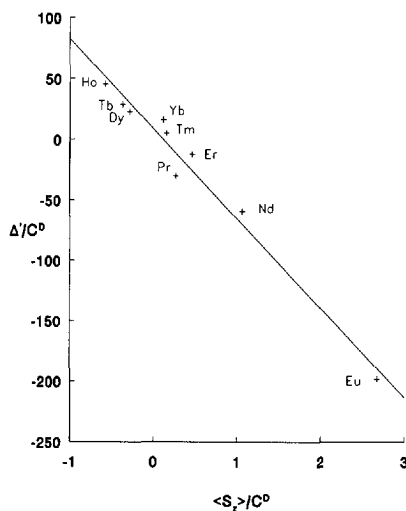


Figure 2. Plot of Δ'/C^D versus $\langle S_z \rangle/C^D$ for the ^{17}O signal in the Ln-DTPA-BGLUCA system at 75 °C.

In Figure 2 this is illustrated for DTPA-BGLUCA³⁻. These results show that there is no change in the hydration number of these complexes along the Ln-series. The values of nF and nG determined by means of a multiple regression method¹⁸ are given in Table 1.

structures and dynamics of Ln(III) complexes of sugar-based DTPA-bis(amides)

Previous investigations have shown that the values of F for Ln(III)-bound oxygens fall in a narrow range of -70 ± 11 at 73°C .¹⁹⁻²¹ It can be concluded that the hydration number does not change across the lanthanide series. Therefore, the stoichiometry of the chelates mentioned above in solution ($\rho_L \leq 1$) is $[\text{Ln}(\text{DTPA-bis}(\text{amide}))(\text{H}_2\text{O})]$.

¹³C NMR spectra

Upon octadentate binding of the DTPA-bisamide ligands to Ln(III) ions in a mode as suggested by the results of the ¹⁷O measurements, inversion of the three nitrogen atoms of the diethylenetriamine backbone is precluded. Therefore these atoms are chiral and the ligand can occur in eight enantiomeric forms. If it is assumed that the coordination polyhedron of the nine-coordinated Ln(III) ion in these complexes can be described by a tricapped trigonal prism, this gives rise to the eight complex geometries depicted in Figure 3. Similar isomers are possible for a monocapped square antiprism.

Recently, it has been shown that all eight isomers occur in aqueous solutions of the Ln(III) complexes of DTPA-BPA³⁻.¹⁰ Two dynamic processes play an important role: (i) racemization of the central nitrogen atom via the interconversions of 1-4 and 1'-4' which are associated with the interconversions of the two gauche conformations of the ethylenediamine bridges ("wagging"); and (ii) racemization at the terminal nitrogens via the interconversions $1 \rightleftharpoons 2 \rightleftharpoons 3 \rightleftharpoons 4$ and $1' \rightleftharpoons 2' \rightleftharpoons 3' \rightleftharpoons 4'$, which is relatively slow because it requires decoordination of a nitrogen and its two neighbouring oxygens (Figure 3).

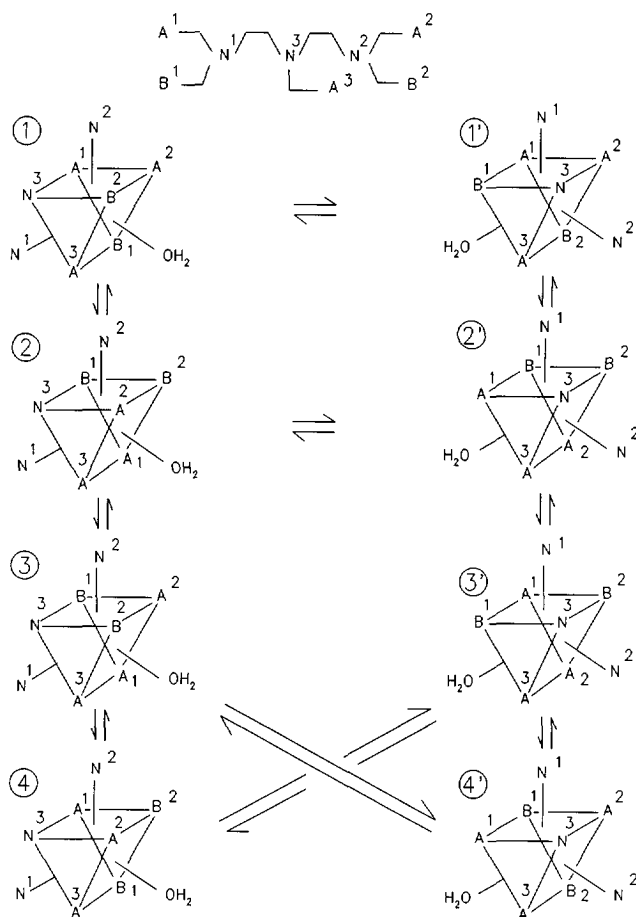


Figure 3. The coordination polyhedrons of the (possible) enantiomers of the $\text{Ln}(\text{DTPA-bisamide})$ complexes (under study), assuming that the geometry is a tricapped trigonal prism. It should be noted that with non-chiral side chains no discrimination can be made between A^1 and A^2 , B^1 and B^2 , and N^1 and N^2 . These groups are labeled in order to be able to follow them during the rearrangements; $A^1=A^2=A^3=\text{COO}^-$; $B^1=B^2=\text{CO-NH-sugar}$.

The ^{13}C NMR spectra of the diamagnetic ($\text{La}(\text{III})$) and paramagnetic ($\text{Nd}(\text{III})$) complexes of the ligands DTPA-BEA^{3-} , DTPA-BPDA^{3-} , DTPA-BGLUCA^{3-} , and DTPA-

BENGALAA³⁻ displayed several resonances for each atom, which is consistent with the occurrence of various isomers in solution. In the static situation of compounds with a chiral side chain, each ligand nucleus would give rise to eight resonances. In addition to this, it should be noted that the two amide groups and the two terminal carboxylate groups in each isomer are chemically inequivalent. Thus for the amide C- α atom, for example, 16 resonances are expected. When the "wagging" process is rapid on the NMR time scale the number of signals is reduced to eight. Accordingly, the ¹³C NMR spectrum of the Nd(DTPA-BGLUCA) complex in D₂O at 100.6 MHz and 80 °C (δ 37 - 41, Figure 4) shows eight signals for the amide C- α (C-1 in Scheme 1). Upon decreasing the temperature to 0°C, substantial line-broadening occurred. However, the slow-exchange region for the racemization around the central nitrogen atom could not be reached because further cooling, after addition of methanol, caused precipitation of the complex. The ¹³C spectrum of the Nd(DTPA-BEA) complex, in which the amide side-chains are not chiral, shows less resonances than the Nd(DTPA-BGLUCA) complex. In this case, the isomers 1'-4' are the mirror images of 1-4 and thus not distinguishable with NMR. Consequently, only four resonances are observed for the amide C- α atom under conditions of rapid exchange on the NMR time scale between 1-4 and 1'-4'. This simplification is also observed in the ¹³C NMR spectra of the Nd(III) complexes of DTPA-BPDA³⁻ and DTPA-BENGALAA³⁻, which both display only four signals in the C- α window at 80°C and 100.6 MHz (Supplementary Material). The chiral entity in DTPA-BENGALAA is probably too far away to be sensed by C- α , whereas the effects of chirality in the ¹³C spectrum of DTPA-BPDA are possibly averaged-out by fast rotations in the PDA side-chain.

The various isomers present in solution of each Nd(III) complex studied occur in non-equivalent amounts which can be seen from the different signal intensities of e.g. the amide C- α (Supplementary Material; Table S1).

The region in the ¹³C spectrum between 56 and 74 ppm (DTPA-backbone and sugar chain), in which the other signals appeared, was very complex due to severe overlapping. The methylene carbons of the diethylenetriamine group and the central glycine unit of the Ln(III) complexes (Ln = La, Nd) of the discussed chelates are at approximately the same chemical shifts as those of LnDTPA and LnDTPA-BPA complexes^{10,22} (Supplementary Material; Table S1). This confirms that there is both a similarity amongst the various Ln

complexes discussed in this work and between these complexes and LnDTPA and LnDTPA-BPA.

In Table 2 the kinetic data for the racemization at N¹, N² in LaDTPA-BGLUCA and LaDTPA-BENGALAA as determined by coalescence temperatures of the ¹³C NMR signals at 100.6 MHz are presented. The activation parameters for this process are in good agreement with those obtained for LaDTPA-BPA indicating that the presence of the polyhydroxy chain does not alter significantly the dynamics of this particular intramolecular rearrangement.

Table 2. Kinetic Data for the Racemization at N¹, N² in La(DTPA-bis(amide) Complexes at 283 K.

| Ligand | $\Delta G_{283}^{\#}$ (kJ mol ⁻¹) | $\Delta H^{\#}$ (kJ mol ⁻¹) | $\Delta S^{\#}$ (J mol ⁻¹ K ⁻¹) | k^{283} (s ⁻¹) |
|------------------------------|--|--|---|---------------------------------|
| DTPA-BGLUCA ^{3-a} | 66 | 34 | -116 | 2.7 |
| DTPA-BENGALAA ^{3-a} | 65 | 37 | -100 | 5.2 |
| DTPA-BPA ^{3-b,c} | 71 | 47 | -84 | 0.7 |

^a From coalescence temperatures of ¹³C NMR signals (100.6 MHz); ^b From ¹³C NMR line shapes (100.6 MHz); ^c Reference 10.

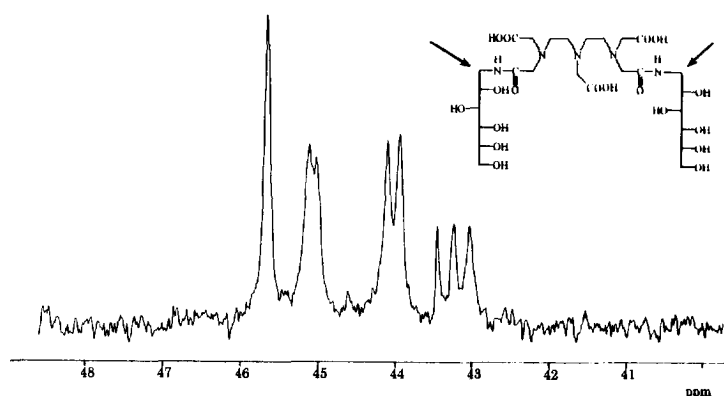


Figure 4. ¹³C NMR spectrum (C-α (C-1) region) of 0.1 M [Nd(DTPA-BLUCA)(H₂O)] in D₂O at 80 °C and 100.6 MHz.

Nd(III)-Induced Relaxation Rates Enhancements

Among the lighter Ln(III) ions (Ln = Ce → Eu), Nd(III) having the longest electron relaxation times,²³ was selected for the ¹³C NMR longitudinal relaxation rate study on the coordination with the ligands discussed in this work. The Nd(III)-induced ¹³C NMR relaxation enhancements have been measured for DTPA-BEA³⁻, DTPA-BPDA³⁻, DTPA-BGLUCA³⁻ and DTPA-BENGALAA³⁻ at 9.4 T and 80°C. Under these conditions fast exchange on the NMR time scale occurs between several ligand nuclei which is due to the racemization at N³. In order to correct for diamagnetic contributions the relaxation rates for the corresponding La(III) complex were subtracted from the measured values of the Nd(III) complex.

Assuming that there are two species A and B, which are in fast exchange on the NMR time scale, the observed longitudinal relaxation rate of a nucleus ($1/T_{1,obs}$) is given by:^{24,25}

$$\frac{1}{T_{1,obs}} = \frac{f_A}{T_{1,A}} + \frac{f_B}{T_{1,B}} \quad (3)$$

where $T_{1,A}$ and $T_{1,B}$ are the intrinsic relaxation times in the absence of exchange and f_A and f_B are the molar fractions of A and B. For exchange between more than two species, an analogous expression can be derived. Since it is only for remote nuclei that the outer-sphere contribution ($1/T_{1,OS}$) becomes significant, this contribution was neglected in our study. The electron relaxation for Nd(III) is very fast ($T_{1e} \approx 10^{-13}$ s) with the result that the contact contribution to the paramagnetic relaxation is negligible. Two contributions are of importance: the "classical" dipolar relaxation and the Curie relaxation. From a simplified Solomon-Bloembergen equation^{23,26} and the equation for the Curie relaxation,^{27,28} expression 4 can be derived, which relates the relaxation rate for each isomer to its structure.

$$\frac{1}{T_1} = \left[\frac{4}{3} \left(\frac{\mu_0}{4\pi} \right)^2 \mu^2 \gamma_I^2 \beta^2 T_{1,e} + \frac{6}{5} \left(\frac{\mu_0}{4\pi} \right)^2 \frac{\gamma_I^2 H_0^2 \mu^4 \beta^4}{(3kT)^2} \tau_r \right] \frac{1}{r^6} \quad (4)$$

The first term between the brackets represents the "classical" dipolar contribution and the

second term the Curie contribution. Here $\mu_0/4\pi$ is the magnetic permeability in a vacuum, μ is the effective magnetic moment of the lanthanide ion, γ_1 is the magnetogyric ratio of the nucleus under study, β is the Bohr magneton, $T_{1,e}$ is the electron spin relaxation time, r is the distance between the ^{13}C nucleus in question and the lanthanide ion, H_0 is the magnetic field strength, k is the Boltzmann constant, T is the temperature, and τ_r the rotational tumbling time of the complex. The contribution of the Curie spin mechanism to the total relaxation becomes significant for larger molecules (τ_r increases), particularly at higher fields.

Table 3. Relaxation Data.

| Assign. | DTPA-BEA ³⁻ | DTPA-BPDA ³⁻ | DTPA-BGLUCA ³⁻ | DTPA-BENGALAA ³⁻ | |
|------------------------------------|---|-------------------------|---------------------------|-----------------------------|-----------------------|
| | <u>$1/T_1$ (s⁻¹)^a</u> | | | | |
| CO | 4.86-7.71 | 6.78-10.9 | 7.60-10.4 | 13.0-15.6 | 8.6-13.1 ^b |
| CH ₂ CO | 4.94-6.01 | 4.22-7.21 | 4.31-7.88 | 10.4-12.4 | 7.2-8.8 ^b |
| NCH ₂ CH ₂ N | 4.53-4.95 | 5.18-6.21 | 5.78-6.43 | 9.14-12.3 | 7.0-13.5 ^b |
| C- α | 0.42-0.49 | 0.22-0.24 | 0.70-1.32 | 0.70-0.9 | 0.44 ^b |
| | <u>τ_r (x 10⁻¹¹ s)^c</u> | | | | |
| DTPA-moiety | 3.7 | 7.4 | 9.8 | 9.3 | |
| sugar chain | | 3.7 | 5.6 | 5.4 | |

^a ^{13}C relaxation rates of the Nd(III) complexes in D₂O at 80 °C and 100.6 MHz; ^b Values obtained at 50.3 MHz; ^c Rotational correlation times τ_r as determined by ^{13}C relaxation rates measurements of the La(III) complexes at 353 K and using eq 5.

The relative paramagnetic relaxation rates (Table 3) are about the same for all ligands studied and they are also the same as those for the previously studied Nd(DTPA-BPA).¹⁰ These data therefore support the conclusions from the Ln(III) induced water ^{17}O shifts: the Ln(III) ion is coordinated by the ligand in an octadentate binding mode via three carboxylate oxygens, two amide oxygens and the three nitrogens of the diethylenetriamine unit. Additionally, the low relaxation rates of the sugar side-chains indicate that the hydroxyl groups of the ligands are not involved in the coordination of Ln(III).

If τ_r and $T_{1,e}$ are known, the absolute distances between Nd(III) and the ligand nuclei can be calculated from the relaxation rates and eq 4. The value of τ_r , under the conditions applied, can be estimated from the intramolecular dipole-dipole relaxation rate ($1/T_{1,DD}$) of a ^{13}C nucleus of the ligand in the corresponding diamagnetic La complex using eq 5:

$$\frac{1}{T_{1,DD}} = N \left(\frac{\mu_0}{4\pi} \right)^2 \frac{\hbar^2 \gamma^2 [^{13}\text{C}] \gamma^2 [^1\text{H}]}{r_{CH}^6} \tau_r \quad (5)$$

Here \hbar is the Dirac constant, and N is the number of protons bound to the ^{13}C nucleus. The $1/T_{1,DD}$ value is determined from the diamagnetic relaxation rate according to a standard NMR procedure.

In Table 3 the τ_r values for the various ligands are as determined from ^{13}C relaxation rates in the corresponding La(III) complexes are summarized. The increase in molecular weight is clearly reflected in the decrease of τ_r , going from DTPA-BEA $^{3-}$ to DTPA-BENGALAA $^{3-}$ via DTPA-BPDA $^{3-}$ and DTPA-BGLUCA $^{3-}$. The molecular weights of DTPA-BGLUCA and DTPA-BENGALAA have the same magnitude; consequently, the rotational correlation times of these chelates are similar. The results show that in all ligands, the DTPA-backbone rotates approximately two times slower than the sugar entity.

It has been shown that the $T_{1,e}$ value is usually rather independent of the ligation of the Ln(III) cation.²⁹⁻³¹ For lanthanides other than Gd, large deviations from $T_{1,e}$ are only expected for complexes that are very rigid and for symmetrical macrocyclic ligands.³² By using data reported by Alsaadi et al. on Nd(III) complexes of DTPA $^{5-}$ and related poly(amino carboxylate) ligands,²⁹ $T_{1,e}$ for the Nd-complexes of DTPA-BEA $^{3-}$, DTPA-BPDA $^{3-}$, and DTPA-BGLUCA $^{3-}$ at 80 °C is estimated to be 0.9×10^{-13} s. Then distances r were calculated for DTPA-BEA $^{3-}$, DTPA-BPDA $^{3-}$, and DTPA-BGLUCA $^{3-}$ from the paramagnetic relaxation rates using eq 4. The distances obtained are compiled in Table 4. The carbon atoms, except for the amide C- α , in the polyhydroxy chain are relatively far away from the Nd(III)-ion compared to these C-atoms present in the DTPA-backbone. Consequently, the Nd(III)-induced relaxation rate enhancement is small causing the corresponding Nd(III)-C distances to be inaccurate, hence these data were not taken into consideration.

The magnitudes of the relaxation rates for DTPA-BENGALAA³⁻ (Table 3) are approximately 1.7 times larger than those of the other chelates, which would result in relatively short (and hence improbable) Nd(III)-C distances upon implementation of the procedure described above. The τ_r values obtained from the relaxation rate measurements of the LaDTPA-BENGALAA complex agree with the observed trend. This leaves a higher value for $T_{1,e}$ as an explanation for the relatively large relaxation rates in DTPA-BENGALAA³⁻. We therefore have also performed relaxation rate measurements on this ligand at lower magnetic field (4.7 T). With the use of eq 4, it can be estimated that under these conditions the contribution of the Curie mechanism to the total relaxation is negligible (< 3%). Based upon the distances in the solid-state structure of Gd(DTPA-EA))³³ and the relaxation data obtained at 4.7 T, $T_{1,e}$ for Nd(DTPA-BENGALAA) was estimated to be $1.5 \cdot 10^{-13}$ s.

Table 4. Nd(III)-C Distances, r (Å), in the Isomers of Nd-Complexes of the Ligands Concerned; Comparison with Distances in the Nd(DTPA)²⁻ Complex, Nd(DTPA-BPA) Complex and in the Solid-State Structure of Gd(DTPA-EA₂).

| Complex | CO | CH ₂ CO | NCH ₂ CH ₂ N | C- α |
|--|-----------|--------------------|------------------------------------|-------------|
| Nd(DTPA-BEA) | 3.14-3.30 | 3.28-3.39 | 3.38-3.44 | 4.98-5.11 |
| Nd(DTPA-BPDA) | 3.04-3.28 | 3.25-3.55 | 3.33-3.43 | 5.21-5.53 |
| Nd(DTPA-BGLUCA) | 3.10-3.26 | 3.25-3.59 | 3.36-3.42 | 4.38-4.86 |
| Nd(DTPA-BENGALAA) ^a | 3.08-3.17 | 3.20-3.29 | 3.20-3.37 | 4.95-5.16 |
| | 3.05-3.27 | 3.26-3.39 | 3.04-3.39 | 5.37 |
| Nd(DTPA) ^{2-,b} | 3.15-3.20 | | 3.21-3.48 | |
| Nd(DTPA-BPA) ^c | 3.08-3.19 | 3.25-3.37 | 3.36-3.43 | 5.33-5.47 |
| Gd(DTPA-EA ₂) ^d | 3.25-3.31 | 3.40-3.56 | 3.46-3.51 | 5.13-5.23 |

^a Upper row values obtained at 400 MHz; lower row values obtained at 200 MHz; distances calculated with $T_{1,e} = 1.5 \cdot 10^{-13}$ s⁻¹; ^b Reference 22; ^c Reference 10; ^d From X-ray analysis.³³

Variable temperature and pressure ¹⁷O NMR measurements

From the measured ¹⁷O NMR relaxation rates and angular frequencies of the [Gd(DTPA-bis(amides))(H₂O)] solutions, $1/T_1$, $1/T_2$, and ω , and of the acidified water reference, $1/T_{1A}$, $1/T_{2A}$, and ω_A , one can calculate the reduced relaxation rates and chemical shifts, $1/T_{1r}$, $1/T_{2r}$, and $\Delta\omega_r$, which may be written as in eqs 6-8.^{34,35}

$$\frac{1}{T_{1r}} = \frac{1}{P_m} \left[\frac{1}{T_1} - \frac{1}{T_{1A}} \right] = \frac{1}{T_{1m} + \tau_m} + \frac{1}{T_{1os}} \quad (6)$$

$$\frac{1}{T_{2r}} = \frac{1}{P_m} \left[\frac{1}{T_2} - \frac{1}{T_{2A}} \right] = \frac{1}{\tau_m} \frac{T_{2m}^{-2} + \tau_m^{-1} T_{2m}^{-1} + \Delta\omega_m^2}{(\tau_m^{-1} + T_{2m}^{-1})^2 + \Delta\omega_m^2} + \frac{1}{T_{2os}} \quad (7)$$

$$\Delta\omega_r = \frac{1}{P_m} (\omega - \omega_A) = \frac{\Delta\omega_m}{(1 + \tau_m T_{2m}^{-1})^2 + \tau_m^2 \Delta\omega_m^2} + \Delta\omega_{os} \quad (8)$$

where $1/T_{1m}$, $1/T_{2m}$ are the relaxation rates in the bound water, $\Delta\omega_m$ is the chemical shift difference between the bound and bulk water (in the absence of a paramagnetic interaction with the bulk water), P_m is the mole fraction of bound water and τ_m is the residence time of water molecules in the inner coordination sphere. The total outer sphere contributions to the reduced relaxation rates and chemical shift are represented by $1/T_{1os}$, $1/T_{2os}$, and $\Delta\omega_{os}$.

It has been shown that the outer sphere contributions in eqs 6 and 7 can be neglected.^{36,37}

In addition, it can be shown from the analysis below that the contribution of $\Delta\omega_m$ in eq 7 is negligibly small, so that one can simplify eqs 6 and 7, giving

$$\frac{1}{T_{1r}} = \frac{1}{T_{1m} + \tau_m} \quad (9)$$

$$\frac{1}{T_{2r}} = \frac{1}{T_{2m} + \tau_m} \quad (10)$$

The maxima observed in the temperature dependence of $1/T_{2r}$ are characteristic of a changeover from the "fast exchange" limit at high temperatures, where T_{2m} is the principal term in the denominator of eq 10, to the "slow exchange" limit at low temperatures, where τ_m is the principal term. Since $T_{1m} > T_{2m}$, the maximum in $1/T_{1r}$ is shifted to lower temperatures as can be seen from the results shown in Figures 5A-C.

The changeover between fast and slow exchange limits is also manifested in $\Delta\omega_r$, the maxima in $1/T_{2r}$ corresponding to the points of inflection in $\Delta\omega_r$. At high temperatures, the inner sphere contribution to $\Delta\omega_r$ is given by the chemical shift of the bound water molecules, which is determined by the hyperfine interaction between the Gd(III) electron spin and the ^{17}O nucleus via³⁸

$$\Delta\omega_m = \frac{g_L \mu_B S(S+1)B}{3k_B T} \frac{A}{\hbar} \quad (11)$$

where g_L is the isotropic Landé g -factor ($g_L = 2.0$ for Gd(III)), S is the electron spin ($S=7/2$ for Gd(III)), A/\hbar is the hyperfine or scalar coupling constant and B is the magnetic field. We assume that the outer sphere contribution to $\Delta\omega_r$ has a temperature dependence similar to $\Delta\omega_m$ and is given by:

$$\Delta\omega_{os} = C_{os} \Delta\omega_m \quad (12)$$

where C_{os} is an empirical constant.

The ^{17}O longitudinal relaxation rates in Gd(III) solutions are dominated by the dipole-dipole and quadrupolar mechanisms³⁶, and to a good approximation³⁷, may be expressed by:

$$\frac{1}{T_{1m}} = \left[\frac{2}{5} \left(\frac{\mu_0}{4\pi} \right) \frac{\hbar^2 \gamma_I^2 \gamma_S^2}{r^6} S(S+1) + \frac{3\pi^2}{10} \frac{2I+3}{I^2(2I-1)} \chi^2 (1 + \eta^2/3) \right] \tau_c \quad (13)$$

where $\gamma_S = g_L \mu_B / \hbar$ is the electron gyromagnetic ratio ($\gamma_S = 1.76 \times 10^{11} \text{ rad s}^{-1} \text{ T}^{-1}$ for $g_L = 2.0$), γ_I is the nuclear gyromagnetic ratio ($\gamma_I = -3.626 \times 10^7 \text{ rad s}^{-1} \text{ T}^{-1}$ for ^{17}O), r is the effective distance between the electron charge and the ^{17}O nucleus (the metal-oxygen distance in the point dipole approximation), τ_c is the overall correlation time of the complex, I is the nuclear spin ($I = 5/2$ for ^{17}O), χ is the quadrupolar coupling constant and η an asymmetry parameter (we use here the value for acidified water³⁹, $\chi(1 + \eta^2/3)^{1/2} = 7.58 \text{ MHz}$). In general, for Gd(III) complexes with low molecular weight τ_c is equal to the rotational correlation time, τ_r . We estimate that $r = 0.25 \text{ nm}$ from neutron

diffraction measurements of lanthanide aqua ions in solution⁴⁰ and from the X-ray crystal structure of a structural analogue $[\text{Gd}(\text{DTPA-BMA})(\text{H}_2\text{O})]^{41}$ of the $[\text{Gd}(\text{DTPA-bis(amide)})(\text{H}_2\text{O})]$ complexes investigated. Using this r value, the dipole-dipole mechanism (the first term in eq 13) contributes about 90% of $1/T_{1m}$.

We assume that the rotational correlation time, τ_c (and thus τ_r), has a simple exponential temperature dependence as in eq 14:

$$\tau_c = \tau_c^{298} \exp \left[\frac{E_c}{R} \left(\frac{1}{T} - \frac{1}{298.15} \right) \right] \quad (14)$$

where τ_c is the correlation time at 298.15 K and E_c is the activation energy. The binding time (or exchange rate, k_{ex}) of water molecules in the inner sphere is assumed to obey the Eyring equation as written in eq 15:

$$\frac{1}{\tau_m} = k_{ex} = \frac{k_B T}{h} \exp \left[\frac{\Delta S^\ddagger}{R} - \frac{\Delta H^\ddagger}{RT} \right] = \frac{k_{ex}^{298} T}{298.15} \exp \left[\frac{\Delta H^\ddagger}{R} \left(\frac{1}{298.15} - \frac{1}{T} \right) \right] \quad (15)$$

where ΔS^\ddagger and ΔH^\ddagger are the entropy and enthalpy of activation for the exchange process and k_{ex}^{298} is the exchange rate at 298.15 K. The transverse relaxation rate of the bound water $1/T_{2m}$ has an exponential temperature dependence as in eq 16:

$$\frac{1}{T_{2m}} = \frac{1}{T_{2m}^{298}} \exp \left[\frac{E_m}{R} \left(\frac{1}{298.15} - \frac{1}{T} \right) \right] \quad (16)$$

where E_m is the activation energy of the relaxation of the bound water and $1/T_{2m}^{298}$ the relaxation rate of the bound water at 298.15 K.

A more detailed approach to the ^{17}O transverse relaxation rates in Gd(III) bound water molecules, which are dominated by the scalar relaxation mechanism,^{36,42} employs the following relationship:³⁷

$$\frac{1}{T_{2m}} = \frac{S(S+1)}{3} \left(\frac{A}{\hbar} \right)^2 \tau_{sl} \quad (17)$$

where $1/\tau_{s1} = 1/\tau_m + 1/T_{1e}$. The line width can be described by assuming a relaxation mechanism arising from modulation of a static or transient zero field splitting (ZFS).⁴³ In order to explain the $1/T_{2r}$ values in earlier studies,⁴¹ we needed to assume a second magnetic field dependent mechanism for $1/T_{1e}$. The ZFS contribution to $1/T_{1e}$ falls off rapidly with magnetic field (for $\omega_s\tau_v > 1$), so that it is quite likely that a second mechanism could come into play at high magnetic fields as used in this NMR study (9.4 T). In particular, the asymmetry of the chelate complex may lead to anisotropy of the g_L tensor so that the spin rotation (SR) mechanism may become important.^{44,45} We therefore assume, that $1/T_{1e}$ is a sum of ZFS and SR contributions as in eq 18.

$$\frac{1}{T_{1e}} = \left(\frac{1}{T_{1e}}\right)^{ZFS} + \left(\frac{1}{T_{1e}}\right)^{SR} \quad (18)$$

It was shown that the ZFS mechanism of longitudinal electronic relaxation to a good approximation should be a single exponential that can be described by the analytical expression of McLachlan,⁴⁶ given in eq 19:

$$\left(\frac{1}{T_{1e}}\right)^{ZFS} = \frac{1}{25} \Delta^2 \tau_v [4S(S+1) - 3] \left(\frac{1}{1 + \omega_s^2 \tau_v^2} + \frac{4}{1 + 4\omega_s^2 \tau_v^2} \right) \quad (19)$$

where ω_s is the Larmor frequency, Δ^2 is the trace of the square of the ZFS tensor and τ_v is the correlation time for the modulation of ZFS. The modulation of the ZFS may be due to the lifetime of transient distortions⁴⁷ and we assume that the correlation time has Arrhenius behaviour

$$\tau_v = \tau_v^{298} \exp\left[\frac{E_v}{R} \left(\frac{1}{T} - \frac{1}{298.15}\right)\right] \quad (20)$$

The SR contribution is given approximately by eq 21:^{44,45}

$$\left(\frac{1}{T_{1e}}\right)^{SR} = \frac{\delta g_L^2}{9\tau_c} \quad (21)$$

where $\delta g_L^2 = \sum_i \delta g_{Li}^2$, δg_{Li} , being the deviations of the g_L values along the principal axes of the g_L tensor from the free electron value. We have performed a simultaneous least squares fit of the data in Figures 5A-C using 6-8, and 11-16 with eight fitted parameters: ΔH^\ddagger , ΔS^\ddagger (or k_{ex}^{298}), A/\hbar , C_{os} , τ_c^{298} , E_c , T_{2m} , and E_m . The resulting curves are shown in Figures 5A-C and the fitted parameters are given in Table 5. In order to prove that the rather crude treatment of the bound water relaxation has no significant effect on the fitting parameters, a simultaneous least squares fit of the data in Figures 5A-C using eqs 6-8, 11-15, and 17-21, with τ_v^{298} , E_v , Δ^2 and δg^2 instead of E_m and T_{2m}^{298} as parameters for the bound water relaxation was carried out. Varying the value of Δ^2 from $2 \times 10^{19} \text{ s}^{-2}$ to $5 \times 10^{19} \text{ s}^{-2}$ and fixing Δg^2 around 0.017 (values for $[\text{Gd}(\text{DTPA-BMA})(\text{H}_2\text{O})]$: $3.8 \times 10^{19} \text{ s}^{-2}$ and 0.017)⁴¹ with τ_v^{298} and E_v as adjustable parameters did not alter k_{ex}^{298} nor the ΔH^\ddagger or A/\hbar values (within the statistical errors) presented in Table 5.

The pressure dependence of the reduced transverse relaxation rates, $1/T_{2r}$, at temperatures between 302 and 312 K and at 9.4 T is shown in Figures 5A-C. At this magnetic field and the temperatures chosen, the systems are in the slow exchange limit and $1/T_{2r}$ equals τ_m . The decrease of $1/T_{2r}$ with pressure in Figures 5A-C is therefore due to deceleration of the water exchange process. The pressure dependence of the water exchange rate may be written as in eq 22:

$$\frac{1}{\tau_m} = k_{ex} = (k_{ex})_0^T \exp \left[-\frac{\Delta V_0^*}{RT} P + \frac{\Delta \beta^*}{2RT} P^2 \right] \quad (22)$$

where ΔV_0^\ddagger is the activation volume at zero pressure and temperature T , $(k_{ex})_0^T$ is the exchange rate at zero pressure and temperature T and $\Delta \beta^\ddagger$ is the compressibility coefficient of activation. In the fitting procedure we included a possible pressure dependence of the bound water relaxation rate $1/T_{2m}$ as given in eq 23. Upon fixing ΔV_m^\ddagger at values from -5 to $+5 \text{ cm}^3 \text{ mol}^{-1}$, the results remained, within the statistical error, the same as those given in Table 5.

$$\frac{1}{T_{2m}} = \frac{1}{T_{2m}^0} \exp \frac{-\Delta V_m^\ddagger}{RT} P \quad (23)$$

We performed a least squares fit of the data in Figures 5A-C using eqs 7, 11, 15, 16, 22, and 23 with $(k_{\text{ex}})_0^T$ and ΔV_0^\ddagger as fitted parameters. In previous studies,⁴⁸ the pressure dependence of $\ln(k_{\text{ex}})$ has been found to be nearly linear, so we assume that $\Delta\beta^\ddagger = 0$. The scalar coupling constant was found previously to be independent of pressure, so we assume that it is constant and equal to the value in Table 5. The fitted function is shown in the Figures 5A-C, the corresponding obtained kinetic parameters are included in Table 6. The kinetic parameters that describe the water exchange in the Gd(III) aqua ion and several other poly(amino carboxylates) chelate complexes are also tabulated in Table 6.^{36,37,41} The water exchange rates at zero pressure and temperature T compared with those calculated from the variable temperature ^{17}O NMR data, using eq 15, are in good agreement as exemplified in Table 7.

Table 5. Parameters Obtained from Least Squares Fits of the ^{17}O NMR Data for [Gd(DTPA-BPDA)(H₂O)], [Gd(DTPA-BGLUCA)(H₂O)] and [Gd(DTPA-BENGALAA)(H₂O)] in Aqueous Solution^a.

| Parameter | Gd(DTPA-BPDA) | Gd(DTPA-BGLUCA) | Gd(DTPA-BENGALAA) |
|--|-----------------------------|-----------------------------|-----------------------------|
| k_{ex}^{298} ($\times 10^5 \text{ s}^{-1}$) | 3.6 \pm 0.3 | 3.9 \pm 0.2 | 2.1 \pm 0.1 |
| ΔH^\ddagger (kJ mol ⁻¹) | 39.4 \pm 2.7 | 44.0 \pm 2.1 | 37.8 \pm 2.2 |
| ΔS^\ddagger (J K ⁻¹ mol ⁻¹) | -6.2 \pm 9.6 | +9.8 \pm 7.2 | -16.4 \pm 7.3 |
| A/\hbar ($\times 10^6 \text{ rad s}^{-1}$) | -4.0 \pm 0.8 | -3.2 \pm 0.3 | -3.4 \pm 0.6 |
| C_{os} | 0.09 \pm 0.07 | 0.08 \pm 0.05 | 0.09 \pm 0.07 |
| τ_r^{298} ($\times 10^{-10} \text{ s}$) | 2.06 \pm 0.16 | 2.93 \pm 0.13 | 3.83 \pm 0.29 |
| E_r (kJ mol ⁻¹) | 22.0 \pm 1.5 | 29.4 \pm 0.7 | 20.3 \pm 1.2 |
| T_{2m}^{298} (10^{-8} s) | 8.0 \pm 5.7 | 7.2 \pm 1.8 | 2.9 \pm 2.2 |
| E_m^{298} (kJ mol ⁻¹) | -30.3 \pm 9.3 | -31.4 \pm 3.0 | -39.2 \pm 8.6 |
| ΔV_0^\ddagger (cm ³ mol ⁻¹) | +6.5 \pm 0.2 ^b | +6.4 \pm 0.2 ^c | +5.2 \pm 0.2 ^d |

^a The errors quoted correspond to one standard deviation; ^b T = 302.6 K; ^c T = 302.5 K;

^d T = 311.9 K

The values for the scalar coupling constant, A/\hbar , obtained from the VT ^{17}O NMR data (Table 5), are very similar to those obtained for several other Gd(III) chelate complexes with one inner sphere water molecule: $A/\hbar = -(3.8 \pm 0.2) \times 10^6 \text{ rad s}^{-1}$ and $A/\hbar = -(3.6 \pm 0.3) \times 10^6 \text{ rad s}^{-1}$ for DTPA⁵⁻ and DTPA-BMA³⁻ complexes respectively,^{36,41} and agree also with the F-value observed in many previous Ln(III) water ^{17}O shift studies.^{10,22} It

was shown using VT UV-visible absorption experiments for DTPA⁵⁻ and DTPA-BMA³⁻ complexes that the number of inner sphere water molecules did not change as a function of temperature.^{36,41} We can therefore be confident in our assignment of the stoichiometry of the Gd(III)-complexes concerned in solution over the temperature range employed in the ¹⁷O NMR study.

As already has been observed, the water exchange rate decreases dramatically from [Gd(H₂O)₈]³⁺ to the chelate complexes with one inner sphere water molecule [Gd(DTPA)(H₂O)]²⁻, [Gd(DOTA)(H₂O)]⁻, and [Gd(DTPA-BMA)(H₂O)] (Table 6). This rate decrease is accompanied by an increase of ΔH^\ddagger and a change of sign of ΔS^\ddagger and ΔV_0^\ddagger . The negative ΔV_0^\ddagger values for [Gd(H₂O)₈]³⁺ indicates associatively activated water exchange (I_a mechanism), whereas the large positive ΔV_0^\ddagger values for [Gd(DTPA)(H₂O)]²⁻ and [Gd(DOTA)(H₂O)]⁻ indicate more dissociatively activated water exchange. This can be understood if we consider that the latter two chelate complexes can accommodate only one inner sphere water molecule. The incoming water molecule cannot participate in water exchange, which will have a dissociative activation mode and probably a limiting dissociative D mechanism. Without participation of the incoming water molecule, more energy is required to break the bond between the outgoing water molecule and the highly charged Gd(III), leading to the higher ΔH^\ddagger and lower k_{ex}^{298} values. The results for the [Gd(DTPA-bis(amide)(H₂O))] complexes investigated obey this trend and we conclude that the water exchange on these chelate complexes takes place most probably via a limiting dissociative D mechanism.

The water-exchange rate, k_{ex}^{298} is an order of magnitude lower for the three Gd-complexes studied, than for [Gd(DTPA)(H₂O)]²⁻ and [Gd(DOTA)(H₂O)]⁻.³⁶ In addition to this, the k_{ex}^{298} values for [Gd(DTPA-BPDA)(H₂O)] and [Gd(DTPA-BGLUCA)(H₂O)] are similar to that obtained for [Gd(DTPA-BMA)(H₂O)].⁴¹ Compared to the water-exchange rate for the latter compound the value found for [Gd(DTPA-BENGALAA)(H₂O)] is a factor of two lower. The activation enthalpies for the six chelate complexes are very similar, which means that the differences in exchange rates are entropy driven. A positive activation entropy for a dissociative process is mainly due to the increasing disorder obtained upon breaking the metal-water bond. There are however, also contributions arising from the arrangement of the remaining coordination sites and the disruption of the structure of the outer sphere water at the transition state. These contributions may be

different for each chelate complex. Previous studies of the Ln(III) aqua ions demonstrated that the systematic errors in activation enthalpies and entropies are correlated, hence over-interpretation of the observed differences in ΔS^\ddagger for the above six chelates should be avoided.

Table 6. Water Exchange Kinetic Parameters Obtained for Different Gd(III) Complexes Compared with Those Obtained in This Study.

| Complex | k_{ex}^{298} (s^{-1}) | ΔH^\ddagger (kJ mol^{-1}) | ΔS^\ddagger ($\text{J K}^{-1} \text{mol}^{-1}$) | ΔV_0^\ddagger ($\text{cm}^3 \text{mol}^{-1}$) | ref. |
|--|--|---|--|--|-----------|
| $\text{Gd}(\text{H}_2\text{O})_8^{3+}$ | $(8.30 \pm 0.95) \times 10^8$ | 14.9 ± 1.3 | -24.1 ± 4.1 | -3.3 ± 0.2 | 42 |
| $\text{Gd}(\text{DTPA})^{2-}$ | $(4.1 \pm 0.3) \times 10^6$ | 52.0 ± 1.4 | $+56.2 \pm 5.0$ | $+12.5 \pm 0.2$ | 36 |
| $\text{Gd}(\text{DOTA})^-$ | $(4.8 \pm 0.4) \times 10^6$ | 48.8 ± 1.6 | $+46.6 \pm 6.0$ | $+10.5 \pm 0.2$ | 36 |
| $\text{Gd}(\text{DTPA-BMA})$ | $(4.3 \pm 0.2) \times 10^5$ | 46.6 ± 1.3 | $+18.9 \pm 4.0$ | $+7.3 \pm 0.2$ | 41 |
| $\text{Gd}(\text{DTPA-BPDA})$ | $(3.6 \pm 0.3) \times 10^5$ | 39.4 ± 2.7 | -6.2 ± 9.6 | $+6.5 \pm 0.2$ | this work |
| $\text{Gd}(\text{DTPA-BGLUCA})$ | $(3.9 \pm 0.2) \times 10^5$ | 44.0 ± 2.1 | $+9.8 \pm 7.2$ | $+6.4 \pm 0.2$ | this work |
| $\text{Gd}(\text{DTPA-BENGALAA})$ | $(2.1 \pm 0.1) \times 10^5$ | 37.8 ± 2.2 | -16.4 ± 7.3 | $+5.2 \pm 0.2$ | this work |

Table 7. Comparison of the water exchange rates at zero pressure and temperature T and those calculated from the variable temperature data.

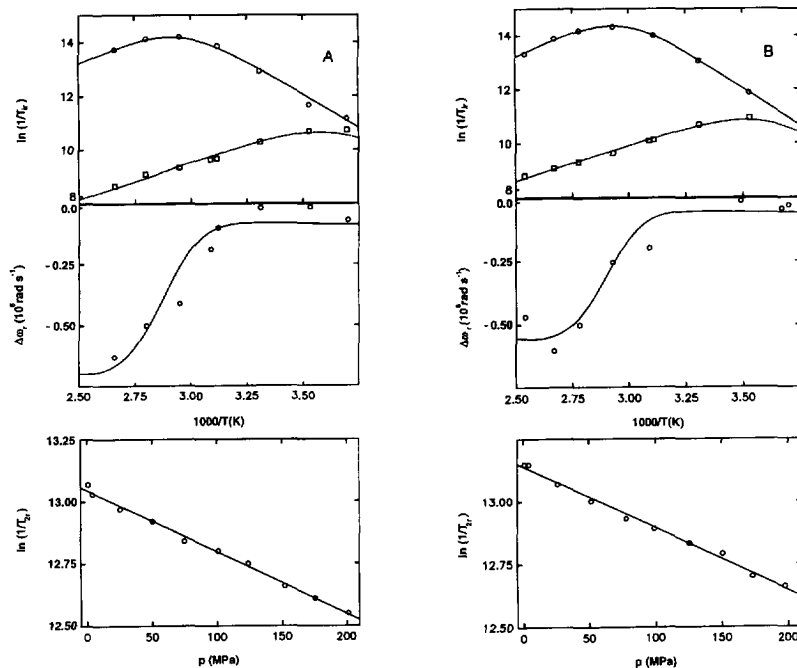
| Complex | T (K) | k_{ex}^T (VT) ^a (s^{-1}) | k_0^T (VP) ^b (s^{-1}) |
|---|---------|---|---|
| $[\text{Gd}(\text{DTPA-BPDA})(\text{H}_2\text{O})]$ | 302.5 | 5.08×10^5 | $5.33 \pm 0.4 \times 10^5$ |
| $[\text{Gd}(\text{DTPA-BGLUCA})(\text{H}_2\text{O})]$ | 311.9 | 4.31×10^5 | $4.41 \pm 0.4 \times 10^5$ |
| $[\text{Gd}(\text{DTPA-BENGALAA})(\text{H}_2\text{O})]$ | 302.6 | 4.68×10^5 | $4.84 \pm 0.4 \times 10^5$ |

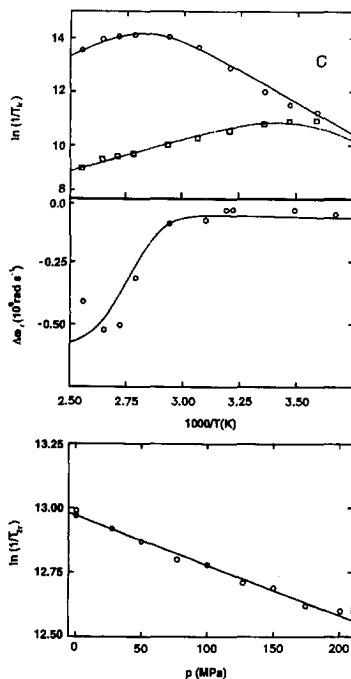
^a values obtained by calculation from eq 15; ^b exchange rate at zero pressure and temperature T .

The rotational correlation time, τ_r^{298} , of $[\text{Gd}(\text{DTPA-BPDA})(\text{H}_2\text{O})]$ is similar to that obtained for $[\text{Gd}(\text{DTPA-BMA})(\text{H}_2\text{O})]$ ($\tau_r^{298} = 1.67 \times 10^{-10}$ s), as expected from the similarity in their molecular size. Relatively longer τ_r^{298} values are obtained for $[\text{Gd}(\text{DTPA-BGLUCA})(\text{H}_2\text{O})]$ and $[\text{Gd}(\text{DTPA-BENGALAA})(\text{H}_2\text{O})]$ due to their larger molecular sizes. Surprisingly the activation energy for the molecular reorientation of

structures and dynamics of Ln(III) complexes of sugar-based DTPA-bis(amides)

[Gd(DTPA-BGLUCA)(H₂O)] ($E_r = 29.4 \text{ kJ mol}^{-1}$) is significantly higher than that of [Gd(DTPA-BPDA)(H₂O)] ($E_r = 22.0 \text{ kJ mol}^{-1}$) and [Gd(DTPA-BENGALAA)(H₂O)] ($E_r = 20.3 \text{ kJ mol}^{-1}$).





Figures 5A-C (also on previous page). Temperature dependence of reduced ^{17}O transverse and longitudinal relaxation rates $\ln(1/T_{ip})$ and of chemical shifts $\Delta\omega_p$, and pressure dependence of transverse relaxation rates for the complexes $[\text{Gd}(\text{DTPA-BPDA})(\text{H}_2\text{O})]$ (A), $[\text{Gd}(\text{DTPA-BGLUCA})(\text{H}_2\text{O})]$ (B) and $[\text{Gd}(\text{DTPA-BENGALAA})(\text{H}_2\text{O})]$ (C) at 9.4 T. The curves represent simultaneous least squares fits using eqs 6-8 and 11-16 for the variable temperature ^{17}O NMR data and eqs 7, 11, 15, 16, 22, and 23 for the variable pressure ^{17}O NMR data.

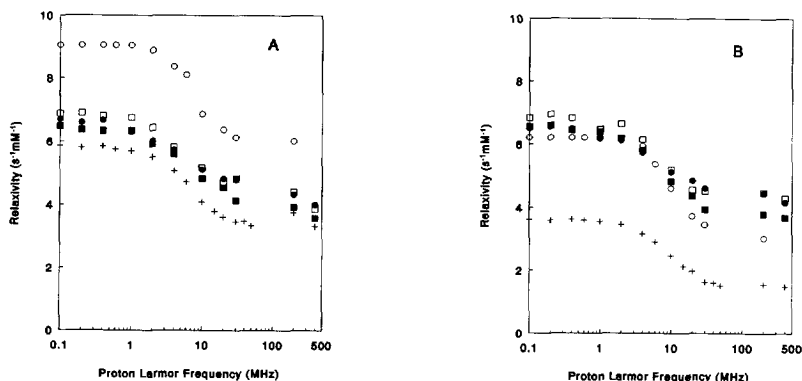
Water proton relaxation

The magnetic field dependences of longitudinal proton relaxation of $[\text{Gd}(\text{DTPA-BPDA})(\text{H}_2\text{O})]$, $[\text{Gd}(\text{DTPA-BGLUCA})(\text{H}_2\text{O})]$ and $[\text{Gd}(\text{DTPA-BENGALAA})(\text{H}_2\text{O})]$ were recorded at several temperatures. The curves obtained at 5 °C and 37 °C, compared to those of $[\text{Gd}(\text{DTPA})(\text{H}_2\text{O})]^{2-}$, are depicted in Figures 6A-B. The relaxivities at 200 and 400 MHz are included in the profiles as well. In the absence of solute-solute interactions,

the solvent relaxation rates are linearly dependent on the concentration of the paramagnetic species; relaxivity is defined as the slope of this dependence in units of $M^{-1}s^{-1}$ (or $mM^{-1}s^{-1}$).

In general, the data are treated using the Solomon-Bloembergen-Morgan's set of equations.^{49,50} The outer sphere contribution to the relaxivity, arising from diffusing water molecules external to the chelate complex, is determined using the Gd(III) complex of triethylenetetramine-*N,N,N',N'',N''',N''''*-hexaacetic acid ($Gd(TTHA)^{3-}$) which is so far considered as a standard outer sphere system since the hydration number, q , is zero. The profiles recorded with the three Gd(III) complexes at 37 °C closely resemble that of $Gd(DTPA)^{2-}$ at low fields (< 10 MHz). However at higher frequencies (> 20 MHz), the relaxivities for all three complexes become larger than for $Gd(DTPA)^{2-}$. In this high-field region, the dominant parameters involved, are τ_m and τ_r . The water-exchange rates of the three Gd(III) complexes are about ten times lower compared to those of $[Gd(DTPA)(H_2O)]^{2-}$ at 37 °C (Table 6) which should result in lower relaxivity values for the DTPA-bis(amide) complexes. The increase in molecular weight results in higher τ_r values for the Gd(III) chelates investigated as compared with $[Gd(DTPA)(H_2O)]^{2-}$ which apparently overcomes the decrease in high field relaxivity due to the above mentioned slower exchange. According to the SBM theory, the low-to-high relaxivities ratio should be 10/3 when $\tau_{SO} \gg \tau_r$, τ_m and $\tau_m \ll T_{1m}$. Since the observed profiles do not exhibit this typical behaviour, the obtained low field relaxivities at 5 °C as well as at 37 °C are limited by τ_{SO} and/or τ_m . The relaxivities obtained for each Gd(III) complex at the various temperatures (Supplementary Material) demonstrate that the relaxivity is almost temperature independent, in contrast to $[Gd(DTPA)(H_2O)]^{2-}$ which displays a typical τ_r -governed relaxivity evolution.³ This temperature independence has already been observed for several other DTPA-bis(amides).^{5,51} At 5 °C, the relaxivity of the three complexes over the whole frequency range is just above that of $[Gd(TTHA)]^{3-}$ and significantly below that of $[Gd(DTPA)(H_2O)]^{2-}$. This is due to the fact that the proton relaxation is limited both by fast electronic relaxation and by slow water chemical exchange, the latter being most distinct at lower temperatures. It was therefore not possible to obtain reliable values for the modulation parameters and as a consequence the comparison with the relaxation data calculated from the ^{17}O NMR measurements could not be made. Further studies are in progress to investigate the as yet not understood temperature dependence of

the relaxivity of the sugar-based DTPA-bis(amides) described in this chapter.



Figures 6A-B. NMRD profiles for the $[Gd(DTPA\text{-bis(amide)})(H_2O)]$ complexes in aqueous solution at 5 °C (A) and 37 °C (B); $[Gd(DTPA)(H_2O)]^{2-}$ (○); $[Gd(DTPA\text{-BPDA})(H_2O)]$ (■); $[Gd(DTPA\text{-BGLUCA})(H_2O)]$ (□); $[Gd(DTPA\text{-BENGALAA})(H_2O)]$ (●); $[Gd(TTHA)]^{3-}$ (+).

CONCLUSIONS

In conclusion, we have shown that $DTPA\text{-BEA}^{3-}$, $DTPA\text{-BPDA}^{3-}$, $DTPA\text{-BGLUCA}^{3-}$ and $DTPA\text{-BENGALAA}^{3-}$ are coordinated to Ln(III) ions in an octadentate fashion via the three N atoms of the diethylenetriamine backbone, three carboxylate oxygens and the two amide oxygens. All Ln(III) complexes contain one inner sphere water molecule. The kinetic parameters for water exchange of the Gd(III) complexes of the ligands under study, when compared with results for similar chelate complexes, indicate a limiting dissociative, D, mechanism. The relatively slow water exchange effects the inner sphere proton relaxivity which is especially reflected in the NMRD profiles recorded at lower temperatures.

EXPERIMENTAL

Materials

All chemicals were purchased from Aldrich Chemical Co. unless otherwise specified and were used without any further purification.

Synthesis of ligands; general procedure

Compounds DTPA-BGLUCA³⁻ and DTPA-BENGALAA³⁻ were prepared analogous to a procedure described by Sherry et al.⁵² DTPA-bis(anhydride) (0.02 mol) was added in small portions to a stirred solution of 0.1 mol of the appropriate amine,^{53,54} dissolved in 25 mL distilled water. An excess of amine was used to avoid the formation of mono-substituted DTPA derivatives. After 2 h the solvent was evaporated and the resulting mixture was separated on a Dowex-H⁺ (25 x 4 cm) column applying a gradient from 0 - 2.0 M aqueous HCl. The fractions containing the product were collected and, after adjustment of the pH to 7, were desalted by membrane filtration (UTC 60, Toray Industries, Inc., Tokyo, Japan, 20 bar pressure) and freeze-dried.

N,N''-bis[N-(D-gluco-2,3,4,5,6-pentahydroxyhexyl)-carbamoylmethyl]-diethylenetriamine-N,N',N''-triaceticacid (DTPA-BGLUCA). A white solid was obtained; yield = 3.5 g (45 %). ¹H-NMR (400 MHz, D₂O, pH 1.44): δ 4.23 (s, 4H, N²CH₂CO), 4.22 (s, 4H, N²CH₂CO), 3.88 (m, 2H, H-2, J_{1,2} = 3.98, J_{1',2'} = 7.99, J_{2,3} = 5.49), 3.78 (dd, 2H, H-6, J_{5,6} = 2.95, J_{6,6'} = -11.49), 3.75 - 3.71 (m, 4H, H-3 and H-5), 3.65 (s, 2H, N¹CH₂COOH), 3.64 (m, 2H, H-4, J_{3,4} = 2.28, J_{4,5} = 8.0 Hz), 3.61 (dd, 2H, H-6', J_{5,6'} = 6.04), 3.56 (t, 2H, N²CH₂CH₂N¹, J_{H,H} = 6.26), 3.49 (dd, 2H, H-1, J_{1,1'} = -14.02), 3.34 (dd, 2H, H-1'), 3.18 (t, 2H, N²CH₂CH₂N¹). ¹³C-NMR (50.3 MHz, D₂O, pH 2.56): δ 43.70 (C-1), 51.10 (N³CH₂CH₂N¹), 54.92 (N³CH₂CH₂N¹), 55.32 (N³CH₂COO), 56.93, 57.89 (N¹CH₂COO, N¹CH₂CON), 64.31 (C-6), 71.80 (C-2), 72.42, 72.55, 72.76 (C-3, C-4, C-5), 167.54 (N¹CH₂CON), 170.32 (N³CH₂COO), 175.08 (N¹CH₂COOH). MS: m/e = 720 (MH⁺). Anal. Calcd (found) for C₂₆H₄₉N₅O₁₈: C, 43.39 (43.17); H, 6.82 (6.79); N, 9.74 (9.68); O, 40.06 (40.0).

N,N''-bis[N-(3-aza-D-galacto-5,6,7,8,9-pentahydroxynonyl)-carbamoylmethyl]-diethylenetriamine-N,N',N''-triaceticacid (DTPA-BENGALAA). A slightly yellow hygroscopic solid was obtained; yield = 6.0 g (32%). ¹³C-NMR (50.3 MHz, D₂O, pH

9.12): δ 38.70 (C-1), 48.87 (C- β), 52.57 (C- α), 54.45, 57.03 (N^3CH_2COO), 60.41, 60.48 (N^1CH_2COO , N^1CH_2CON) 64.80 (C-6), 68.58 (C-2), 70.90, 71.62, 72.10 (C-3, C-4, C-5), 174.28 (N^1CH_2CON), 175.91 (N^3CH_2COO), 180.60 (N^1CH_2COO). MS (m/e): = 806 (MH^+).

NMR measurements

The La(III), Nd(III) and Gd(III) complexes of the ligands were prepared by mixing equimolar amounts of hydrated $LnCl_3$ and ligand. The absence of free Ln(III) was verified using a xylenol orange indicator. After adjustment of the pH to approximately 7, NaCl was removed by membrane filtration. The solutions were freeze-dried and the complexes were obtained as the trihydrates. Samples of the Ln(III) complexes for the NMR measurements were prepared by dissolution of solid Ln-complex or by dissolving equimolar amounts of Ln(III) complex and hydrated $LnCl_3$. The pH of the solutions was measured at room temperature with a calibrated micro-combination probe purchased from Aldrich Chemical Co. The pH values given are direct meter readings. For the variable temperature and variable pressure ^{17}O NMR measurements the samples were dissolved in 10% ^{17}O enriched water and the pH was adjusted with weighted amounts of 0.01 m (mol per kg water) $HClO_4$. The compositions of all the solutions used in the variable temperature and variable pressure measurements are given in Table 8.

Table 8. Compositions of the Aqueous Solutions Used in the Variable Temperature ^{17}O NMR and Variable Pressure ^{17}O NMR Spectrometry Measurements^a.

| No | Solution | [Ln(III)], mol kg ⁻¹ | 10 ³ P _m | pH |
|----|---------------------------------------|---------------------------------|--------------------------------|------|
| 1 | acidified water | | | 4.35 |
| 2 | [Gd(DTPA-BPDA)(H ₂ O)] | 0.155 | 2.79 | 4.38 |
| 3 | [Gd(DTPA-BGLUCA)(H ₂ O)] | 0.191 | 3.44 | 4.38 |
| 4 | [Gd(DTPA-BENGALAA)(H ₂ O)] | 0.204 | 3.68 | 4.35 |

^a All solutions were in ^{17}O -enriched water (2-10% enrichment).

The complete spectral assignment of DTPA-BGLUCA³⁻ has been carried out by means of 1H homonuclear correlation spectroscopy (COSY) and 1H - ^{13}C chemical shift correlation spectroscopy (HETCOR).

The ^{17}O and ^{13}C NMR spectra were recorded with a Nicolet NT-200 WB or a Varian VXR-400 S spectrometer. For ^{13}C NMR *t*-BuOH (methyl signal at 31.2 ppm) was used as the internal standard. The ^{17}O chemical shifts were recorded with respect to D_2O as external standard; the chemical shifts were determined by fitting the observed signal with a Lorentzian line function. Downfield shifts are denoted as positive.

Variable temperature ^{17}O NMR measurements were performed at one magnetic field of 9.4 T using either a Varian VXR-400 S spectrometer equipped with a cold junction temperature control unit (Thermo Electric) or a Bruker AM-400 spectrometer equipped with Bruker VT-1000 temperature control units. The temperature was stabilized within 0.1 °C of the desired value and was measured by a substitution technique.⁵⁵ The samples were sealed in glass spheres, fitting into 10 mm NMR tubes, in order to eliminate bulk susceptibility effects on the chemical shift.⁵⁶ Longitudinal relaxation rates, $1/T_1$, were obtained by the inversion-recovery method⁵⁷ and transverse relaxation rates, $1/T_2$, were measured by the Carr-Purcell-Meiboom-Gill spin-echo technique⁵⁸ or, for line widths larger than 1 kHz, directly from the line widths. Variable pressure NMR measurements were carried out up to 200 MPa on a Bruker AM-400 spectrometer equipped with a home-built probe head.⁵⁹ The temperature was controlled by circulating fluid from a temperature bath and was measured using a built-in Pt-resistor. The transverse relaxation rates were measured in the same way as had been done for the variable temperature work.

NMRD measurements

The $1/T_1$ Nuclear Magnetic Relaxation Dispersion (NMRD) profiles of the solvent protons at several temperatures were obtained on an IBM Research Relaxometer, using the field cycling method, and covering a continuum of magnetic fields from 2.5×10^{-4} to 1.4 T (corresponding to a proton Larmor frequency range of 0.01 MHz to 50 MHz). The absolute uncertainty in the $1/T_1$ for the NMRD measurements was $\pm 3\%$. The spin-lattice proton relaxation rates at 20 MHz were measured on a spin analyzer Bruker PC-20. Based on the T_1 values at 20 MHz the samples were diluted in order to obtain relaxation rates in the range of 4 - 8 s^{-1} . The proton relaxation rates at 4.7 T (proton Larmor frequency of 200 MHz) were recorded on a Bruker MSL-200 spectrometer. The proton relaxation rates at 9.4 T (proton Larmor frequency of 400 MHz) were measured on a Varian VXR-400 S spectrometer.

Fast atom bombardment (FAB) spectra were obtained with a VG 70-250 SE mass spectrometer. Elemental analyses were performed by Mikroanalytisches Labor Pascher, Remagen (Germany).

ACKNOWLEDGEMENTS

Thanks are due to Ms. A.M. van der Heijden and Mr. R. Demange for their contribution in synthesizing several compounds. This work has been supported by the Dutch National Innovation Program Carbohydrates (IOP-K), Akzo Nobel Central Research (ACR), the Swiss National Science Foundation and the Swiss OFES, and the European COST D1 action (Coordination Chemistry in the Context of Biological and Environmental Studies).

REFERENCES

1. Lauffer, R.B. *Chem. Rev.* **1987**, *87*, 901.
2. Tweedle, M.F. In *Lanthanide Probes in Life, Chemical and Earth Sciences*; Bünzli, J.-C.G.; Choppin, G.R., Eds.; Elsevier: Amsterdam 1989; Chapter 5.
3. Tweedle, M.F. *J. Alloys Comp.* **1992**, *180*, 317.
4. Koenig, S.H.; Brown, R.D., III *Prog. Nucl. Magn. Reson. Spectrosc.*, **1990**, *22*, 487 and references therein.
5. Geraldes C.F.G.C.; Sherry, A.D.; Cacheris, W.P.; Kuan, K.T.; Brown III, R.D.; Koenig, S.H.; Spiller, M. *Magn. Reson. Med.* **1988**, *8*, 191.
6. Peters, J.A.; Kieboom, A.P.G. *Recl. Trav. Chim. Pays-Bas* **1983**, *102*, 381.
7. Sherry, A.D.; Geraldes, C.F.G.C. In *Lanthanide Probes in Life, Chemical and Earth Sciences*; Bünzli, J.-C.G.; Choppin, G.R., Eds.; Elsevier: Amsterdam 1989; Chapter 4.
8. Alpoim, M.C.; Urbano, A.M., Geraldes, C.F.C.G.; Peters, J.A. *J. Chem. Soc., Dalton Trans.* **1992**, 463, and references therein.
9. Kowall, Th.; Foglia, F.; Helm, L.; Merbach, A.E. *J. Am. Chem. Soc.* **1995**, *117*, 3790.
10. Geraldes, C.F.G.C.; Urbano, A.M.; Hoefnagel, M.A.; Peters, J.A. *Inorg. Chem.* **1993**, *32*, 2426.

11. Golding, R.M.; Halton, M.P. *Aust. J. Chem.* **1972**, *25*, 2577.
12. Bleaney, B. *J. Magn. Reson.* **1972**, *8*, 91.
13. Bleaney, B.; Dobson, C.M.; Levine, B.A.; Martin, R.B.; Williams, R.J.P.; Xavier, A.V. *J. Chem. Soc. Chem. Commun.* **1972**, 791.
14. Golding, R.M.; Pyykkö, P. *Mol. Phys.* **1973**, *26*, 1389.
15. Pinkerton, A.A.; Rossier, M.; Spiliadis, S. *J. Magn. Reson.* **1985**, *64*, 420.
16. Reuben, J. *J. Magn. Reson.* **1982**, *50*, 233.
17. Peters, J.A. *J. Magn. Reson.* **1986**, *68*, 240.
18. Reilley, R.N.; Good, B.W.; Allendoerfer, R.D. *Anal. Chem.* **1976**, *48*, 1446.
19. Vijverberg, C.A.M.; Peters, J.A.; Kieboom, A.P.G.; van Bekkum, H. *Recl. Trav. Chim. Pays-Bas* **1980**, *99*, 403.
20. Peters, J.A.; Nieuwenhuizen, M.S.; Raber, D.J. *J. Magn. Reson.* **1985**, *65*, 417.
21. Nieuwenhuizen, M.S.; Peters, J.A.; Sinnema, A.; Kieboom, A.P.G.; van Bekkum, H. *J. Am. Chem. Soc.* **1985**, *107*, 12.
22. Peters, J.A. *Inorg. Chem.* **1988**, *27*, 4686.
23. Dwek, R.A. *Nuclear Magnetic Resonance in Biochemistry*; Clarendon Press: Oxford, 1973.
24. Leigh, J.S., Jr. *J. Magn. Reson.* **1971**, *4*, 308.
25. McLaughlin, A.C.; Leigh, J.S., Jr. *J. Magn. Reson.* **1973**, *9*, 296.
26. Reuben, J.; Fiat, D. *J. Chem. Phys.* **1969**, *51*, 4918.
27. Gueron, M., *J. Magn. Reson.* **1975**, *19*, 58.
28. Vega, A.J.; Fiat, D. *Mol. Phys.* **1976**, *31*, 374.
29. Alsaadi, B.M.; Rossotti, F.J.C.; Williams, R.J.P. *J. Chem. Soc. Dalton Trans.* **1980**, 2151.
30. Alsaadi, B.M.; Rossotti, F.J.C.; Williams, R.J.P. *J. Chem. Soc. Dalton Trans.* **1980**, 2147.
31. Burns, P.D.; LaMar, G.N. *J. Magn. Reson.* **1982**, *46*, 61.
32. Sherry, A.D.; Brown, R.D., III; Geraldès, C.F.G.C.; Koenig, S.H.; Kuan, K.-T.; Spiller, M. *Inorg. Chem.* **1989**, *28*, 620.
33. Konings, M.S.; Dow, W.C.; Love, D.B.; Raymond, K.N.; Quay, S.C.; Rocklage, S.M. *Inorg. Chem.* **1990**, *29*, 1488.
34. Swift, T.J.; Connick, R.E. *J. Chem. Phys.* **1962**, *37*, 307.
35. Zimmerman, J.R. Brittin, W.E. *J. Phys. Chem.* **1957**, *61*, 1328.
36. Micskei, K.; Helm, L.; Brücher, E.; Merbach, A.E. *Inorg. Chem.* **1993**, *32*, 3844.
37. Micskei, K.; Powell, D.H.; Helm, L.; Brücher, E.; Merbach, A.E. *Magn. Reson. Chem.* **1993**, *31*, 1011.

38. Bloembergen, N. *J. Chem. Phys.* **1957**, *27*, 595.
39. Halle, B.; Wennerstrom, H. *J. Chem. Phys.* **1981**, *75*, 1928.
40. Helm, L.; Merbach, A.E. *Eur. J. Solid State Inorg. Chem.* **1991**, *28*, 245.
41. González, G.; Powell, D.H.; Tissières, V.; Merbach, A.E. *J. Phys. Chem.* **1994**, *98*, 53.
42. Southwood-Jones, R.V.; Earl, W.L.; Newman, K.E.; Merbach, A.E. *J. Chem. Phys.* **1980**, *73*, 5909.
43. Powell, D.H.; Merbach, A.E.; González, G.; Brücher, E.; Micskei, K.; Ottaviani, M.F.; Köhler, K.; von Zelewsky, A.; Grinberg, O. Ya.; Lebedev, Ya. S. *Helv. Chim. Acta* **1993**, *76*, 2129.
44. Atkins, P.W.; Kivelson, D. *J. Chem. Phys.* **1966**, *44*, 169.
45. Nyberg, G. *Mol. Phys.* **1967**, *12*, 69.
46. McLachlan, A.D. *Proc. R. Soc. London* **1964**, *A280*, 271.
47. Friedman, H.L. In *Protons and Ions Involved in Fast Dynamics Phenomena*; Laszlo, P., Ed.; Elsevier: Amsterdam 1978, pp 27-42.
48. Cossy, C.; Helm, L.; Merbach, A.E. *Inorg. Chem.* **1989**, *28*, 2699.
49. Solomon, I. *Phys. Rev.* **1955**, *99*, 559.
50. Bloembergen, N.; Morgan, L.O. *J. Chem. Phys.* **1961**, *34*, 842.
51. Geraldès, C.F.C.G.; Urbano, A.M.; Alpoim, M.C.; Sherry, A.D.; Kuan, K.-T.; Rajagopalan, R.; Maton, F.; Muller, R.N. *Magn. Reson. Imaging* **1995**, *2*, 13.
52. Sherry, A.D.; Cacheris, W.P.; Kuan, K.T. *Magn. Reson. Med.* **1988**, *8*, 180.
53. Kelkenberg, H. *Tens. Surf. Det.* **1988**, *25*, 8.
54. Lammers, H.; Peters, J.A.; van Bekkum, H. *Tetrahedron* **1994**, *50*, 8103.
55. Amman, C.; Meyer, P.; Merbach, A.E. *J. Magn. Reson.* **1982**, *46*, 319.
56. Hugi, A.D.; Helm, L.; Merbach, A.E. *Helv. Chim. Acta*, **1985**, *68*, 508.
57. Vold, R.V.; Waugh, J.S.; Klein, M.P.; Phelps, D.E. *J. Chem. Phys.* **1968**, *48*, 3831.
58. Meiboom, S.; Gill, D. *Rev. Sci. Instrum.* **1958**, *29*, 688.
59. Frey, U.; Helm, L.; Merbach, A.E. *High Pressure Res.* **1990**, *2*, 237.

SUPPLEMENTARY MATERIAL.

Table S1

Measured ^{13}C chemical shifts of 0.10 M $[\text{Nd}(\text{DTPA-bisamide})(\text{H}_2\text{O})]$ complexes in D_2O at 80 °C and 100.6 MHz.

Table S2A-C

Measured longitudinal and transverse relaxation times and chemical shifts of the acidified water reference (T_{1A} , T_{2A} and $\Delta\omega_A$) and of the paramagnetic solutions (T_1 , T_2 and $\Delta\omega$), at molar ratios of bound water P_m . The calculated values of reduced relaxation rates and chemical shifts ($1/T_{2r}$, T_{2r} and $\omega\omega_r$) of the variable temperature study on the $[\text{Gd}(\text{DTPA-bisamide})(\text{H}_2\text{O})]$ complexes are also tabulated. The variable temperature ^{17}O NMR measurements were mainly carried out on a Varian VXR-400 S spectrometer. Several measurements, denoted with an asterisk, were recorded using a Bruker AM-400 spectrometer. All measurements were carried at 9.4 T.

Table S3A-C

Measured transverse relaxation times of the $[\text{Gd}(\text{DTPA-bisamide})(\text{H}_2\text{O})]$ complexes (T_2) and of the acidified water (0.9 m perchloric acid) reference ($1/T_{2A}$) and the calculated reduced relaxation times ($1/T_{2r}$) at variable pressure. The reduced relaxation times were calculated taking into account an activation volume of $+1.09 \text{ cm}^3 \text{ mol}^{-1}$ for the reference. The measurements were recorded on a Bruker AM-400 spectrometer at 9.4 T.

Table S4A-D

Longitudinal proton relaxation rates (T_1) for the $[\text{Gd}(\text{DTPA-bisamide})(\text{H}_2\text{O})]$ complexes and the $\text{Gd}(\text{TTHA})^{3-}$ complex at several temperatures T . The data at 0.01 MHz to 50 MHz were obtained on an IBM Research Relaxometer using the field cycling method. The spin-lattice proton relaxation rates at 200 MHz and 400 MHz were measured on a Bruker MSL-200 spectrometer and a Varian VXR-400 S spectrometer, respectively.

Table S1.

| Assign. | DTPA-BEA | DTPA-BPDA | DTPA-BGLUCA | DTPA-BENGALAA | DTPA-BPA ^a |
|---|------------------------|------------------------|------------------------|--------------------------------|-----------------------|
| C=O | 186.54 | 186.54 | 187.04 | 187.15 | 186.38 |
| | 182.75 | 183.32 | 183.23 | 183.04 | 182.95 |
| | 180.18 | 176.55 | 176.46 | 177.65 | 177.04 |
| | 178.97 | 173.48 | 174.70 | 176.01 | 175.99 |
| | 172.78 | 171.24 | 171.35 | 173.54 | 172.68 |
| | 170.56 | 168.29 | 168.07 | 170.70 | 170.84 |
| | 167.70 | 164.63 | 164.06 | 167.48 | 168.07 |
| | 164.04 | | | 164.70 | |
| CH ₂ COOH | 70.20 | 67.55 | 67.69 | 62.39 | 70.67 |
| | 66.78 | 62.58 | 66.15 | 57.44 | 67.24 |
| | 65.26 | 60.56 | 63.17 | 55.79 | 61.18 |
| | 62.70 | 56.62 | 60.64 | | 55.57 |
| | 55.23 | | 59.28 | | |
| | | 56.22 | | | |
| | | 55.31 | | | |
| N ¹ CH ₂ CH ₂ N ³ | 32.52 | 33.31 | 32.62 | 32.35 | 33.11 |
| N ¹ CH ₂ CH ₂ N ³ | 24.09 | 25.34 | 24.29 | 24.08 | 25.08 |
| C- α (C- β) | | | | 40.11 (1) ^b (48.37) | |
| | | | | 39.32 (3) (46.70) | |
| | | | | 37.78 (3) (46.49) | |
| | | | | 36.79 (1) (46.22) | |
| C-1 | 44.88 (1) ^b | 45.48 (2) ^b | 45.64 (4) ^b | 52.41 | 45.02 |
| | 44.45 (2) | 45.00 (2) | 45.11 (2) | 51.33 | 44.47 |
| | 43.81 (2) | 43.81 (2) | 44.93 (2) | | 43.37 |
| | 42.25 (1) | 43.06 (1) | 44.10 (2) | | 42.58 |
| | | | 43.94 (2) | | |
| | | | 43.46 (1) | | |
| | | | 43.24 (1) | | |
| | | | 43.04 (1) | | |

^a reference 10; ^b ratio of the signal intensities.

structures and dynamics of Ln(III) complexes of sugar-based DTPA-bis(amides)

Table S2A. [Gd(DTPA-BPDA)(H₂O)] P_m = 2.79 10⁻³

| T (K) | T _{1A} (s) | T ₁ (s) | T _{2A} (s) | T ₂ (s) | v _A (s ⁻¹) | v (s ⁻¹) |
|-------|---------------------|--------------------|---------------------|--------------------|-----------------------------------|----------------------|
| 271* | | | 2.85E-03 | 1.84E-03 | 720 | 690 |
| 283 | 4.45E-03 | 2.90E-03 | 4.09E-03 | 1.76E-03 | 208 | 201 |
| 302 | 7.76E-03 | 4.76E-03 | 6.17E-03 | 7.69E-04 | 161 | 153 |
| 321 | 1.13E-02 | 7.51E-03 | 8.38E-03 | 3.25E-04 | 117 | 71 |
| 323 | 1.19E-02 | 7.89E-03 | 8.71E-03 | 3.54E-04 | 602 | 530 |
| 338 | 1.65E-02 | 1.08E-02 | 9.02E-03 | 2.36E-04 | 69 | -114 |
| 358 | 2.24E-02 | 1.42E-02 | 1.44E-02 | 2.50E-04 | 24 | -195 |
| 375 | 2.72E-02 | 1.86E-02 | 1.47E-02 | 3.27E-04 | -21 | -302 |

Table S2B. [Gd(DTPA-GLUCA)(H₂O)] P_m = 3.44 10⁻³

| T (K) | T _{1A} (s) | T ₁ (s) | T _{2A} (s) | T ₂ (s) | v _A (s ⁻¹) | v (s ⁻¹) |
|-------|---------------------|--------------------|---------------------|--------------------|-----------------------------------|----------------------|
| 270* | | | | | 720 | 702 |
| 273* | | | | | 710 | 686 |
| 283 | 4.29E-03 | 2.37E-03 | 3.95E-03 | 1.35E-03 | | |
| 287* | | | | | 701 | 694 |
| 302 | 7.82E-03 | 3.62E-03 | 6.03E-03 | 5.62E-04 | | |
| 322 | 1.20E-02 | 5.87E-03 | 7.81E-03 | 2.35E-04 | | |
| 324* | 1.19E-02 | 5.99E-03 | | | 603 | 494 |
| 341 | 1.57E-02 | 8.58E-03 | 9.33E-03 | 1.73E-04 | 82 | -57 |
| 360 | 2.23E-02 | 1.20E-02 | 1.11E-02 | 2.00E-04 | 42 | -233 |
| 374 | 2.67E-02 | 1.48E-02 | 1.32E-02 | 2.64E-04 | 76 | -257 |
| 393 | 3.34E-02 | 1.89E-02 | 1.23E-02 | 4.53E-04 | -47 | -304 |

Table S2C. [Gd(DTPA-BENGALAA)(H₂O)] P_m = 3.68 10⁻³

| T (K) | T _{1A} (s) | T ₁ (s) | T _{2A} (s) | T ₂ (s) | v _A (s ⁻¹) | v (s ⁻¹) |
|-------|---------------------|--------------------|---------------------|--------------------|-----------------------------------|----------------------|
| 273* | | | | | -1584 | -1619 |
| 279 | 3.73E-03 | 2.12E-03 | 3.67E-03 | 1.81E-03 | | |
| 287* | | | | | -1590 | -1615 |
| 288 | 5.09E-03 | 2.54E-03 | 4.48E-03 | 1.70E-03 | | |
| 297 | 6.68E-03 | 3.03E-03 | 5.16E-03 | 1.26E-03 | | |
| 311* | | | | | -1601 | -1625 |
| 312 | 9.28E-03 | 4.08E-03 | 6.20E-03 | 6.16E-04 | | |
| 314* | | | | | -1613 | -1638 |
| 323* | | | | | -1620 | -1669 |
| 326 | 1.19E-02 | 5.26E-03 | 7.43E-03 | 3.05E-04 | | |
| 340 | 1.68E-02 | 7.04E-03 | 8.45E-03 | 2.08E-04 | 48 | -9 |
| 359 | 2.23E-02 | 9.66E-03 | 6.86E-03 | 1.94E-04 | 2 | -182 |
| 368 | 2.53E-02 | 1.07E-02 | 1.32E-02 | 2.09E-04 | -21 | -315 |
| 377 | 2.76E-02 | 1.18E-02 | 9.12E-03 | 2.30E-04 | -38 | -344 |
| 391 | 3.46E-02 | 1.57E-02 | 5.83E-03 | 3.33E-04 | -70 | -310 |

Table S3A. [Gd(DTPA-BPDA)(H₂O)] P_m = 2.79 10⁻³ T = 302.6 K

| P (MPa) | T ₂ (s) | T _{2A} (s) | 1/T _{2r} (s ⁻¹) | ln(1/T _{2r}) |
|---------|--------------------|---------------------|--------------------------------------|------------------------|
| 0.60 | 6.95E-04 | 8.46E-03 | 4.73E+05 | 13.07 |
| 4.00 | 7.17E-04 | 8.48E-03 | 4.58E+05 | 13.03 |
| 25.00 | 7.63E-04 | 8.55E-03 | 4.28E+05 | 12.97 |
| 50.00 | 7.96E-04 | 8.65E-03 | 4.09E+05 | 12.92 |
| 75.00 | 8.59E-04 | 8.74E-03 | 3.76E+05 | 12.84 |
| 101.00 | 8.90E-04 | 8.84E-03 | 3.62E+05 | 12.80 |
| 124.00 | 9.32E-04 | 8.93E-03 | 3.45E+05 | 12.75 |
| 152.00 | 1.01E-03 | 9.04E-03 | 3.16E+05 | 12.66 |
| 172.50 | 1.06E-03 | 9.12E-03 | 2.99E+05 | 12.61 |
| 201.20 | 1.12E-03 | 9.23E-03 | 2.81E+05 | 12.55 |

structures and dynamics of Ln(III) complexes of sugar-based DTPA-bis(amides)

Table S3B. [Gd(DTPA-BGLUCA)(H₂O)] P_m = 3.44 10⁻³ T = 302.5 K

| P (MPa) | T ₂ (s) | T _{2A} (s) | 1/T _{2r} (s ⁻¹) | ln(1/T _{2r}) |
|---------|--------------------|---------------------|--------------------------------------|------------------------|
| 0.60 | 5.30E-04 | 8.44E-03 | 5.14E+05 | 13.15 |
| 4.00 | 5.30E-04 | 8.46E-03 | 5.14E+05 | 13.15 |
| 26.00 | 5.73E-04 | 8.54E-03 | 4.73E+05 | 13.07 |
| 51.50 | 6.12E-04 | 8.63E-03 | 4.41E+05 | 13.00 |
| 78.00 | 6.51E-04 | 8.73E-03 | 4.13E+05 | 12.93 |
| 99.00 | 6.78E-04 | 8.81E-03 | 3.96E+05 | 12.89 |
| 126.00 | 7.19E-04 | 8.92E-03 | 3.72E+05 | 12.83 |
| 151.00 | 7.46E-04 | 9.01E-03 | 3.57E+05 | 12.79 |
| 173.00 | 8.08E-04 | 9.10E-03 | 3.28E+05 | 12.70 |
| 198.00 | 8.38E-04 | 9.20E-03 | 3.15E+05 | 12.66 |

Table S3C. [Gd(DTPA-BENGALAA)(H₂O)] P_m = 3.67 10⁻³ T = 311.9 K

| P (MPa) | T ₂ (s) | T _{2A} (s) | 1/T _{2r} (s ⁻¹) | ln(1/T _{2r}) |
|---------|--------------------|---------------------|--------------------------------------|------------------------|
| 0.60 | 5.86E-04 | 1.04E-02 | 4.39E+05 | 12.99 |
| 0.60 | 6.00E-04 | 1.04E-02 | 4.28E+05 | 12.97 |
| 28.00 | 6.30E-04 | 1.05E-02 | 4.07E+05 | 12.92 |
| 50.00 | 6.56E-04 | 1.07E-02 | 3.90E+05 | 12.87 |
| 77.00 | 7.03E-04 | 1.08E-02 | 3.62E+05 | 12.80 |
| 100.00 | 7.19E-04 | 1.09E-02 | 3.54E+05 | 12.78 |
| 127.00 | 7.68E-04 | 1.10E-02 | 3.30E+05 | 12.71 |
| 150.00 | 7.81E-04 | 1.11E-02 | 3.24E+05 | 12.69 |
| 174.50 | 8.36E-04 | 1.12E-02 | 3.02E+05 | 12.62 |
| 201.00 | 8.52E-04 | 1.14E-02 | 2.96E+05 | 12.60 |

Table S4A. $[\text{Gd}(\text{TTHA})]^{3-}$ $c = 1\text{mM}$ $\text{pH} = 6.84$

| ω_1 (MHz) | T_1 (s) | | | | |
|------------------|-----------|-------|-------|-------|-------|
| | 5 °C | 15 °C | 25 °C | 37 °C | 45 °C |
| 0.01 | 5.819 | 4.891 | 4.190 | 3.675 | 3.366 |
| 0.02 | 5.791 | 5.012 | 4.254 | 3.554 | 3.267 |
| 0.04 | 5.853 | 4.950 | 4.286 | 3.660 | 3.368 |
| 0.100 | 5.864 | 4.924 | 4.218 | 3.618 | 3.245 |
| 0.200 | 5.793 | 4.999 | 4.221 | 3.591 | 3.274 |
| 0.400 | 5.838 | 4.849 | 4.151 | 3.622 | 3.407 |
| 0.600 | 5.749 | 4.875 | 4.170 | 3.595 | 3.329 |
| 1.000 | 5.689 | 4.653 | 4.131 | 3.552 | 3.414 |
| 2.000 | 5.506 | 4.654 | 4.096 | 3.457 | 3.177 |
| 4.000 | 5.067 | 4.184 | 3.710 | 3.167 | 3.017 |
| 6.000 | 4.719 | 4.083 | 3.454 | 2.903 | 2.582 |
| 10.000 | 4.077 | 3.453 | 2.989 | 2.471 | 2.074 |
| 15.000 | 3.792 | 3.078 | 2.629 | 2.125 | 1.875 |
| 20.000 | 3.611 | 2.902 | 2.426 | 1.978 | 1.717 |
| 30.000 | 3.460 | 2.713 | 2.183 | 1.631 | 1.304 |
| 40.000 | 3.476 | 2.659 | 2.087 | 1.610 | 1.317 |
| 50.000 | 3.324 | 2.597 | 2.061 | 1.524 | 1.255 |
| 200.00 | 3.747 | 2.579 | 2.026 | 1.565 | 1.378 |
| 400.00 | 3.309 | 2.518 | 1.969 | 1.487 | 1.273 |

structures and dynamics of Ln(III) complexes of sugar-based DTPA-bis(amides)

Table S4B. [Gd(DTPA-BPDA)(H₂O)] c = 1mM pH = 7.37

| ω_1 (MHz) | T_1 (s) | | | | |
|------------------|-----------|-------|-------|-------|-------|
| | 5 °C | 15 °C | 25 °C | 37 °C | 45 °C |
| 0.01 | 6.397 | 5.994 | 6.344 | 6.472 | 6.313 |
| 0.02 | 6.428 | 5.832 | 6.356 | 6.528 | 6.263 |
| 0.04 | 6.393 | 5.971 | 6.157 | 6.489 | 6.265 |
| 0.100 | 6.478 | 5.929 | 6.227 | 6.552 | 6.364 |
| 0.200 | 6.357 | 5.904 | 6.248 | 6.591 | 6.246 |
| 0.400 | 6.329 | 5.930 | 6.233 | 6.455 | 6.417 |
| 1.000 | 6.338 | 5.791 | 6.202 | 6.390 | 6.271 |
| 2.000 | 5.908 | 5.712 | 6.055 | 6.199 | 6.013 |
| 4.000 | 5.600 | 5.359 | 5.710 | 5.812 | 5.741 |
| 10.000 | 4.825 | 4.524 | 4.967 | 4.828 | 4.616 |
| 20.000 | 4.541 | 3.949 | 4.432 | 4.373 | 3.857 |
| 30.000 | 4.133 | 4.020 | 4.198 | 3.938 | 3.539 |
| 200.00 | 3.915 | 3.824 | 3.893 | 3.800 | 3.436 |
| 400.00 | 3.582 | 3.576 | 4.002 | 3.687 | 3.286 |

Table S4C. [Gd(DTPA-BGLUCA)(H₂O)] c = 1mM pH = 7.35

| ω_1 (MHz) | T_1 (s) | | | | |
|------------------|-----------|-------|-------|-------|-------|
| | 5 °C | 15 °C | 25 °C | 37 °C | 45 °C |
| 0.01 | 7.012 | 6.438 | 6.839 | 6.949 | 6.753 |
| 0.02 | 6.886 | 6.434 | 6.879 | 6.846 | 6.755 |
| 0.04 | 6.879 | 6.429 | 6.890 | 6.865 | 6.847 |
| 0.100 | 6.882 | 6.357 | 7.005 | 6.832 | 6.755 |
| 0.200 | 6.896 | 6.321 | 6.922 | 6.948 | 6.745 |
| 0.400 | 6.805 | 6.432 | 6.923 | 6.829 | 6.644 |
| 1.000 | 6.746 | 6.250 | 6.880 | 6.741 | 6.705 |
| 2.000 | 6.429 | 6.092 | 6.570 | 6.640 | 6.479 |
| 4.000 | 5.820 | 5.740 | 6.262 | 6.152 | 6.018 |
| 10.000 | 5.169 | 4.892 | 5.275 | 5.189 | 5.175 |
| 20.000 | 4.705 | 4.498 | 4.724 | 4.563 | 4.396 |
| 30.000 | 4.826 | 4.226 | 4.544 | 4.517 | 4.187 |
| 200.00 | 4.398 | 4.180 | 4.412 | 4.479 | 4.268 |
| 400.00 | 3.869 | 3.787 | 4.430 | 4.293 | 3.834 |

structures and dynamics of Ln(III) complexes of sugar-based DTPA-bis(amides)

Table S4D. [Gd(DTPA-BENGALAA)(H₂O)] c = 1mM pH = 6.88

| ω_1 (MHz) | T_1 (s) | | | | |
|------------------|-----------|-------|-------|-------|-------|
| | 5 °C | 15 °C | 25 °C | 37 °C | 45 °C |
| 0.01 | 6.727 | 6.041 | 6.088 | 6.558 | 6.462 |
| 0.02 | 6.547 | 5.977 | 6.115 | 6.661 | 6.699 |
| 0.04 | 6.729 | 5.861 | 6.235 | 6.534 | 6.596 |
| 0.100 | 6.694 | 5.978 | 6.092 | 6.515 | 6.714 |
| 0.200 | 6.590 | 5.908 | 6.038 | 6.564 | 6.689 |
| 0.400 | 6.663 | 5.903 | 6.041 | 6.489 | 6.585 |
| 1.000 | 6.300 | 5.803 | 5.917 | 6.216 | 6.488 |
| 2.000 | 6.013 | 5.585 | 5.718 | 6.114 | 6.181 |
| 4.000 | 5.726 | 5.182 | 5.503 | 5.744 | 5.938 |
| 10.000 | 5.102 | 4.523 | 4.857 | 5.126 | 5.300 |
| 20.000 | 4.822 | 4.264 | 4.437 | 4.856 | 4.638 |
| 30.000 | 4.769 | 4.143 | 4.264 | 4.611 | 4.652 |
| 200.00 | 4.316 | 4.088 | 4.176 | 4.449 | 4.496 |
| 400.00 | 4.003 | 3.929 | 4.017 | 4.170 | 4.077 |

Chapter 9

PROTONATION AND METAL ION COORDINATION STUDIES OF A SUGAR-BASED DTPA-BIS(AMIDE) DERIVATIVE AS STUDIED BY POTENTIOMETRY AND MULTINUCLEAR NMR SPECTROSCOPY

ABSTRACT

The macroscopic and microscopic protonations of DTPA-BGLUCA (DTPA-bis(glucamide)) have been investigated using potentiometry, ^1H and ^{13}C NMR. The transmetallation of LaDTPA and LaDTPA-BGLUCA with Zn(II) has been studied using ^{13}C and ^{139}La NMR. It is shown that in the case of LaDTPA-BGLUCA the sugar side chains are not participating in the transmetallation. With the aid of ^{11}B NMR it is demonstrated that the polyhydroxy side chains are involved in the formation of borate ester species. The stoichiometry of the various borate ester species derived from DTPA-BGLUCA and its Ln(III)-complexes is investigated by recording the corresponding Job's plots. A major species has a borate moiety linking the two glucitol side chains under the formation of a macrocyclic compound. The stability constants of the occurring borate ester species as determined by ^{11}B NMR are reported.

INTRODUCTION

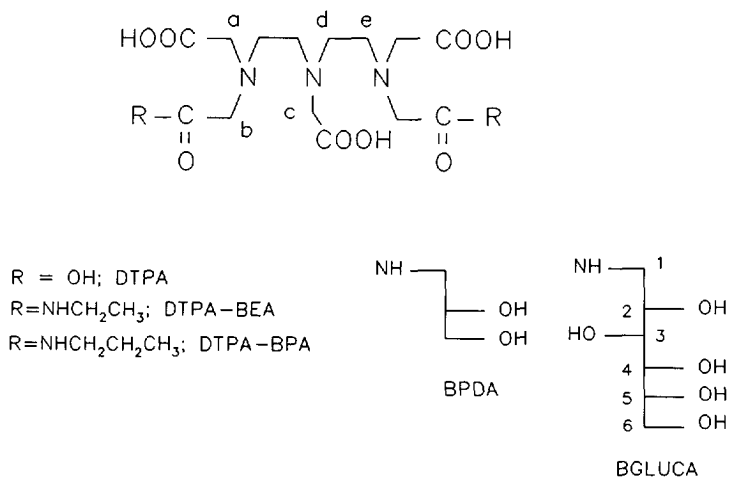
The rapid development of magnetic resonance imaging (MRI) has been of great

importance to medical diagnosis.^{1,2} The emergence of MRI as a major medical diagnostic modality has created the need for safe and effective contrast agents. These agents can be applied to enhance contrast of images, allowing for example an easier recognition of abnormal tissue. Among paramagnetic contrast agents, stable and water soluble Gd(III) chelates have the ideal properties of high water relaxivity, high thermodynamic and kinetic stability, low toxicity in vivo and rapid and complete excretion after the diagnostic exam. The Gd(III) complexes of diethylenetriamine-N,N,N',N'',N'''-pentaacetate (Gd(DTPA)²⁻) and 1,4,7,10-tetraazacyclododecane-N,N',N'',N'''-tetraacetate (Gd(DOTA)⁻) are commercially the most important products on the market today.

One of the options to improve these commercial contrast agents involves the attachment of Gd(DTPA)²⁻ to macromolecules such as polysaccharides (dextran)³ and dendrimers⁴ which will lead to an increase in relaxivity. The diagnostic utility of these latter type of contrast agents is that they are limited to the intravascular blood pool space and therefore may be useful in magnetic resonance angiography (MRA). The physicochemical properties of these DTPA-linked macromolecules and their model compounds are currently under scrutiny in order to obtain optimal relaxivity.

We reported earlier⁵ on the synthesis and dynamics in aqueous solution of DTPA-bis(glucamide) (DTPA-BGLUCA, for structural formula see Scheme 1) and the corresponding Ln(III) complexes. This poly(amino carboxylate) chelate was designed as a model compound for the DTPA-linked polysaccharides in order to investigate the influence of the hydroxyl groups in the second coordination sphere on e.g. the water exchange rates and relaxivity. It has been shown that the sugar chains are not involved in the coordination with the Ln(III) cation.

In this paper, ligand protonation studies are performed in order to investigate the effect of the polyhydroxy chains present in DTPA-BGLUCA on the macroscopic and microscopic protonation. The sugar side chains might be potential binding sites for metal ions (e.g. Zn(II)). These interactions may affect the thermodynamic and kinetic stability of the Ln(III) complexes concerned. Therefore the transmetallation of LaDTPA-BGLUCA with Zn(II) has been studied using ¹³C and ¹³⁹La NMR. In order to investigate whether the geometry of the Ln(DTPA-BGLUCA) complexes allows the coordination of a second metal ion, the interaction of borate (as metalloprobe) with these systems has been studied using ¹¹B NMR.



Scheme 1. The structural formulas of the ligands discussed in this work.

RESULTS AND DISCUSSION

Ligand protonation using potentiometry and NMR pH titration curves

The protonation constants ($\log K_i$) of DTPA-BGLUCA as obtained with potentiometry and ^{13}C and ^1H NMR pH titration curves (Figures 1,2) are given in Table 1. The $\log K_i$ values from the NMR pH titration curves were obtained by applying the Henderson-Hasselbach equation⁶ to the δ values near the point of inflection. For comparison literature data of various DTPA-bis(amide) derivatives have been included in Table 1.⁷ In general, three protonation constants for the DTPA-bis(amide) ligands as well as for DTPA can be determined using potentiometry. The value of $\log K_2$ for DTPA-GLUCA is 4 units lower than that of DTPA. Similar behaviour has been observed previously for other DTPA-bis(amides).⁷

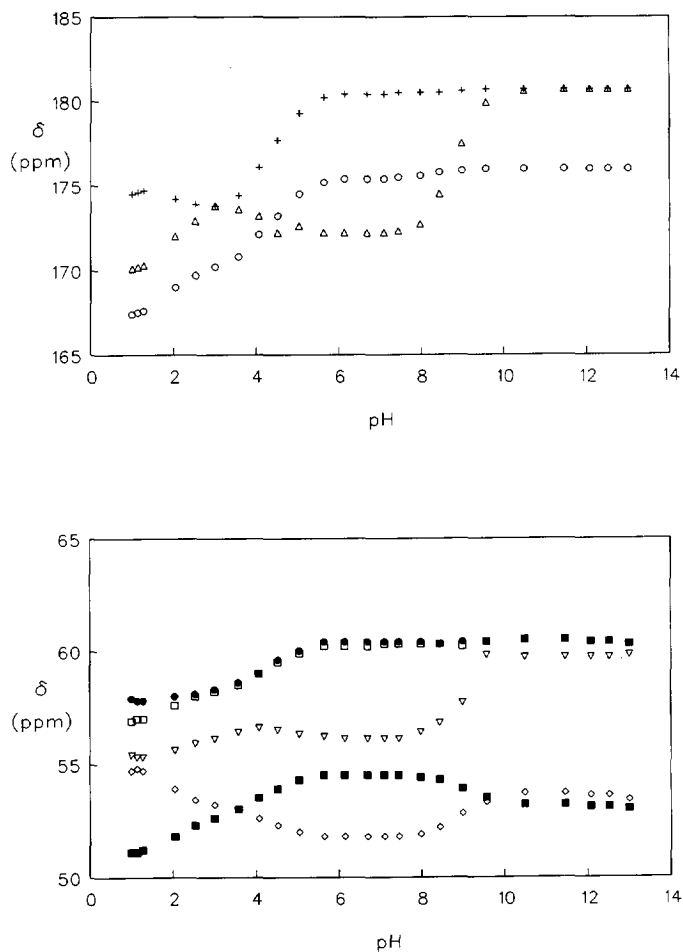


Figure 1. The ^{13}C NMR pH titration curve of DTPA-BGLUCA at 100.6 MHz and 25 °C.
 + terminal COOH; Δ central COOH; \circ CONH; \bullet $C_{a'}$; \square $C_{b'}$; ∇ $C_{c'}$; \diamond $C_{e'}$; \blacksquare $C_{d'}$

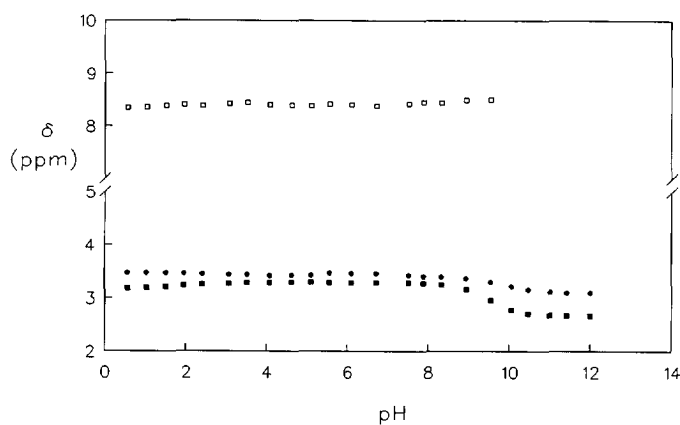
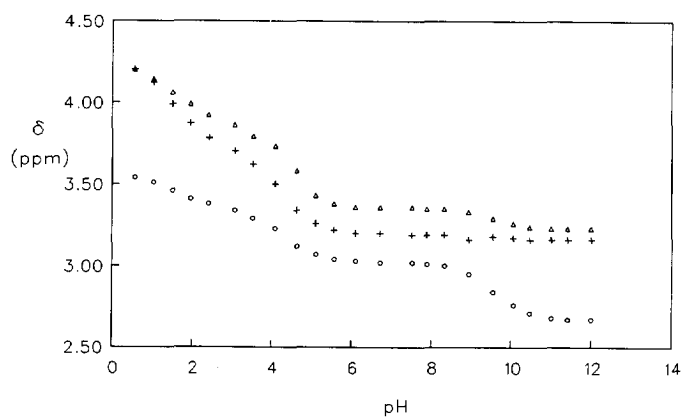


Figure 2. The ^1H NMR pH titration curve of DTPA-BGLUCA at 400 MHz and 25 °C. Δ $H_a + H_b$; \circ H_e ; \bullet H_c ; \blacksquare H_d ; \square amide H.

protonation and metal ion coordination studies of DTPA-bis(glucamide)

Table 1. Protonation constants for DTPA-GLUCA compared with those of DTPA and various DTPA-bis(amide) derivatives.^a

| Ligand | log K ₁ | log K ₂ | log K ₃ | log K ₄ | log K ₅ |
|--------------------------|--------------------|--------------------|--------------------|--------------------|--------------------|
| DTPA-BGLUCA ^b | 9.2 | 4.5 | 3.3 | 2.3 | ^c |
| | 8.7 | 4.5 | 2.7 | 1.8 | ^c |
| DTPA-BPDA ^d | 9.2 | 4.3 | 3.0 | ^c | ^c |
| DTPA-BPA ^d | 9.4 | 4.5 | 3.4 | ^c | ^c |
| DTPA ^d | 10.4 | 8.6 | 4.2 | 2.9 | 2.4 |

^a Measured by potentiometry in 0.1 M NaCl at 25 °C. All values are within ± 0.05 . The values of pK_a were converted into protonation constants (log K_i) using the expression $\log K_i = pK_{a(n+a-i)}$, where n is the number of pK_a values determined for each ligand and $i = 1, 2, \dots, n$; ^b Lower row values obtained from ¹³C NMR, values within ± 0.1 ; ^c Could not be determined; ^d Ref. 7

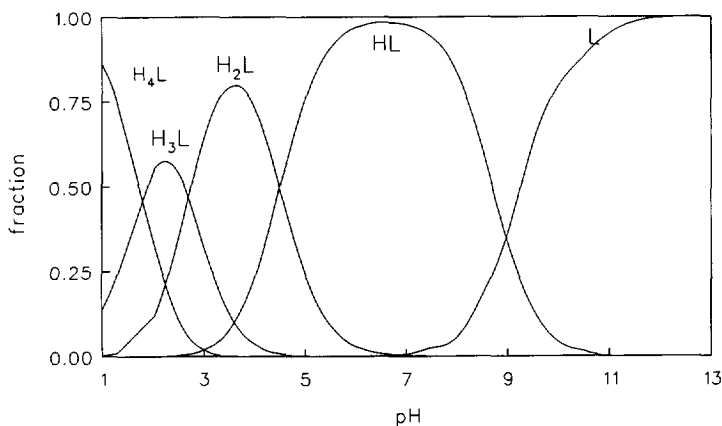


Figure 3. The speciation of a 0.25 M solution of DTPA-BGLUCA at various pH and 25 °C.

The quantitative estimation of the microscopic sites of protonation of DTPA-BGLUCA can be evaluated from ¹H NMR pH titration curves following the empirical procedure of Sudmeier and Reilley.⁸ The protonation of the donor atoms in the DTPA-backbone will

result in a deshielding of the non-labile hydrogens and changes in chemical shifts indicate the site of protonation.

The observed average chemical shift of nucleus i is given by $\delta_{\text{obs}}^i = \sum \delta_n^i X_{\text{H}_n\text{L}}$, where δ_n^i are the proton intrinsic chemical shifts of the H_nL species and $X_{\text{H}_n\text{L}}$ is the mole fraction of each species. This can be rearranged to $\delta_{\text{obs}}^i = \delta_L + \sum V_n^i X_{\text{H}_n\text{L}}$ in which V_n^i is the chemical difference between H_nL and the unprotonated form L. The speciation at various pH of DTPA-BGLUCA was calculated from the protonation constants obtained from potentiometry, the ligand mass balance and the equilibria equations (Figure 3). The V_n^i values were calculated for each set of shift data using a multiple linear regression program, which minimizes the sums of the squares of the deviation between the observed and calculated values δ_{obs}^i . The obtained V_n^i of the various forms H_nL were then used to calculate the fractions of protonation of the nitrogen (N) and of the carboxylate (O) sites (f_N and f_O , respectively). The average number of ligand bound protons at all basic sites is $n = \alpha_N f_N + \alpha_O f_O$, where α_N and α_O are the number of equivalent N and O sites, respectively. It has been shown for linear poly(amino carboxylate) chelates that each observed shift effect of protonation at various basic sites (V_n^i) are additive and can be calculated ($V_{n(c)}^i$) using eq 1:⁸

$$V_{n(c)}^i = \sum C_N f_N + \sum C_N f_N + \sum C_O f_O \quad (1)$$

where the pH-independent shielding constants $C_O = 0.20$, $C_N = 0.75$ and $C_N = 0.35$ ppm can be used (these constants are the changes in proton chemical shift of the CH_2 groups under study due to α -carboxylate protonation (C_O) or protonation of a N atom in the α -position (C_N) or in the β -position (C_N)). The values of f_N and f_O were calculated through minimization of the sum of the squares of the differences between the calculated and observed protonation shifts ($V_{n(c)}^i$ and V_n^i , respectively).

In Table 2 the values of f_N (f_1, f_2) and f_O (f_3, f_4) calculated for DTPA-BGLUCA are compared with those obtained for DTPA, DTPA-BPA and DTPA-BEA.⁹ A quantitative determination of the microscopic sites of protonation of DTPA-BLUCA was also attempted using the ^{13}C NMR pH titration curves (Figure 1). However, no satisfactory fit was obtained (negative f_N and f_O values were found). Probably, the ^{13}C chemical shifts are more sensitive to conformational changes accompanying the protonation than ^1H shifts

and consequently the substituent effects for the carbon chemical shifts are no longer valid. The trends observed in the titration curves (Figure 1), however, agree with the f_N values obtained from the evaluation of the ^1H data (Table 2).

Table 2. Percent protonation fractions of the different basic sites of DTPA-BGLUCA compared with DTPA and various DTPA-bis(amide) derivatives for different values of n . (for identification of f_i sites, see text). The errors of f_i are $\pm 5\%$.

| Ligand | n | f_1 | f_2 | f_3 | f_4 |
|-----------------------|-----|-------|-------|-------|-------|
| DTPA-BGLUCA | 1 | 19 | 62 | 0 | 0 |
| | 2 | 75 | 35 | 15 | 0 |
| DTPA-BPA ^a | 1 | 13 | 74 | 0 | 0 |
| | 2 | 65 | 59 | 11 | 0 |
| DTPA-BEA ^a | 1 | 12 | 76 | 0 | 0 |
| | 2 | 60 | 58 | 22 | 0 |
| DTPA ^a | 1 | 26 | 41 | 0 | 0 |
| | 2 | 87 | 16 | 0 | 5 |

^a Ref. 9

The preference of the first protonation ($n=1$) for the central diethylenetriamine backbone nitrogen (f_2) over the terminal ones (f_1) is larger for DTPA-BGLUCA (and DTPA-BPA and DTPA-BEA) than for DTPA. Accordingly, the $\log K_2$ values for DTPA-BGLUCA and for the other DTPA-bis(amides) are significantly lower than that for DTPA (Table 1). The larger electron withdrawing ability of the amide group compared with the carboxylate group cannot account for the large decrease of $\log K_2$; replacement of the carboxylate group (COO^-) of glycine with a carboxamide function results in a decrease of the pK_a of only 1.7 units.^{10,11} It has been proposed^{8,9,12,13} that migration of the positive charge to the terminal nitrogens to form the diprotonated DTPA species is favoured by positive charge repulsion and by formation of two hydrogen bond rings involving each protonated terminal nitrogen and their two attached acetate groups. The two carboxylate anions present on these acetate groups exert a strong electrostatic field on the attached proton, giving the hydrogen bonding ring system extra strength. Consequently, this structure of

the diprotonated DTPA is very stable, and the value of $\log K_2$ for DTPA is relatively high. It has also been suggested that the non- and mono-protonated DTPA-bis(amides) are stabilized by hydrogen bond formation between the amide protons, the terminal N atoms, and the adjacent carboxylates.^{9,14} In order to check this for DTPA-BGLUCA, we have performed the ^1H NMR titrations in $\text{H}_2\text{O}-\text{D}_2\text{O}$ (90/10 v/v) solutions and using a spinecho pulse sequence to suppress the water signal. In this way it was possible to observe ^1H shifts between pH 0 and 9.6. Surprisingly, the chemical shift appeared to be independent of the pH, which makes an involvement of these protons in intramolecular hydrogen bonds very unlikely. If such hydrogen bonds were present, they would be disrupted during the second protonation step (pH \approx 4.5), which should be reflected in the chemical shift. The absence of hydrogen bonding of the amide NH is supported by the dynamic behaviour of these protons. At about pH 5, two triplets (intensity ratio 9:1, $J = 5.6$ Hz) were observed for these nuclei. The occurrence of two resonances can be explained by the hindered rotation around the amide C-N bond, which has partial double bond character. At both higher and lower pH values, the resonances broadened and coalesced, whereas the coupling could no longer be observed. This shows that the exchange between the amide NH protons and water and the exchange between the two rotamers increases under these conditions. Above pH 9.5 the signals could no longer be observed, probably because the exchange rate is so fast that both water and the NH protons are suppressed by the spinecho pulse sequence. A pH dependence of amide NH exchange with a minimum at pH 4-5 and high rates at both high and low pH is typical for aminoacids.¹⁵ Any involvement in hydrogen bonds would have been reflected in a substantial reduction of the exchange rate. Further support was obtained from the signals for the methylene hydrogens of the acetate groups, which are singlets rather than AB systems as should be expected in case of restricted rotation due to hydrogen bonding. It may be concluded that the difference in protonation behaviour and $\text{p}K_{\text{a}2}$ between DTPA and DTPA-bis(amides) can be explained by a difference in strength of the electrostatic field experienced by the terminal NH in the diprotonated species. The basicities of the various groups of DTPA-BGLUCA are very similar to those in other bisamides and, therefore, it may be expected that the affinities for metal ions are similar as well.

The ^1H and ^{13}C chemical shifts of the sugar moiety are independent of the pH, indicating that its hydroxyl groups are also not involved in intramolecular hydrogen bonds with the

DTPA-backbone. The vicinal HH coupling constants (Table 3) are the same as those in sorbitol (D-glucitol).¹⁶ It can be concluded that the conformation of the sugar side chain is the same as that of sorbitol in solution, which is similar to the solid state structure (see Figure 4).

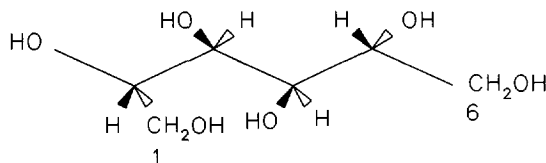


Figure 4. Conformational structure sorbitol.¹⁶

Table 3. The proton coupling constants of DTPA-GLUCA at 400 MHz and 25 °C compared with those of sorbitol.^a

| Coupling constant (Hz) | DTPA-BGLUCA | D-sorbitol |
|------------------------|-------------|------------|
| $J_{1,1'}$ | -14.0 | -12.0 |
| $J_{1,2}$ | 3.97 | 3.55 |
| $J_{1',2}$ | 7.99 | 6.55 |
| $J_{2,3}$ | 5.49 | 6.00 |
| $J_{3,4}$ | 2.28 | 1.79 |
| $J_{4,5}$ | 8.00 | 8.25 |
| $J_{5,6}$ | 2.95 | 2.95 |
| $J_{5,6'}$ | 6.04 | 6.30 |
| $J_{6,6'}$ | -11.49 | -11.80 |

^a Ref. 16

Transmetalation

The resonances of the DTPA backbone in ¹³C NMR spectra of La(III) complexes of the DTPA-derivatives have chemical shifts that are typically 2-7 ppm smaller than those of

the corresponding Zn(II) complexes. This is illustrated for the parent compounds in Table 4. Therefore, ^{13}C NMR is very useful for the study of transmetallation of La(III) complexes of DTPA-derivatives with Zn(II).

Table 4. ^{13}C NMR chemical shifts (ppm) of the DTPA ligand in La(III) and Zn(II) chelates of 0.1 M solutions in D_2O at 80°C at 9.4 T.

| | 0.1 M soln pure complex | | 0.1 M LaDTPA in the presence of 0.1 M Zn(II) | |
|---------------------------------------|-------------------------|--------------------|---|--------------------|
| | LaDTPA | ZnDTPA | LaDTPA | ZnDTPA |
| COO (terminal) | 182.3 | | 182.3 | 179.4 ^a |
| | 181.7 | 179.0 ^a | 182.0 | |
| COO (central) | 182.3 | | 183.2 | 179.3 |
| CH ₂ COO (terminal) | 64.9 | 61.4 | 64.7 | 61.3 ^a |
| | | | 64.5 | |
| CH ₂ COO (central) | 66.4 | 59.1 | 65.4 | 59.3 |
| N-CH ₂ -CH ₂ -N | 59.1 | 54.3 ^a | 58.9 | 54.7 ^a |
| | 57.7 | | 57.7 | |

^aCoalescing and broad resonances.

Upon stepwise addition of ZnCl_2 to a 0.1 M solution of LaDTPA-BGLUCA, the ^{13}C resonances shifted somewhat (≤ 1 ppm) and at the same time a set of new signals appeared, which could be assigned to the corresponding Zn(II) complex. The chemical shifts of the latter species were also dependent on the Zn(II) concentration. The intensities of the signals for ZnDTPA-BGLUCA increased at the expense of those for LaDTPA-BGLUCA upon increase of the molar ratio Zn(II)/La(III). Similar phenomena were observed upon addition of ZnCl_2 to a sample of LaDTPA (see Table 4). At molar ratio La(III)/Zn(II) = 1, the molar ratios of the La(III) and Zn(II) chelates were 2:3 and 3:2 for DTPA and DTPA-BGLUCA, respectively. In all cases the thermodynamic equilibrium

was obtained almost immediately after preparation of the samples. On the basis of the stability constants of LaDTPA and ZnDTPA (at 80 °C $\log K = 19.0$ and 17.8 , respectively¹⁷), a higher ratio of the La(III) and Zn(II) complexes would be expected. This and the dependence of the chemical shifts of the two species on the molar ratio La(III)/Zn(II) indicate that an interaction occurs between these complexes and the excess of metal ions. Most likely the free oxygens of the carboxylate groups in the La(III) and Zn(II) chelates bind the second metal ion (La(III) or Zn(II)) under the formation of the complexes $[\text{La}(\text{DTPA})]\text{Zn}$, $[\text{Zn}(\text{DTPA})]\text{La}$, $\{[\text{La}(\text{DTPA})]\text{La}\}^+$, and $\{[\text{Zn}(\text{DTPA})]\text{Zn}\}^-$. It should be noted that, upon addition of Zn(II) to LaDTPA and LaDTPA-BGLUCA, the largest induced ^{13}C NMR shifts were observed for the central glycine unit. Apparently, the counter-ions have a preference for the central carboxylate group. The chemical shifts of the signals for the sugar side-chains were almost independent of the molar ratio Zn(II)/La(III), which suggests that no interaction occurs between these groups and the metal ions. The occurrence of binuclear complexes $\{[\text{Ln}(\text{DTPA})]\text{Ln}\}^+$ has been previously suggested based on ^1H NMR measurements¹⁸ and kinetics¹⁹, and ^6Li shift and relaxation studies showed that Li^+ interacts with all carboxylates in $[\text{Nd}(\text{DTPA})]^{2-}$.²⁰ The formation of these binuclear complexes was supported by ^{139}La NMR spectra. The relaxation of ^{139}La is governed by the quadrupole mechanism. In the extreme narrowing region ($\omega_0^2\tau_c^2 \ll 1$), the relaxation rates can be approximated by eq 2.²¹

$$\frac{1}{T_1} = \frac{1}{T_2} = \frac{1}{98} \left(\frac{e^2qQ}{\hbar} \right)^2 \left(1 + \frac{\eta^2}{3} \right) \tau_c \quad (2)$$

Here e^2qQ is the nuclear quadrupole coupling constant, eq is the electric field gradient, η the asymmetry parameter, and τ_c the rotational correlation time. The relaxation of ^{139}La hence depends on both the electric field gradients, produced by the surrounding ligands, and the molecular tumbling, which is also related to the nature of the ligands via the molecular volume. The high sensitivity of the ^{139}La relaxation for the chemical environment of the La^{III} ion can be employed in coordination studies. Furthermore, it has been shown that the ^{139}La chemical shift is strongly dependent on the number of coordinated carboxylate groups.^{22,23} Both 0.1 M solutions of LaDTPA and LaDTPA-

BGLUCA displayed very broad resonances ($\Delta\nu_{1/2} = 8\text{-}9$ kHz) at about 200 ppm. Upon addition of Zn(II) to the 0.1 M LaDTPA or LaDTPA-BGLUCA sample, the chemical shift of the ^{139}La signal steeply decreased (see Figure 5) but the signal remained very broad ($\Delta\nu_{1/2} \geq 6$ kHz). Since the linewidth of La(III) aquo ion is only 80 Hz, it can be concluded that La(III) released by the transmetallation reaction is predominantly associated to the chelates of the DTPA or DTPA-BGLUCA. The sugar side chains have no significant influence on the transmetallation; the affinity of these groups for metal ions is low in comparison with that of the DTPA-backbone.

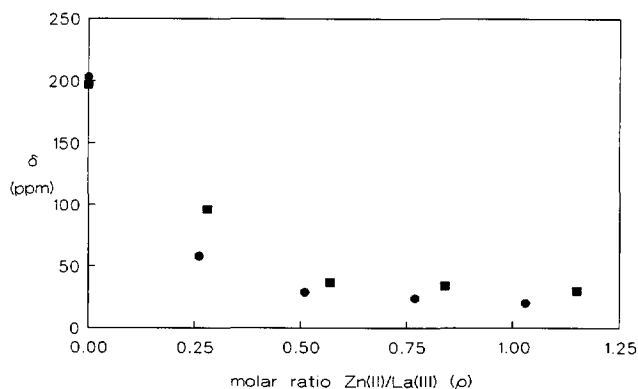


Figure 5. The ^{139}La chemical shifts (ppm) versus the Zn(II)/La(III) ratio (ρ) at 80 °C in D_2O for 0.1 M DTPA (●) and DTPA-BGLUCA (■).

Borate ester formation as studied with ^{11}B NMR

In order to investigate the geometry of the Ln(DTPA-BGLUCA) allows the coordination of second metal ion via the sugar chains, we studied the interaction of borate with these systems. Boron(III) can be considered as an extremely hard metal ion. Previously, it has been outlined that an ion with such a high charge density has a relatively high affinity for (ionized) hydroxyl groups.²⁴ Usually, the preferred donor sites in a polyhydroxyalkyl chain are the same for borate and metal ions. Under the conditions applied in this study (pH 12), borate has no affinity for carboxylates, so exchange between borate and the Ln(III) ion can be excluded. It is well known that in mixtures of boric acid/borate and

polyhydroxy compounds borate esters are formed involving adjacent (1,2-diol type) or alternate (1,3-diol type) (Figure 6).^{25,26} It has been shown that the stabilities of borate esters generally follow the order threo-1,2-diol > terminal 1,2-diol ≥ erythro-1,2-diol > syn-1,3-diol > anti-1,3-diol. Two types of borate esters are possible with diols: borate monoesters, in which a borate is bound to a single diol unit (BD) and borate diesters, in which two diol functions are bound (DBD). ¹¹B NMR is ideally suited to study borate ester formation as the exchange between borate (B), borate monoesters (BD) and borate diesters (DBD) is slow on the ¹¹B NMR time scale and because the various borate esters have characteristic chemical shifts. This enables one to identify them and to determine the boron association constants.

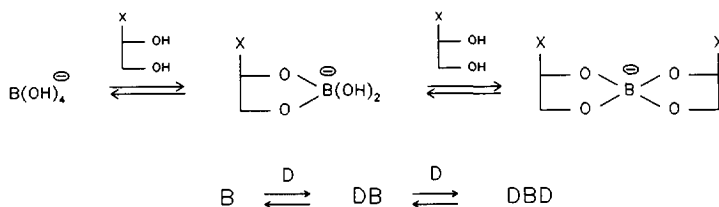


Figure 6. The equilibria between borate (B) and a diol function (D) of a polyhydroxy compound ($X = CHO, CH_2OH, COO, C=NOH$).

Previously, it has been shown that sorbitol forms threo-2,3- or 3,4- (BD, $\delta = -13.4$ ppm; DBD $\delta = -9.3$ ppm), erythro-4,5- (BD, $\delta = -14.4$ ppm), and syn-2,4-borate esters (BD, $\delta = -18.1$ ppm).^{27,28} Based on the structure of DTPA-BGLUCA various possibilities for the formation of borate esters can be envisaged. Firstly, the intra- and intermolecular DBD species ($\delta = -9$ ppm) might be formed. In the case of intramolecular DBD formation only one ligand molecule (DTPA-BGLUCA or L_n DTPA-BGLUCA) will be involved whereas in the formation of intermolecular borate diesters two ligand molecules are required. The formation of polymeric DBD esters is possible which would cause an increase of the viscosity of the borate/ligand solution.

In Figure 7 the ¹¹B NMR spectra of DTPA-BGLUCA and L_n DTPA-BGLUCA with 1 eq borate at pH 12.2 are presented. It can be seen that borate ester species described above are present next to free borate ($\delta = -16.8$ ppm). The formation of erythro borate esters at

the 5,6-position can be excluded on the basis of the ^{13}C NMR spectra: the ^{13}C signal corresponding to C_6 is the only sugar signal that remains unaltered after the addition of borate. The predominant species is of the DBD type. In order to determine the stoichiometry of the various borate ester species Job's plots²⁹ were recorded. In these plots the molarity of bound borate (as obtained from peak integrals) is plotted against $[\text{B}]/([\text{B}]+[\text{L}])$, in which $[\text{B}]+[\text{L}]$ is kept constant. Here L is DTPA-BGLUCA or its lanthanide complex. In Figure 8 the Job's plots for the DBD species at - 9 ppm are shown for DTPA-BGLUCA as well as for LaDTPA-BGLUCA.

From this plot it can be concluded that stoichiometry of the DBD species in the case of DTPA-BGLUCA is BL (x-value is 0.50), which means that there are predominantly intramolecular borate species formed. In general, the borate esters of threo-diols are more stable those of erythro-diols. Consequently, it is very likely that the intramolecular borate diester species is bound at the threo-positions, either the 2,3- or the 3,4-position. The discrimination between the latter two positions cannot be made using ^{11}B NMR in this particular case but molecular models show that for sterical reasons the 3,4-position is the most favourable one.

At the chemical shift characteristic for the DBD species ($\delta=-9$ ppm), at least two resonances were observed for LaDTPA-BGLUCA (Figure 7). The maximum of the Job's plot for these species, compared to that obtained from the free ligand, is slightly shifted to a lower x-value, indicating that the intramolecular DBD species (with stoichiometry BL) are present predominantly in addition to a small amount of intermolecular DBD species (stoichiometry BL_2).

Surprisingly, the Job's plots demonstrate that stoichiometries of the 4,5-erythro BD ester for DTPA-BGLUCA and LaDTPA-BGLUCA are B_2L (x-value is 0.67) and BL, respectively. Thus in the corresponding species each of the sugar chains in DTPA-BGLUCA binds via the 4,5-diol functions to a borate, whereas LaDTPA-BGLUCA forms a cyclic borate ester in which a single borate links the two sugar chains. Presumably, the LaDTPA-BGLUCA is somewhat better preorganized for the 4,5-erythro DBD ester. The Job's plot for the threo BD esters (not presented) show that the stoichiometry for DTPA-BGLUCA as well as for LaDTPA-BGLUCA is B_2L . In Table 5 the borate association constants for the intramolecular diester ($K_{\text{intramolecular}}$) and threo monoester (K_{threo}) for DTPA-BGLUCA and several corresponding Ln(III) complexes are presented. From the

protonation and metal ion coordination studies of DTPA-bis(glucamide)

data in Table 4 it can be concluded that there are no large discrepancies in boron stability constants between the two Ln(III) complexes and the free ligand. These stability constants are similar to those in sorbitol.²⁷ It is also clear that borate is capable of linking the two sugar chains in LnDTPA-BGLUCA.

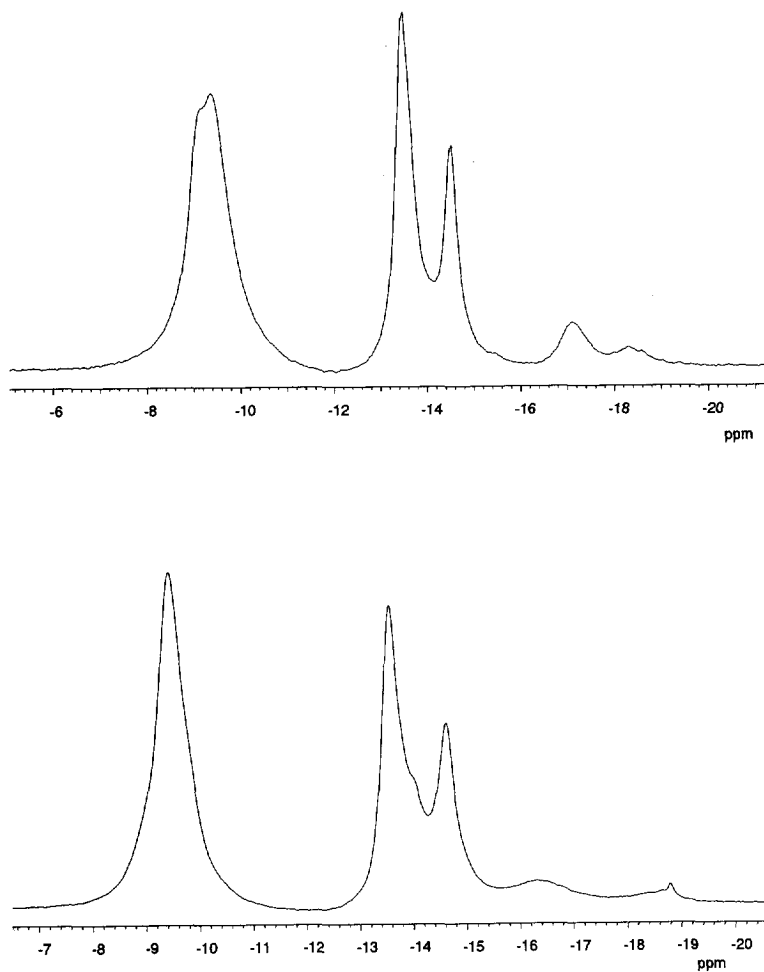


Figure 7. The ^{11}B NMR spectra of a 0.15 M solution of DTPA-BGLUCA (top) and LaDTPA-BGLUCA (bottom), respectively and an equimolar amount of borate at pH 12.2 and 25 °C.

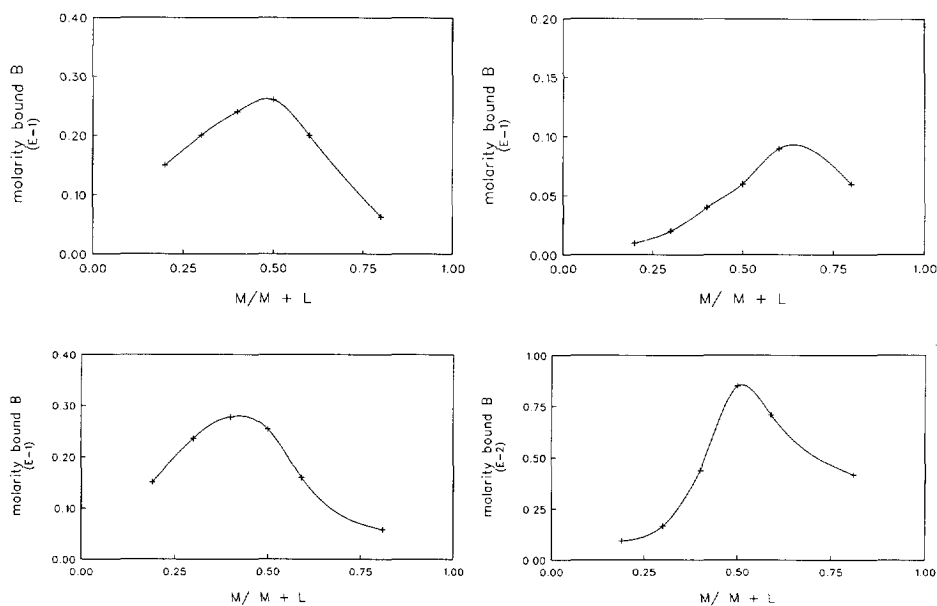


Figure 8. The Job's plots of the borate diester (DBD, $\delta = -9$ ppm) and the 4,5-erythro borate monoester (BD) for DTPA-BGLUCA/ borate (top) and LaDTPA-BGLUCA/ borate (bottom), respectively at pH 12.2 and 25 °C.

Table 5. The boron stability constants (log values) of DTPA-BGLUCA and the corresponding La(III) and Nd(III) complexes.

| Complex | K_{threo} | $K_{\text{intramolecular}}$ |
|---------------|--------------------|-----------------------------|
| DTPA-BGLUCA | 4.21 | 5.31 |
| LaDTPA-BGLUCA | 3.67 | 5.11 |
| NdDTPA-BGLUCA | 4.21 | 5.31 |

CONCLUSIONS

The presence of the polyhydroxy side chains in this novel type of DTPA-bis(amides) does not affect significantly both the macroscopic and the microscopic protonation of this ligand when compared to various DTPA-bis(amides), e.g. DTPA-BEA, DTPA-BPA and DTPA-BPDA. Therefore, the basicities and thus the affinities for metal ions of the amino functions in these ligands are similar. Also transmetallation studies of the Ln(III) chelates of these ligands with Zn(II) reveal large similarities. In all complexes Zn(II) competes with Ln(III) for the binding sites in the DTPA backbone. Any excess of metal ion (Zn(II) or Ln(III)) is bound in the second coordination sphere of the metal ion in the complexes concerned. This second sphere coordination appears to be preferred over coordination to hydroxyl groups of the sugar side chain. However, borate, which can be considered as a model for hard metal ions, is able to intramolecularly link the sugar chains in the LnDTPA-BGLUCA complexes. In order to achieve similar phenomena with divalent metal ions that occur in biological systems (Zn(II), Ca(II), etc), it will be needed to functionalize the sugar side chains with groups that have a somewhat higher affinity for these ions. A terminal carboxylate group, for example, might improve this affinity substantially. It may be expected that those modified complexes show synergistic binding of the divalent ions, which will result in a higher kinetic stability.

EXPERIMENTAL

Potentiometry

The potentiometric titrations were conducted at 298 K in a double-walled vessel. Millivolt readings obtained with a glass electrode were converted to pH values using a calibration curve which was determined from standard buffer solutions. The ionic strength was maintained at 0.1 M using NaClO₄. The protonation constants were determined by titration of a 0.01 M ligand solution with 0.02 M HCl. The calculations for the potentiometric titrations were performed using a spreadsheet program.^{30,31}

NMR measurements

^1H NMR spectra were recorded on Varian VXR-400 S NMR and Varian Unity 500 spectrometers with $\text{D}_2\text{O}/\text{H}_2\text{O}$ (4:1 v/v) as the solvent and *t*-BuOH as the internal reference (δ (ppm); 1.20). For the ^1H NMR pH titration curves at 25 °C a 0.2 M solution of DTPA-BGLUCA was used. The pH was adjusted to 1 using 1 M HCl. Subsequently, the pH was raised from 1 to 12 in intervals of approximately 1 using 1 M NaOH. The pH was measured with a calibrated Z11,344-1 Aldrich combination pH electrode. The values are direct meter readings. The ^{13}C NMR spectra were recorded on a Nicolet NT-200 WB NMR spectrometer (50.3 MHz) and on a Varian VXR-400 S NMR spectrometer (100.6 MHz) using 30% D_2O (for locking) in water as the solvent with *t*-BuOH (δ (ppm); 31.2) as the internal reference. The ^{13}C NMR pH titration curves at 25 °C were measured on a Varian XL-200 FT spectrometer (50.3 MHz) in a similar method as described for the ^1H NMR pH titration curves. The pH was measured on a Crison micropH 2002 equipped with a glass electrode. The values are direct meter readings. The ^{11}B NMR spectra (external 0.1 M boric acid in D_2O) were recorded at 25 °C with Varian Unity 500 (160.5 MHz), Varian VXR-400 S (128.3 MHz) and Nicolet NT-200 WB (64.2 MHz) spectrometers. Baseline correction was applied to remove the broad signal of the boron incorporated in the glass sample tube and in the insert. Usually a deconvolution program was used to obtain all the signal characteristics. The ^{139}La spectra were recorded at 80 °C on a Varian VXR-400 S NMR spectrometer (56.5 MHz) using 0.1 M LaCl_3 as the external reference.

ACKNOWLEDGEMENTS

This investigation was carried out with the support of the Dutch National Innovation Program Carbohydrates. We are grateful to Akzo Nobel Central Research (ACR) for their financial support. Many thanks are due to Mrs A.H. van der Heijden for performing the larger part of the NMR experiments. The authors are also indebted to Prof. dr. C.F.G.C. Geraldes (University of Coimbra, Portugal) for having A.M. v.d.H. as a guest at his institute. The EC Erasmus program is thanked for funding the stay of A.M.v.d.H. at the University of Coimbra.

REFERENCES

1. Lauffer, R.B. *Chem. Rev.* **1987**, *87*, 901.
2. Goldstein, H.; Lumma, W.; Rudzik, A. *Ann. Rep. Med. Chem.* **1989**, *24*, 265.
3. Armitage, F.E.; Richardson, D.E.; Li, K.C.P. *Bioconjugate Chem.* **1990**, *1*, 365.
4. Wiener, E.C.; Brechbiel, M.W.; Brothers, R.L.; Magin, R.L.; Gansow, O.A.; Tomalia, D.A.; Lauterbur, P.C. *Magn. Reson. Med.* **1994**, *31*, 1.
5. Lammers, H.; Maton, F.; Pubanz, D.; van Laren, M.W.; van Bekkum, H.; Merbach, A.E.; Muller, R.N. Peters, J.A. *to be submitted to Inorg. Chem.*
6. Breitmaier, E.; Völler, W. *Carbon-13 NMR Spectroscopy*, 3rd ed.; VCH: New York, 1987, pp. 122-123.
7. Sherry, A.D.; Cacheris, W.P.; Kuan, K.-T. *Magn. Reson. Med.* **1988**, *8*, 180.
8. Sudmeier, J.L.; Reilley, C.N. *Anal. Chem.* **1964**, *9*, 1698.
9. Geraldes, C.F.G.C.; Urbano, A.M.; Alpoim, M.C.; Sherry, A.D.; Kuan, K.-T.; Rajagopalan, R.; Maton, F.; Muller, R.N. *Magn. Reson. Imaging* **1995**, *2*, 13.
10. King, E.J. *J. Am. Chem. Soc.* **1951**, *73*, 155.
11. Li, N.C.; Doody, E.; White, J.M. *J. Am. Chem. Soc.* **1957**, *79*, 5859.
12. Fujiwara, Y.; Reilley, C.N. *Anal. Chem.* **1968**, *40*, 890.
13. Letkeman, P.; Martell, A.E. *Inorg. Chem.* **1979**, *18*, 1284.
14. White, D.H.; DeLearie, L.A.; Dunn, T.J.; Rizkalla, E.N.; Imura, H.; Choppin, G.R., *Invest. Radiol.* **1991**, *26*, S229.
15. Bai, Y.; Milne, J.S.; Mayne, L.; Englander, S.W. *Proteins Struct. Funct. Genet.* **1993**, *17*, 75 (1993).
16. Hawkes, G.E.; Lewis, D. *J. Chem. Soc. Perkin Trans. II* **1984**, 2073.
17. Martell, A.E.; Smith, R.M. *Critical Stability Constants*; Plenum New York, 1974; Vol. 1.
18. Kostromina, N.A.; Ternovaya, T.V. *Russ. J. Inorg. Chem. (Engl. Transl.)* **1979**, *24*, 1024.
19. Brücher, E.; Laurenczy, G. *J. Inorg. Nucl. Chem.* **1981**, *43*, 2089.
20. Peters, J.A. *Inorg. Chem.* **1988**, *27*, 4686.
21. Reuben, J.; Luz, Z. *J. Phys. Chem.* **1976**, *80*, 1357.
22. Peters, J.A.; Kieboom, A.P.G. *Recl. Trav. Chim. Pays-Bas* **1983**, *102*, 381.

23. Geraldes, C.F.G.C.; Sherry, A.D. *J. Magn. Reson.* **1986**, *66*, 274.
24. van Duin, M.; Peters, J.A.; Kieboom, A.P.G., van Bekkum, H. *Recl. Trav. Chim. Pays-Bas* **1989**, *108*, 57 .
25. Henderson, W.G.; How, M.J.; Kennedy, G.R.; Mooney, E.F. *Carbohydr. Res.* **1973**, *28*, 1.
26. van Duin, M.; Peters, J.A.; Kieboom, A.P.G.; van Bekkum, H. *Tetrahedron* **1984**, *40*, 2901.
27. van Duin, M.; Peters, J.A.; Kieboom, A.P.G.; van Bekkum, H. *Tetrahedron* **1985**, *41*, 3411.
28. Makkee, M.; Kieboom, A.P.G.; van Bekkum, H. *Recl. Trav. Chim. Pays-Bas* **1985**, *104*, 230.
29. Gil, V.M.S.; Oliveira, N.C. *J. Chem. Educ.* **1990**, *67*, 473.
30. Huskens, J.; van Bekkum, H.; Peters, J.A. *Comput. Chem.* in press.
31. Huskens, J.; Lammers, H.; van Bekkum, H.; Peters, J.A. *Magn. Reson. Chem.* **1994**, *32*, 691.



SUMMARY

This thesis deals with the synthesis of alkylamino sugars and derivatives thereof. The metal ion coordination behaviour of these compounds in aqueous systems has been studied extensively using multinuclear NMR and potentiometry.

Chapter 1 is a general introduction on the various synthetic routes to alkylamino sugars. Several industrial applications of amino sugars are also given. This chapter is concluded with an overview of this thesis.

In chapter 2, an introduction on MRI (Magnetic Resonance Imaging) is presented. This chapter has been included in this thesis because several of the synthesized alkylamino sugars (chapter 3) were used as starting materials for the synthesis of potential contrast agents for MRI.

Chapter 3 describes a ^1H and ^{13}C NMR study on the speciation of aqueous systems ($\text{pH}=11.5\text{-}11.8$) containing equimolar amounts of aldohexose (D-glucose, D-galactose and D-mannose) and mono- or bifunctional amines. β -N-propylgalactosylamine is the major species present in solutions of D-galactose and propylamine. In equimolar solutions of aldohexoses and ethylenediamine or 1,3-diaminopropane, in addition to mono- and diglycosylamines, the tetrahydro-imidazole and hexahydropyrimidine derivatives, respectively, are formed. The hydrogenation of solutions of aldohexoses and ethylenediamine using platinum on activated carbon as the catalyst gives the corresponding alkylamino sugars in good yields. The latter type of amino sugar can be simply converted into EDTA-type complexing agents having similar sequestering capacities (Ca(II) and Cd(II)) as EDTA.

The reductive amination of D-galactose with propylamine in water over a platinum-on-graphite catalyst in a three-phase continuous stirred tank reactor, is reported in chapter 4. The hydrogen pressure is varied from 5 to 20 bar, the D-galactose concentration from 125 to 750 mol m^{-3} and the amine concentration from 125 to 500 mol m^{-3} . The reaction temperature is fixed at 323 K. The reaction kinetics of the hydrogenation can be described satisfactorily using a relatively simple rate equation for the range of the applied reaction conditions.

Chapter 5 deals with the synthesis, borate ester formation and metal ion sequestration of secondary alditylamines and their N-carboxymethyl derivatives. ^{11}B and ^{13}C NMR measurements show that these compounds form diborate diesters leading to macrocyclic structures. The N-carboxymethyl derivatives possess strong Ca(II) ($\text{pH}>11$) and Cd(II)

complexing properties both in the presence and absence of borate.

In chapter 6, the Cd(II) coordination of the aldohexoses obtained by reductive amination with bifunctional amines (see chapter 3), using ^{113}Cd NMR and potentiometry is described. The protonation constants of these compounds are determined from ^{13}C pH titration curves. The obtained values are in good agreement with those obtained by potentiometry. The Cd(II) stability constants are determined with potentiometry. ^{113}Cd NMR demonstrates that at neutral pH, both the primary and secondary N-atoms are involved in the coordination. At high pH, additional coordination of one of the hydroxyl groups of the sugar side chains occurs.

In chapter 7, the use of NMR in the determination of metal ligand complex stability constants is discussed. Three examples are provided in which NMR is applied to determine stability constants. For one of the compounds already described in chapter 3 and 6, the Cd(II) stability constants are determined using ^{113}Cd NMR speciations. The stability constants of the ternary complexes of trimetaphosphate with Ln(III) aminopolycarboxylates were determined using ^{31}P NMR shifts. The third example is the determination of the stability of the ternary complex of tripolyphosphate, Nd(III) and NTA using ^{31}P NMR shifts and relaxation rate enhancements.

Chapter 8 deals with the synthesis of several sugar-based DTPA-bis(amides) in which the alkylamino sugars discussed in chapter 3 are used as starting materials. The structure and dynamics of the corresponding Ln(III) complexes in aqueous solution are studied using ^{13}C and ^{17}O NMR. The NMR results show that the organic ligand binds to the Ln(III)-ion in an octadentate fashion via the three nitrogens of the diethylenetriamine backbone, the three carboxylate groups, and the two amide oxygens. The sugar side chains are not involved in the coordination. ^{17}O NMR measurements indicate that the coordination sphere is completed by one water ligand. A variable temperature and pressure ^{17}O NMR study on the corresponding Gd(III) complexes is performed to evaluate their water exchange kinetics. These complexes may be of relevance as potential MRI contrast agents (see chapter 2), and the water exchange rate is one of the crucial parameters determining the efficacy of a contrast agent. The water exchange rates obtained are compared with that obtained for GdDTPA-bis(methylamide). The conclusion is that the structural changes in the second coordination sphere do not influence the water exchange significantly. The activation volumes obtained from the variable pressure ^{17}O NMR measurements show that the water exchange reaction is strongly dissociatively activated. The nuclear magnetic relaxation dispersion (NMRD)

profiles at several temperatures are recorded. The data confirm the relatively slow water exchange process of these complexes in comparison with $\text{Gd}(\text{DTPA})^{2-}$.

In chapter 9, the quantitative determination of the microscopic sites of protonation of DTPA-BGLUCA obtained from ^1H NMR pH titration curves is reported. In the second protonation step, a substantial migration occurs from the central nitrogen atom to the terminal ones. In addition, the transmetallation of LaDTPA and LaDTPA-BGLUCA with Zn(II) is investigated using ^{13}C and ^{139}La NMR. The results show that the sugar side chains are not involved in the transmetallation. On the other hand, the sugar side chains are involved in the coordination of borate which results in the formation of borate esters as studied by ^{11}B NMR. The ^{11}B NMR data demonstrate that intramolecular macrocyclic borate diester are formed. The stoichiometry of the various borate esters species is investigated by recording the corresponding Job's plot. The boron stability constants of each type of borate ester obtained for DTPA-BGLUCA compared to the ones obtained for its corresponding Ln(III) complexes, show no large discrepancies.



SAMENVATTING

Dit proefschrift is gewijd aan de synthese van aminosuikers en afgeleiden daarvan. De metaalioncoördinerende eigenschappen van deze verbindingen in waterige systemen zijn uitvoerig bestudeerd met multikern NMR en potentiometrie.

Hoofdstuk 1 is een algemene inleiding over de verschillende syntheseroutes die bestaan om aminosuikers te bereiden. De verschillende toepassingsmogelijkheden van aminosuikers worden eveneens beschreven. Tenslotte wordt in dit hoofdstuk een overzicht van de indeling van het proefschrift gegeven.

In hoofdstuk 2 wordt een inleiding over MRI (Magnetic Resonance Imaging) gegeven. Het hoofdstuk is opgenomen in het proefschrift omdat de in dit onderzoek gesynthetiseerde aminosuikers (hoofdstuk 3) zijn gebruikt als uitgangsstof voor een mogelijk nieuw type contrastreagens voor MRI.

Hoofdstuk 3 beschrijft een ^1H en ^{13}C NMR studie verricht naar de evenwichten en intermediairen die aanwezig zijn in waterige oplossingen (pH=11.5-11.8) die equimolaire hoeveelheden aldohexose (D-glucose, D-galactose en D-mannose) en mono- of bifunctionele amine bevatten. Het meest voorkomende intermediair aanwezig in een oplossing van D-galactose en propylamine is β -N-propylgalactosylamine. In equimolaire oplossingen van bovengenoemde aldohexosen en ethyleendiamine of 1,3-diaminopropaan zijn naast, mono- en biglycosylamines, respectievelijk tetrahydro-imidazool en hexahydro-pyrimidine aanwezig. De hydrogenering van een mengsel met aldohexose en ethyleendiamine met platina op kool als de katalysator geeft een produkt dat eenvoudig omgezet kan worden naar een EDTA derivaat. De metaalioncoördinerende capaciteiten (Ca(II) en Cd(II)) van dit type verbinding zijn vergelijkbaar met die van EDTA.

De reactiekinetiek van de reductieve aminering van D-galactose met propylamine met platina op kool als de katalysator, in een driefase continu geroerde reactor, staat centraal in hoofdstuk 4. De waterstofdruk werd gevarieerd van 5 tot 20 bar, de D-galactoseconcentratie van 125 tot 750 mol m^{-3} en de amine concentratie van 125 tot 500 mol m^{-3} . De reactietemperatuur was 323 K. De reactiekinetiek van de hydrogenering kan met een relatief eenvoudige snelheidsvergelijking beschreven worden.

Hoofdstuk 5 beschrijft de synthese, boraatstervoming en metaalioncomplexering van secundaire alditylamines en hun N-carboxymethylderivaten. De ^{11}B en ^{13}C -NMR metingen tonen aan dat deze verbindingen diboraatesters vormen, waarbij macrocyclische structuren ontstaan. De N-gecarboxymethyleerde verbindingen bezitten sterke Ca(II) (pH>11) en Cd(II)-

complexerende eigenschappen, zowel in aan- als afwezigheid van boraat.

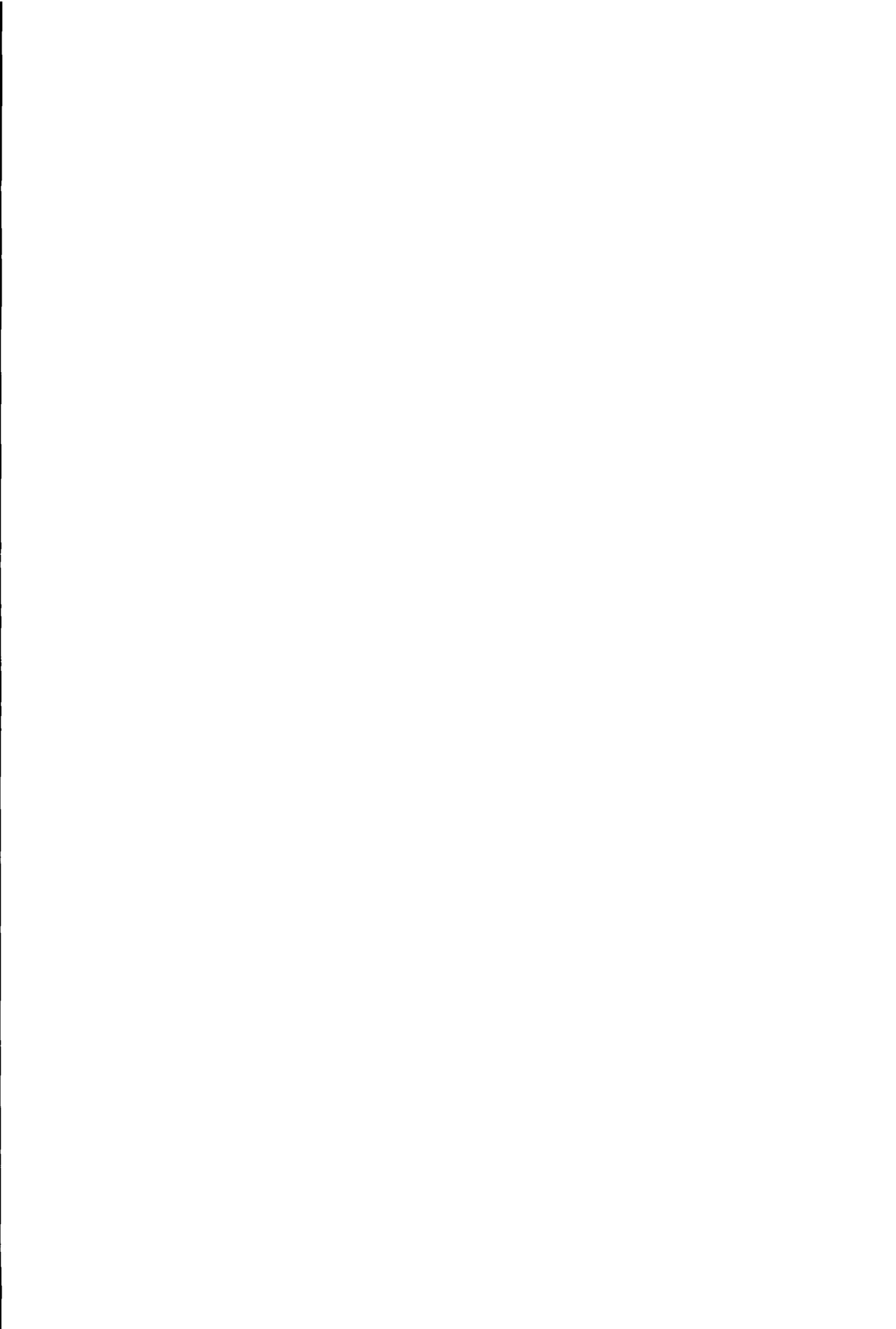
In hoofdstuk 6 wordt de Cd(II)-complexering van aminosuikers, verkregen door reductieve aminering van aldohexosen met bifunctionele amines (hoofdstuk 3), met ^{113}Cd NMR en potentiometrie bestudeerd. De protoneringsconstanten van deze verbindingen zijn bepaald met zowel potentiometrie als ^{13}C NMR. De gevonden waarden zijn goed met elkaar in overeenstemming. De Cd(II)-stabiliteitsconstanten zijn bepaald met potentiometrie. ^{113}Cd NMR toont aan dat bij neutrale pH zowel het secundaire als primaire stikstofatoom zijn betrokken bij de Cd(II)-coördinatie. Eveneens blijkt uit ^{113}Cd NMR dat bij hoge pH (>12) één van de hydroxylgroepen van de suikerketen participeert in de Cd(II)-chelering.

In hoofdstuk 7 wordt aandacht geschonken aan het gebruik van NMR voor de bepaling van stabiliteitsconstanten van metaal-ligand-complexen. Er worden drie voorbeelden gegeven. Voor één van de verbindingen in hoofdstuk 6 is de stabiliteit van het Cd(II)-complex bepaald met ^{113}Cd NMR. De verkregen waarde blijkt goed overeen te komen met de waarde verkregen met potentiometrie. De stabiliteitsconstanten van de ternaire complexen van cyclisch trifosfaat met aminopolycarboxylaatcomplexen van Ln(III) worden bepaald met ^{31}P NMR-shifts. Als laatste voorbeeld wordt de stabiliteit van het ternaire complex van lineair trifosfaat Nd(III) and NTA bepaald met ^{31}P NMR-shifts besproken.

Hoofdstuk 8 gaat over de synthese van op suiker gebaseerde DTPA-bisamiden waarbij de aminosuikers behandeld in hoofdstuk 3 worden gebruikt als uitgangsstof. De structuur en dynamica in waterig milieu van de overeenkomstige Ln(III)-complexen zijn bestudeerd met ^{13}C en ^{17}O NMR. Het DTPA-derivaat blijkt octadentaat aan het Ln(III)-ion te binden, waarbij de drie stikstofatomen van de diethyleentriamine unit, de drie carboxylaat groepen en de twee zuurstofatomen van de amide functies fungeren als donor. De eerste coördinatiesfeer van het Ln(III) wordt gecompleteerd met één water molecuul. De uitwisselingssnelheid van water in de Gd(III) complexen is bepaald met variabele temperatuur ^{17}O NMR. Het blijkt dat de suikerketens in het complex de snelheid van wateruitwisseling, vergeleken met DTPA-bis(methylamide), niet significant beïnvloeden. Het mechanisme van de wateruitwisseling, bestudeerd met variabele druk ^{17}O NMR, blijkt volgens een dissociatief mechanisme te verlopen. De uitwisselingssnelheid van water van dit type DTPA-derivaten ten opzichte van $\text{Gd}(\text{DTPA})^{2-}$ is relatief langzaam. Dit laatste aspect wordt duidelijk zichtbaar wanneer de NMRD ("nuclear magnetic resonance dispersion") profielen, opgenomen bij 5 and 37 °C, met elkaar worden vergeleken.

In hoofdstuk 9 wordt een kwantitatieve studie van het protoneringsschema van DTPA-BGLUCA met ^1H NMR beschreven. Het blijkt dat bij de eerste protonering ($\text{pK}_a = 9.2$)

voornamelijk het centrale N-atoom is betrokken. Bij de tweede protoneringsstap ($pK_a = 4.5$) treedt er een duidelijke migratie van protonen op naar de terminale N-atomen. Eveneens wordt in dit hoofdstuk de transmetallering van LaDTPA en LaDTPA-BGLUCA met Zn(II) bestudeerd met ^{13}C en ^{139}La NMR. De resultaten laten zien dat de suikerketens niet zijn betrokken bij de transmetallering. Uit ^{11}B NMR blijkt dat de suikerketens wel betrokken zijn bij de vorming van boraatesters. De stabiliteitsconstanten van dezelfde type boraatesters van DTPA-BGLUCA en de overeenkomstige Ln(III)-complexen liggen in dezelfde orde van grootte.



DANKWOORD

Het onderzoek wat in dit proefschrift staat beschreven is tot stand gekomen met de hulp van velen. Ik wil dan ook iedereen die eraan heeft bijgedragen hartelijk danken. Een aantal mensen verdient het om hier met name genoemd te worden.

In het bijzonder wil ik Herman van Bekkum en Joop Peters bedanken voor hun stimulerend enthousiasme en enorme kennis van zaken. De vrijheid en het vertrouwen die zij mij hebben gegeven tijdens het onderzoek heb ik de afgelopen vier jaar zeer gewaardeerd.

Dr. J.G. Batelaan, Dr. E. Boelema, Dr. C.M. Navarro en Dr. J.C. Speelman, allen van Akzo Nobel Central Research, worden bedankt voor de stimulerende discussies tijdens de Akzo Nobel/ TU Delft bijeenkomsten.

Dr. ir. B.F.M. Kuster en Geert Ingenbleek beiden werkzaam in de Vakgroep Chemische Proceskunde (o.l.v. prof. dr. ir. G.B. Marin) van de TU Eindhoven ben ik zeer erkentelijk voor hun belangrijke bijdrage in hoofdstuk 4.

Jacco van Haveren ben ik dankbaar voor zijn belangrijk aandeel in hoofdstuk 5.

Speciale dank aan Jurriaan Huskens voor zijn grote bijdrage in hoofdstuk 7 en eveneens voor de fijne manier waarop ik enkele jaren met hem heb samengewerkt.

Special thanks are also due to Prof. dr. A.E. Merbach Head of Department, Inorganic and Analytical Chemistry, the University of Lausanne, who kindly invited me to work in his group. I am greatly indebted to Dirk Pubanz for his daily supervision during my stay in Lausanne.

Furthermore I would like to thank Prof. dr. R.N. Muller Head of Department, Laboratory of Organic Chemistry and NMR, the University of Mons-Hainaut, for inviting me to his institute and Frédéric Maton for his supervision during my stay in Mons.

Anneke van der Heijden en Martijn van Laren ben ik veel dank verschuldigd voor hun inzet en enthousiasme tijdens hun hoofdvakstages. Hun resultaten zijn terug te vinden in de hoofdstukken 8 en 9.

Anton Sinnema en Anton van Esterik ben ik erkentelijk voor het opnemen van NMR-spectra. Ernst Wurtz ben ik erg dankbaar voor alle praktische problemen die hij voor mij heeft opgelost.

Mieke van der Kooy-van Leeuwen ben ik zeer erkentelijk voor het helpen bij allerlei administratieve werkzaamheden.

Theo en Ton Hoefnagel worden bedankt voor hun zinvolle discussies wat betreft de organische synthese en Wim Jongeleen voor zijn grafische ondersteuning.

Bert van der Hulst en Chris van Drongelen worden bedankt voor hun niet altijd zinvolle discussies over van alles behalve de wetenschap.

I also would like to acknowledge my three IAESTE-students Anna Kennedy, Raynald Demange and Ingrid van Uffelen. The former for performing the potentiometric measurements described in chapter 6 and the latter two for synthesizing various compounds as described in chapter 8.

Een belangrijke bijdrage aan het dagelijks plezier in het werk hebben mijn directe collega's geleverd, te weten (naast reeds enkele bovengenoemde personen) Fokko Venema, Edwin Boers, Ron van den Berg, Kees de Graauw, Dorine Verraest, Emrin Bovens en Annemieke Heinen. Verder wil ik alle Böesekenzaal-bewoners en andere koffieclubleden bedanken voor de gezellige koffie-uren.

De Geertruida Stichting van het Groene Hart Lyceum te Alphen aan den Rijn ben ik zeer erkentelijk voor de financiële tegemoetkoming in de drukkosten van het proefschrift.

Tenslotte ben ik mijn ouders, familie, vrienden en speciaal Louise zeer dankbaar voor alle ondersteuning die zij mij de afgelopen jaren hebben gegeven.

CURRICULUM VITAE

René Lammers werd op 29 mei 1965 te Aalten geboren. Na het behalen van het HAVO en VWO diploma aan het Groene Hart Lyceum te Alphen aan den Rijn begon hij in september 1984 aan de Leidse Hogeschool een HLO-studie (Organische Chemie). Het examen werd in juni 1988 afgelegd. Vanaf juli 1988 tot en met augustus 1989 vervulde hij zijn militaire dienstplicht. In september 1989 begon hij met de studie Scheikunde aan de Rijksuniversiteit Leiden. Het doctoraal examen werd in juni 1991 afgelegd (cum laude) met als hoofdvak Organische Chemie (dr. C.L. Habraken). Het in dit proefschrift beschreven onderzoek werd verricht van augustus 1991 tot en met augustus 1995. Vanaf 1 november 1995 is de auteur werkzaam bij Unilever Nederland B.V.